Anti-inflammatory Effects of 15-Lipoxygenase Metabolites of α-Linolenic acid: Studies on Signalling Pathways Involved

Thesis submitted for the degree of

DOCTOR OF PHILOSOPHY

By

Naresh Kumar

Department of Animal Biology
School of Life Sciences
University of Hyderabad
Hyderabad-500 046, INDIA

Enrolment No. 08LAPH12
June, 2016

University of Hyderabad
(A Central University established in 1974 by act of parliament)
Hyderabad-500 046, INDIA

CERTIFICATE

This is to certify that **Mr. Naresh Kumar** has carried out the research work embodied in the present thesis under my supervision and guidance for a full period prescribed under the Ph.D. ordinance of this University. We recommend his thesis entitled **"Anti-inflammatory Effects of 15-Lipoxygenase Metabolites of α-Linolenic acid: Studies on Signalling Pathways Involved"** for submission for the degree of Doctor of Philosophy of this University.

Prof. P. Reddanna
Research Supervisor _____

Head
Department of Animal Biology _____

Dean
School of Life Sciences _____

University of Hyderabad
(A Central University established in 1974 by act of parliament)
Hyderabad-500 046, INDIA

DECLARATION

I hereby declare that the work embodied in this thesis entitled **"Anti-inflammatory Effects of 15-Lipoxygenase Metabolites of α-Linolenic acid: Studies on Signalling Pathways Involved"** has been carried out by me under the supervision of **Prof. P. Reddanna** and this work has not been submitted for any degree or diploma of any other university earlier.

Prof. P. Reddanna
(Research Supervisor)

Naresh Kumar
(Research Scholar)

ACKNOWLEDGEMENTS

I express my deepest sense of gratitude to my mentor, ***Prof. P. Reddanna*** *for giving me an opportunity to work under his able guidance, providing the lab facilities and constant support throughout my work. It gives me immense pleasure to admit that Prof. P. Reddanna, a man of integrity, patience and perseverance has been a constant source of inspiration throughout my doctoral discourse.*

I would like to thank members of doctoral committee, ***Prof. Aparna Dutta Gupta*** *and* ***Dr. Mrinal Kanti Bhattacharyya*** *for their valuable suggestions and guidance. I thank all the other faculty members of School of Life Sciences for their help during the course of my Ph.D. work*

I would like to thank the Head of the department, Animal Biology, ***Prof. Jagan Pongubala*** *and the former Heads of the department* ***Prof. B. Senthilkumaran, Prof. Manjula Sritharan*** *and* ***Prof. S. Dayananda,*** *for their support and encouragement and for letting me use the department facilities.*

I would like to thank the Dean of School of Life Sciences, ***Prof P. Reddanna*** *and the former Deans of School of Life Sciences,* ***Prof. R.P. Sharma, Prof. Aparna Dutta Gupta, Prof. M. Ramanadham*** *and* ***Prof. A.S. Raghavendra,*** *for their support and encouragement during my research tenure and also for allowing me to use the School facilities.*

I thank ***Dr. A. Bindu Madhava Reddy*** *and* ***Dr. M.K. Arunasree*** *for their support and encouragement.*

I am extremely thankful individually to all the faculty members of the school for their kind help and cooperation at various stages of my stay in the campus.

My heartfelt thanks to ***Dr. G. V. Reddy*** *for his timely guidance, help and critical views all throughout my PhD work.*

Special heartfelt thanks to ***Dr. Anilkumar Kotha*** *and* ***Dr. Karnati Roy*** *for their unwavering support and constant encouragement during my entire research period. Their critical comments and patience have helped me improve my research skills largely.*

I wish to thank my senior colleagues ***Dr. Chandramohan, Dr. Nishanth, Dr. Kishore, Dr. Aparna, Dr. Aparoy, Dr. Pulla reddy, Dr. Ramakrishna, Dr. Smita, Dr. Sandhya*** *and* ***Dr. Vasundhra*** *for their guidance and help in acquiring the technical skills and scientific insight.*

I wish to thank all my cooperative lab mates ***Geetika, Chandrani, Jyotsna, Praveen, Suresh, Naireen, Kumar, Vanaja, Preethi, Azad, Dinesh*** *and* ***Priyanka*** *for their help and creating a cheerful work atmosphere*

My special thanks to ***Ashutosh, Shivendra, Venkat, Madhubabu, Kishor, Shreesh, Ravi, Baburao, Jagdish,*** *and* ***Samuel*** *for their ever responsiveness and timely help.*

I thank all my teachers since my childhood whose guidance and encouragement at each step was instrumental in shaping my career.

I would also like to thank the administrative and technical staff of Department of Animal Biology ***Mr. Ankineedu, Ms. Jyothi and Mr. Jagan,*** *for their timely help. Assistance received from* ***Mr. Balram, Mr. Shiva kumar, Mr. Nagesh*** *and* ***Mr. Bangariah*** *is greatly appreciated.*

I acknowledge CSIR, New Delhi for providing JRF and SRF in the form of financial assistance. I also acknowledge the infrastructural support received from UPE-I & II programs, which helped me to carry out this work.

I would like to make a special mention of my friend ***Chandrashekhar*** *for always being there for me when I needed. His support, love and inspiration through all times kept me going. I wish him all success and happiness in his life.*

Words fall short in expressing my appreciation to my friend ***Mridula*** *who was always a source of energy, whose emotional and financial support through all the time kept me going while love, suggestions and inspiration made me feel special.*

At this juncture, I remember with gratitude my beloved parents for their wholehearted support and immense blessings to achieve this goal in my life. This dissertation is cordially devoted to them. What I am today is by the Grace of God Almighty. I stoop before him for having strengthened me to complete this endeavor.

Naresh….

Table of Contents

List of Figures and Tables

1 List of Abbreviations

AA	:	Arachidonic acid
ALA	:	α-Linolenic Acid
BSA	:	Bovine serum albumin
CLP	:	Cecal Ligation and Puncture
COX	:	Cyclooxygenase
DAPI	:	4',6-diamidino-2-phenylindole
DCFH-DA	:	2',7'-Dichlorofluorescein Diacetate
DHA	:	Docosahexaenoic acid
DMEM	:	Dulbecco's Modified Eagle Medium
DMSO	:	Dimethyl sulfoxide
DNA	:	Deoxyribonucleic acid
EDTA	:	Ethylene diamine tetra acetic acid
EFA	:	Essential fatty acids
ELISA	:	Enzyme linked immunosorbent assay
EPA	:	Eicosapentaenoic acid
FACS	:	Fluorescence-activated cell Sorter
FBS	:	Fetal bovine serum
FFA	:	Free fatty acids
FITC	:	Fluorescein isothiocyanate
g	:	Gram
GC-MS	:	Gas chromatography-mass spectrometry
h	:	Hour(s)
HRP	:	Horseradish peroxidase
IL-1β	:	Interleukin-1β

iNOS	:	Inducible nitric oxide synthase
kDa	:	Kilo Dalton
l	:	litre
LA	:	Linolenic acid
LOX	:	lipoxygenase
LPS	:	Lipopolysaccharide
LT	:	Leukotriene
LX	:	Lipoxin
mg	:	Milli gram
min	:	Minute(s)
mL	:	Milli liter
mM	:	Milli molar
mRNA	:	Messanger Ribonucleic acid
MTT	:	3-(4, 5-dimethylthiazol-2-yl)-2,5- Diphenyl tetrazolium bromide
NAC	:	N-acetylcystein
nm	:	Nano meter(s)
NO	:	Nitric oxide
NSAIDs	:	Non-steroidal anti-inflammatory drugs
PAGE	:	Polyacrylamide gel electrophoresis
PBS	:	Phosphate buffered saline
PCR	:	Polymerase chain reaction
PG	:	Prostaglandin
PI	:	Propidium iodide
PMSF	:	Phenyl methane sulphonyl fluoride
PUFAs	:	Polyunsaturated fatty acids

ROS	:	Reactive oxygen species
RP-HPLC	:	Reverse phase- High pressure liquid chromatography
RT-PCR	:	Reverse transcription-polymerase chain Reaction
SDS	:	Sodium dodecyl sulfate
SP-HPLC	:	Straight phase-High pressure liquid chromatography
TNF-α	:	Tumor necrosis factor-α
Tris	:	Tris-(Hydroxymethyl) aminomethane
UV	:	Ultraviolet
µM	:	Micro molar
°C	:	Degree centigrade/ Degree Celsius
13-(S)-HODE	:	13-(S)-hydroxyoctadecadienoic acid
13-(S)-HOTrE	:	13-(S)-hydroxyoctadecatrienoic acid
13-(S)-HPODE	:	13-(S)-hydroperoxyoctadecadienoic acid
13-(S)-HPOTrE	:	13-(S)-hydroperoxyoctadecatrienoic acid
15-(S)-HETE	:	15-(S)-hydroxyeicosatetraenoic acid
15-(S)-HPETE	:	15-(S)-hydroperoxyeicosatetraenoic acid

Chapter 1

GENERAL INTRODUCTION

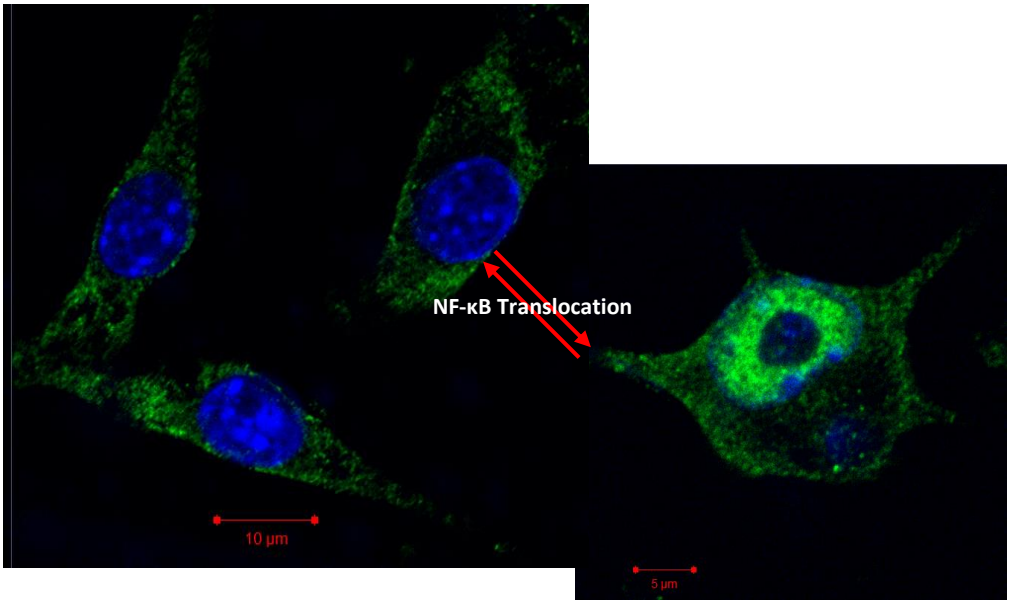

1.1 INFLAMMATION

1.1.1 Introduction

Inflammation is the host's immune response towards any internal or external cue such as tissue damage, injury, infection, artificial agents, or immune disorders. In 1600 BC, Celsus explained four cardinal signs of inflammation as *ruber* (redness), *tumor* (swelling), *calor* (heat), and *dolar* (pain). Galen added the 5th sign of inflammation: *functio laesa* (loss of function) (Figure 1-1). Inflammatory response involves three events, vasodilation, increase in blood capillary permeability and the influx of phagocytes from blood capillaries to specific tissue. The initiation of the inflammatory response is mediated by a complex series of events through a variety of

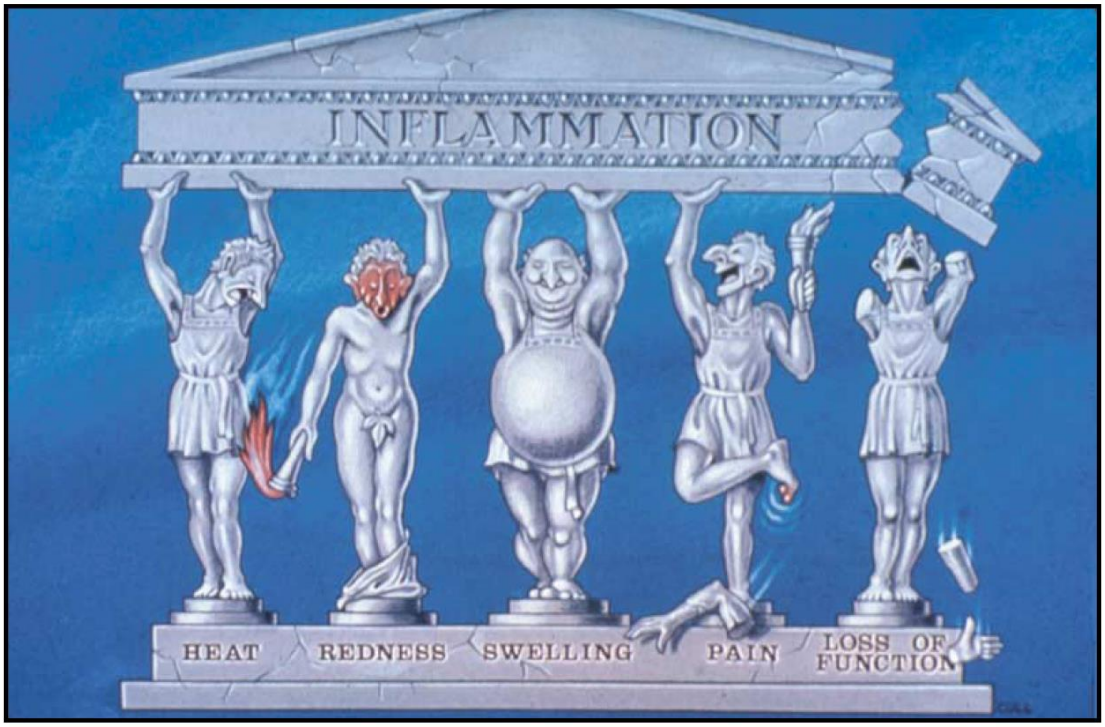

Figure 1-1: ***Inflammation: Five cardinal signs.***

Source: Lawrence et al., Anti-inflammatory lipid mediators and insights into the resolution of inflammation. Nat. Rev. Immunol. 2, 787–795 (2002)

mediators. These mediators may be originated either from pathogenic microbes, from the molecules released by the damaged cells in case of tissue injury, or from some plasma enzymes or from the product of leukocytes (WBCs).

Vascular endothelial cell line serves as a guard for regulating the migration of molecules and leukocytes into the tissue. The movement of these molecules and leukocytes at the site of tissue injury through endothelium lining is called **extravasation.** This process is based on the interaction between **cell adhesion molecules (CAMs)** present on endothelium cells and migrating cells. CAMs are divided into four families based on the differences in the structure and the pattern of glycosylation**: selectin family, integrin family, mucin-like family and immunoglobulin superfamily.** As the initiation of inflammatory response originates, many cytokines and inflammatory mediators act on local blood capillaries and induce the expression of CAMs on the endothelial membrane. This state of vascular endothelium is called **inflamed** or **activated.** Generally, neutrophils are among the first cell type that binds to inflamed endothelium and extravasates into tissue. Neutrophils first recognize the inflamed endothelium and then attach strongly to adhesion molecules. Lymphocytes circulate continuously from the vascular system (Cardiovascular system and lymphatic system) to various lymphoid organs. The circulation process of lymphocytes increases the possibility of activated lymphocytes to encounter antigen, presented by antigen presenting cells and thus determine the removal of pathogens or microorganisms either by inhibiting their growth or by killing them.

Acute phase proteins are serum originated chemical mediators of the inflammatory response whose concentration can either increase or decrease in the

serum during inflammation thus called as **positive acute phase proteins** and **negative acute phase proteins** [1,2]. C- reactive protein, Serum amyloid, mannose binding lectin, complement factors, ferritin, and coagulation factors are positive acute phase proteins while albumin, retinol binding protein, and transferrin are negative acute phase proteins [3]. The majority of bacterial and fungal cell walls are composed of C-polysaccharide, providing strength to their cell wall and thus offering protection. However, the C-reactive protein uses these polysaccharides for pathogen identification. C-reactive protein binds to C-polysaccharide [4] leading to complement system activation which results in complement-mediated phagocytosis or lysis of pathogens [5], and thus avoiding any damage or infection by the microbes. Another factor, blood-clotting factor in blood circulatory system arrests the pathogen or toxic agent, locally in blood clots and limit the infection from spreading [6].

Histamine is an important chemical mediator of inflammatory response released by the various cell during inflammation. It is a biological molecule that plays various vital roles in the body. Apart from functioning as a neurotransmitter and maintaining a role in the physiology of digestive track, it has a critical role associated with local immune responses [7]. It causes vasodilation and increases the permeability of capillaries after binding to its receptor and thus recruits leukocytes and macrophages at the site of infection. Next, a significant group of inflammatory mediators is small peptide-kinin which is generally present in an inactive form in the blood. This peptide gets activated after tissue damage. Like histamine, it also causes vasodilation and increases the permeability of blood capillaries. Bradykinin- a type of kinin also activates pain receptors present in the skin. Such inflammatory mediators recruit neutrophils and macrophages at inflammatory site and assist in pathogen killing or its removal.

1.1.2 Types of Inflammation

Inflammation can be classified into two different groups, acute inflammation and chronic inflammation, based on time of persistence and tissue damage.

Acute Inflammation (Either Localized or Systemic inflammation):

The acute inflammation may be either localized or systemic in nature. Tissue injuries of any kind can induce rapid and acute immune response. The immediate immune response is initiated by chemical mediators [8]. These mediators appear at the site of tissue injuries within few seconds and start action in the microenvironment. As a consequence, edema (fluid accumulation) development takes place along with hallmarks of inflammation as described above [9]. Extravasation of leukocytes further increases swelling and blood flow in that area which further generates heat, and at the same time fluid from bloodstream exudates, activates kinin, and fibrinogen-blood clotting system. The plasma enzyme mediators- fibrinopeptide and bradykinin directly initiate vascular modification that takes place during the early local response. The complement system, however, plays an indirect role in local vascular changes through its complement anaphylatoxins-C3a, C4a, and C5a [10–12]. These molecules also induce mast cell degranulation to release histamine- a potent inflammatory mediator that induces smooth muscle contraction and vasodilation.

The tissue neutrophils actively participate at the site of inflammation within a minute after tissue damage or any infection encountered, however, the blood neutrophils extravasate from blood vessels to the local site of inflammation after few

hours of the onset of initial inflammatory response. After recruitment at the local site of inflammation, neutrophils devour invading particles, pathogens and/or other foreign particles and release chemical mediators that further enhance the inflammatory response. Generally, chemotactic chemokine- **Macrophage Inflammatory Proteins** (MIP-1) are released by neutrophils, which attract macrophages at the site of inflammation [7]. After 5-6 hours of initiation of the inflammatory response, macrophages arrive at the site of inflammation. Like neutrophil, these activated macrophages also phagocytose the pathogen and secret 3 different types of cytokines- IL-1β, IL-6, and tumor necrosis factor-α (TNF-α) which further enhance the systemic and localized inflammatory responses. These cytokines work in paracrine fashion and increase expression of adhesion molecules on endothelial cells and increase permeability. As a result, extravasation of lymphocytes, neutrophils and monocytes take place, which are thus recruited, to the inflammation site. TNF-α and IL-1β act in an autocrine manner, induce macrophages and endothelial cells to produce chemokine that in turn increases neutrophil influx in tissue. On the other hand, TNF-α and INF-γ activate macrophage and neutrophils to enhance the phagocytic properties and release of the lytic enzymes in tissue at inflammation site [9].

Mechanism of acute inflammation is beautifully planned which regulates its amplitude and time period to control tissue damage and starts tissue repair process. The presence of leukocytes, neutrophils, macrophages, monocytes and other phagocytic cells enhance pathogen clearance and increase tissue repair. Unlike TNF-α and INF-γ, TGF-β plays an anti-inflammatory role and inhibits leukocytes recruitment by inhibiting extravasation through endothelial layer [13] thus limiting the pro-inflammatory process. TGF-β also assists in tissue repairing by increasing the deposition

of extracellular matrix at the damaged tissue thus helping in wound healing. Hence, the inflammatory response terminates with the removal of pathogen followed by resolution of inflammation and tissue repair [9].

Systemic inflammatory response (Also called **Acute-Phase Response**) is a consequence of local inflammatory response and results from its failure to control the release of cytokines and acute phase proteins. In another way, it can be defined as the effects of local inflammation on different organs. The characteristics systemic inflammation includes the production of acute phase proteins in liver, initiation of fever, increase in leukocytes production and synthesis of hormones. The Cytokines-IL-1, TNF-α, and IL-6 act on the hypothalamus and induce fever which decreases microbial growth and its pathogenic effects. TNF-α, on the other hand, activates macrophages and endothelial cells to secret colony stimulating factors such as GM-CSF, G-CSF, and M-CSF. These secreted CSFs activate hematopoiesis that leads to leukocytes production, which eliminates the infection. The serum components- C-reactive protein also assists the removal of pathogens and/or other foreign particles from the site of infection. It deposits opsonin C3b on pathogens and boosts its killing by phagocytic cells [10–12]. In worse circumstances, systemic inflammatory response leads to deleterious outcomes such as **systemic Inflammatory Response Syndrome** (SIRS) and **Multi Organ Dysfunction Syndrome** (MODS).

Chronic Inflammation:

Chronic inflammation occurs when acute inflammatory response fails to eliminate pathogen and infection persists. Activation and assembly of macrophages for a prolonged period of time is the hallmark of chronic inflammation. These activated macrophages activate proliferation of fibroblasts and production of collagen. As a result, excess fibrous connective tissue is formed that leads to **fibrosis** and the aggregates of leukocytes and lymphocytes lead to **granulomas**.`

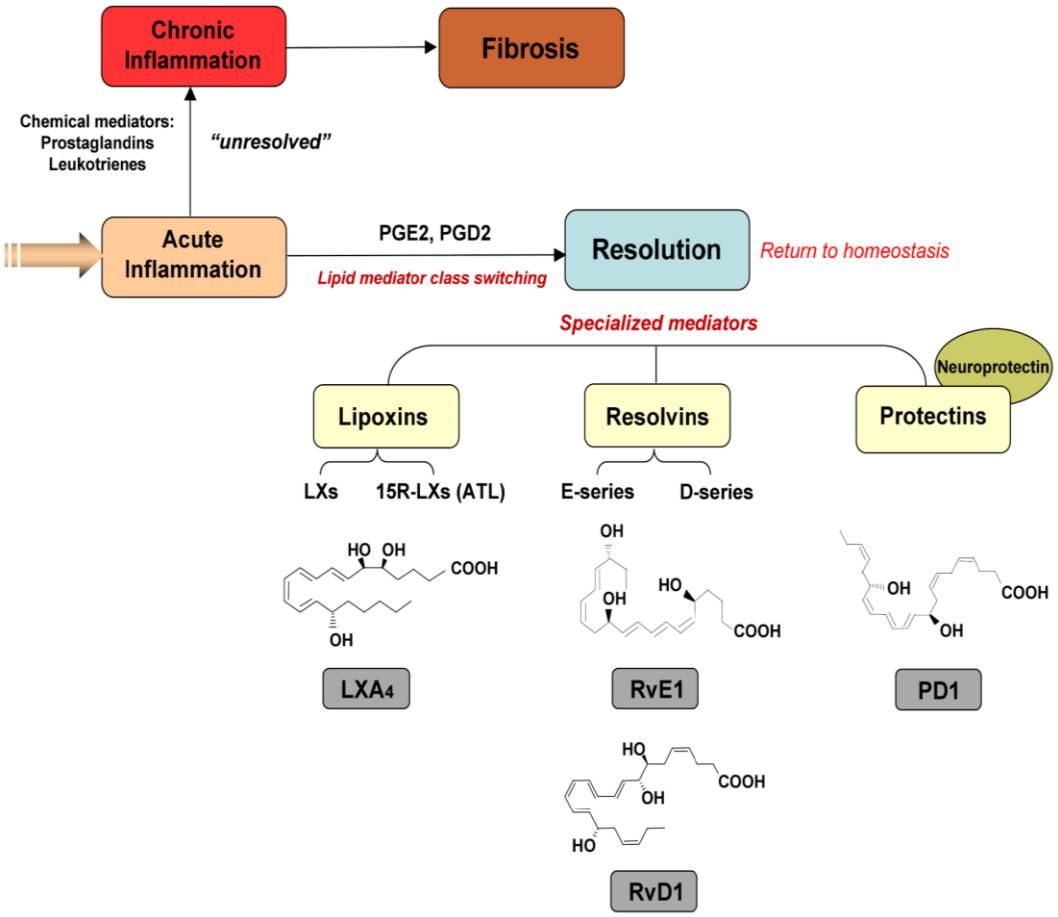

Figure 1-2 : ***Acute inflammation, Resolution of Inflammation and development of chronic inflammation***

Source: Serhan et al., Resolving inflammation: dual anti-inflammatory and pro-resolution lipid mediators. *Nat. Rev. Immunol*. **8,** 349–361 (2008).

Players of Chronic inflammation: INF-γ and TNF-α

INF-γ and TNF-α are two cytokines which play a vital role in chronic inflammation development. The activated macrophages secrete TNF-α while T_C cells, NK cells and T_H1 cells secret INF-γ. The virus-infected cells, on the other hand, secret interferons that protect the neighboring cells from the viral infections. [9]. However, the nature of interferons production depends on the type of a cell infected. The infected leukocytes produce INF-α, the fibroblast secret INF-β, while NK cells and T cells produce INF-γ. Among the interferons, INF-γ has a unique characteristic- the pleiotropic effects that make it different from others. One of the remarkable effects of INF-γ is its capacity to activate macrophages. Activated macrophages produce more cytokines and increase the expression of MHC II molecules on membranes. As a result, these activated macrophages efficiently function as APC (Antigen presenting cells) and exhibit increased cytokine production and increased pathogens killing activity (phagocytic property) in comparison to non-activated macrophages. Other than phagocytic property, these activated macrophages also produce many hydrolytic enzymes, ROS and RNS (Reactive Nitrogen species) that kill microorganisms. However, these hydrolytic enzymes are also responsible for tissue damage, even leading to autoimmune disorders [14], in case the activation of macrophages persists for longer time period.

1.1.3 Inflammation meets cancer (7th hallmark of cancer)

The relation of inflammation with cancer was established long back in the 19th century. Based on multiple pieces of evidence from epidemiological and molecular studies; the general concept is that cancer and inflammation are interlinked. There are many points of control in chronic inflammation that increase the possibility of cancer development [14–16].

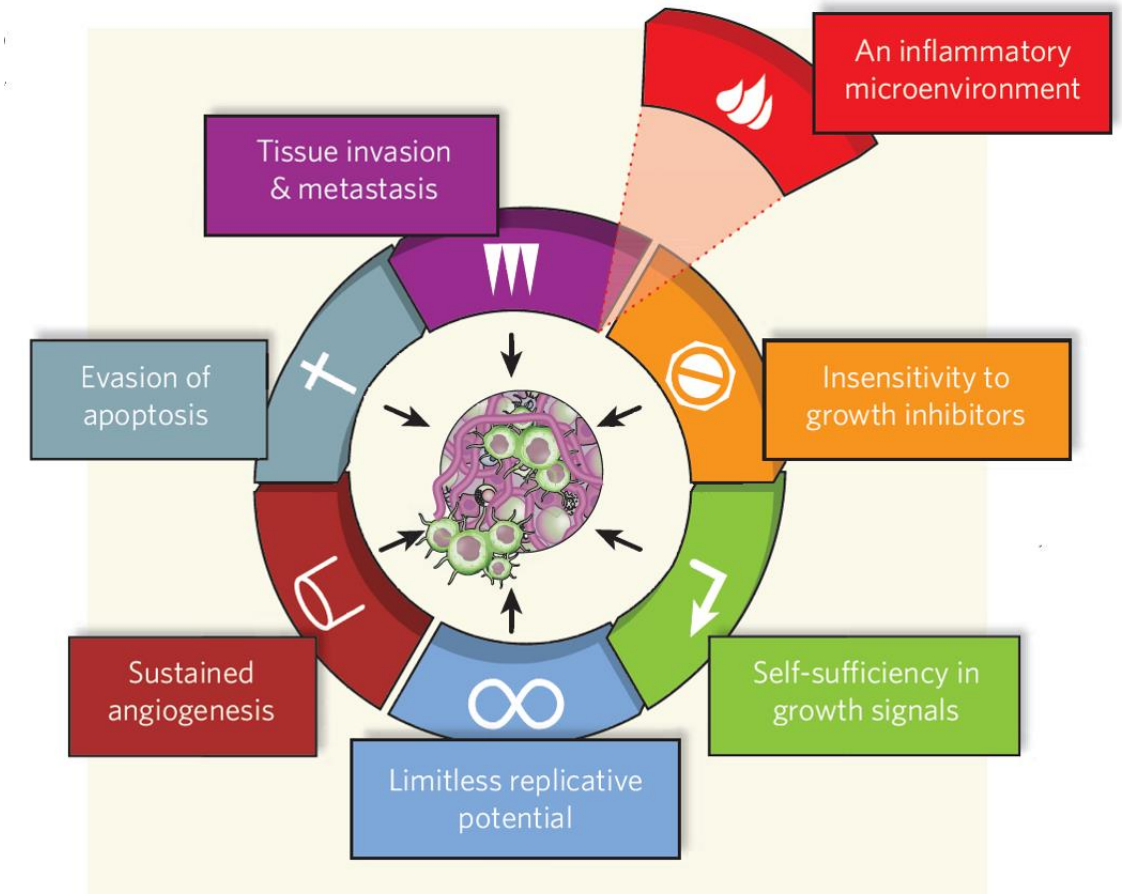

Figure 1-3: ***Inflammation: 7th Hallmark of Cancer***

Source: Mantovani A. Cancer: Inflaming metastasis. *Nature* **457,** 36–37 (2009)

Connecting Links between Inflammation and Cancer:

Inflammation and cancer share some common intermediates. Basically, two pathways correlate the functional relation of inflammation with cancer. These are- extrinsic and intrinsic pathways [17,18]. In intrinsic pathways, genetic mutation or modification that originate neoplasia development also initiate the program related to inflammatory response and build microenvironment of inflammation [19]. Different oncogenes such as ras, and tyrosine kinase coordinate with pro-inflammatory switches such as an angiogenic switch to guide the development of inflammatory microenvironment. In extrinsic pathways, inflammatory response promotes cancer progression. The significant mediators of extrinsic and intrinsic pathways include transcription factors such as NF-κB and STAT3, cytokines such as IL-1β, IL-6, TNF-α and IL-23, and chemokines. NF-κB is a key molecule of inflammation and adaptive immunity thus important for both inflammation and cancer progression [20,21].

1.1.4 Inflammation: Anti-Tumor activity !!!

In some tumor environments, the presence of inflammatory cells exhibit more prognosis and reveal the facts that inflammatory cells such as macrophages kill cancer cells [15,21,22]. Recently, studies indicated that NF-κB is associated with balancing between the pro-tumor and anti-tumor activity of macrophages [23]. The exact mechanism, which triggers anti-cancer property of immune response, is not clear. In future, it will be interesting to find out the external stimuli to convert tumor-promoting environment (M2 macrophages and TH2) into the tumor-killing environment (M1 macrophages and TH1 cells).

1.2 INFLAMMASOME

1.2.1 Introduction

Germline encodes sensor to monitor signal of infection or tissue damage in extracellular and intracellular compartments. Inflammasome - multimeric protein complex is a key molecule associated with cytosolic surveillance. It is also called cytoplasmic equivalent to TLRs. This complex can be classified into two major families- **Nod-Like receptor family** (NLR family) and **PYHIN family** (Pyrin and HIN 2000). The human genome encodes 23 NLRs while mouse genome encodes 34 NLRs [24]. NLRs are composed of three domains: **a) Effector domain** (N-terminal domain) consists of either PYD, CARD (caspase recruitment domain) or BIR (Baculovirus inhibitor of apoptosis

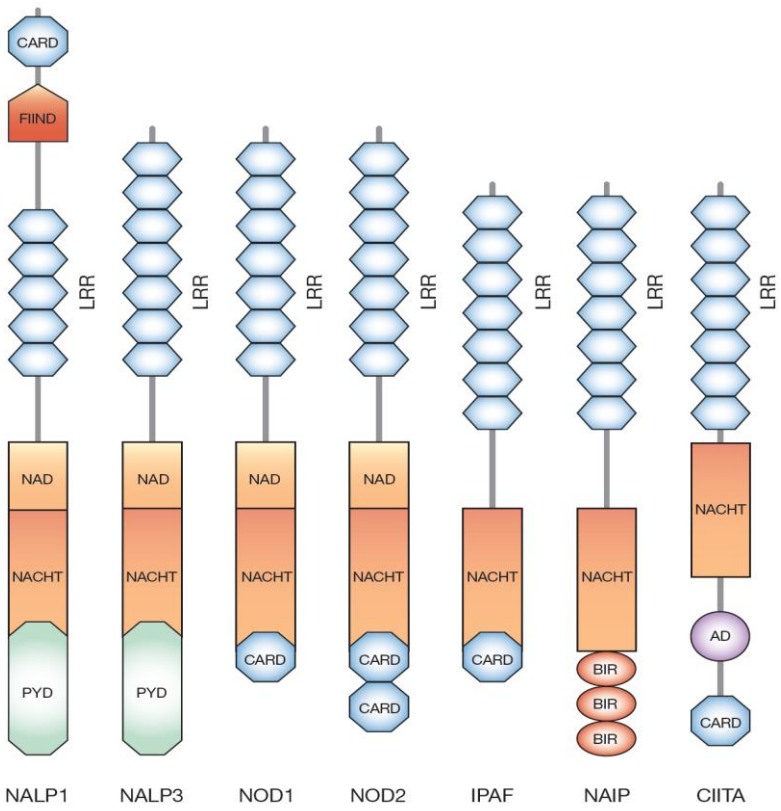

Figure 1-4: ***Different types of inflammasomes***

Source: Church et al., Primer: inflammasomes and interleukin 1β in inflammatory disorders. *Nat. Clin. Pract. Rheumatol.* **4,** 34–42 (2008)

protein repeat), **b). Nucleotide binding domain** (NBD; NAD, NOD; or NATCH), **C). LLR domain** (Leucine-rich repeats-C terminal domain) [24].

NLRPs are the largest family having PYD proteins. 14 NLRP genes are present in the human genome. Among these; NLRP1, NLRP3, IPAF (NLRC4), NLRP6 and NLRP12 form inflammasome complexes. NLRPs consists of PYD domain, NACHT domain and variable LRRs (22-28 Leucine residue repeats) (Figure1-4) [25]. Activated Inflammasome complex processes pro-caspase-1 (Inactive form) into caspase-1 (Active form). Then Caspase-1 initiates processing of Pro-IL-1β and Pro-IL 18 into their mature forms IL-1β and IL 18, respectively [26]. These pro-inflammatory cytokines initiate the complex cascade of cytokines that have been implicated in inflammation, pain and even auto-immune disorders [27] .

1.2.2 Inflammasome complex formation

The initiation of oligomerization of NLRs takes place through intermediate NACHT domain [**NA**IP (neuronal apoptosis inhibitory protein), **C**IITA (class II MHC transcription activator), **H**ET-E (incompatibility locus protein) and **T**P1 (telomerase-associated protein)] while CARD domain of NLRs interacts with pro-caspase-1 that leads to its recruitment in the complex. Those NLRs in which CARD domain is lacking but containing PYDs domain, ASC adaptor (PYD domain + CARD domain) protein is required for interactions [28]. The PYD domain of ASC adaptor protein interacts with PYD domain of NLRs while CARD domain of ASC adaptor protein recruits pro-caspase-1 into inflammasome complex [28]. The activation of Inflammasome takes place by its oligomerization into big disc shape structure while ASC adaptor protein functions as a platform for protein-protein interactions.

Multimerization of proteins in Inflammasome complex initiates autoproteolytic cleavage of recruited pro-caspase-1. Pro-caspase-1 is fragmented into a large p35 fragment (CARD+caspase1) and a small p10 fragment. p35 fragment subsequently fragmented into p20 subunit and CARD [24]. An active caspase-1 enzyme consists of two p10s and two p20s subunits (Figure1-5).

Caspase-1 is cysteine protease specific to aspartate and cleaves IL-1β and IL-18 at specific recognition site next to aspartic acid residues [29]. Inflammasome containing ASC adaptor induces autoproteolysis of pro-caspase-1 that promotes maturation of pro-inflammatory cytokines while ASC-independent caspase-1 multimeric complex initiates **pyroptosis-** a caspase-1 dependent programmed cell death [24] [28].

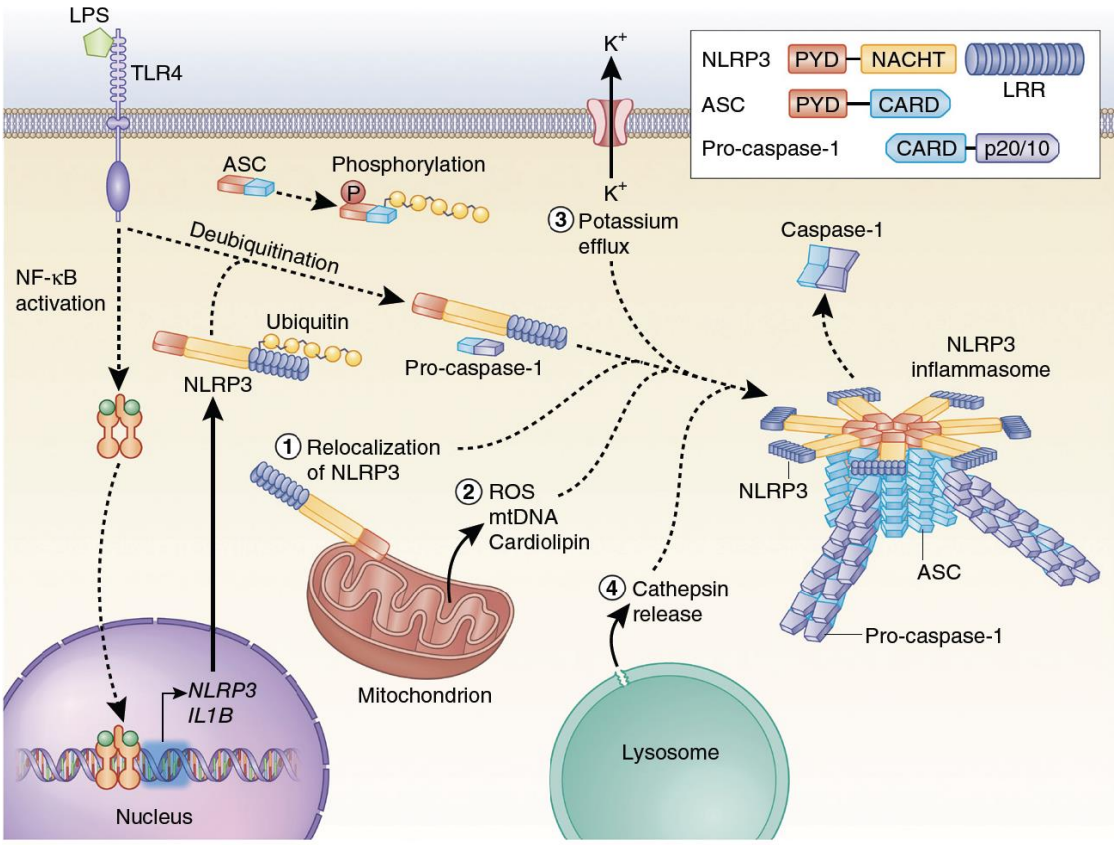

Figure 1-5: ***Assembly and activation of NALP3 inflammasome***

Source: Guo et al., Inflammasomes: mechanism of action, role in disease, and therapeutics. *Nat. Med.* **21,** 677–87 (2015)

1.2.3 NLRP3 Inflammasome

The NLRP3 inflammasome (**N**OD, **LR**R, and **p**yrin-containing domain-**3)** is the best-studied member of NLRs family and activated by various types of stimuli such as pathogenic, environmental, endogenous or viral [24]. The pathogenic stimuli originated from the pathogens such as influenza A virus [30], *N. gonorrhoeae* [31], *L. monocytogenes* [32], *C. albicans* [33] *S. aureus* [34], *and K. pneumoniae* [35] trigger NLRP3 inflammasome. In addition, the endogenous signals that release during tissue damage such as hyaluronan, extracellular ATP, uric acid crystals also activate NLRP3 inflammasome complex [36] (Figure 1-6, 1-7).

Despite the identification of several NLRP3 activators and immunostimulatory properties of several molecules, the exact mechanism of NLRP3 activation is not much clear. However, the activation of NLRP3 is proposed by three different phenomena such

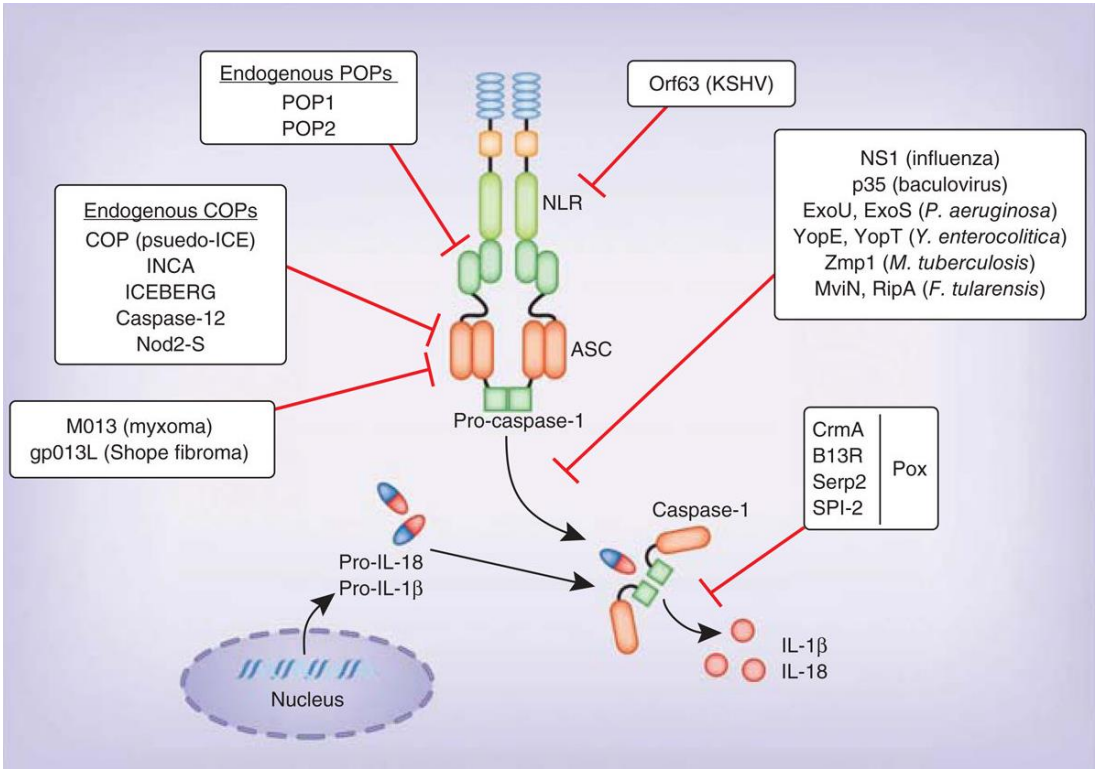

Figure 1-6: ***Regulation of inflammasome***

Source: Rathinam *et al*., Regulation of inflammasome signaling. Nat. Immunol. **13,** 332–333 (2012)

as ROS generation from mitochondria, potassium efflux, and phagolysosomal destabilization. The importance of NLRP3 can be determined by the fact that mutation [37] in nalp3 gene gives rise to auto-inflammatory disorder and other several deformities [38–41].

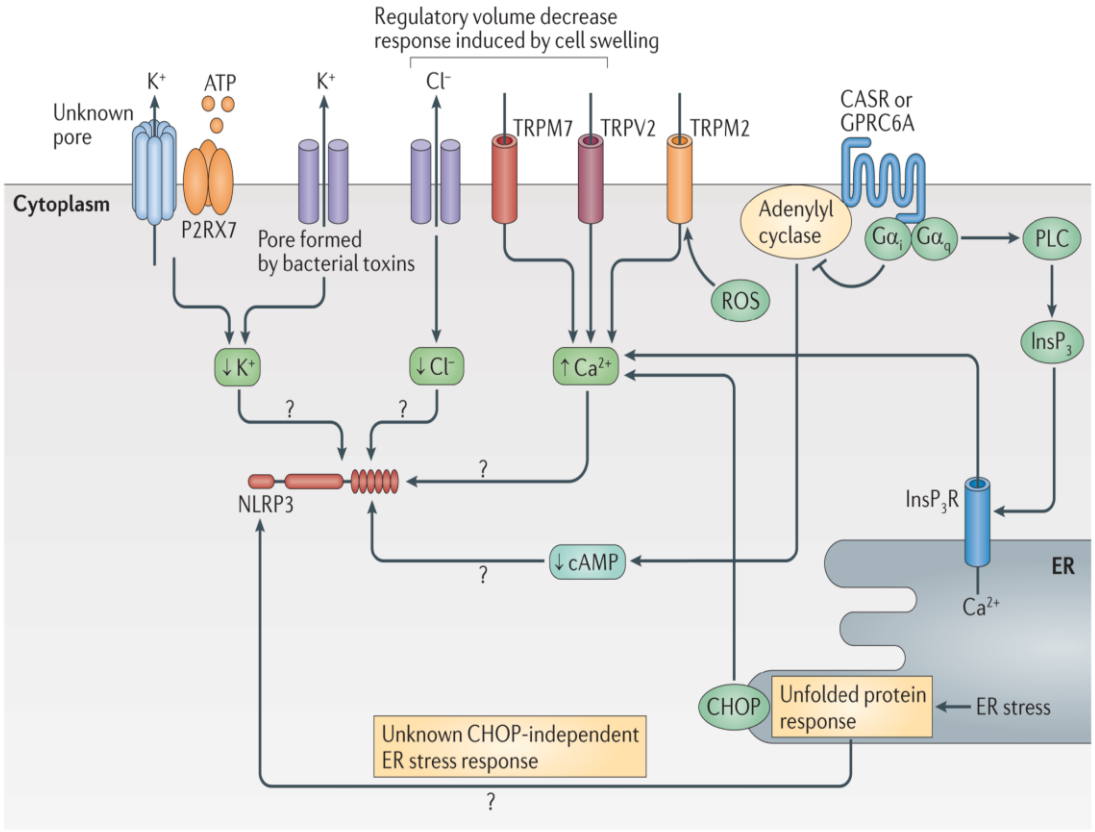

Figure 1-7: ***Regulation of inflammasome by Cell stress and ion flux***

Source: Latz et al., Activation and regulation of the inflammasomes. *Nat. Rev. Immunol.* **13,** 397–411 (2013)

1.3 POLYUNSATURATED FATTY ACIDS

1.3.1 Introduction

Polyunsaturated fatty acids (PUFAs) are made up of long-chain carbon in which a methylene group separates multiple double bonds having cis-configuration. Based on the position of the double bond in carbon backbone, two major families of PUFAs, omega-6 (ω-6) and omega-3 (ω-3), have been characterized. Oleic acid (18:1Δ9) is a precursor for most of the plants PUFAs [42]. In the plants, Δ12 desaturase introduces a double bond in Oleic acid at 12th position to form Linoleic acid (LA, 18:2 Δ9, 12, ω-6). Further desaturation of LA on 15th position catalyzed by Δ15 desaturase forms α-Linolenic acid (ALA, 18:3 Δ9, 12, 15, ω-3). In animals, LA and ALA are required for the growth, reproduction, and other metabolic processes, however; animals lack the synthesis of these fatty acids. Therefore, LA and ALA are essential fatty acids and are made available to animals only through dietary sources. These essential fatty acids give rise to two series of PUFAs, omega-ω-6 series and ω-3 series. LA catalyzed by Δ6 desaturase, elongase, and Δ5 desaturase give rise to Arachidonic acid (AA, 20:4 Δ5, 8, 11, 14). On the other hand, when these enzymes catalyze ALA then give raise to Eicosapentaenoic acid (EPA, 20:5 Δ5, 8, 11, 14, 17). Further, elongase and Δ4 desaturase catalyze EPA and generate Docosahexaenoic acid (DHA, 20:5 Δ4, 7, 10, 13, 16, 19) (Figure 1-8) [43]. As with other complications, age, diabetes and food habit affect the enzymatic activities of these enzymes and thus alter the proportion of PUFAs in the body.

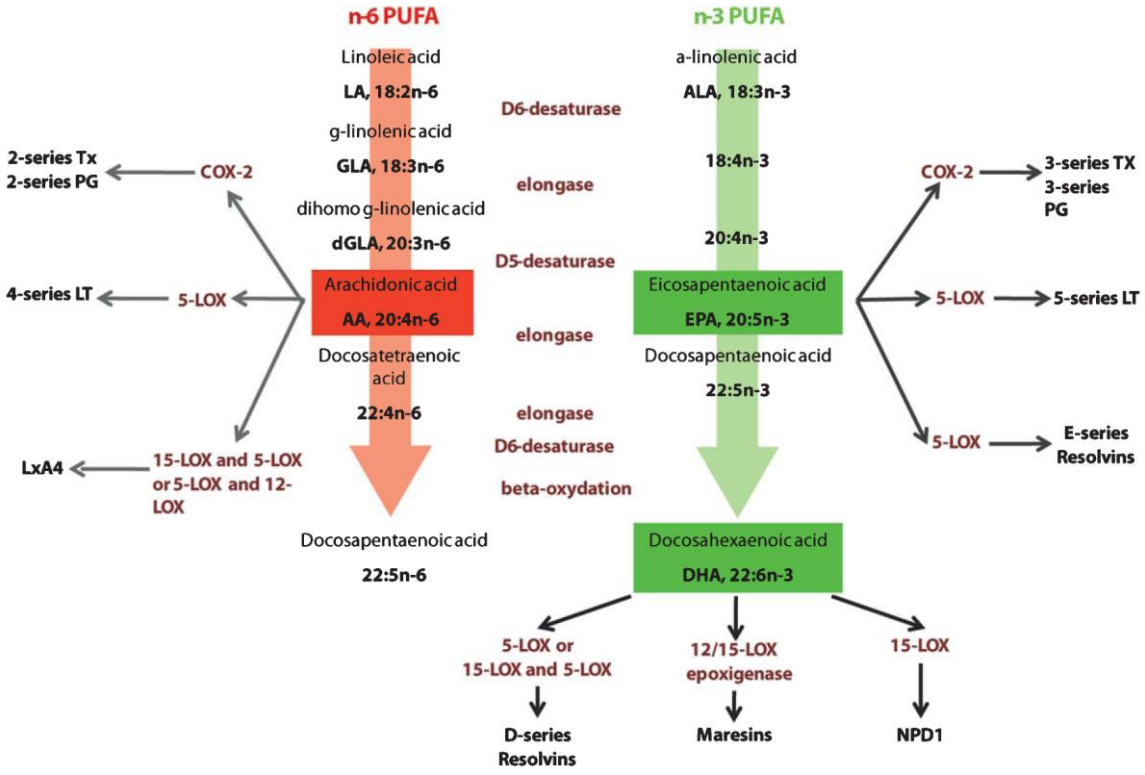

Figure 1-8: ***The conversion of ω-3 PUFAs and ω-6 PUFAs into longer chain unsaturated derivatives***

Source: Layé *et al.,* N-3 polyunsaturated fatty acid and neuroinflammation in aging and Alzheimer's disease. *Nutr. Aging* **3,** 33–47 (2015)

1.3.2 Role of ω-6 and ω-3 PUFAs in inflammation

Inflammation, in general, is the host's response of its immune system and is associated with the prognosis of various autoimmune disorders, arthritis, and cancer. However, the manifestation of inflammation is mediated through various chemical mediators including lipid molecules. Lipid mediators are among the biomolecules that are generated by LOXs and COXs pathways, whose nature depends on the types of PUFAs utilized as the substrate. The eicosanoids generated from AA include prostaglandins (PGs), leukotrienes (LTs), and Thromboxane (Tx). PLA2 releases free fatty acids (AA) from membrane phospholipids, which is acted upon by COX-2 and generates series-2 PGs and thromboxanes such as PGE2 and TXA2 while 5-LOX uses AA

as a substrate for generation of 4-series leukotrienes LTA4, LTB4, LTC4, LTD4 and LTE4 and hydroperoxyeicosatetraenoic acids (HPETEs) and hydroxyeicosatetraenoic acids (HETEs). When ω-3 PUFAs such as EPA and DHA are available, then LOXs and COXs use these fatty acids and generate series-3 TXs and PGs; and series-5 LTs.

Now it is well established that there is a correlation between the increased ratio of ω-6 to ω-3 PUFAs and emergence of various metabolic disorders as well as life-threatening complications such as autoimmune disorders and cancer [44]. Several other findings also supported such type of relation in which the decrease in ω-6 PUFAs intake and/or increase ω-3 PUFAs intake (decrease ω-6 to ω-3 PUFAs ratio) reduces the severity of these diseases [45]. Based on several studies, the information suggests that during the ancient times the ratio of ω-6 to ω-3 PUFAs in the diet was 1/1 [44]. However, during the course of evolution the proportion of ω-3 PUFAs decreased drastically, a typical western diet contains 20% of ω-6 PUFA (AA) [46,47] while the proportion of ω-3 PUFA (ALA) is less than 1% [44,48,49] having average ratio of 15/1 to 16.7/1 (ω-6 to ω-3 PUFAs ratio) [44]. Observations based on several reports show that excessive high ratio of ω-6 to ω-3 PUFAs as present in western food habit, stimulate prognosis of numerous disorders and diseases such as cancer, cardiovascular diseases, autoimmune disorders, and inflammation [44]. However, a decreased ratio of 4/1 significantly reduced 70% mortality in cardiovascular disease while a 2.5/1 ratio was linked with a decrease in colorectal cancer [44]. Moreover, the ratio of 5/1 revealed beneficial effects on Asthma patients [44]. In converse to this , the ratio of 10/1 showed adverse consequences [44]. In another experiment, *C. elegans* fat 1, a gene which

converts ω-6 into ω-3 PUFAs has lowered the ratio of ω-6 to ω-3 PUFAs in treated mice and has shown a protective effect against pathological angiogenesis in the retina [50].

These studies demonstrate the role of ω-6 and ω-3 PUFAs and the importance of their ratio in the manifestation of various inflammatory disorders. In general, the ω-6 PUFAs are pro-inflammatory in nature while ω-3 PUFAs are anti-inflammatory (Figure 1-9).

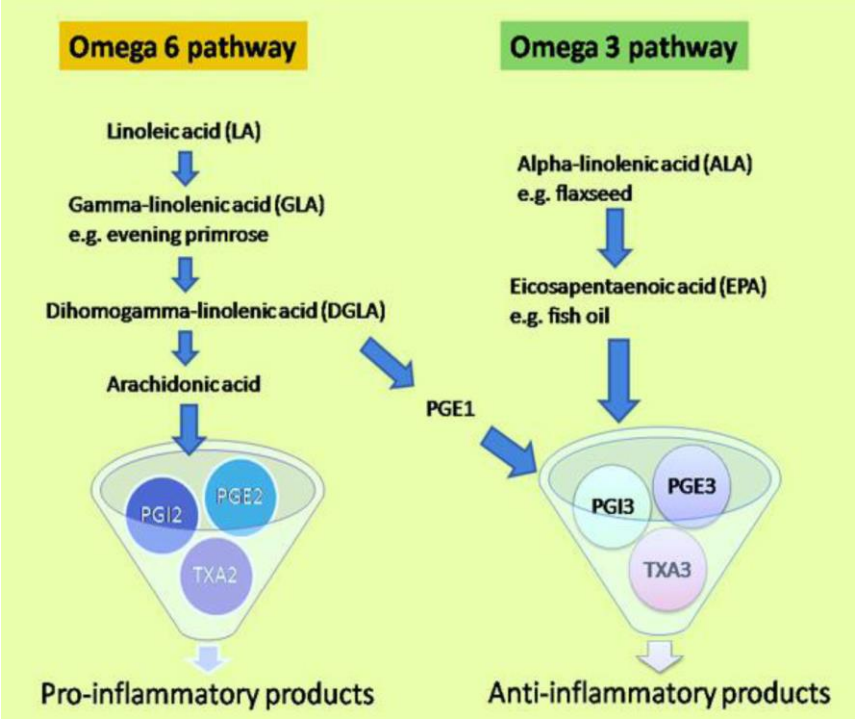

Figure 1-9 : ***Role of ω-6 and ω-3 PUFAs in Inflammation***

The increase in the proportion of ω-3 PUFAs in cell membrane leads to a decrease of pro-inflammatory mediator generated by ω-6 fatty acids in several ways. The first one is a generation of differential metabolites of COX-2 and 5-LOX that depends on the type of substrate available. In ω-6 PUFAs rich diet, AA is dominant substrate among PUFAs available for eicosanoids synthesis that gives rise to the most effective pro-inflammatory mediators. On the other hand, intake of ω-3 PUFAs replaces

AA in the plasma membrane and thus decreases the availability of AA for eicosanoid biosynthesis. The lipid mediators generated by ω-3 PUFAs are less potent for inducing inflammation than the lipid mediators generated by AA [51]. One of the best examples is LTB4- ω-6 PUFA based metabolite and LTB5-ω-3 PUFA based metabolite, both generated by 5-LOX. Both metabolites are chemoattractant to neutrophils at the inflammatory site; however, LTB5 attracts neutrophils with 10 times less efficiency than LTB4. Next is antagonistic nature of ω-3 PUFAs based lipid mediators. In this scenario, apart from the generation of differential metabolites, the metabolites of ω-3 PUFAs bind to same receptors and thus act as antagonists for AA based lipid mediators. Moreover, COX-2 and 5-LOX generate E-series resolvins by using EPA as a substrate, which act as anti-inflammatory molecules. Therefore, the ratio of ω-3 fatty acids to ω-6 in the body is very important and sufficiently high ratio in the diet decreases the production of several pro-inflammatory mediators and supports resolution phase of inflammation thereby helping the body to maintain homeostasis (Figure 1-10).

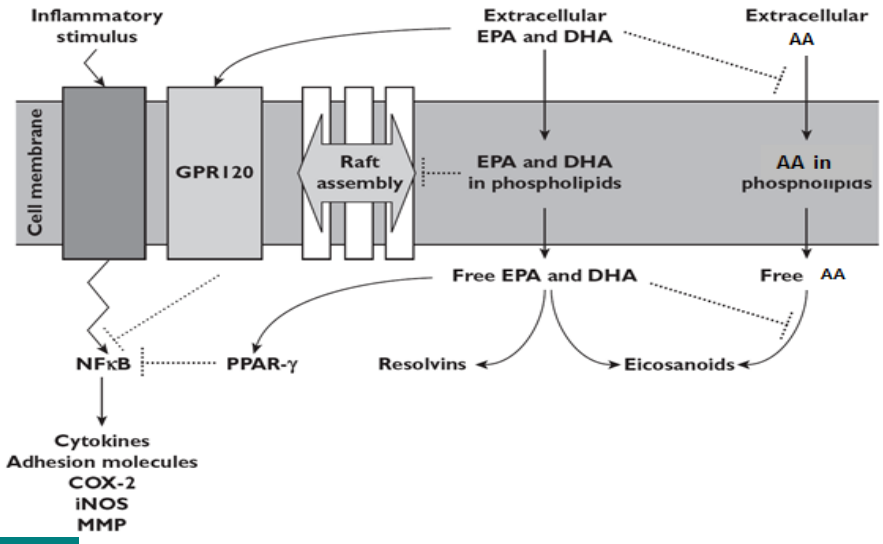

Figure 1-10: ***Summary of the anti-inflammatory actions of marine n-3 polyunsaturated fatty acids.***

Source: Calder et al., Omega-3 polyunsaturated fatty acids and inflammatory processes: Nutrition or pharmacology? Br. J. Clin. Pharmacol. **75,** n/a-n/a (2012)

1.4 EICOSANOIDS

1.4.1 Introduction

Eicosanoids term is generally used for 20 carbon fatty acids and their metabolites, which are very short-lived but active lipid mediators. These metabolites act mostly in a paracrine manner. In the early 1930s, kurzrok and Lieb reported that human uterus either strongly contracted or relaxed in the presence of human seminal fluid. Von Euler and Goldblatt independently found out that lipid fraction of ram seminal vesicular gland contained this activity. This active fatty acid fraction was named as **"prostaglandin"** which later opened a sea of signaling molecules associated with countless significant signaling pathways. PGE1 and $PGF_{1\alpha}$ are first two prostaglandins isolated in the form of the crystal structure. The nomenclature is based on the backbone of 20 C acid in which C_8 and C_{12} form a 5 C member ring also called **prostanoic acid**. E-series and F-series prostaglandins have keto and hydroxyl group, respectively, at C_9 position, while 1, 2 and 3 represent a number of double bonds present and α represent stereochemistry of hydroxyl group.

1.4.2 Types of Eicosanoids

Although prostaglandins were discovered first but now it is known that essential fatty acids are precursors for generation of eicosanoids. Eicosanoids include prostaglandins, prostacyclins, thromboxanes, leukotrienes and other oxygenated metabolites produced mainly through three enzymes: Cyclooxygenases (COX), Lipoxygenases (LOX) and Cyt 450 (epoxygenase). ω-6 (dihomo-γ- linolenic acid and AA)

and ω-3 PUFAs (EPA and DHA) are the precursors for eicosanoids biosynthesis. The non-enzymatic free radical peroxidation of PUFAs leads to the generation of prostaglandin-like molecules called **isoprostanes**. In plants, jasmonates generated from ALA are analogous to eicosanoids generated from AA.

Biosynthesis of eicosanoids starts as soon as the free fatty acids (FFA) are available in the cytoplasm. PLA2 releases FFA from cell membrane phospholipids in response to various physiological factors such as hormones, cytokines or tissue injuries. Cyclooxygenase pathways produce **prostanoids** (prostacyclins, thromboxanes, and prostaglandins) while lipoxygenase pathways produce leukotrienes, lipoxins, and hydroperoxyeicoastetraenoic acids (HPETEs) [52].

1.4.3 Cyclooxygenases (COX)

Cyclooxygenases (EC 1.14.99.1) are enzymes that oxygenate free PUFAs available in cytoplasm into prostanoids. They are also called as prostaglandin endoperoxide H synthases. COX includes two different forms-cyclooxygenase-1 (COX-1) which are generally constitutive and cyclooxygenase-2 (COX-2), an inducible form of COX. Both, COX-1 and COX-2 are very similar in structure and share 60% homology but are coded by two different genes.

1.5 LIPOXYGENASES

1.5.1 Introduction

Lipoxygenases (EC 1. 13. 11. 12); are members of a class of dioxygenases (non-heme iron-containing) which catalyze the addition of molecular oxygen to fatty acids containing at least one cis, cis-1, 4-pentadiene system and give rise to unsaturated fatty acid hydroperoxides. The mechanism of dioxygenation of fatty acids catalyzed by LOXs involves three main steps (Figure 1-11). First, abstraction of a hydrogen atom from the double allylic methylene carbon atom (the first and rate-limiting step). Second, conjugation of double bonds followed by rearrangement of the radical electron, and third, addition of molecular oxygen (this occurs at a diffusion-controlled rate under ambient O_2 concentrations) [53].

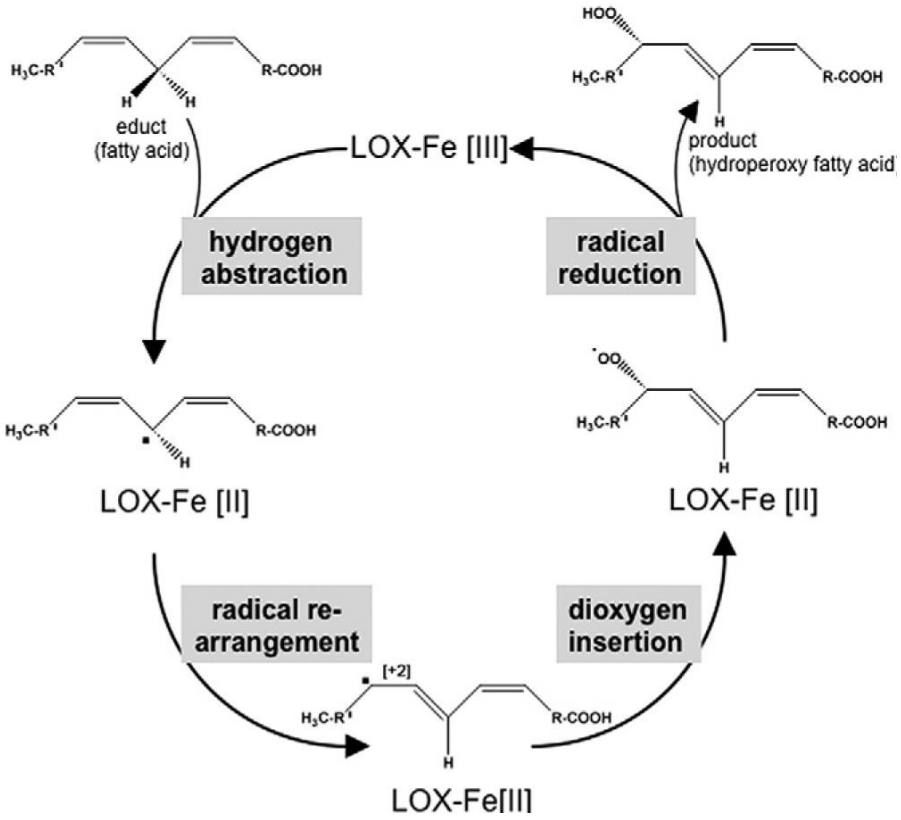

Figure 1-11: ***Mechanism of Lipoxygenase reaction***

Source: Ivanov *et al.,* Molecular enzymology of lipoxygenases. *Arch. Biochem. Biophys.* **503,** 161–174 (2010)

Structure

The three-dimensional structure of soybean LOX-1 has been determined. It is a single polypeptide chain enzyme having two domains (Figure 1-12). The N-terminal domain contains 146 amino acid residues having β-barrel and called domain I while C-terminal domain contains 693 amino acid residues having a helix and called domain II [54]. The active site is present in the center of domain II and contains iron which is connected with 4 conserved Histidines and one Isoleucine [54]. Molecular oxygen and substrates reached to active site through two different cavities: cavity I and cavity II. Molecular oxygen reaches at the active site through cavity I while substrate such as AA

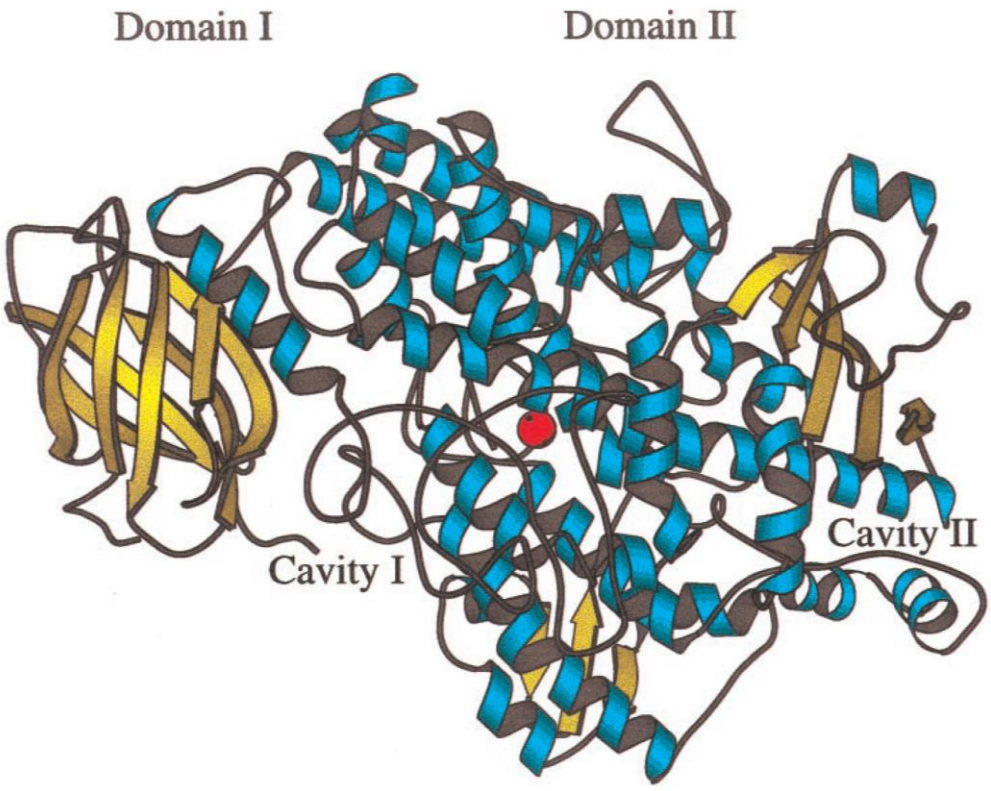

Figure 1-12: ***3D structure of Glycine max (Soybean) lipoxygenases***

Source: Ivanov *et al.,* Molecular enzymology of lipoxygenases. *Arch. Biochem. Biophys.* **503,** 161–174 (2010)

and other larger fatty acids reach through cavity II (Figure 1-13) [53]. Mammalian LOXs are lesser smaller in molecular mass (75-80 kDa) in comparison to plant LOXs (94-104 kDa) because it lacks domain I (N-terminal domain) as present in LOX-1 and other related plants LOXs [54]. The crystal structure of several mammal and plant LOXs available now, along with X-ray data of human 12-LOX. Most of the LOXs composed of single polypeptide chain like soybean LOX-1. However, LOXs in lower organisms may present in the form of fusion proteins where LOX domain attached to a different catalytic domain [53,55].

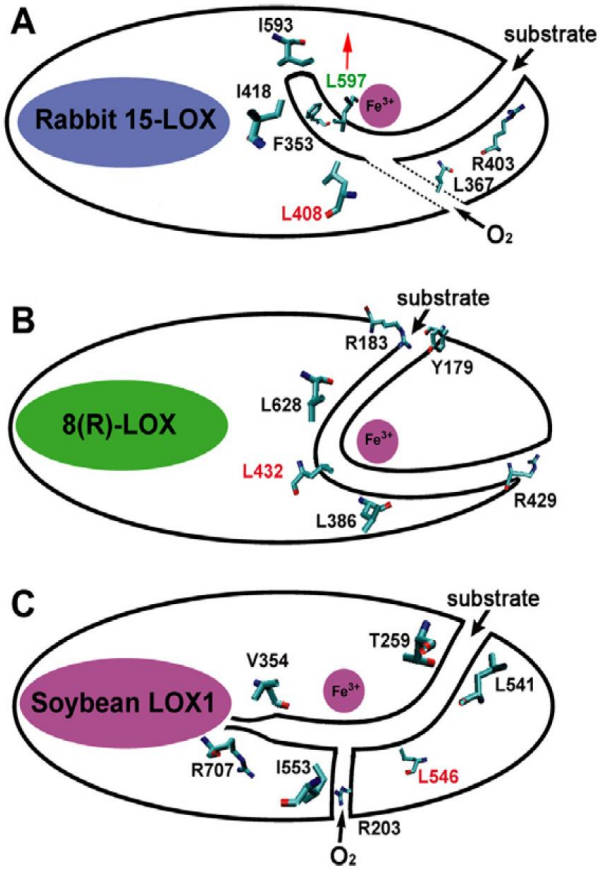

Figure 1-13: ***Substrate binding site in lipoxygenases***

Source: Ivanov, I. *et al.* Molecular enzymology of lipoxygenases. *Arch. Biochem. Biophys.* **503,** 161–174 (2010)

1.5.2 Distribution and Classification of LOXs

LOXs are broadly distributed in mammals [56,57], aquatic organisms [58] and plant [59,60]. Recently, various prokaryotes also reported to have different LOXs isoforms [61–63]. LOXs sequences are found in eukaryotes and prokaryotes while not reported in archaea. In conventional nomenclature, animal LOXs are classified into five different types. These are 5-LOX, 8-LOX, 11-LOX, 12-LOX and 15-LOX [53]. Although in 1947, Theorell *et al*, [64] crystallized the lipoxygenase the progress was limited until 1974 when Axelrod and coworkers first separated and purified different isoforms of lipoxygenase from soybean (*Glycin max*) and further confirmed in 1988 that soybean cotyledons contain three isozymes (LOX-1, 2 and 3) [65,66]. All these are water soluble having 5.68, 6.25 and 6.15 isoelectric values, respectively. All LOXs contain one atom of non-heme iron/protein molecule. LOX-1, 2 and 3 are composed of 838, 865 and 859 amino acids having a molecular weight of 94, 97 and 96 kDa, respectively [67,68]. It also shows different pH optima, LOX-1 has optimum activity at pH 9.0 while LOX-2 and LOX-3 have around pH 6.5 and pH 7.0, respectively [69].

LOXs regiospecificity changed by surrounding pH and oxygen concentration. Soybean LOX-1 (15-LOX) catalyzes linoleate into 9-(S)-HPODE (25%) and 13-(S)-HPODE (75%) at pH 6.0 while at pH 9.0 it oxidizes linoleate exclusively into 13-(S)-HPODE[70]. 9-(S)-HPODE is formed from linoleic acid (non-dissociated carboxylic acid form) because substrate in this form can enter the active site of LOX in any orientation, however, carboxylate ion (linoleate) can be recognized only from $-CH_3$ end [70]. In normal condition, soybean LOX-1 oxidizes linoleate into 95% 13-(S)-HPODE. However, it loses its regiospecificity in low oxygen concentration and oxidizes linoleate into an equal

amount of 9-and 13-(S)-HPODE [71]. LOX-2 and LOX-3 oxidize linoleate into an equal amount of 9-(S)-HPODE and 13-(S)-HPODE product [69].

1.5.3 Role of Lipoxygenases in Plants and animals

LOXs are broadly expressed in animal and plant systems and initiate the production of signaling molecules. LOX pathways in plants and animals differ because of availability of substrate. In plants, linoleate and α-linolenate are the most abundant substrates while lacking arachidonic acid and eicosapentaenoic acid. However, in animals, the main fatty acids available as substrates are arachidonic acid and eicosapentaenoic acid [72]. Generally, LOXs prefer free PUFAs as substrates. However, some LOXs also act on esterified fatty acids *in vivo* suggesting a direct role of membrane lipids in the synthesis of oxylipins [73–75]. In the plant, the LOXs hydroperoxy metabolites of LA and ALA can be further metabolized by at least six different enzymes into different compounds (Figure 1-14).

Plant LOXs are generally present in seeds [69], have various functions such as lipid mobilization [73] and storage of proteins in vegetative plants [76]. It also plays vital

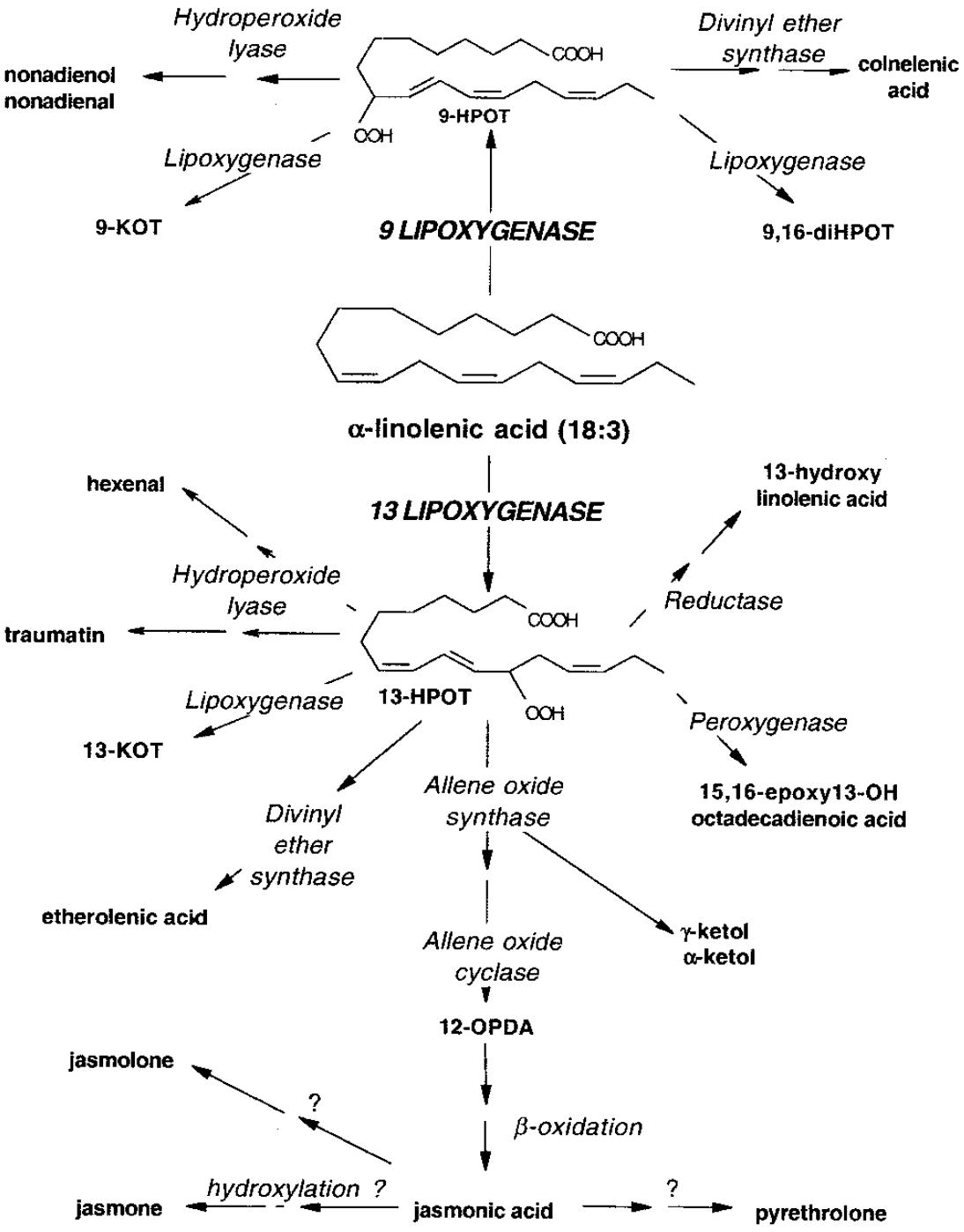

Figure 1-14: ***The dioxygenation of ALA by lipoxygenases in Plants***

Source: Porta, H. Plant Lipoxygenases. Physiological and Molecular Features. *Plant Physiol.* **130,** 15–21 (2002)

roles during several developmental processes [69]. The expression of LOXs genes are associated with various biotic and abiotic factors such as pathogen attack [77], abscisic acid [77], jasmonates [78], deficiency of water [79], wound [79], drought, temperature [76].

In vegetative plants such as potato, LOXs are associated with tuber growth and development, most likely by oxylipin synthesis[80]. In legume plants, the presence of LOX mRNA and proteins is associated with the development of nodule[79].The presence of LOX activity and its regulation by ethylene during fruit ripening also advocates LOX defense role. The C_6 aldehydes of LOX metabolites also give aroma and flavor to tomato plants [81]. Plant tissues also synthesize **vegetative storage protein (VSP)**- a LOX family protein. There are three VSPs- VSPa (VSP27), VSPb (VSP29) and VSP94 in soybean, which stores amino acids and provides nitrogen and other nutrients if needed [82,83]. Lipoxins provide a defense to the plants from the wound as well as from herbivores [84]. Several studies reported induced expression of LOXs during wounding and herbivore attack in several plants including potatoes [78,85]. **Jasmonic acid (JA)** and **phytodienic acid** levels increase during wounding and herbivores attack where they function as signaling molecules [78,86]. They stimulate the synthesis of molecules such as C 6 volatile alcohols and aldehydes that protect against herbivores attack. These volatile molecules attract natural predators of attacking herbivores [87].

SCOPE OF STUDY

Inflammation is a crucial part of the immune response of a host to an infection or injury in order to sustain cellular homeostasis. Abnormal or uncontrolled inflammation is associated with various disorders mediated by hyperactivation of inflammasome complexes and up-regulation of pro-inflammatory enzymes like iNOS, LOXs, and COXs [88–92]. The inflammatory response generated by eicosanoids is known to be mediated by pro-inflammatory cytokines such as IL-1β and tumor necrosis factor-α (TNF-α) [93].

A balanced diet is always known to be associated with proper maintenance of health. Imbalanced diet or nutritional deficiency, on the other hand, is associated with prognosis of various disorders and diseases [94]. Several studies also show that many of inflammatory disorders in the modern era are not caused by pathogens or injuries but due to altered lifestyles such as lack of physical activities, high calories food, and expose to toxic compounds in daily life [95]. Obesity, atherosclerosis, neurodegenerative diseases , type 2 diabetes, and asthma are the outcome of these conditions, wherein inflammation is a major component [95]. The impact of fatty acids on inflammation have been well established [96,97]. In several comparative studies, PUFAs have been shown to have several beneficial and protective properties [98] over saturated fatty acids when treated with pathogenic bacteria [98]. It is well established that the two types of PUFAs, ω-6, and ω-3 regulate homeostasis in body but have opposing effects [96,99]. The ω-6 PUFAs mediate the generation of eicosanoids family of lipid mediators such as prostaglandins, prostacyclin, and thromboxane maintain homeostasis. However, their uncontrolled production shifts the homeostasis towards pathogenesis. Dietary

intake of ω-3 PUFAs, on the other hand, increase the ratio of ALA, EPA, and DHA in the body [100,101], which leads to the generation of less potent pro-inflammatory mediators on one side and on the other side they compete with ω-6 mediated pro-inflammatory mediators for the same receptors [96,100]. Several of these studies demonstrated that beneficial effects of ω-3 PUFAs are mediated in part by their oxygenated metabolites mainly via the LOXs and COXs pathways. However, the downstream signaling pathways mediating these anti-inflammatory effects of ω-3 PUFAs have not been elucidated.

The present study, therefore, is aimed at understanding the signalling pathways involved in the mediation of anti-inflammatory effects of 13-(S)-hydroperoxy octadecatrienoic acid [13-(S)-HPOTrE] and 13-(S)-hydroxyoctadecatrienoic acid [13-(S)-HOTrE], the 15-LOX metabolites of alpha-linolenic acid (ALA), a ω-3 PUFA. As the macrophages actively participate during inflammation and secrete inflammatory mediators, it is a preferable cell type for inflammatory studies. However, established and immortalized cell lines are tools for various researchers working in the area of cell biology, immunology, and biochemistry. Hence RAW 264.7 cells, an immortalized cell line derived from male BALB/c mice, were employed in the present study. Moreover, RAW 264.7 cells are the most preferred for inflammatory studies because their fast growing nature with doubling time of 2-3 days, easy to handle, easy to propagate, expression of complement system factor-C3, high transfection efficiency ratio, and sensitivity to siRNA [102]. Hence, in the present study, the anti-inflammatory effects of 15-LOX metabolites of ALA (13-(S)-HPOTrE and 13-(S)-HOTrE) were elucidated on mouse macrophage cell line, RAW 264.7 cells. As RAW 264.7 cells are immortalized cell line, the primary peritoneal macrophages were also employed in this study. For further

validation of these in vitro findings, studies were also carried *in vivo* on BALB/c male mice.

The specific objectives of the present study are:

1. Evaluate the role of ω-6 PUFAs and ω-3 PUFAs in inflammation *in vitro* by employing mouse macrophage cell line, RAW 264.7 as a model system.
2. Generation of 15-Lipoxygenase (15-LOX) metabolites of ω-6 and ω-3 PUFAs and their characterization.
3. Study the effects of 15- LOX metabolites of ALA (13-(S)-HPOTrE and 13-(S)-HOTrE) on inflammation *in vitro* and *in vivo* and elucidate the signalling pathways involved.

Chapter 2

EVALUATION OF THE ROLE OF OMEGA-6 AND OMEGA-3 PUFAS IN INFLAMMATION *IN VITRO* BY EMPLOYING MOUSE MACROPHAGE CELL LINE, RAW 264.7 AS A MODEL SYSTEM

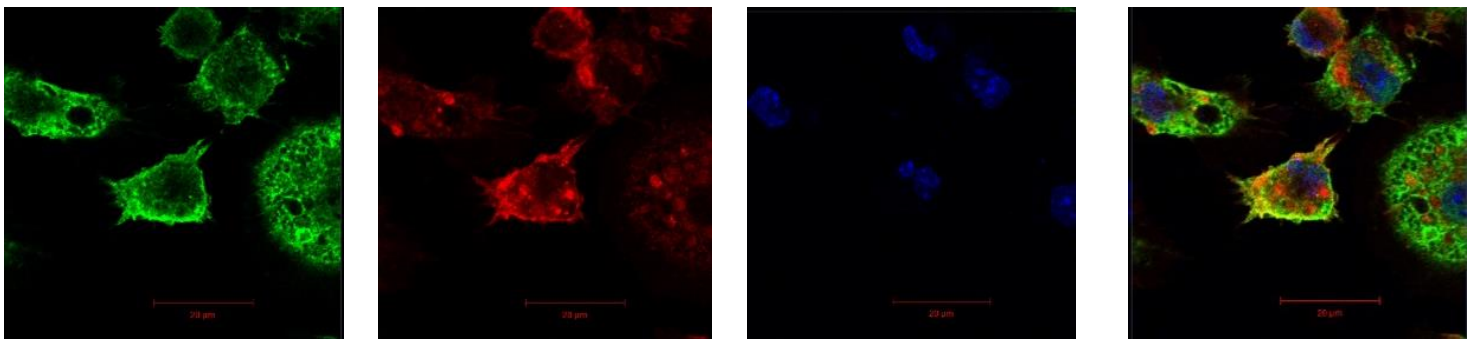

2.1 INTRODUCTION

Inflammation is the host's immune response towards any cue like tissue damage, injury, infection, artificial agents, or immune disorders and it is associated with the prognosis of various autoimmune disorders, arthritis, and cancer. The state of inflammation depends on the severity of infection and pathogenesis. Neutrophils and tissue macrophages are among the initial mediators that migrate at the site of infection during initial inflammatory responses and generate a state of inflammation called acute inflammation. These inflammatory mediators are accompanied by infiltration of leukocytes, monocytes, and other phagocytic cells, which actively participate in the removal of pathogens and strengthen wound healing process. When acute inflammatory response fails to eliminate pathogen and infection still persists, then macrophages and other immune cells get activated and release cytokines such as INF-γ and TNF-α, that initiate the development of chronic inflammation. These activated macrophages produce many hydrolytic enzymes, ROS and NOS that kill microorganisms and help in removing pathogens.

It is well established that the two types of PUFAs, ω-6, and ω-3 regulate homeostasis in body but have opposing effects [96,99]. The ω-6 PUFAs mediate the generation of eicosanoids family of lipid mediators such as prostaglandins, prostacyclins, and thromboxanes, and shift the homeostasis towards pathogenesis. On the other hand, intake of ω-3 PUFAs increases the ratio of ALA, EPA, and DHA in the body [100,101] as a result less potent pro-inflammatory mediators are generated [96,100]. It is reported that beneficial effects of ω-3 PUFAs are mediated via the LOXs and COXs pathways

mainly by their oxygenated metabolites. However, the downstream signalling pathways mediating these anti-inflammatory effects of ω-3 PUFAs have not been elucidated.

In the present study, the role of ω-6 and ω-3 PUFAs in inflammation was studied on mouse macrophages cell line, RAW 264.7 cells. Cytotoxicity of ω-6 and ω-3 PUFAs was determined by MTT (3-(4, 5-dimethylthiazol-2-yl)-2, 5-diphenyl tetrazolium bromide) assay. A low dose of endotoxin (LPS) was used to stimulate RAW 264.7 cells for generation of inflammatory state inside cells, and then pro-inflammatory markers and cytokines were analyzed.

2.2 MATERIALS AND METHODS

2.2.1 Chemicals and Reagents

Culture medium DMEM, penicillin, streptomycin, PBS, Trypsin-EDTA and fetal bovine serum (FBS) were purchased from Gibco. MTT, DCFH-DA (2'-7'-Dichlorodihydrofluorescein diacetate), LPS (lipopolysaccharide from *E. coli, 0127:B8)*, and Griess reagent were purchased from Sigma-Aldrich, USA. Enzyme immunoassay kit for IL-1β was purchased from R&D system, Inc. (MN, USA). AA, LA, ALA, and DHA were procured from Nu-Chek-Prep (MN, USA).

2.2.2 Cell culture and Treatments

The mouse macrophage cell line, RAW 264.7 cell was obtained from NCCS (Pune, India). It was grown and maintained in DMEM supplemented with 10% heat-inactivated FBS, 100 IU/ml penicillin, and 100 µg/ml streptomycin in a humidified atmosphere with 5% CO_2 at 37°C. Subculturing of cells was done twice a week. Fresh culture medium was used before each treatment. For MTT assay, cells were pre-incubated with different concentrations (1, 10, 100 and 200 µM) of ω-6 PUFAs (AA, and LA) and ω-3 PUFAs (ALA, and DHA) for different time points (24 h, and 36 h). For apoptosis study and IL-1β measurement, RAW 264.7 cells were pre-incubated with 100 µM of ω-6 PUFAs (AA, and LA) and ω-3 PUFAs (ALA, and DHA) for 3 h then primed with LPS (100 ng/ml) for 24 h. For IL-1β measurements, RAW 264.7 cells were incubated with 1mM ATP for 30 min prior to end time point. While, for ROS measurement, RAW 264.7 cells were pre-incubated with 100 µM of ω-6 PUFAs (AA, and LA) and ω-3 PUFAs (ALA, and DHA) for 3 h then primed with LPS (100 ng/ml) 16 h.

2.2.3 Cytotoxicity Assay

Cytotoxicity of ω-6 PUFAs (AA, and LA) and ω-3 PUFAs (ALA, and DHA) was assayed by MTT assay. To perform this assay, RAW 264.7 cells were seeded in 96 well plates at a density of $5X10^4$ cells/well then treated with ω-6 PUFAs (AA, and LA), ω-3 PUFAs (ALA and DHA) at various concentrations (1, 10, 100 and 200µM) for different time points (24 h, and 36 h). Cell viability was measured colorimetrically by MTT assay as described by Mossman [103].

2.2.4 Nitrite Estimation

RAW 264.7 cells were seeded in 6 well plates for 12 h then pre-incubated with 100 µM of ω-6 PUFAs (AA, and LA) and ω-3 PUFAs (ALA, and DHA) for 3 h then stimulated with or without LPS (100 ng/ml) for the next 24 h. At the end of the time point, stable nitrite level in the culture supernatant was measured by Griess Reagent. For this, 50 µl of cell culture medium was mixed with 50 µl of Griess reagent and incubated at room temperature for 10 min in the dark. Then absorbance was measured at 540 nm using multi-mode ELISA reader (BioTek, SynergyMx). Nitrite level in samples was determined by using the standard curve of sodium nitrite. Culture medium was taken as blank for all experiments.

2.2.5 Estimation of IL-1β

RAW 264.7 cells were seeded in 6 well plates for 12 h then pre-incubated with 100 µM of ω-6 PUFAs (AA, and LA) and ω-3 PUFAs (ALA and DHA) for 3 h then stimulated with or without LPS (100 ng/ml) for the next 24 h. Then cells were incubated with 1 mM ATP for 30 min prior to end time point. At the end of the time point, the culture supernatant was collected. Levels of IL-1β (R&D system, Inc. MN, USA) in culture medium were measured by ELISA kit according to manufacturer's protocol. Their levels

in culture medium were determined by using standard curves of IL-1β standard provided along with the kit.

2.2.6 Measurement of Reactive Oxygen Species (ROS)

RAW 264.7 cells were seeded in 6 well plates at a density of $2x10^5$ cells/well then pre-incubated with 100 µM of ω-6 PUFAs (AA, and LA) and ω-3 PUFAs (ALA, and DHA) for 3 h. Then these cells were stimulated with or without LPS (1 µg/ml) for next 16 h. After this, cells from each well were harvested and washed twice with PBS and further incubated with 10 mM of DCFH-DA for 30 min in dark at 37°C and then further washed twice with PBS. 10,000 cells per sample were taken for analysis. The quantification was performed on a Flow Cytometer and data analysis was done by Cell Quest software (FACS Calibur, Becton Dickinson, CA, USA) with excitation of DCF at λ 488 nm and emission at λ 525 nm.

2.2.7 Analysis of Apoptosis by FACS

RAW 264.7 cells were seeded in 6 well cultures plate. When cells were 60 % confluent, pre-incubated with 100 µM of ω-6 PUFAs (AA, and LA) and ω-3 PUFAs (ALA and DHA) and/or doxorubicin (10 µM) for 3 h. Then stimulated with or without LPS (100 ng/ml) for 24 h. Staining of cells was done by Propidium iodide. Samples were run on Flow Cytometer (BD, LSR Fortessa, CA, USA) and data analyses were done on BD FACSDiva™ software.

2.3 Statistical Analyses

All the experiments were performed in triplicates and the values represented as mean ± SD. Data were correlated, analyzed and p-values were obtained using student's t-test. The p-value < 0.05 was considered as statistically significant.

2.4 RESULTS

2.4.1 ω-6 and ω-3 PUFAs show less cytotoxic effect on RAW 264.7 cells.

The cytotoxic effects of ω-6 and ω-3 PUFAs were evaluated by MTT assay on RAW 264.7 cells. There was no significant cytotoxicity of either ω-6 or ω-3 PUFAs at 24 h. Therefore, the percentage of cell death was calculated for 200 µM PUFAs at 36 h. As shown in the

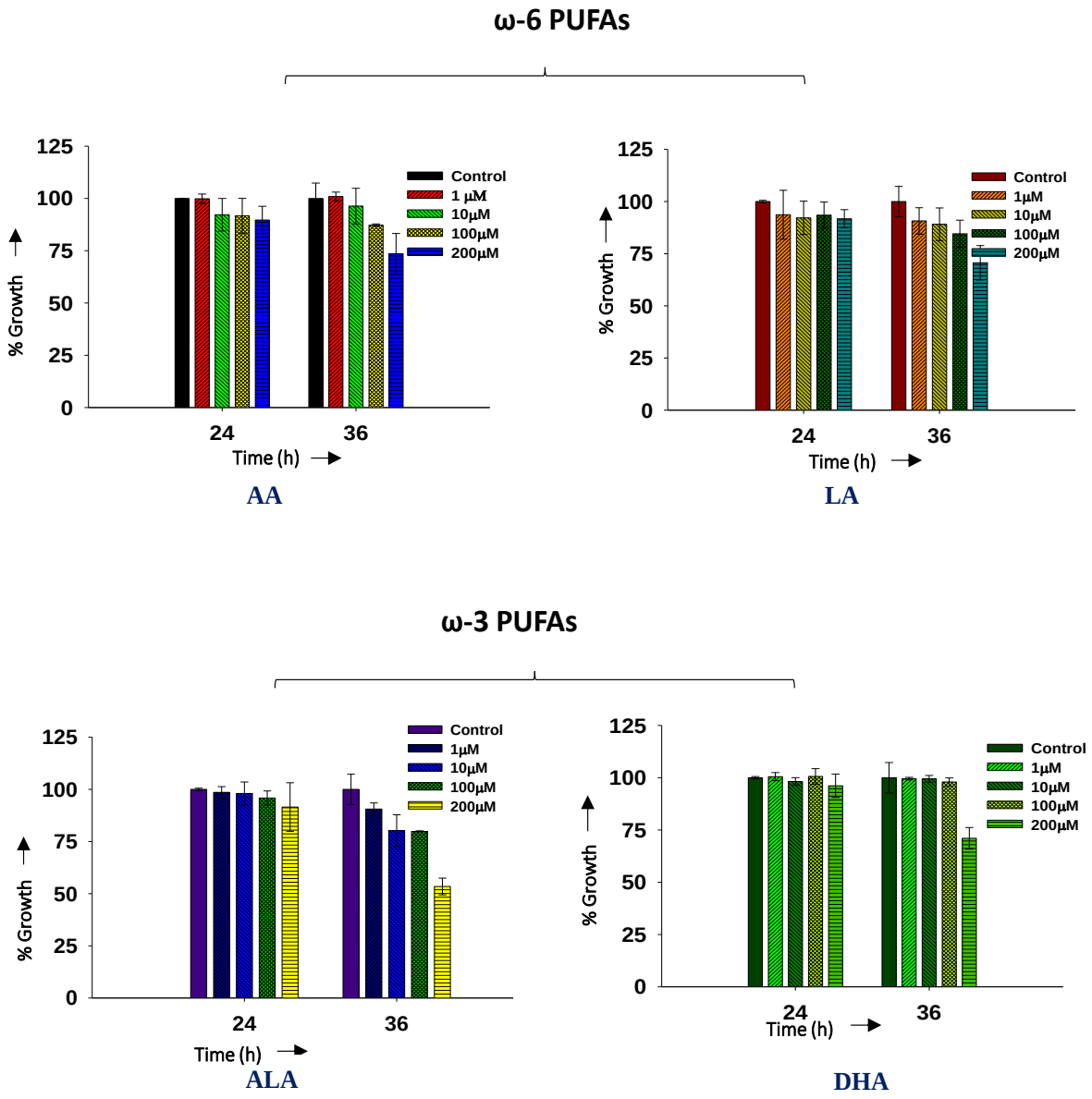

Figure 2-1: ***Effects of ω-6 PUFAs (AA, and LA) and ω-3 PUFAs (ALA, and DHA) on viability of mouse macrophage cell line, RAW 264.7 cells.*** In MTT assay, cells were pre-incubated with different concentrations (1, 10, 100 and 200 µM) of ω-6 PUFAs (AA, and LA) and ω-3 PUFAs (ALA, and DHA) for different time points (24 h and 36 h). The percent cell growth following treatment was calculated, in comparison with untreated control cells.

figure 2-1, RAW 264.7 cells treated with ALA and DHA (ω-3 PUFAs) showed 46.6% and 29% cell death, respectively. However, AA and LA (ω-6 PUFAs) showed only 26.4% and 29.4% cell death, respectively; at 36 h. Treatment of these PUFAs decreased the growth of the cells in a dose and time-dependent manners. The cell death was less than 50% in RAW 264.7 cells treated with ω-6 and ω-3 PUFAs, therefore, IC50 values of any of PUFAs could not be calculated. Based on these results, further experiments were carried out at 100 µM concentrations of ω-6 and ω-3 PUFAs.

2.4.2 Effects of ω-6 and ω-3 PUFAs on Nitrite level in culture medium in LPS induced RAW 264.7 Cells.

Next, it was aimed to evaluate the effects of ω-6 and ω-3 PUFAs on LPS induced inflammation by examining effects on pro-inflammatory chemical mediator: NO- a second messenger. For this, RAW 264.7 cells were first treated with or without PUFAs and challenged with LPS (100 ng/ml) as described in the methods. There was a significant elevation in NO production in RAW 264.7 cells when stimulated with LPS and this elevated level was reduced by 13% and 12.45% in the presence of ALA and DHA, respectively (Figure 2-2). However, there was no significant changes in NO level in AA and LA treated and LPS stimulated macrophages. The significant reduction in NO production by ALA and DHA suggests their strong anti-inflammatory effects on LPS stimulated macrophages.

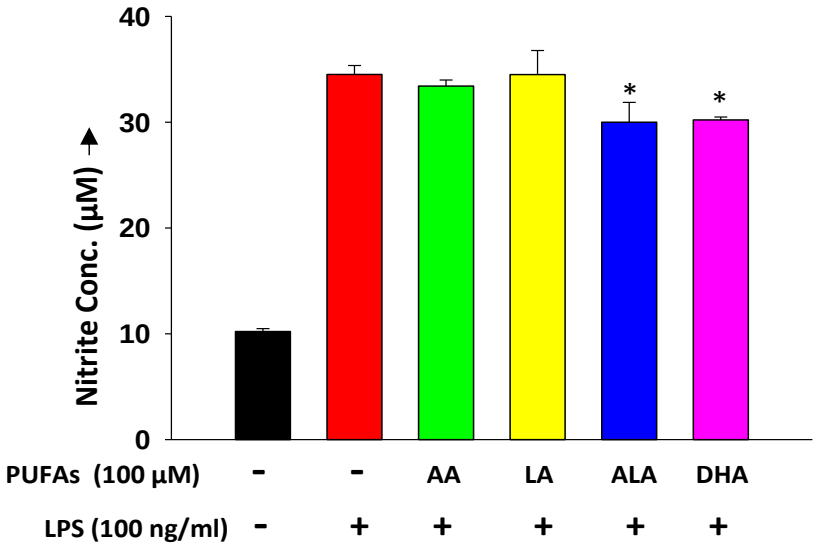

Figure 2-2: ***Effects of ω-6 PUFAs (AA, and LA) and ω-3 PUFAs (ALA, and DHA) on NO generation in RAW 264.7 cells.*** Nitrite level measured in culture medium of RAW 264.7 cells pre-incubated with ω-6 PUFAs (100 µM) and ω-3 PUFAs (100 µM) for 3 h and further stimulated with or without LPS (100 ng/ml) for the next 24 h. ω-3 PUFAs reduced NO level more efficiently compared to ω-6 PUFAs. The values represent mean ± SD of three independent experiments. * indicates significance ($p<0.05$) compared to LPS alone treated cells.

2.4.3 ω-6 and ω-3 PUFAs reduce Reactive Oxygen Species (ROS) generation in LPS induced RAW 264.7 cells.

Next, it was aimed to evaluate the effects of ω-6 and ω-3 PUFAs on LPS induced inflammation by examining effects on pro-inflammatory chemical mediator: ROS- an oxidative stress marker. For this, RAW 264.7 cells were first treated with or without PUFAs and challenged with LPS (100 ng/ml) as described in the methods. There was a significant elevation in ROS production in RAW 264.7 cells, when stimulated with LPS and this elevated level was reduced by 73.1% and 88.2% in the presence of ALA and DHA, respectively (Figure 2-3). However, AA and LA (ω-6 PUFAs) showed 61.5% and

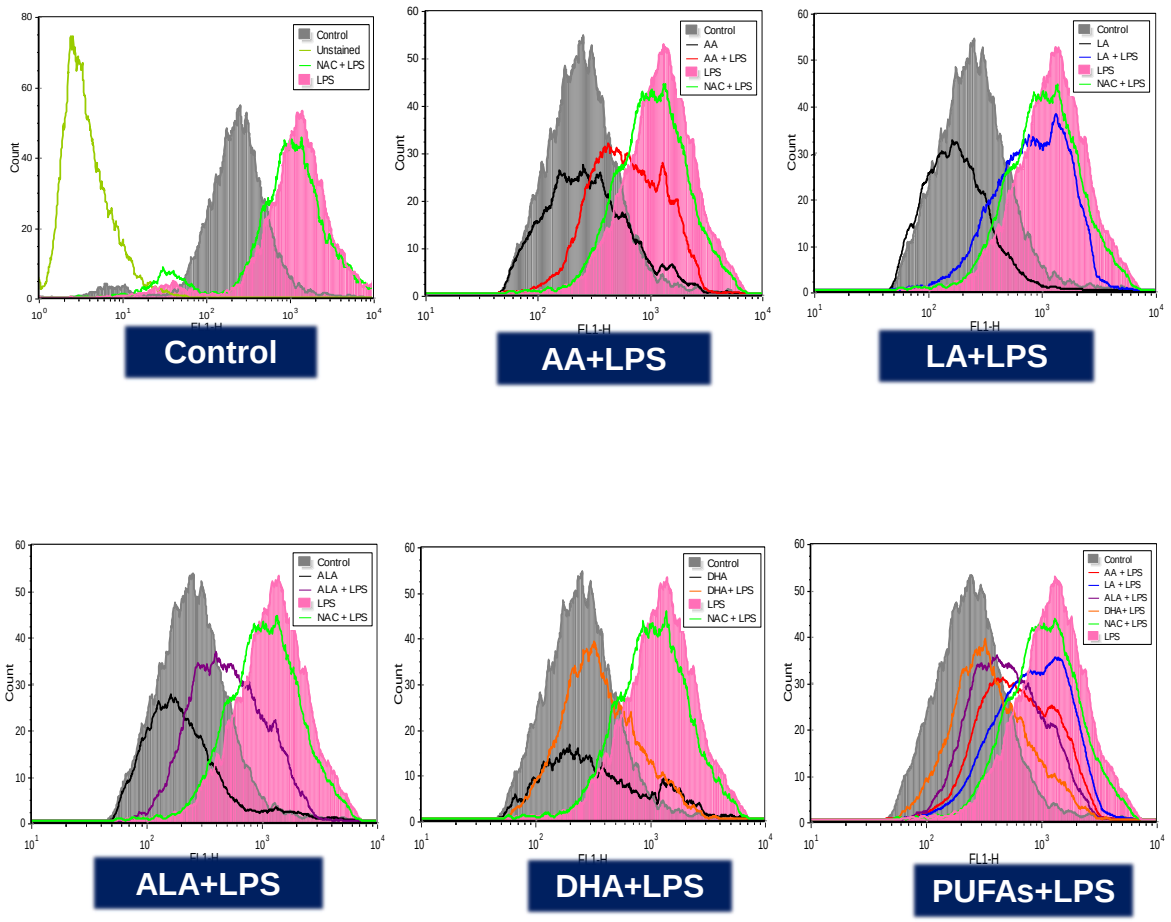

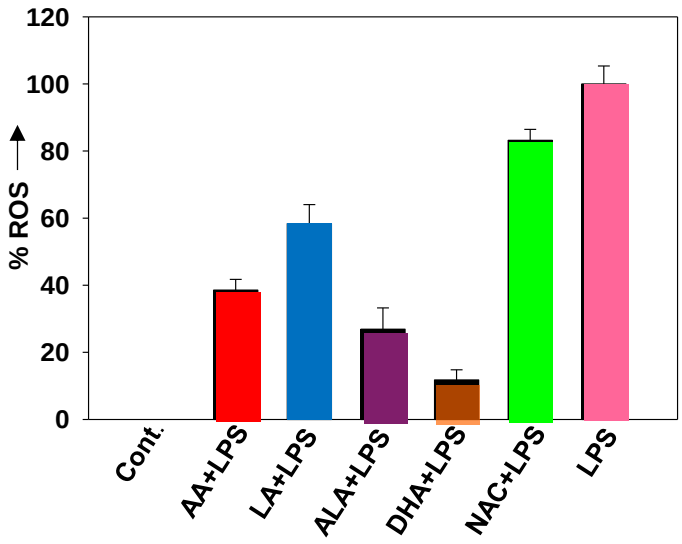

Figure 2-3: ***Effects of ω-6 PUFAs (AA, and LA) and ω-3 PUFAs (ALA, and DHA) on ROS generation in RAW 264.7 cells.*** Intracellular ROS level measured in cells following pre-incubation with ω-6 PUFAs (100 µM) and ω-3 PUFAs (100 µM) for 3 h then stimulated with LPS for 16 h. ω-3 PUFAs reduced ROS level more efficiently compared to ω-6 PUFAs. N-Acetyl Cysteine (NAC, 5mM), a ROS inhibitor was used as positive control.

41.6% reduction in ROS generated by LPS stimulation. NAC- an anti-oxidant compound also decreased 16.8% ROS generated by LPS. The result showed that ω-3 PUFAs reduced LPS induced ROS generated in RAW 264.7 cells more efficiently than ω-6 PUFAs and even NAC- an anti-oxidant molecule.

2.4.4 ω-6 and ω-3 PUFAs show a decrease in IL-1β level in culture medium in LPS induced RAW 264.7 Cells.

The identification of IL-1β is registered in the 1980s [104] but its existence noticed in the form of Pus much before the advent of the microscope [27,105]. Its significance can be analyzed by the fact that before the 1980s, it was studied with different names such as haematopoietin 1, leukocytes endogenous mediators, catabolin, endogenous pyrogens depending on diverse functions noticed [105]. Now, it is well established that most potent molecule of innate immune system-IL-1β, is also pro-inflammatory in nature. The above studies indicated the anti-inflammatory nature of ω-3 PUFAs. Therefore, it was aimed to evaluate the effects of ω-6 and ω-3 PUFAs on the level of pro-inflammatory cytokine-IL-1β. The level of IL-1β in the culture medium of RAW 264.7 cells were measured by ELISA kit. There was an increase in IL-1β level in RAW 264.7 cells challenged with LPS. However, macrophages pre-treated with ω-6 and ω-3 PUFAs and challenged with LPS showed decreased IL-1β level. The ω-3 PUFAs, ALA and DHA significantly decreased IL-1β level by 52.7% and 54% respectively, while ω-6 PUFAs, AA, and LA decreased IL-1β by 50% and 41.7%, respectively in LPS induced RAW 264.7 cells (Figure 2-4).

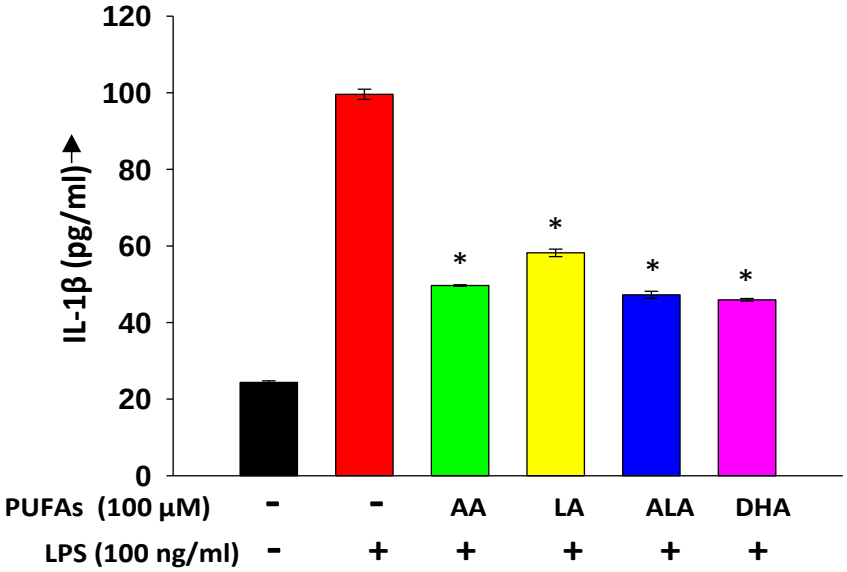

Figure 2-4: ***Effects of ω-6 PUFAs (AA, and LA) and ω-3 PUFAs (ALA, and DHA) on IL-1β level in RAW 264.7 cells.*** Cells were pre-incubated with 100 µM of ω-6 PUFAs and ω-3 PUFAs for 3 h then stimulated with or without LPS (100 ng/ml) for the next 24 h. The values represent mean ± SD of three independent experiments. *Indicates significance ($p<0.05$) compared to LPS treated cells.

2.4.5 ω-3 PUFAs show increased apoptosis than ω-6 PUFAs in LPS induced RAW 264.7 Cells.

Apoptosis enhances anti-inflammatory effects and it plays a vital role in the resolution of inflammation [106]. Moreover, LPS and activated inflammasomes also induce autophagy in mesothelial cells [107]. Since ω-3 PUFAs showed anti-inflammatory effects, we examined whether they affected induction of apoptosis in LPS stimulated RAW 264.7 cells. FACS analysis of RAW 264.7 cells stimulated with LPS showed increased apoptosis. However, macrophages pre-treated with PUFAs and challenged with LPS showed a further increase in apoptosis. Macrophages pre-treated with ALA and DHA and challenged with LPS showed 47% and 57.6% increase in apoptosis while AA and LA showed 32.2% and 35.2% increase in apoptosis, respectively (Figure 2-5).

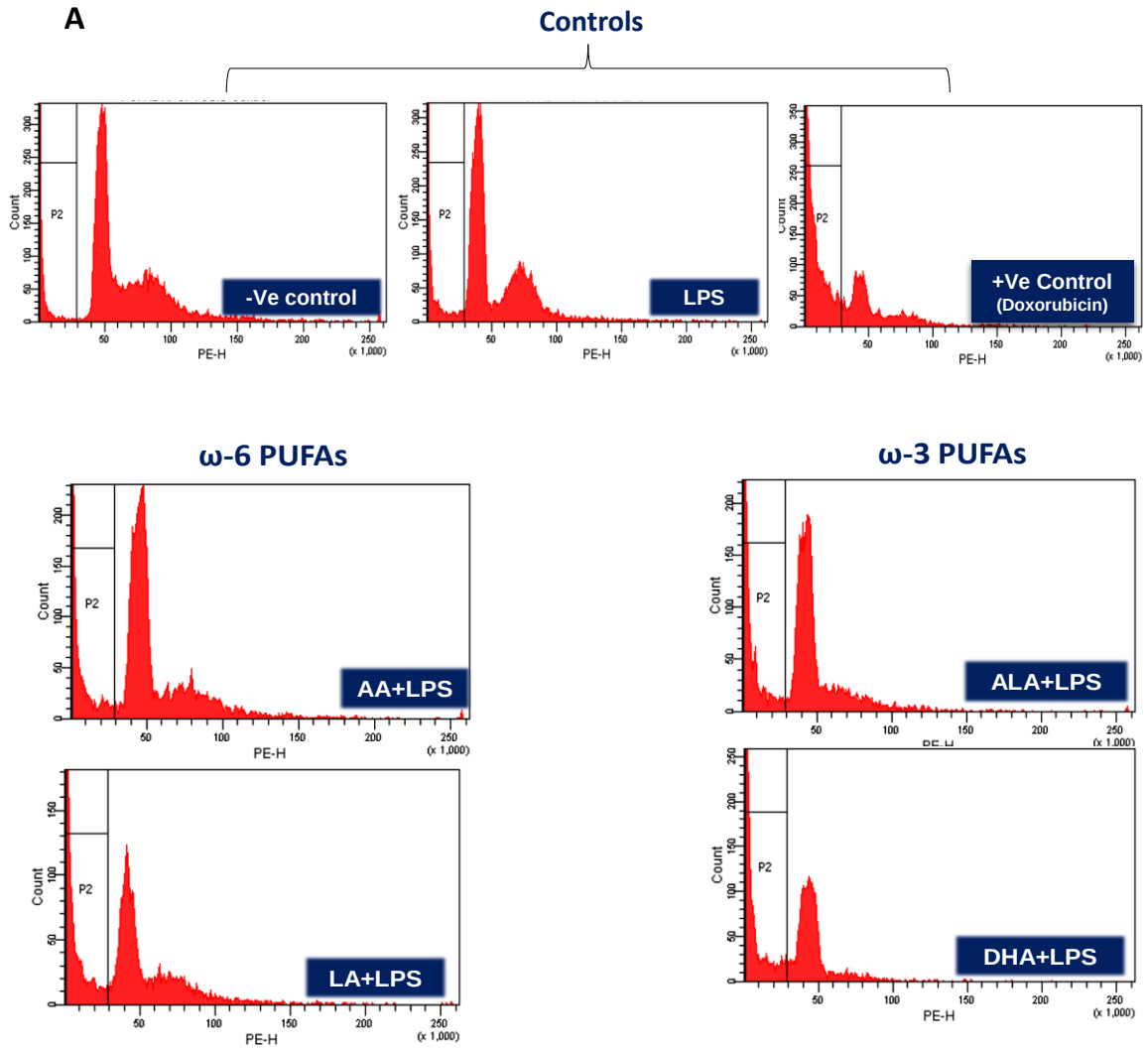

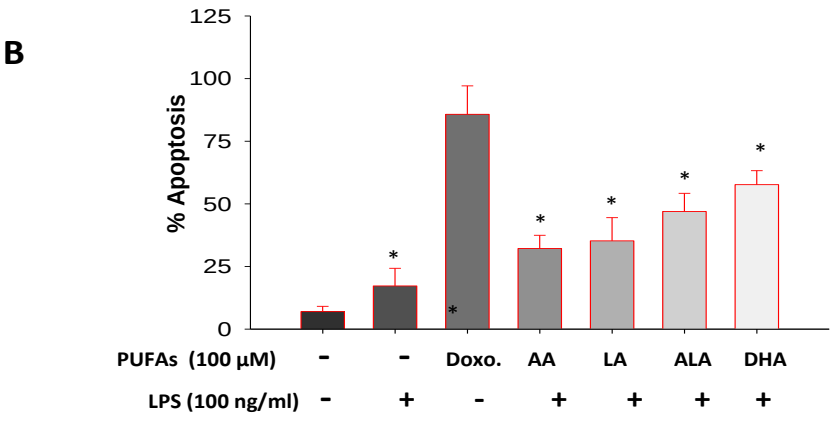

Figure 2-5: ***Flow cytometric analysis showing the effects of ω-6 PUFAs (AA, and LA) and ω-3 PUFAs (ALA, and DHA) on apoptosis in RAW 264.7 cells challenged with LPS.*** **A)** Apoptosis was assayed by Propidium iodide at 24 h, by flow cytometric analysis. The dead cells were gated and analysis was performed only on live cells. **B)** Bar graph representation of above studied apoptosis. *Indicates significance ($p<0.05$) compared to LPS treated cells.

2.5 Discussion

According to Merriam-Webster's Learner's Dictionary, “food” is defined as “Material consisting essentially of protein, carbohydrate, and fat used in the body of an organism to sustain growth, repair, and vital processes and to furnish energy” [108]. In addition to this, types of food (diet) is also associated with health, prognosis of various disorders and diseases [94]. Several studies also show that all the inflammatory diseases are not caused by foreign pathogens or injuries but seems to be linked with situations such as less or lack of physical activities, high calories food, and expose to toxic compounds in daily life [95]. Obesity, atherosclerosis, neurodegenerative diseases, type 2 diabetes, and asthma are the outcome of these conditions [95]. These states are also called **para-inflammation** or **chronic low-grade inflammation**. If these conditions persist for a longer time then contribute to further disease progression.

The dietary intake of PUFAs decides the ratio of ω-6 and ω-3 PUFAs in the body. Increased ratio of ω-6 to ω-3 PUFAs is hypothesized to elevate pro-inflammatory eicosanoid production and thus the onset of inflammatory diseases. A sufficiently high intake of ω-3 PUFAs, on the other hand, has shown to offer protection from inflammatory diseases by decreasing the production of pro-inflammatory eicosanoids, cytokines, ROS and RNS [100,101].

In the present study, mouse macrophage cell line, RAW 264.7 was used as *in vitro* model system to elucidate ω-6 and ω-3 PUFAs role in inflammation. The findings of the present study supports above thought wherein, FACS analysis of RAW 264.7 cells stimulated with LPS showed increased intracellular ROS level, while the macrophages

pre-treated with ω-6 and ω-3 PUFAs and stimulated with LPS showed a significant decrease in generation of ROS. ω-3 PUFAs, however, decreased the intracellular ROS level more efficiently as compared to ω-6 PUFAs. In MTT cytotoxicity assay, ω-6 PUFAs (AA, and LA) showed very less cytotoxic effects as compared to ω-3 PUFAs (ALA, and DHA) in RAW 264.7 cells. On the other hand, both, ω-6 and ω-3 PUFAs decreased IL-1β level significantly.

NO is a signalling molecule and generally considered as a pro-inflammatory marker [46]. It also regulates growth and inhibition of cell type which are associated with inflammatory responses such as macrophages, immune cells and mast cells [109]. In the present study, NO level in culture medium was measured by Griess reagent. The results showed that LPS increase the level of NO generation in RAW 264.7 cells while macrophages pre-treated with ω-3 PUFAs showed decreased NO level. Nevertheless, among both ω-6 and ω-3 PUFAs, ω-3 PUFAs appear to be relatively more effective.

The apoptosis actively participates in the removal of neutrophils and other inflammatory mediators thus enhance strength during resolution phase. RAW 264.7 cells challenged with LPS showed increased apoptosis, which was further increased in macrophages pre-treated with ω-6 and ω-3 PUFAs and challenged with LPS. However, apoptosis induced by ω-3 PUFAs was more prominent than ω-6 PUFAs. Hence, the involvement of ω-3 PUFAs (ALA, and DHA) to increase apoptosis in comparison to ω-6 confirms its importance during the resolution of inflammation.

ALA is the precursor for EPA and DHA and the anti-inflammatory properties of ω-3 PUFAs might be mediated through various pathways. The maturation of inflammation mediated through various chemical mediators in which, lipid mediators

play a vital role. Lipid mediators are generated by LOXs and COXs pathways, whose nature depends on the types of PUFAs available. The ω-6 PUFAs generate eicosanoids family, which on excess production shift the homeostasis towards pathogenesis. On the other hand, ω-3 PUFAs gives raise to less potent pro-inflammatory mediators [96]. Also, the presence of EPA and DHA decreases the availability of AA for LOXs and COXs as substrate. As a result, on one side, there is an increase in the EPA and DHA-mediated eicosanoids generation while on the other side, there is a decrease in AA based eicosanoids and lipid mediators. Furthermore, DHA and EPA based eicosanoids and lipid mediators are less potent than AA based analogs [51].

It is also reported that ω-3 PUFAs show anti-inflammatory effects through several mechanisms [51,100], among these, NF-κB and MAP kinase pathways are two major signalling cascades involved. In NF-κB signalling pathway, it prevents the phosphorylation and degradation of Iκ-Bα protein by proteasome complex while in MAP kinase pathways it is mediated through JNK, ERK, p38 and AP-1 [110]. In addition, this effect also mediated by showing anti-oxidant properties by inhibiting the intracellular accumulation of peroxides [111]. Therefore, the reduction in production of NO and ROS by ω-3 PUFAs in LPS primed macrophage might be mediated through any of the above mechanisms, either directly or through their metabolites. In order to understand these mechanisms, further studies were undertaken to evaluate the anti-inflammatory effects of the metabolites of ω-3 PUFAs (Chapter 4). As this involves the pure metabolites of these PUFAs, their generation and characterization was taken up first by employing 15-lipoxygenase (Chapter 3).

Chapter 3

GENERATION OF 15-LIPOXYGENASE (15-LOX) METABOLITES OF OMEGA-6 AND OMEGA-3 PUFAS AND THEIR CHARACTERIZATION

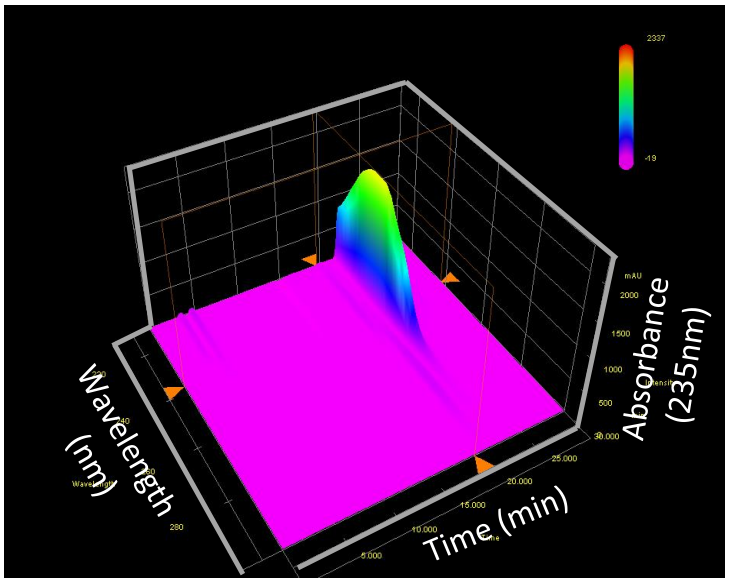

3.1 INTRODUCTION

Lipoxygenases are found in various plants such as peas, green beans, peanuts, mung beans, soybean, mustard, cucumber and in cereals such as rice, oat, rye, corn barley, and wheat [69,112–115]. LOXs are also reported in vegetables such as potato tubers and brinjal [116,117]. However, soybean LOXs are well known and extensively studied for several decades. In soybeans, all the three lipoxygenase isozymes (lipoxygenase-1, 2 and 3) are water-soluble and globular proteins and consist of a single polypeptide of approximate 96 kDa molecular weight [69].

Linseed (*Linum usitatissimum*), also known as flaxseed, is a food and fiber yielding annual plant. The linseed seeds have been used for a long time as a source of food as well as for oil called linseed oil. Linseed is rich in fatty acids and consists 35-40% fatty acids out of which 8-10% saturated fatty acids, 15-20% monounsaturated and more than 70% ALA [118]. LOX activity has also been reported in linseed seeds [119]. In 1970, Zemmerman showed LOXs activity in linseed [120] that was further confirmed by Grosch [121] in 1976 and found that linseed seed LOXs perform catalysis similar to soybean LOX-1. On the other hand, In 1982, Vernoov demonstrated that unlike soybean, linseed seed lack LOX-2 activity [122].

All the plant LOXs studied above have a common feature, i.e., as the seedling develops there is an increase in LOXs activity in initial 50 to 72 h and further followed by a significant decrease. In rice, there was a 20 fold increase in LOXs activity in day three seedling [114]. So far, all the LOX activities in linseed were demonstrated in defatted seeds. In the present study, instead of linseed seed, we demonstrated LOXs activity in linseed seedling and found as a novel source of LOX enzyme and day two seedling

showed maximum enzyme activity. The enzyme was extracted and purified by column chromatography, enzyme activity was measured on oxygraph using Clark's Oxygen electrode and molecular mass determination was done by SDS-PAGE. Further, metabolites of AA, ALA, and LA were generated from two different enzyme sources- Linseed seedling enzymes as well as from soybean LOX (commercially available) and purified on HPLC. Co-chromatography was done to compare metabolites generated from these two different enzyme sources. Then these metabolites were also characterized on LC-MS/MS.

3.2 Materials and Methods

3.2.1 Chemicals and Reagents

Column Chromatography matrices and Q Sepharose™ fast flow were purchased from Amersham Pharmacia Biotech, Uppsala, Sweden and G-50 Sephadex was obtained from Sigma chemical company, St. Louis, USA. All the solvents used for HPLC were of HPLC grade and procured from Merck Specialities Pvt. Ltd, Mumbai, India. AA, LA, and ALA were purchased from Nu-Chek Prep, Inc. MN, USA. Soybean Lipoxygenase (cat# L7395) was procured from Sigma, Saint Louis, Missouri, USA

3.2.2 Enzyme source

Dried ripe seeds of Linseed (*Linum usitatissimum*) were surface sterilized using 0.1% sodium hypochlorite for 15 min and subsequently washed in running tap water for 5-6 times. Then linseed seeds were soaked in tap water for overnight and allowed for germination at room temperature. Then seeds were washed rigorously in tap water to remove mucilage, kept for germination at room temperature in a humid environment for 4 days, and further stored in -80 °C for further studies.

3.2.3 Homogenization and (NH4) 2 SO4 precipitation of linseed seedling

Germinated linseed seedlings (Day1-4) were homogenized in homogenization buffer (125 mM Tris-Cl buffer, pH 8.0 containing 1mM EDTA, 2 mM Ascorbic acid, and 2 mM Sodium metabisulphite) at 4°C. Then the homogenate was filtered by double-layered cheesecloth and centrifuged at 17000 rpm for 15 min and supernatant was collected. Then $(NH_4)_2SO_4$ was added under continuous stirring to the supernatant fraction to give a final concentration of 30% saturation and stirred for one hour at 4°C. The precipitated protein was removed by centrifugation at 17,000 rpm for 15 min at 4°C. The resulting supernatant was brought to 30-40% saturation by further addition of solid $(NH_4)_2SO_4$, stirred for one hour at 4°C, and then centrifuged at 17,000 rpm for 15 min at 4°C. Different fractions were obtained by ammonium sulphate fractionation. The homogenization and fractionation process were carried at 0-4°C.

3.2.1 Enzyme Assay

The LOX activity was measured by determining the O_2 consumption with Strathkelvin 782 oxygen system version 3.0, Model 782, Oxygen monitor equipped with Clark's oxygen probe and connected to the computer for data acquisition. The enzyme assay mixture consists of 2 ml enzyme assay buffer, 10 µl substrate (AA-133 µM; ALA, and LA-266 µM), 25 µl linseed homogenate and double distilled water in a total volume of 3 ml reaction mixture. The reaction was carried out in an airtight chamber, molecular O_2 consumption was recorded and enzyme unit was calculated.

One Enzyme Unit= µmole of O_2 consumed/mg protein x min

3.2.2 pH optimization

The LOX activity in linseed seedling was measured by oxygraph at different pHs (pH 6.0 – pH 13.0). For this, Potassium phosphate, Tris-Cl, Sodium bicarbonate and

Potassium chloride buffer systems were used to obtain a wide range of enzyme assay buffers. The homogenates of different day's seedlings (Day1-4) of linseed were used to check enzyme activity at various pH ranges (pH 6.0 – pH 13.0).

3.2.3 Temperature optimization

The LOX activity in linseed seedling was measured by oxygraph compatible to measure enzyme activity at different temperatures. The various temperatures were achieved by attaching oxygraph with water bath fitted with temperature regulator. The enzyme activity in seedling homogenate was assayed at various temperature ranges (5.0-50°C).

3.2.4 Clarification of sample

The pellets obtained from Ammonium sulphate fractionations were redissolved in homogenization buffer containing 0.5 M $CaCl_2$ and 0.2% Dextran sulphate and kept for mild stirring at 4°C for 20 min and then centrifuged at 18,000 rpm for 40 min at 4°C. The supernatant was collected and further filtered through Whatman filter paper followed by Millipore filter of pore size 0.8 and 0.4 µm.

3.2.5 Desalting

Desalting of the sample was done by gel filtration chromatography. Sephadex G-50 matrix was packed into a glass column (30 x 350 mm) and equilibrated with 2 CV (Column Volume) equilibration buffer (50 mM Tris-Cl pH 8.50 containing 1 mM EDTA, 2 mM Ascorbic acid, and 2 mM Sodium metabisulphite). Then the sample was loaded onto the Sephadex G-50 column at 2-3 ml/min flow rate and different fractions were collected. Active fractions were pooled together and further purified by anion exchange chromatography.

3.2.6 Anion Exchange Chromatography

Q-Sepharose fast flow matrix was packed in column (20 x 100 mm) and equilibrated with 4 CV equilibration buffer (50 mM Tris-Cl pH 8.5 containing 100 mM KCl, 1 mM EDTA, 2 mM Ascorbic acid, and 2 mM Sodium metabisulphite). Then the sample was loaded onto the column at 0.8-1 ml/min flow rate. The column was washed with equilibration buffer to remove unbound proteins while bound proteins were eluted with 0.7 M linear KCl gradient at 1.5 ml/min flow rate.

3.2.7 Biosynthesis of Linseed Lipoxygenase metabolites

Linseed enzyme was employed for synthesis of hydroperoxy and hydroxy metabolites of AA, LA, and ALA as per the method described earlier [123,124]. In brief, linseed enzyme was incubated with AA (133 µM), LA (266 µM), or ALA (266 µM), in 100 mM Tris-Cl buffer, pH 8.0 for 3 min and the reaction was terminated by acidifying the reaction mixture to pH 3.0 with 6N HCl. The products formed were extracted with equal volumes of hexane: diethyl ether (1:1) twice and the organic solvent was evaporated under inert conditions. The dried products were then dissolved in HPLC mobile phase consisting of hexane: propane-2-ol: acetic acid (1000:15:1) for purification of these metabolites on HPLC. For biosynthesis of corresponding hydroxides, these dried hydroperoxy products were dissolved in methanol and reduced with sodium borohydride ($NaBH_4$) for 2 min. Then the reduced products were extracted in hexane diethyl system and separated on HPLC as mentioned above.

3.2.8 Purification and analysis of metabolites on SP-HPLC

The metabolites generated using different PUFAs as substrate were purified on preparatory straight phase HPLC (SP-HPLC) (Shimadzu LC 20AP) equipped with the autosampler- (SIL-10AF), detector (SPD-M20A) and connected to a computer with Shimadzu LC solution. The metabolites were separated on SP-HPLC using enable Silica

column (250 x 20mm) and HPLC mobile phase solvent system consisting of hexane: propane-2-ol: acetic acid (1000:15:1) at a flow rate of 6 ml/min and the eluents were monitored at 235 nm. The peaks showing characteristic absorption maximum at 235 nm, as analysed on UV/VIS Perkin Elmer lambda 35 spectrophotometer, were taken for further characterisation. The solvent was evaporated and metabolites were stored in 100% ethanol in an inert environment at -20°C. Analysis of metabolites was performed on analytical HPLC (Shimadzu LC 20AD, equipped with autosampler SIL-20AC HT and diode array detector (SPD-M20A) on Enable silica column (250 x 4.6mm) at 1 ml/min flow rate and solvent system mentioned above.

3.2.9 Characterization on LC-MS/MS

For characterization, equal concentration of linseed metabolites and Soybean 15-(S)-HETE (as the standard) were dissolved in MS grade solvent system separately. The Reverse phase solvent system (methanol: water, 80: 20) was used for purification and characterization of metabolites. These metabolites were injected in LC-MS/MS (LC: Agilent Technologies, 1200 series, Hystar Version 3.2, MS/MS: Bruker Daltonics, micrOTOFQ, micrOTOF control version 2.2) fitted with C-18 column. The fragmentation pattern of linseed metabolites and soybean metabolites were compared for identification

3.3 Statistical Analyses

All the experiments were performed in triplicates and the values represented as mean ± SD. Data were correlated, analyzed and p-values were obtained using student's t-test. The p-value <0.05 was considered as statistically significant.

3.4 RESULTS

3.4.1 Linseed seedlings show abundant LOX activity during early days of germination.

Several plants have shown LOX activity, which varies from type of tissue and their states. LOXs activity reported mostly in plant seeds while high enzymatic activity reported during germination. LOXs activities were also reported in defatted linseed seed [119,125], however, in this study, we report LOX activity in linseed seedlings. The germinated seedlings were homogenized in Tris-Cl buffer at pH 8.0 as described in methodology and fractionated by ammonium sulphate precipitation. The ammonium sulphate fraction of 30-50% showed more enzymatic activity than other fractions. Therefore, this fraction was used for further purification of the enzyme. The homogenates of different day's seedlings (Day1-Day4) of linseed were used to check its enzyme activity on oxygraph and abundant LOX-like activity was detected in linseed seedlings. Oxygraphic assay of linseed seedlings homogenate, using AA, LA, and ALA as the substrates, showed rapid incorporation of molecular O_2 (Figure 3-1). It was further confirmed by the characteristic spectrum of conjugated diene present in LOXs product, which was observed by the spectrophotometer-based assay.

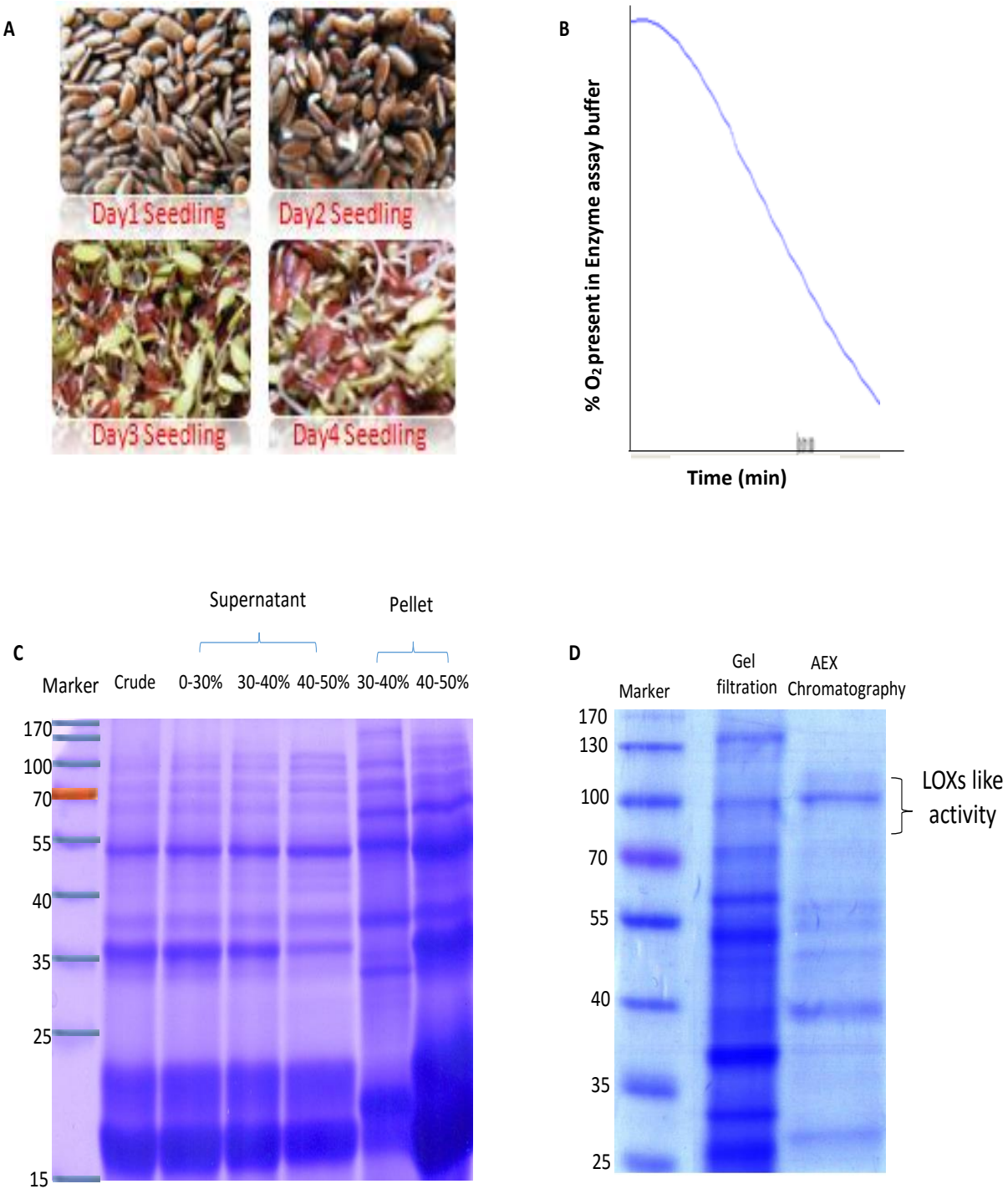

Figure 3-1: ***Homogenization, Isolation and Purification of Linseed seedling enzyme.*** **A)** Different days seedling of Linseed seeds showing the growth of radicle and plumule. **B)** A typical image of Oxygraph showing the enzymatic activities of linseed seedlings. **C)** SDS-PAGE showing proteins of different fractions obtained by ammonium sulphate fractionation of linseed seedling homogenate. D). SDS-PAGE showing partial purification of active enzyme fraction by chromatography.

3.4.2 Linseed enzyme shows pH optima in alkaline pH range

Enzyme assay was carried out as per the methods described in the methodology on an oxygraph (Strathkelvin 782 oxygen system version 3.0, Model 782). Enzyme activity was assayed in homogenates of different day's linseed seedlings (day1-4) against changing pH in a range of pH 6.0 to pH 13.0 at 25°C. The homogenate of day-1 linseed seedling showed two major pH optima, first at pH 10.0 and the second at pH 11.7. In addition, two minor peaks with pH optima of 9.5 and 6.8 were also recorded (Figure 3-2).

The enzyme activity in Day 2 homogenate of linseed seedlings was also analyzed at different pHs (pH 6.0 – 13.0). The optimum enzyme activity was observed at two different pHs. It showed two major pH optima, first at pH 9.7 and the second at pH 11.05. In addition, two minor peaks with pH optima of 8.2 and 12.4 were also recorded The homogenate of day-3 linseed seedling showed one major pH optima at 11.03. In addition, four minor peaks with pH optima of 7.2, 9.0, 9.7 and 12.03 were also recorded The enzyme activity in Day 4 homogenate of linseed seedlings was also analyzed at different pHs (pH 6.0 – 13.0). The maximum enzyme activity was observed at pH 9.6 and pH 11.10. Minor peaks of activity were also observed at pH 7.2 and pH 12.5.

When the specific activity of linseed enzyme at different pH was compared with those from different days of germination, enzymes of Day 2 linseed seedlings showed highest LOX specific activity. Four days analysis of LOX activity and pH optimization showed that linseed homogenate had two pH optima, first at pH 9.6 ($\pm$ 0.07) and second at pH 11.2 ($\pm$ 0.3). Further, linseed enzyme based enzymatic reactions were -

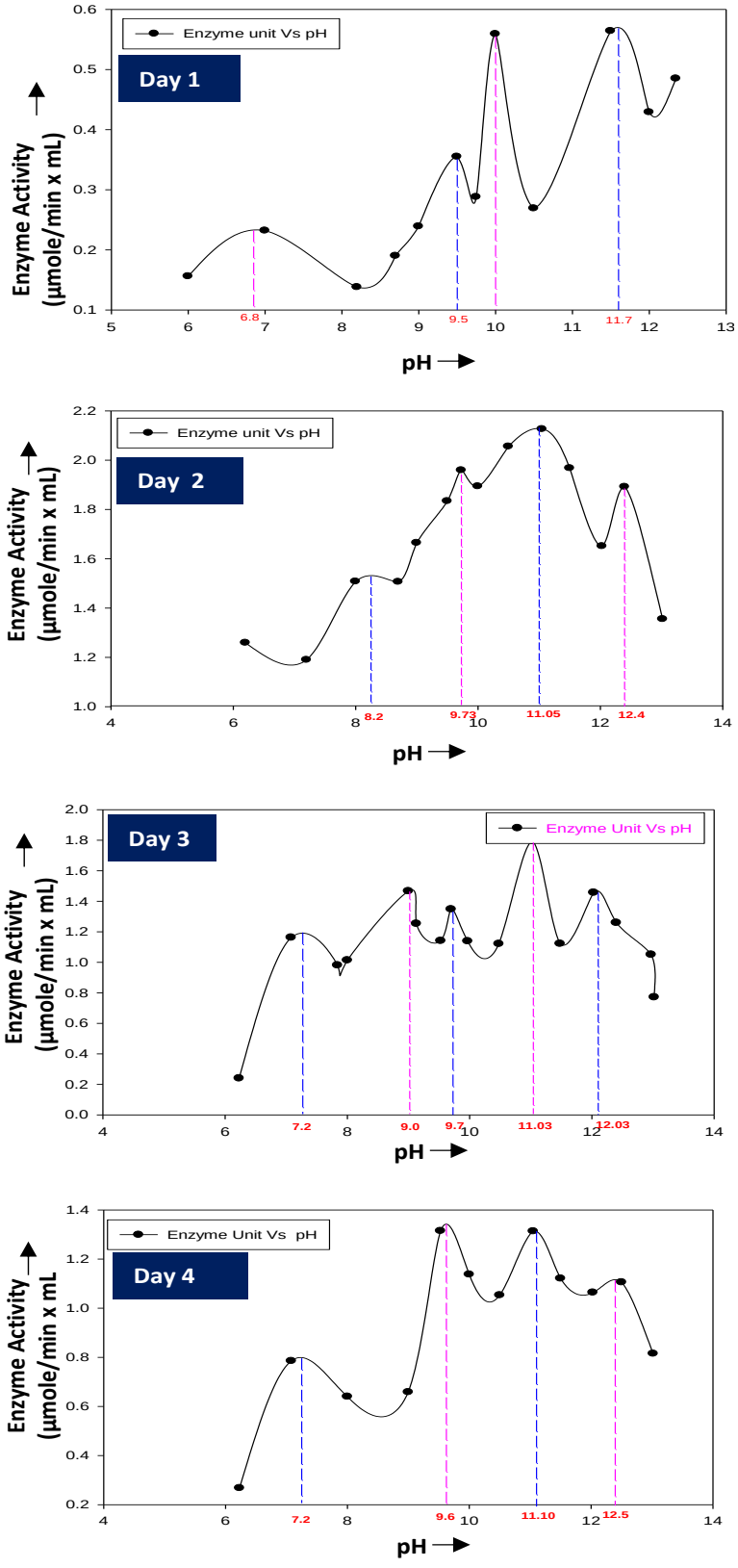

Figure 3-2: ***pH optimization of Linseed seedling enzyme***. Different days linseed seedlings were homogenized in Tris-Cl buffer (125 mM, pH 8.0). Enzyme activity was assayed on oxygraph (Strathkelvin 782 oxygen system version 3.0, Model 782), at various pHs (pH 6.0-pH13.0) at 25°C.

performed at pH 9.6 only. Temperature optimization was performed on Oxygraph, which showed the optimum enzymatic activity of linseed seedling enzyme at 40°C (Figure 3-3).

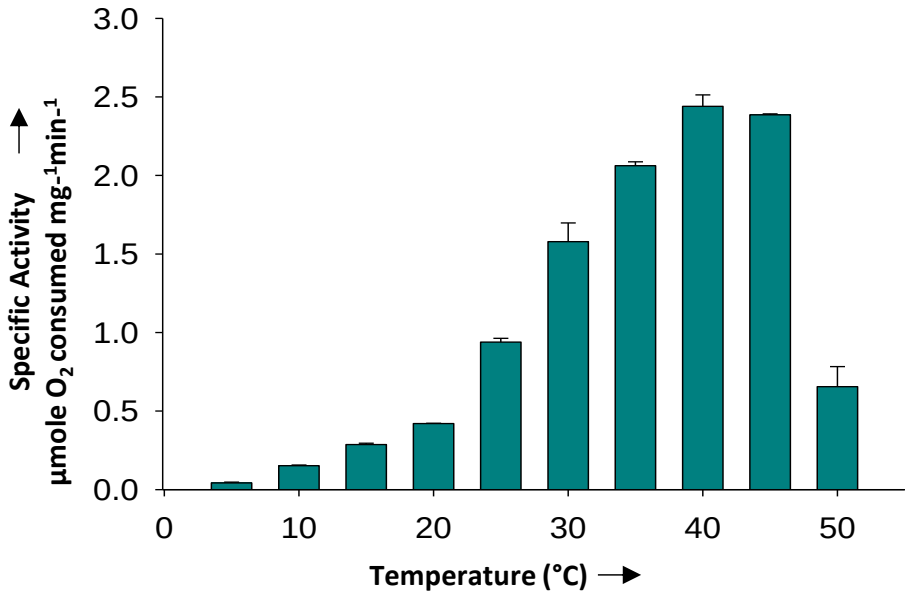

Figure 3-3: ***Temperature optimization of linseed seedling enzyme.*** Enzymatic activity was assayed on oxygraph (Strathkelvin 782 oxygen system version 3.0, Model 782) and the specific activity was calculated by determining protein contents, at various temperatures (5°C to 50 °C) at pH 9.6.

3.4.3 Linseed enzyme uses ω-6 and ω-3 PUFAs as substrate.

The linseed enzyme was incubated with ω-6 PUFAs (AA, and LA) and ω-3 PUFAs (ALA). The reaction mixtures were extracted with organic solvent (described in materials and methods) and purified on HPLC. The HPLC chromatogram showed the formation of products with both the ω-6 and ω-3 PUFAs having absorption maxima at 235 nm but different retention time (Rt) (Figure 3-5). The peaks were collected and wavelength scan was performed, which showed the characteristic spectrum of conjugated diene present in LOXs product (Figure 3-4).

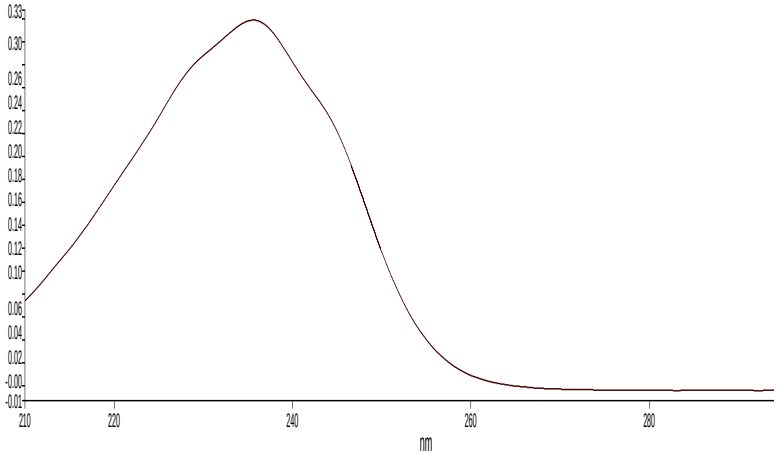

Figure 3-4 : ***Wavelength scan (210nm- 300nm) of HPLC peak collected from SP-HPLC***. It is showing characteristic conjugated diene spectrum at 235 nm measured on UV/VIS spectrophotometer (Perkin Elmer lambda 35)

3.4.4 Purification of metabolites generated by linseed enzyme on preparative straight phase HPLC (SP-HPLC).

The metabolites of linseed enzyme were synthesized by employing partially purified homogenate of Day 2 seedling with AA, LA, and ALA as the substrates at pH 9.6 as described in methodology. The AA, ALA and LA metabolites catalyzed by linseed seedling enzyme were extracted into an organic solvent. The products were purified on SP-HPLC by preparative column. The retention times of hydroperoxy and hydroxy metabolites (products formed with reduction by $NaBH_4$) of AA were 21.3 and 15.0 min respectively, (Figure 3-5A). Similarly, the retention times of hydroperoxy and hydroxy products of ALA were 22.0 and 19.7 min (Figure 3-5B) respectively. The absorption spectra of the metabolites when recorded on UV-VIS spectrophotometer, showed-

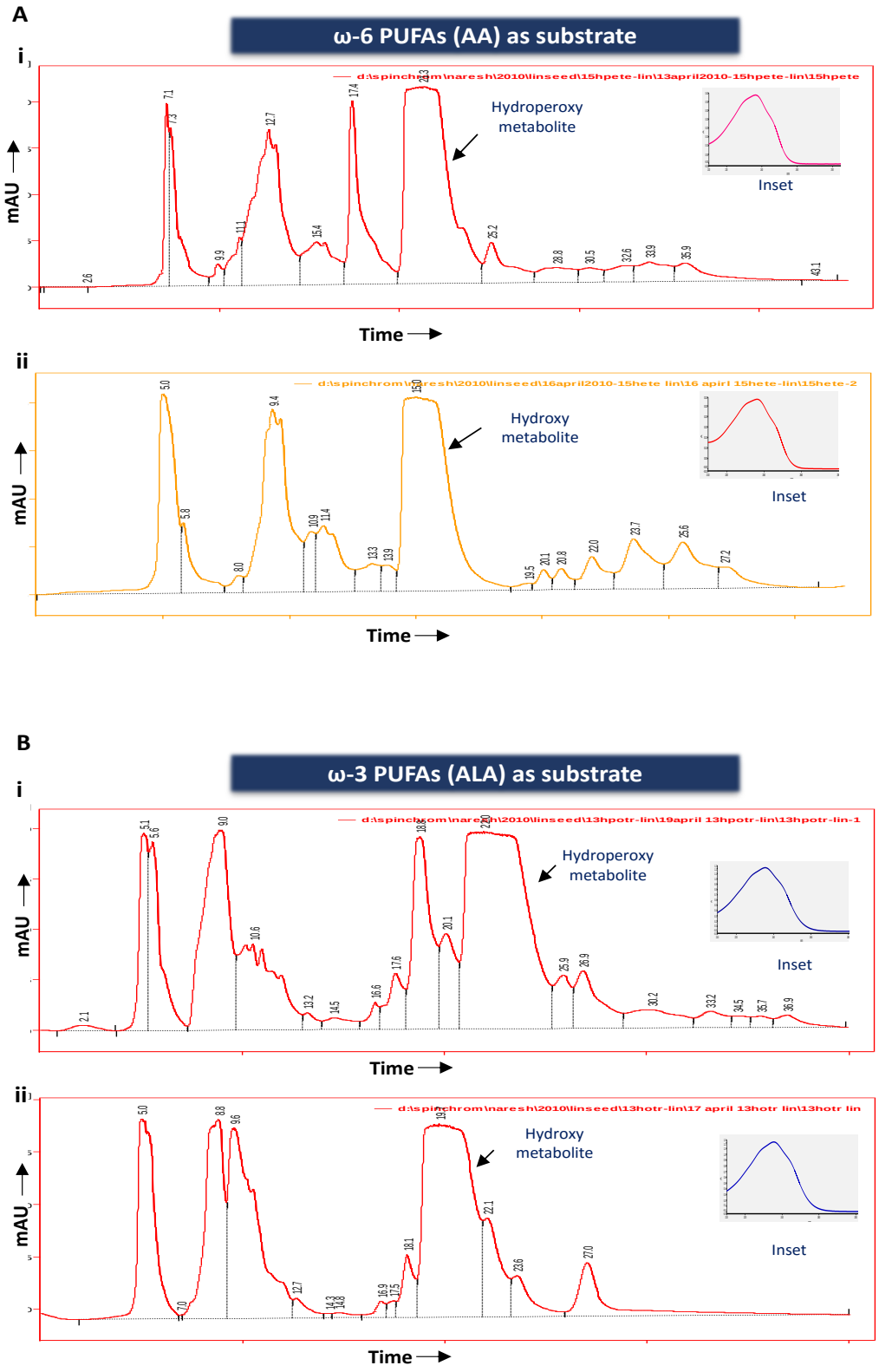

Figure 3-5 : ***HPLC chromatograms of PUFAs metabolites generated using Linseed lipoxygenase.*** The products were synthesized using linseed seedlings enzyme; ω-6 PUFA (AA) and ω-3 PUFA (ALA) were used as substrates. The products were purified on SP-HPLC system using hexane: propane-2-ol: acetic acid (1000:15:1) solvent system at 6 ml/min flow rate. **A).** i) Hydroperoxy and ii) hydroxy metabolites of ω-6 PUFA (AA) generated by employing Linseed seedlings lipoxygenase and purified on SP-HPLC. **B).** i) Hydroperoxy and ii) hydroxy metabolites of ω-3 PUFA (ALA) generated by employing Linseed seedlings lipoxygenase and purified on SP-HPLC. **(Inset)** The absorption spectra of the compounds when recorded on UV-VIS spectrophotometer, show characteristic conjugated diene spectra with maximum absorbance peaks at 235 nm.

Analysis of Linseed hydroperoxy metabolites of ALA on Analytical SP-HPLC

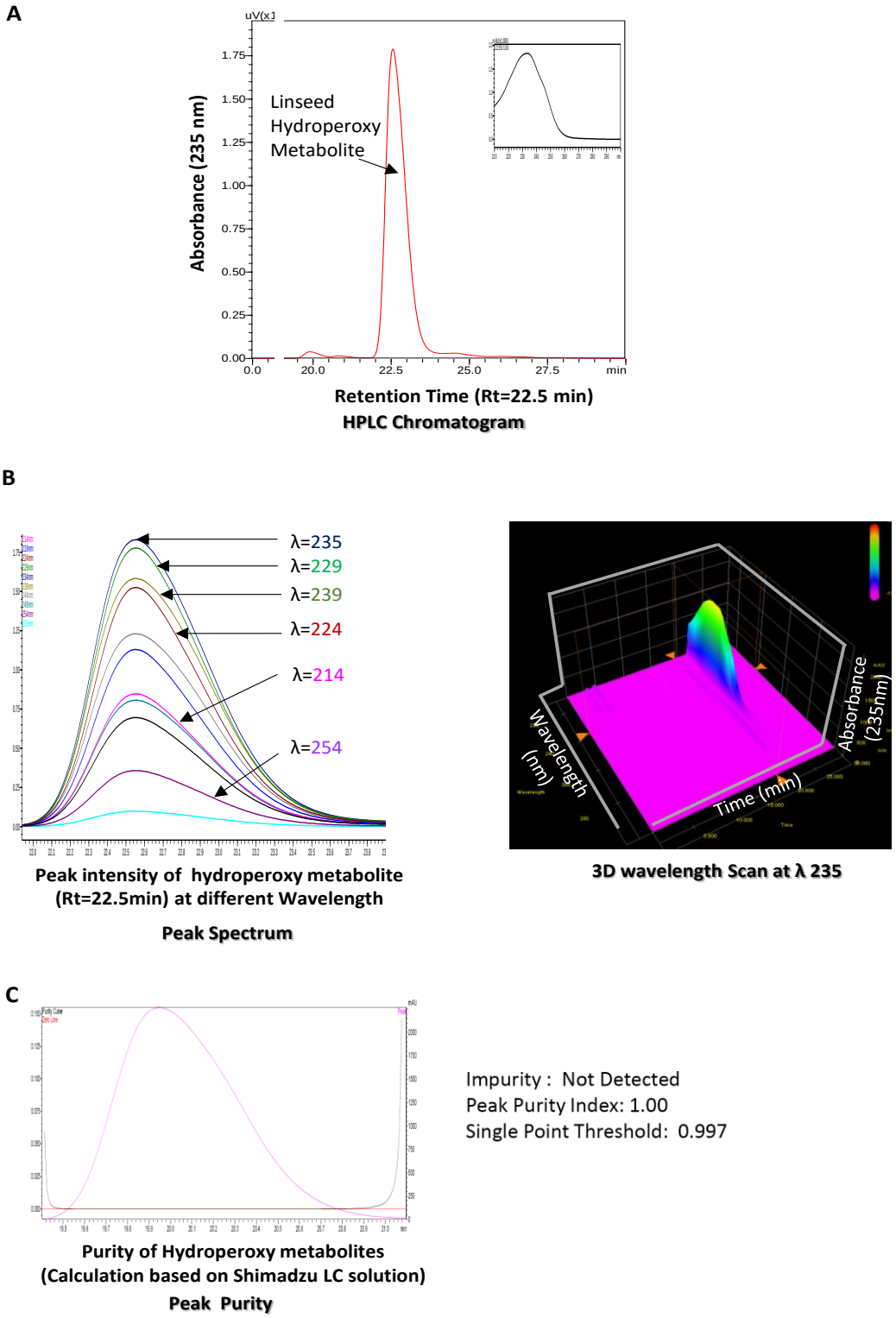

Figure 3-6: ***HPLC analysis of hydroperoxy metabolites of ALA catalyzed by Linseed lipoxygenase.*** **A)** HPLC chromatogram of hydroperoxy metabolite showing single and prominent peak (Rt=22.5 min). **B)** Image showing optimum absorbance of the peak (Rt=22.5 min) obtained above at 235 nm. The image showing real time absorbance of the selected peak at different wavelength obtained from HPLC PDA detector (Shimadzu, Japan). **C)** The image showing peak purity curve of the HPLC peak calculated by LC solution software associated with HPLC. It shows that the metabolite present in selected HPLC peak is free from impurity and having purity index 1.00.

Analysis of Linseed hydroxy metabolites of ALA On Analytical SP-HPLC

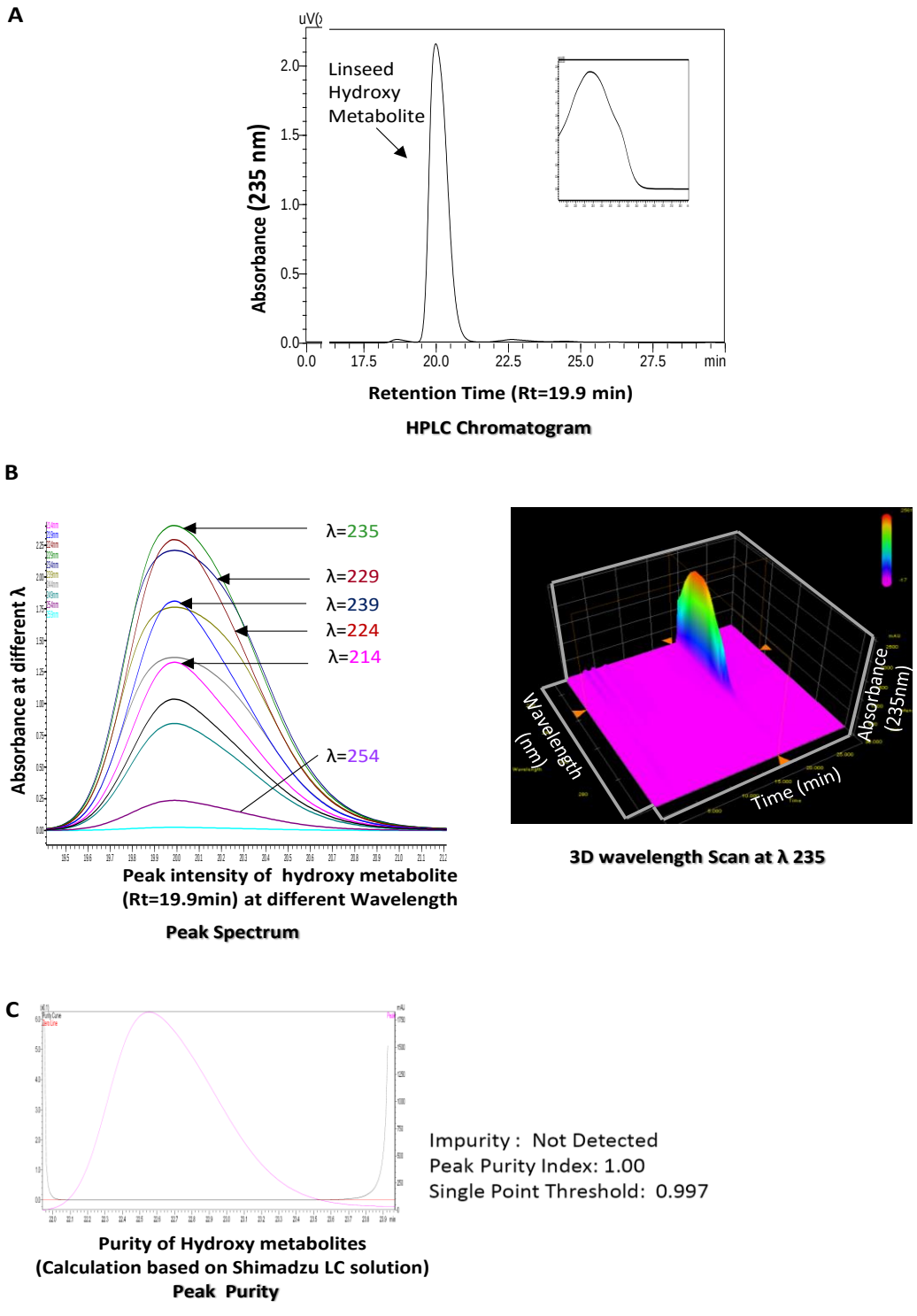

Figure 3-7: ***HPLC analysis of hydroxy metabolites of ALA catalyzed by Linseed lipoxygenase.*** **A)** HPLC chromatogram of hydroxy metabolites showing single and prominent peak (Rt=19.9 min). **B)** Image showing optimum absorbance of peak (Rt=19.9 min) obtained above at 235 nm. The image shows real time absorbance of the selected peak at different wavelength obtained from HPLC PDA detector (Shimadzu, Japan). **C)** The image showing peak purity curve of the HPLC peak calculated by LC solution software associated with HPLC. It shows that the metabolite present in selected HPLC peak is free from impurity and having purity index 1.00.

characteristic conjugated diene feature with peaks at 235 nm (Inset). The metabolites thus separated on SP-HPLC, were initially identified based on retention time in SP-HPLC solvent system. The purity of the metabolites was determined by peak purity curve, which showed 1.0 peak purity index and 0.997 single point threshold (Figure 3-6, 3-7).

3.4.5 Analysis of metabolites generated by linseed enzyme and comparison with soybean LOX metabolites.

The analysis of LOX activity of the enzyme from linseed seedling was initiated upon the reaction with PUFAs (AA, LA, and ALA) as substrate and purifying the hydroperoxy and hydroxy metabolites on SP-HPLC by preparative column. The wavelength scanning spectrum of the hydroperoxy product was observed on a spectrophotometer. The product showing absorption maximum at 235 nm was collected and then compared with soybean 15-LOX hydroperoxy and hydroxy metabolites of corresponding PUFAs by comparing retention times (Rt). The hydroperoxy and hydroxy metabolites of soybean LOX were considered as the standards. The prominent peak showed typical conjugated diene spectrum. The retention time of linseed hydroperoxy and hydroxy metabolites of ALA were 22.5 min and 19.5 min, respectively, while the retention time of hydroperoxy and hydroxy metabolites AA were 14.9 min and 8.8 min, respectively. The hydroperoxy and hydroxy metabolites of LA showed retention times of 22.8 min and 20.1 min, respectively. The HPLC chromatogram of linseed hydroperoxy and hydroxy metabolites of ALA when subjected to overlay with HPLC chromatogram of standard 13-(S)-HPOTrE and 13-(S)-HOTrE of soybean LOX, the two metabolites have shown same retention times corresponding to standard (Figure 3-8). The HPLC chromatogram of linseed hydroxy and

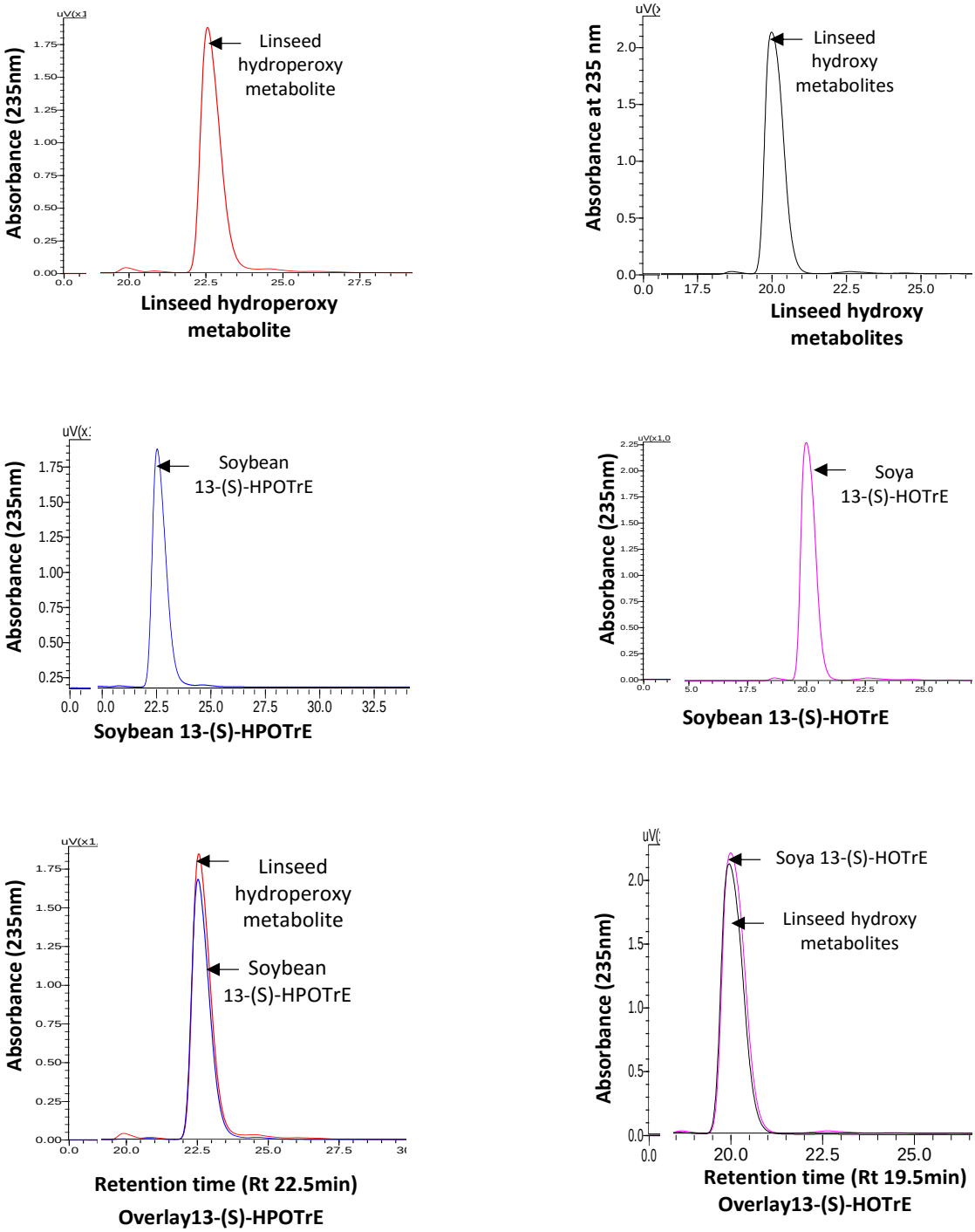

Figure 3-8: ***Comparison of linseed hydroperoxy and hydroxy metabolites of ALA with soybean hydroperoxy (13-(S)-HPOTrE) and hydroxy (13-(S)-HOTrE) metabolites of ALA, respectively.*** Overlay of HPLC chromatogram of linseed hydroperoxy (Red) and hydroxy (Black) metabolites of ALA over soybean (13-(S)-HPOTrE) (Blue) and (13-(S)-HOTrE) (pink) metabolites of ALA shows similarity of linseed hydroperoxy metabolite with 13-(S)-HPOTrE and hydroxy metabolite with 13-(S)-HOTrE. Analysis was performed on analytical SP-HPLC using hexane: propan-2-ol: acetic acid (1000:15:1) solvent system.

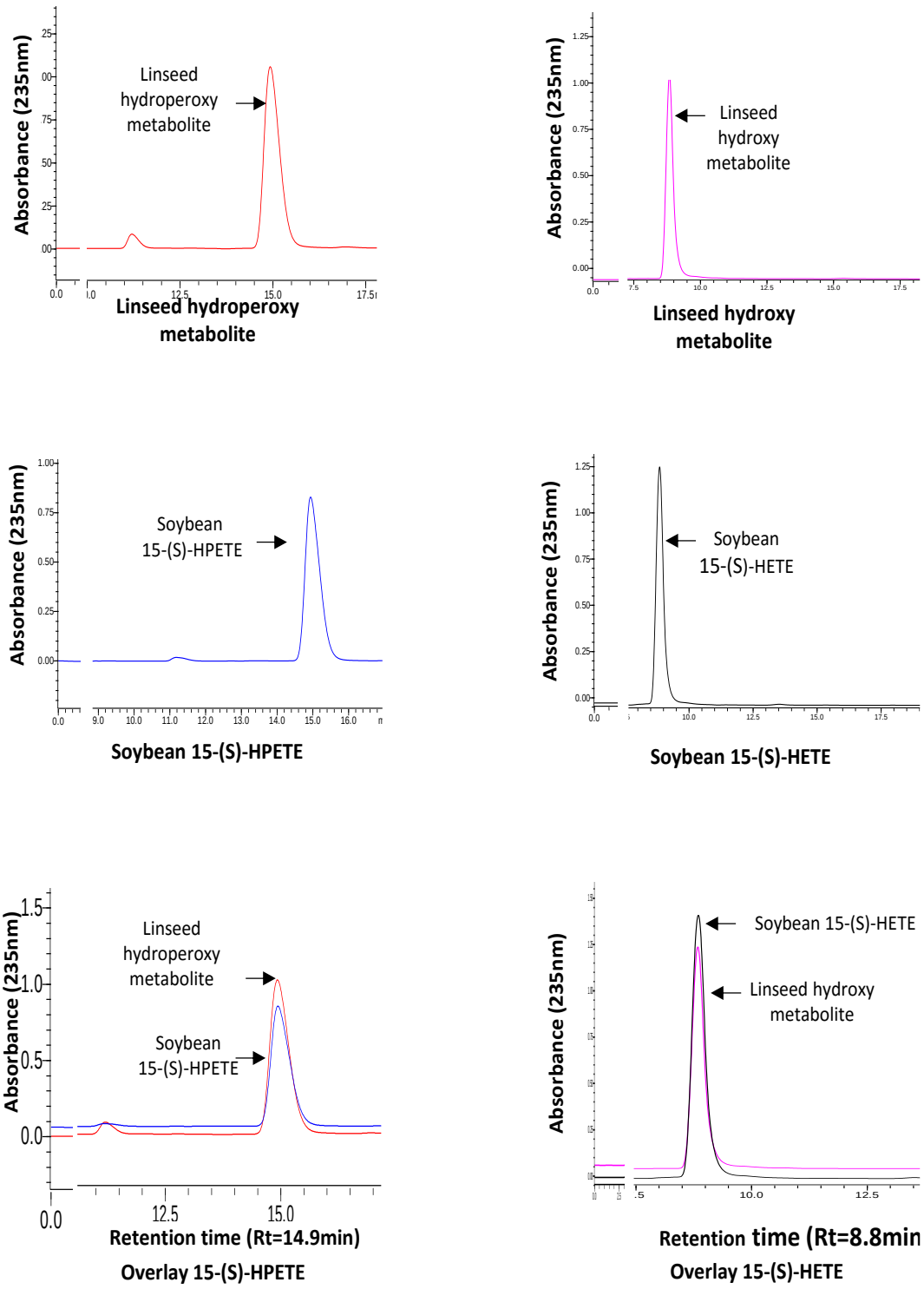

Figure 3-9: ***Comparison of linseed hydroperoxy and hydroxy metabolites of AA with soybean hydroperoxy (15-(S)-HPETE) and hydroxy (15-(S)-HETE) metabolites of AA.*** Overlay of HPLC chromatogram of linseed hydroperoxy (Red) and hydroxy (pink) metabolites of AA over soybean (15-(S)-HPETE) (Blue) and (15-(S)-HETE) (black) metabolites of AA shows similarity of linseed hydroperoxy metabolite with 15-(S)-HPETE and hydroxy metabolite with 15-(S)-HETE. Analysis was performed on analytical SP-HPLC using hexane: propan-2-ol: acetic acid (1000:15:1) solvent system.

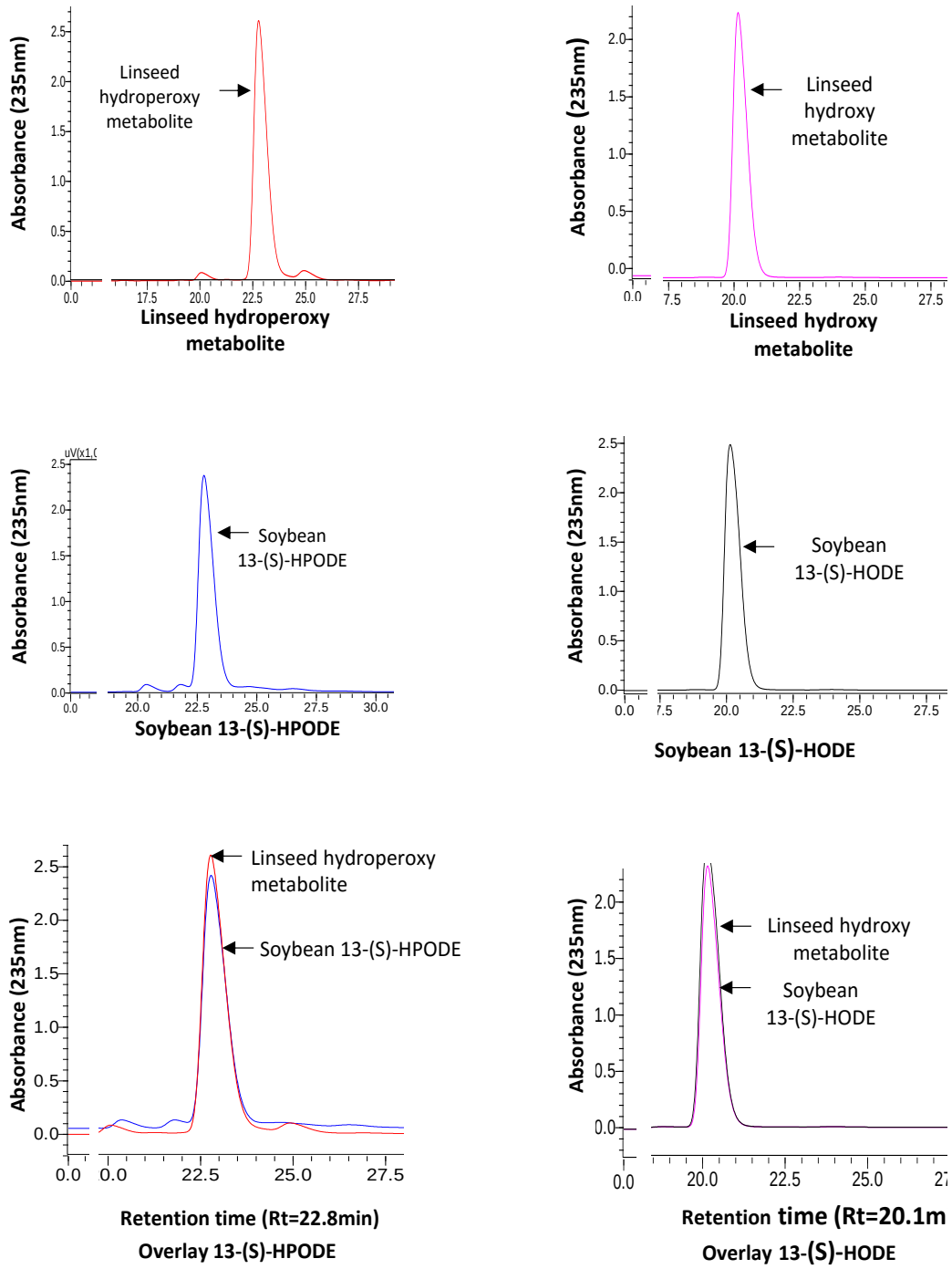

Figure 3-10 ***Comparison of linseed hydroperoxy and hydroxy metabolites of LA with soybean hydroperoxy (13-(S)-HPODE) and hydroxy (13-(S)-HODE) metabolites of LA.*** Overlay of HPLC chromatogram of linseed hydroperoxy (Red) and hydroxy (pink) metabolites of LA over soybean (13-(S)-HPODE) (Blue) and (13-(S)-HODE) (black) metabolites of LA shows similarity of linseed hydroperoxy metabolite with 13-(S)-HPODE and hydroxy metabolite with 13-(S)-HODE. Analysis was performed on analytical SP-HPLC using hexane: propan-2-ol: acetic acid (1000:15:1) solvent system.

and hydroperoxy metabolites of AA when subjected to overlay with HPLC chromatogram of standard 15-(S)-HPETE and 15-(S)-HETE of soybean LOX, the two metabolites have shown same retention times corresponding to standard (Figure 3-9). The similar pattern was observed when the HPLC chromatogram of linseed hydroperoxy and hydroxy metabolites of LA subjected to overlay with HPLC chromatogram of standard 13-(S)-HPODE and 13-(S)-HODE of soybean LOX, these two metabolites have also shown same retention times corresponding to standard (Figure 3-10).

3.4.6 Characterization of Linseed metabolites on LC-MS/MS.

Linseed hydroxy metabolite of AA, purified on SP-HPLC, was further characterized by LC-MS/MS. The metabolites were initially separated on the reverse phase solvent system (Methanol: water 80:20) using analytical silica column (C-18) at a flow rate of 1 ml/min on LC-MS/MS. Similarly, soybean 15-(S)-HETE (standard) was also subjected to LC-MS/MS. Linseed metabolite of AA and Soybean 15-(S)-HETE showed the same retention time (4.0 min) in LC-MS/MS (Figure 3-11). The major fragmentation detected in both linseed metabolite and soybean 15-(S)-HETE were identical with peaks at 321, 301, 251, 219 and 205 (Figure 3-12 and Figure 3-13).

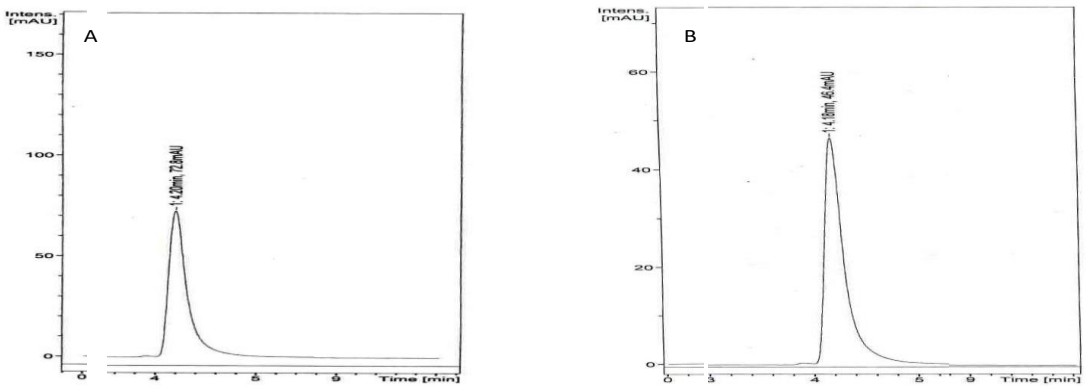

Figure 3-11: ***Comparison of linseed LOX metabolite of AA with soybean 15 LOX metabolites of AA (15-(S)-HETE) on LC-MS/MS using mobile phase solvent, Methanol: Water (80: 20).*** **(A)** RP-HPLC chromatogram showing linseed hydroxy metabolite of AA on LC-MS/MS, retention time 4.0 min. **(B)** RP-HPLC chromatogram showing soybean 15-(S)-HETE on LC-MS/MS, retention time 4.0 min.

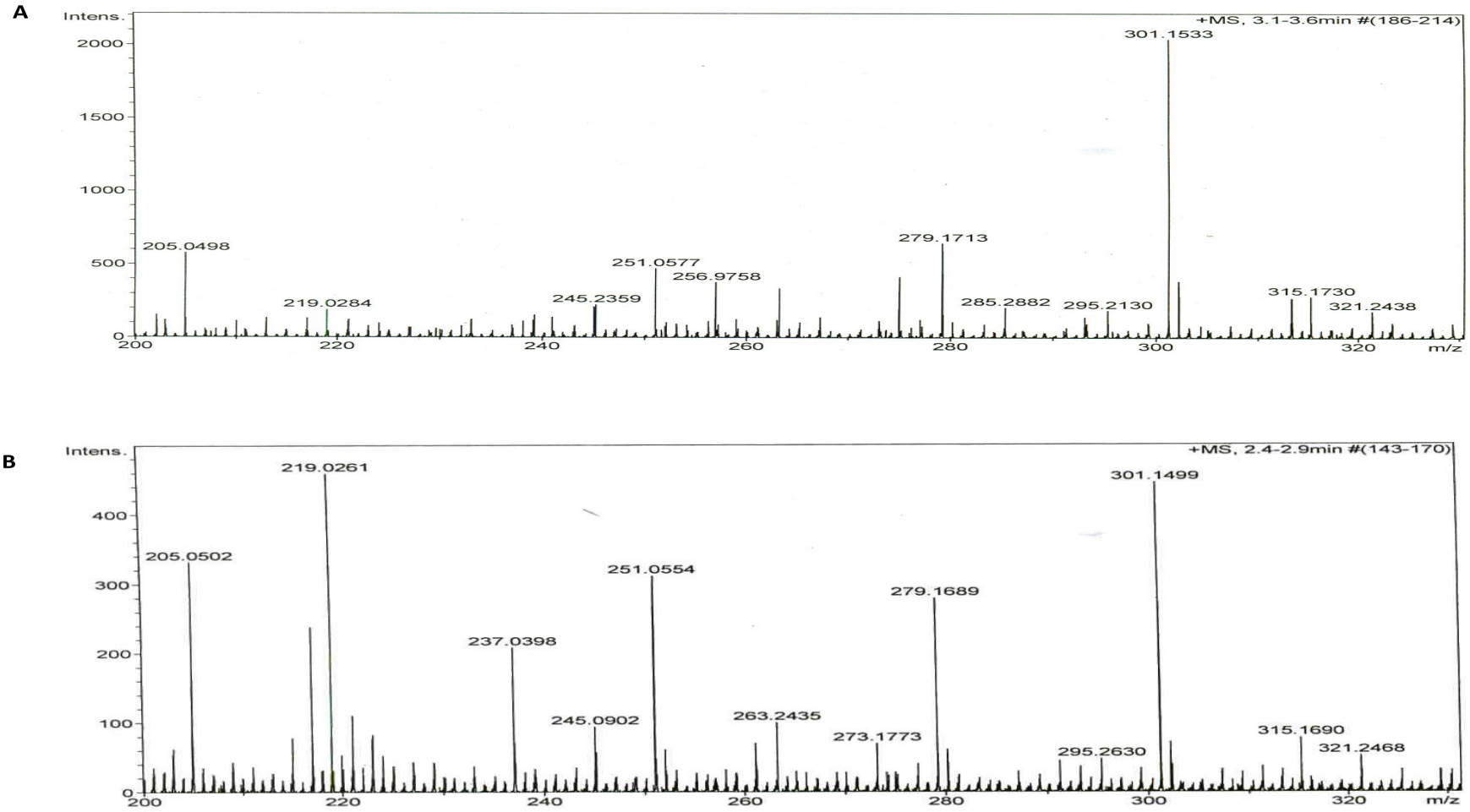

Figure 3-12: ***Comparison of linseed seedling LOX metabolite of AA with soybean 15 LOX metabolite of AA (15-(S)-HETE) on LC-MS/MS in positive mode at capillary volt 3800V and collision cell RF 120V_{pp}.*** **A)** Fragmentation pattern of Linseed hydroxy metabolite of AA in LC-MS/MS in positive mode. **B)** Fragmentation pattern of soybean 15-LOX metabolite 15-(S)-HETE in LC-MS/MS in positive mode.

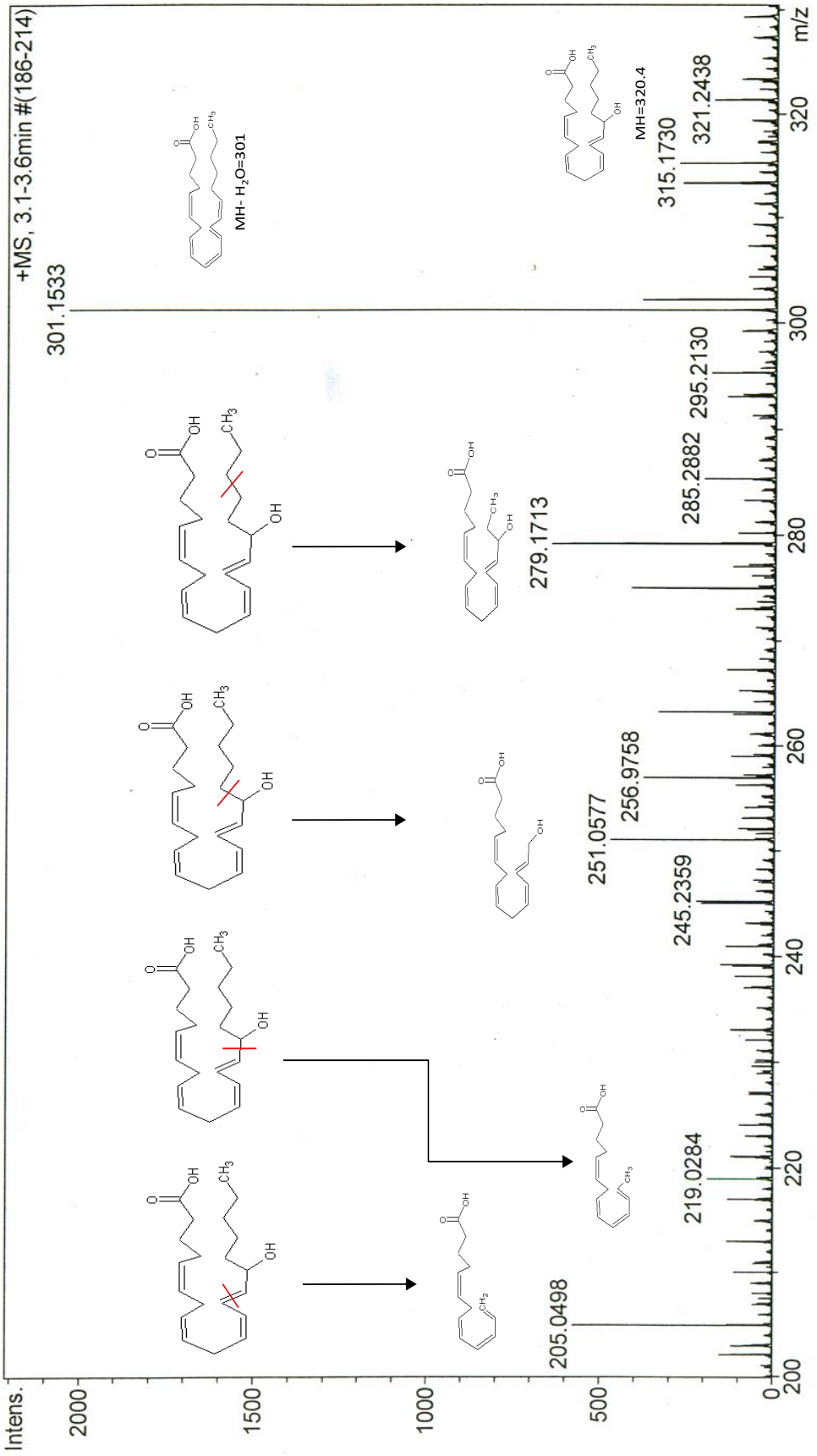

Figure 3-13: The fragmentation of hydroxy metabolite of linseed seedling LOX using AA as substrate, accounting for the peaks observed on LC-MS/MS. It is showing the characteristic fragmentation pattern of 15-(S)-HETE – a 15 LOX metabolite of soybean.

3.5 Discussion

In plants, LOXs play vital role, which starts from seed germination to fruit ripening and plant senescence [126]. Several studies reported that there are many fold increase in LOXs expression during early hours of seed germination [114] and as the seedling develops, the LOXs activity decreases significantly. In the present study, linseed seedling showed abundant LOX activity. Enzymatic activity of seedling was assayed by oxygraph that measures molecular O_2 in the reaction chamber. It showed that linseed seedling contains enzymatic activity, which varies as the seedling develops. It was noticed that the specific activity of the enzyme of day 2 seedling was significantly higher in comparison to the enzyme of the day1-4 seedling. The increase in enzymatic activity in early linseed seedling and a significant decrease in day 3 and day 4 seedling supports the previous findings which reported in other plants during seed germination [114]. The linseed seedling enzyme used ω-6 (AA, LA) and ω-3 PUFAs (ALA) as substrates and showed rapid oxygen consumption, when measured on oxygraph, suggesting the possibility of LOX activity in the linseed seedlings. The enzyme activity of linseed seedling assayed at various pHs ranging from pH 6.0 to 13.0, showed several majors and minor peaks. The presence of such peaks reveals the possibility of different isoforms of LOXs showing different pH optima at different days. The possibility of 15-LOXs in linseed seedling was further strengthened by comparing metabolites of linseed seedling with metabolites of soybean 15-LOX on HPLC. In SP-HPLC, the stationary phase is hydrophilic (polar) in nature while mobile phase contains hydrophobic solvent (nonpolar solvent e.g. heptane, hexane) mixed with more polar solvent (e.g. ethyl acetate, isopropanol, chloroform). Silica and other organic groups such as amino and cyano are generally

used as stationary phase. The Linseed seedling enzyme also catalyzed AA, LA (ω-6 PUFAs) and ALA (ω-3 PUFA) and generated corresponding hydroperoxy metabolites while hydroxy metabolites were generated by further reduction of hydroperoxy metabolites. When purified on SP-HPLC, the soybean hydroperoxy metabolites of ALA, AA and LA (13-(S)-HPOTrE, 15-(S)-HPETE, and 13-(S)-HPODE) showed more retention times and eluted late as compared to corresponding hydroxy metabolites (13-(S)-HOTrE ,15-(S)-HETE, 13-(S)-HODE). The peak purity index showed the purity of PUFAs metabolites synthesized by linseed seedling enzyme.

The hydroperoxy and hydroxy metabolites of linseed seedling enzyme synthesized using ALA, AA, and LA, were compared with corresponding standard hydroperoxy and hydroxy metabolites of soybean LOX using same substrates on SP-HPLC. When the hydroperoxy metabolites of linseed seedlings using ALA as the substrate, compared with hydroperoxy metabolites (13-(S)-HPOTrE) of soybean LOX using ALA as the substrate, showed same retention time (22.5 min). Similarly when the hydroxy metabolites of linseed seedling using ALA as the substrate, compared with hydroxy metabolites (13-(S)-HOTrE) of soybean LOX using ALA as the substrate, also showed same retention time (19.5 min). Similarly, the hydroperoxy and hydroxy metabolites of seedling using ω-6 PUFAs (AA, and LA) as the substrates, showed same retention time of corresponding hydroperoxy and hydroxy metabolites of standard soybean 15-LOX. Thus, the HPLC chromatogram of the hydroperoxy and hydroxy metabolites of linseed seedlings overlay showed same retention times when compared to corresponding hydroperoxy and hydroxy metabolites of soya LOX.

The overlay HPLC chromatogram of hydroperoxy and hydroxy metabolites of linseed seedling with standard soybean hydroperoxy and hydroxy metabolites indicate that linseed seedling enzyme might be 15-LOX, which might catalyze PUFAs and generated the same hydroperoxy and hydroxy metabolites as catalyzed by soybean 15-LOX.

The initial assays based on oxygraph indicated the possibility of LOXs in linseed seedling. Furthermore, the comparison of the retention times of hydroperoxy and hydroxy metabolites of linseed seedling enzyme with the hydroperoxy and hydroxy metabolites of soybean 15-LOX (standard) strengthen such a possibility. The presence of 15-LOX in linseed seedling was confirmed by analyzing the fragmentation patterns of the metabolite of linseed seedling with the corresponding metabolite of soybean 15-LOX on LC-MS/MS.

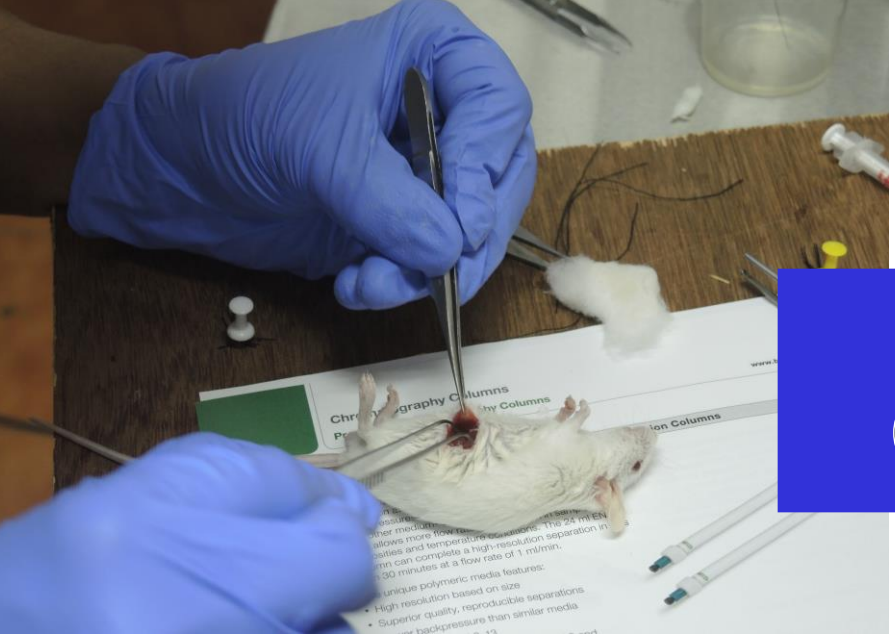

Chapter 4

STUDY THE EFFECTS OF 15-LOX METABOLITES OF ALA [13-(S)-HPOTrE AND 13-(S)-HOTrE] ON INFLAMMATION AND ELUCIDATE THE SIGNALLING PATHWAYS INVOLVED: *IN VITRO* AND *IN VIVO* STUDIES

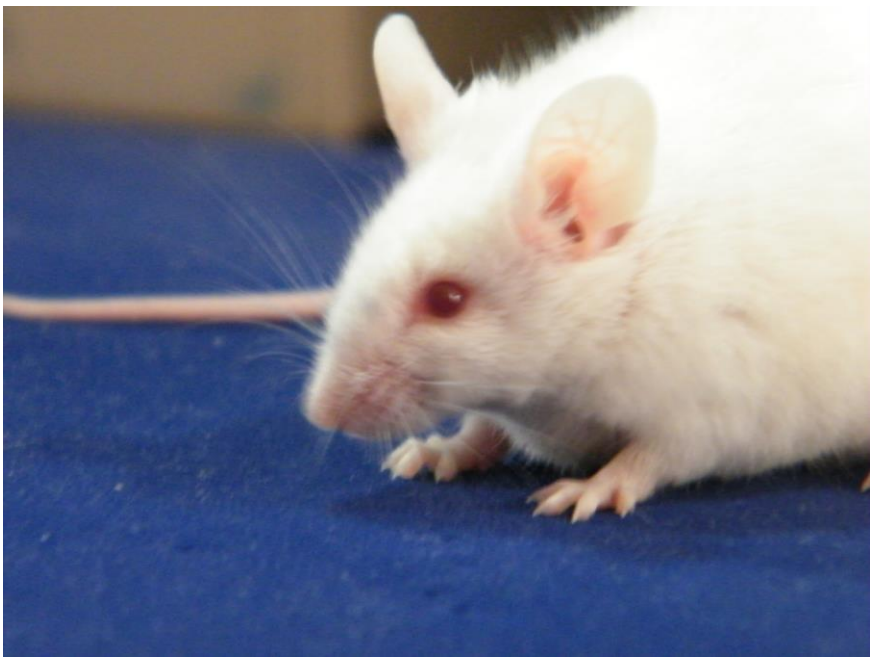

4.1 INTRODUCTION

Inflammation is an essential part of host's response to infection or injury in order to maintain cellular homeostasis. Aberrant inflammation is associated with various disorders mediated by hyperactivation of inflammasome complexes and up-regulation of pro-inflammatory enzymes like iNOS, LOXs and COXs [88–92]. The inflammatory responses generated by eicosanoids, is known to be mediated by pro-inflammatory cytokines such as IL-1β and TNF-α [93].

Increased ratio of ω-6 to ω-3 PUFAs is hypothesized to elevate pro-inflammatory eicosanoid production and thus the onset of inflammatory diseases. A sufficiently high intake of ω-3 PUFAs, on the other hand, is shown to offer protection from inflammatory diseases by decreasing the production of pro-inflammatory eicosanoids, cytokines, ROS and RNS [100,101]. In addition, it is reported that increasing ω-3 PUFAs tissue levels by dietary or genetic means decreases the pathological retinal angiogenesis by suppressing TNF-α [50]. These beneficial effects of ω-3 PUFAs appear to be mediated by the oxygenated metabolites formed via the LOXs and COXs pathways [97,127–130].

COX-2, an inducible enzyme that converts ω-6 PUFAs such as AA to pro-inflammatory prostaglandins, has been widely recognized as the major pathway responsible for inflammation as it triggers the production of other pro-inflammatory chemokines and cytokines [130]. However, this concept is challenged by recent findings on COX-2 derived oxidative metabolites of ω-3 PUFAs possessing anti-inflammatory and anti-oxidant properties [131,132]. These studies suggest that the ultimate pro/anti-inflammatory effects of COX-2 depend on the substrate on which these enzymes act, ω-6 or ω-3 PUFAs [133,134] and their down-stream metabolites-PGE_2 and/or PGD_2. While

PGE_2 is associated to shifting of M1 macrophages (pro-inflammatory) into M2 macrophages (anti-inflammatory) [135,136], PGD_2 exhibits anti-inflammatory effects by its conversion to PGJ_2 and subsequently 15-deoxy-$\Delta^{12,14}$ PGJ_2 (15d-PGJ_2) a well-known ligand with high affinity for peroxisome proliferator-activated receptor-γ (PPAR-γ) [137–139]. LOXs, on the other hand, are majorly classified into 5-, 12- and 15-LOXs, depending on the position at which AA is oxygenated. These LOX isoforms have been implicated in a variety of inflammatory and hyperproliferative and neurodegenerative diseases [140]. While 5-LOX is pro-inflammatory in nature [141], the 15-LOX exhibits anti-inflammatory properties [142,143]. Earlier we have shown the anti-inflammatory and anti-cancer properties of 15-LOX metabolites of AA and elucidated the mechanisms involved [144] [145] [17]. In the present study, we report the anti-inflammatory effects of 15-LOX metabolites of ALA, the precursor for EPA and DHA, on LPS stimulated mouse macrophage cell line, RAW 264.7 and primary peritoneal macrophages isolated from BALB/c mice and demonstrated that these effects are mediated by inactivating NLRP3 inflammasome complex through the PPAR-γ pathway. Further, we report on the extended survival of BALB/c mice in endotoxin-mediated septic shock and polymicrobial sepsis in CLP mouse model.

4.2 Materials and Methods

4.2.1 Chemicals and Reagents

Culture medium DMEM, penicillin, streptomycin, PBS, Trypsin-EDTA and fetal bovine serum (FBS) were purchased from Gibco. MTT, 2’-7'-Dichlorodihydrofluorescein diacetate (DCFH-DA), LPS (lipopolysaccharide from *E. coli, 0127:B8)*, Griess reagent, Dexamethasone (Dex) and GW9662 (2-chloro-5 nitrobenzanilide) were purchased from Sigma-Aldrich, USA. Anti-Beclin-1, anti-Caspase-1, anti-NF-κB and anti-TNF-α antibodies

were purchased from Abcam (MA, USA). Anti-LC-3 antibody was purchased from Cell Signalling while anti-COX-2 antibody was obtained from Santa Cruz Biotechnology Inc. (Texas, USA). Anti-iNOS antibody was purchased from Thermo Fisher Scientific (MA, USA). Enzyme immunoassay kit for IL-1β, IL-10 and PGE_2 were purchased from R&D system, Inc. (MN, USA) whereas PGD_2 assay kit was purchased from Cayman Chemical Company (Ann Arbor, MI, USA). AA, LA, ALA, and DHA were procured from Nu-Chek-Prep (MN, USA). The 15-LOX metabolites of ALA, 13-(S)-HPOTrE and 13-(S)-HOTrE, were generated essentially employing the methods described earlier for generation of 5-LOX metabolites [116,123,124].

4.2.2 Animals

BALB/c, male mice, 4-week old weighing 20-25 g were purchased from Centre for Cellular and Molecular Biology, Hyderabad, India. Mice were housed at constant room temperature (23±1°C) and allowed to water and food *ad libitum* in 12 h dark/light cycle. The mice were kept at least 1 week in animal house before performing any experiment. The mice used in this study were handled carefully and according to the *Guide for the care and use of Laboratory animals* published by NIH (National Institute of Health). The experimental protocol was approved by Institutional Animal Ethics Committee (IAEC), University of Hyderabad, India.

4.2.3 Cell culture and Treatments

The mouse macrophage cell line, RAW 264.7 was obtained from NCCS (Pune, India). The cells were grown and maintained in DMEM supplemented with 10% heat-inactivated FBS, 100 IU/ml penicillin and 100 µg/ml streptomycin in a humidified atmosphere with 5% CO_2 at 37°C. Sub-culturing of cells was done twice a week. Fresh culture medium was used before each treatment. Cells were pre-incubated with

different concentrations (1, 50 and 100 µM) of ALA metabolites, 13-(S)-HPOTrE) and 13-(S)-HOTrE or with Dexamethasone (10 µM) for 3 h then challenged with LPS (100 ng/ml) for different time points as mentioned in experiments. The anti-inflammatory drug, dexamethasone was used as positive control. For inhibitor study, cells were pre-incubated with 10 µM GW9662 for specific time periods as mentioned in experiments. For analysis of the inflammasomes and IL-1β measurements, RAW 264.7 cells and peritoneal macrophages were incubated with 1mM ATP for 30 min prior to end time points.

4.2.4 Isolation of Primary Peritoneal Macrophages

Primary peritoneal macrophages were isolated from thioglycolate-elicited BALB/c male mice as described by Xia Zhang et al [146]. Briefly, in BALB/c male mice, 3% thioglycolate broth (1 ml) was injected through i.p. After 3 days, mice were euthanized by cervical dislocation. 5 ml ice-cold DMEM was injected into the peritoneal cavity. The abdomen was finger tapped 4-5 times and peritoneal lavage was aspirated and collected in a cold sterile centrifuge tube. Further, centrifugation was done at 1500 rpm for 5 min, pellets were resuspended in DMEM and cell counting was done by haemocytometer. The appropriate number of cells were grown and maintained in DMEM, macrophages enrichment was done by washing and removing unattached cells from culture plate, further grown as described above for RAW 264.7 cells, and treated with 13-(S)-HPOTrE and 13-(S)-HOTrE as mentioned in experiments for RAW 264.7 cells.

4.2.5 Cytotoxicity Assay

Cytotoxicity of ALA metabolites was assayed by MTT assay. To perform this assay, RAW 264.7 cells were seeded in 96 well plates at a density of $5X10^4$ cells/well then treated with ω-6 PUFAs (AA, and LA), ω-3 PUFAs (ALA and DHA) and 15-LOX

metabolites of ALA [13-(S)-HPOTrE and 13-(S)-HOTrE] at various concentrations (1, 50, 100 and 200 µM) for different time points. Cell viability was measured colorimetrically by MTT assay as described by Mossman [103].

4.2.6 Nitrite Estimation

RAW 264.7 cells were seeded in 6 well plates for 12 h then pre-incubated with different concentrations (1, 50 and 100 µM) of ALA metabolites [13-(S)-HPOTrE and 13-(S)-HOTrE], or dexamethasone for 3 h then stimulated with or without LPS (100 ng/ml) for the next 24 h. At the end of the time point, stable nitrite level in the culture supernatant was measured by Griess Reagent. For this, 50 µl of cell culture medium was mixed with 50 µl of Griess reagent and incubated at room temperature for 10 min in the dark. Then absorbance was measured at 540 nm using multi-mode plate reader (BioTek, SynergyMx). Nitrite level in samples was determined by using the standard curve of sodium nitrite. Culture medium was taken as blank for all experiments.

4.2.7 Estimation of IL-1β, IL-10, PGD2 and PGE2

Levels of IL-1β, IL-10, PGE_2 and PGD_2 in culture medium were measured by ELISA kit according to manufacturer's protocol. Their levels in culture medium were determined by using standard curves of respective cytokine or prostaglandin standards provided along with the kit.

4.2.8 Measurement of Reactive Oxygen Species (ROS)

RAW 264.7 cells were seeded in 6 well plates at a density of $2x10^5$ cells/well then pre-incubated with different concentrations (1, 50 and 100 µM) of ALA metabolites [13-(S)-HPOTrE and 13-(S)-HOTrE] and/or N-Acetyl Cysteine (NAC, 5 mM), for 3 h. Then cells were further stimulated with or without LPS (1 µg/ml) for next 16 h. After that cells from each well were harvested and washed twice with PBS and further

incubated with 10 mM DCFH-DA for 30 min in dark at 37ºC and then two times washed with PBS. About 10,000 cells per sample were taken for analysis. The measurement was performed on a Flow Cytometer and data analysis was done by Cell Quest software (FACS Calibur, Becton Dickinson, CA, USA) with excitation of DCF at λ 488 nm and emission at λ 525 nm. Primary macrophages isolated from peritoneal cavity were seeded in 12 well plates and grown as mentioned earlier. Then pre-treated with 13-(S)-HPOTrE and 13-(S)-HOTrE at 100 nM for 3 h. Then stimulated with LPS and ROS was measured as described above.

4.2.9 Anti-inflammatory Effects of ALA Metabolites in vitro employing RAW 264.7 cells and Mouse Peritoneal macrophages: Immunoblot Analysis

RAW 264.7 cells seeded in 100 mm plates at a density of $5x10^5$ cells/well and after 12 h pre-incubated with different concentrations (1, 50 and 100 µM) of either ALA metabolites or dexamethasone (10 µM) for 3 h. For Immunoblot analysis of primary cells, mouse peritoneal macrophages were isolated and seeded in 60 mm plates. Then pre-treated with lower doses (100 nM and 400 nM) of ALA metabolites for 3 h. Cells were then stimulated with or without LPS (100 ng/ml) for next 24 h. Cells were harvested at the end of time point, pelleted down and stored at -80°C for further use. Cell pellets were lysed in RIPA buffer containing 1x protease inhibitor at 4°C. Protein estimation was done by Bradford method using BSA as standard. An equal amount of protein was loaded and separated on 8-15% SDS-PAGE and transferred to nitrocellulose membrane. Then membranes were blocked with 5% (w/v) fat-free dry milk in TBST for 1 h at room temperature followed by washing three times with TBST. Membranes were incubated with primary antibodies (0.5-1.0 µg/ml) for 12 h at 4°C on a shaker incubator with gentle shaking followed by thrice washing with TBST. The membranes were then

incubated with respective secondary antibodies conjugated with HRP. Signals were then detected with western lightning plus ECL kit (PerkinElmer) and captured on Kodak Imaging System (KODAK Image station 4000 mm Pro).

4.2.10 Anti-inflammatory Effects of ALA metabolites: Reverse Transcription Polymerase Chain Reaction (RT-PCR)

RAW 264.7 cells were seeded in 6 well culture plate. At 60% confluency, cells were pre-incubated with different concentrations of either ALA metabolites (1, 50 and 100 µM) or dexamethasone (10 µM) for 3 h and then stimulated with LPS (100 ng/ml) for 24 h. Total cellular RNA was extracted from each well using TRIzol® Reagent according to the manufacturer's instructions (Invitrogen Bio Services, India, Pvt. Ltd). RNA quantification was performed by nanodrop (NanoDrop 2000TM, Thermo Scientific, DE, USA). cDNA of each sample was prepared by using 2 µg of RNA, 1µl MLV reverse transcriptase, 1 mM dNTP and 1µl oligo dT according to manufacturer's standardized protocol (Promega Corporation, WI, USA). PCR analyses were performed on aliquots of the cDNA prepared to detect iNOS, TNF-α, NLRP3, Caspase-1, IL-1β, IL-18, and GAPDH. The reactions were carried out in a volume of 20 µl containing (final concentration) 1 U Taq DNA polymerase, 0.2 mM dNTP, 100 pM of forward primers and reverse primers (Table 1), and 10 µl reaction buffer. After amplification, PCR products were electrophoresed on 1% agarose gels and visualized by ethidium bromide staining on UV irradiation (BIO-RAD, Universal hood II).

Table 1:	List of Primers used for RT-PCR
mRNA	**Sequences of Primers**
NLRP3	Forward Primer 5' CTT CCA GAC TGG TGA ACT GCTG 3', Reverse Primer 5' TCT CCA AGG GCA TTG CTT CG 3',
Caspase-1	Forward Primer 5' GAG CTT CAA TCA GCT CCA TCA G 3' Reverse Primer 5' AAT GTC CCG GGA AGA GGT AGA 3',
IL-1β	Forward Primer 5' AGC TTC CTT GTG CAA GTG TC 3', Reverse Primer 5' AAG GGA GCT CCT TAA CAT GCC 3',
IL-18	Forward Primer 5' TTC CTC TTG GCC CAG GAA CAA TG 3' Reverse Primer 5' CAA GGC GCA TGT GTG CTA ATC 3'
GAPDH	Forward Primer 5' AGG TCA TCC CAG AGC TGA ACG 3' Reverse Primer 5' CAC CCT GTT GCT GTA GCC GTA T 3'.
iNOS	Forward primer: 5' CCG CAT GAG CTT GGT GTT TG 3' Reverse primer: 5' AGT GCT TCA GTC AGG AGG TTG 3'
TNF-α	Forward Primer 5' TGT AGC CCA CGT CGT AGC AAA 3' Reverse Primer 5' AGA GGC AAC CTG ACC ACT CT 3',

Table 1 : ***List of Primers used for Semi-quantitative PCR***

4.2.11 Analysis of the inflammasome, autophagy and NF-κB translocation by confocal microscopy

RAW 264.7 cells were seeded in 6 well culture plates on sterile culture grade coverslips. When cells were 60% confluent, pre-incubated with ALA metabolites (100 µM) and/or with GW9662, PPAR-γ inhibitor, for 3 h, then stimulated with LPS (100 ng/ml) for 24 h. For the study of inflammasome and autophagy, stimulation of cells with LPS was done for 24 h and for NF-κB translocation; it was done for 16 h. However, for study NF-κB translocation on peritoneal macrophages, cells were treated with ALA

metabolites at lower concentration (100 nM) for 16 h. Fixation of cells was done by ice-cold 4% paraformaldehyde for 10 min at 4°C followed by washing in PBS with 0.2% Tween 20. Permeabilization in cells was done by ice-cold acetone: methanol (1:3) for 15 min at room temperature followed by washing in PBS with 0.2% Tween 20. To avoid nonspecific binding, blocking was done by incubating cells in 5% FBS in PBST for 1 h at room temperature followed by twice washing in PBS with 0.2% Tween 20. Cells were then incubated with targeted primary antibody (1:100 dilution) in 3% BSA in PBST for 12 h at 4°C followed by washing thrice in PBS with 0.2% tween 20. Cells were then incubated with the fluorescent conjugated respective secondary antibody (1:300 dilutions) in 3% BSA in PBST for 1 h at room temperature in the dark. Finally, washings were done and coverslips mounted on slides by anti-fade reagent with DAPI (ProLong Gold Antifade reagent, Invitrogen, USA). Image analysis was done on a confocal microscope (Zeiss LSM700, USA).

4.2.12 Analysis of Apoptosis by FACS

RAW 264.7 cells were seeded in 6 well cultures plate. When cells were 60 % confluent, pre-incubated with different concentrations of either ALA metabolites (1, 50 and 100 µM) and/or doxorubicin (10 µM) for 3 h, then stimulated with LPS (100 ng/ml) for 24 h. Staining of cells was done by FITC Annexin V Apoptosis Detection Kit (BD Biosciences, CA, USA), according to manufacturer's standardized protocol. Samples were run on Flow Cytometer (BD, LSR Fortessa, CA, USA) and data analyses were done on BD FACS Diva™ software.

4.2.13 Induction of Inflammation in vivo: Septic Shock with LPS

BALB/c male mice (20 to 25 g) were divided into 4 different groups (10 mice in each group), control, LPS, LPS+13-(S)-HPOTrE, and LPS+13-(S)-HOTrE. LPS was dissolved

in saline (0.9% NaCl) and injected (30 mg/kg body weight) intraperitoneally (i.p.) in all mice except control. In control mice, 0.9% saline was injected. ALA metabolites were dissolved in saline having Tween 80 (0.9% NaCl + 0.5% Tween 80). Two i.p. doses of 13-(S)-HPOTrE and 13-(S)-HOTrE (0.1 mg/kg body weight, 2.5 µg/mice) metabolites were injected, first at 1 h prior to LPS and second, soon after LPS administration. 250 µl saline with Tween 80 (vehicle control) was injected in control and LPS treated groups. All mice were kept in normal conditions with an extra vigilance. Mice were monitored initially at 2 h intervals for 12 h then for 4 days.

4.2.14 Induction of Inflammation *in vivo:* Cecal Ligation and Puncture (CLP) model

Cecal Ligation and Puncture was performed in BALB/c male mice (20 to 25 g). Mice were divided into 4 groups (5 mice/group), Sham, CLP, CLP+13-(S)-HPOTrE and CLP+13-(S)-HOTrE. The mice were anesthetized with 60 µg/g ketamine and 10 µg/g xylazine. After cleaning and disinfecting the lower abdomen by iodine solution to prevent infection, a 1.5 to 2 cm incision was made through linea alba. Then, the cecum was spotted and ligated with disinfected 3-0 silk suture and perforated twice using a 22-gauge needle. Wound strength was ensured by squeezing out a small amount of stool. Then the cecum was replaced into the abdomen, and the incision was closed properly. In Sham, mice undergone surgery but ligation and puncture were not performed. Tramadol hydrochloride (20 µg/g body wt.) was injected i.p. with 1 ml warm saline in all mice. In ALA metabolites treated mice, two i.p. doses of 13-(S)-HPOTrE and 13-(S)-HOTrE (0.1 mg/kg body weight, 2.5 µg/mice) metabolites were given, first at 1 h prior to CLP and second, soon after CLP surgery. Finally, all mice were kept at normal conditions

with an extra vigilance. The mice were sacrificed after 24 h of CLP surgery then blood, peritoneal fluid, and liver were collected.

4.3 Statistical Analyses

All the experiments were performed in triplicates and the values represented as mean ± SD. Data were correlated, analyzed and p-values were obtained using student's t-test. The p-value <0.05 was considered as statistically significant.

4.4 Results

4.4.1 Hydroperoxy metabolites exhibit more cytotoxic effects on RAW 264.7 cells as compared to hydroxy metabolites of ALA.

The cytotoxic effects of 15-LOX metabolites of ALA [13-(S)-HPOTrE and 13-(S)-HOTrE] on RAW 264.7 cells were evaluated by MTT assay. Among these metabolites, 13-(S)-HPOTrE showed a more cytotoxic effect compared to the hydroxy metabolite, 13-(S)-HOTrE, when incubated at different concentrations for 24 h (Figure 4-1). Treatment with both metabolites decreased the proliferation of the cells in a dose and time-dependent manner. However, 13-(S)-HPOTrE and 13-(S)-HOTrE showed more cytotoxic effects when compared to ω-3 (ALA, and DHA) and ω-6 (AA, and LA) PUFAs (Figure 2-1). A 50% decrease in RAW 264.7 cell proliferation was observed at a concentration (IC50 value) of 114 µM 13-(S)-HPOTrE, which was much lower than 13-(S)-HOTrE (>200µM) at 24 h. Based on these results, further experiments on RAW 264.7 cells were carried out up to 100 µM concentration of ALA metabolites for analysis of their anti-inflammatory effects.

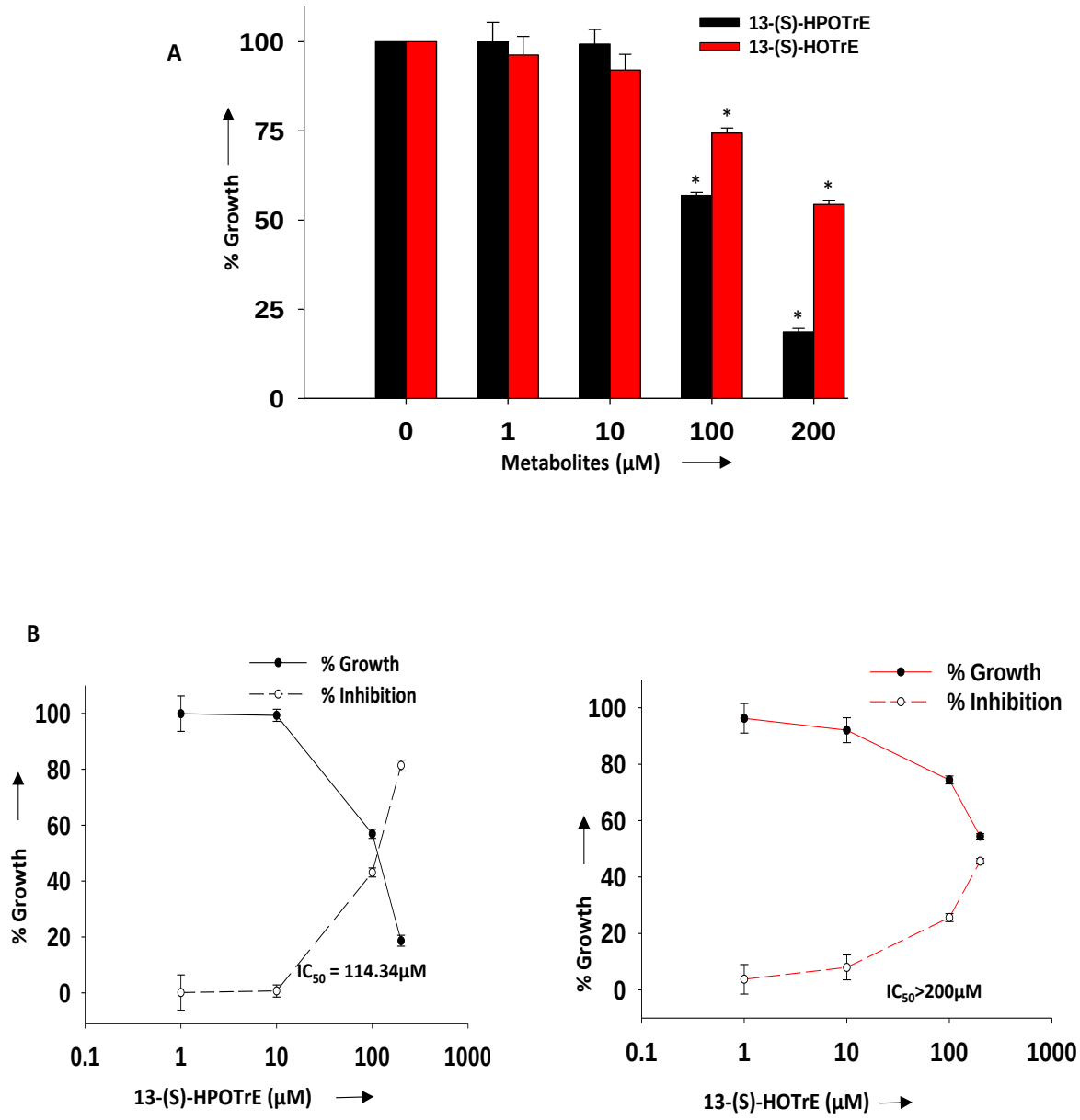

Figure 4-1: ***Effects of 13-(S)-HPOTrE and 13-(S)-HOTrE on cells viability in RAW 264.7 cells.*** **A)** Effects of 13-(S)-HPOTrE and 13-(S)-HOTrE on the viability of RAW 264.7 cells were measured by MTT assay. Cells were treated with different concentrations (1, 10, 100 and 200 µM) of ALA metabolites for 24 h. The percent cell growth following treatment was calculated, in comparison with untreated control cells. The values represent mean ± SD of three independent experiments. *Indicates significance ($p<0.05$) when compared with untreated control cells. **B)** IC50 values of 13-(S)-HPOTrE and 13-(S)-HOTrE calculated at 24 h. The values represent mean ± SD of three independent experiments.

4.4.2 ALA metabolites reduce nitric oxide levels and ROS generation in RAW 264.7 cells and peritoneal macrophages.

Next, it was aimed to evaluate the effects of ALA metabolites on LPS induced inflammation by examining effects on pro-inflammatory parameters: NO- a second messenger and ROS- an oxidative stress marker. For this, RAW 264.7 cells were first treated with or without metabolites and challenged with LPS as described in the methods. There was significant elevation in NO production and ROS generation in cells when stimulated with LPS and this elevated NO level was reduced by 52.7% and 29% in the presence of 13-(S)-HPOTrE and 13-(S)-HOTrE at 100 µM, respectively (Figure 4-2A). Similarly, LPS stimulated RAW 264.7 cells, pre-treated with 13-(S)-HPOTrE and 13-(S)-HOTrE, resulted in the reduction of ROS generation, in a dose-dependent manner and at 100 µM concentration, decreased ROS generation by 96.4% and 92.7% respectively (Figure 4.2B). Not only ALA metabolites, the substrate fatty acid ALA also showed the similar pattern of decreased NO and ROS production in LPS stimulated RAW 264.7 cells, though lower (89.5 % and 8.6%) compared to its metabolites (Figure 2-2, 2-3). Similar effects were observed on ROS level when the mouse peritoneal macrophages were pre-treated with ALA metabolites at lower doses (100 nM) and then challenged with LPS (Figure 4.2C). The significant reduction in the production of the pro-inflammatory markers by the ALA metabolites suggests their strong anti-inflammatory effects on LPS stimulated macrophages.

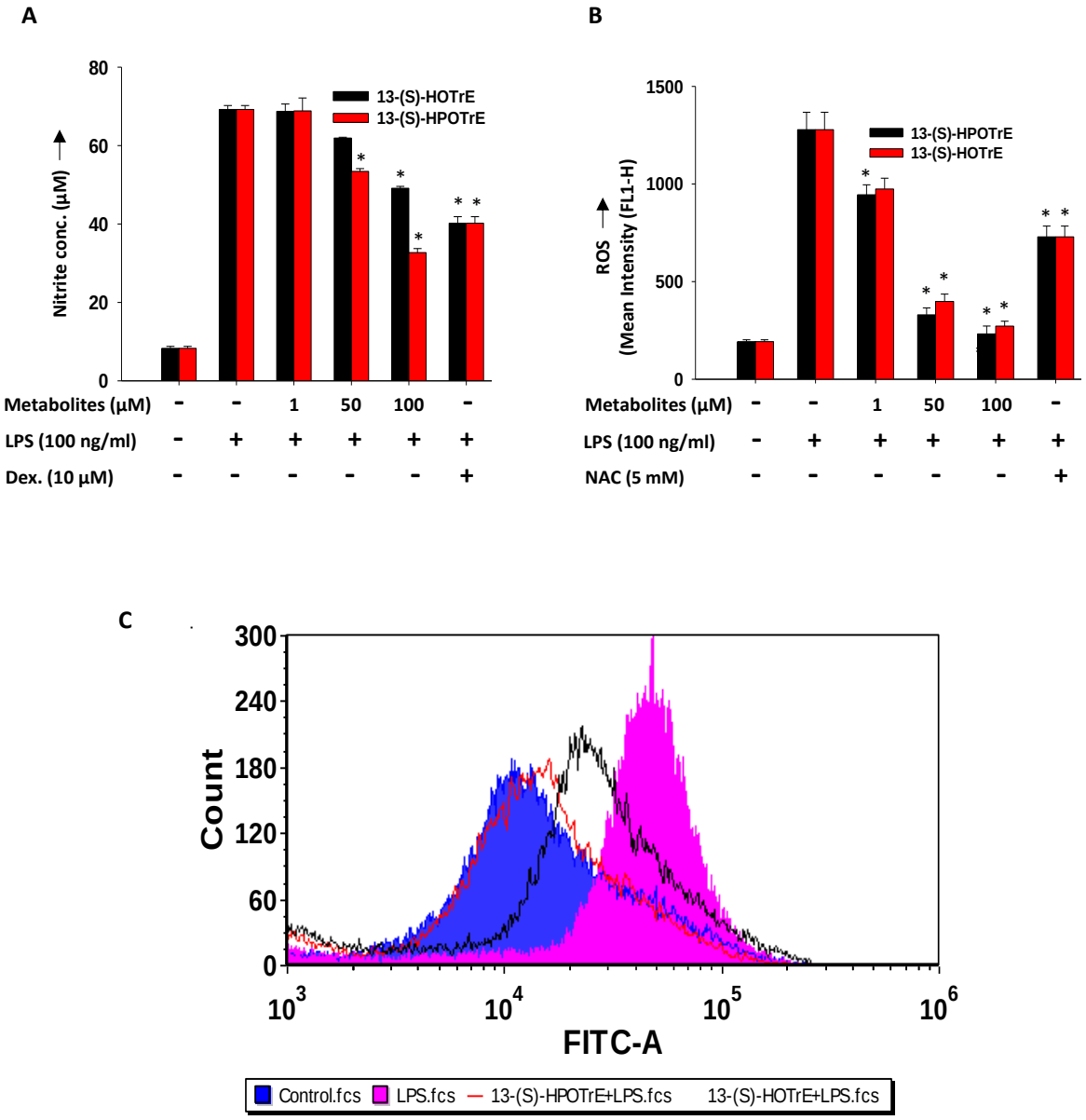

Figure 4-2: ***Effects of 13-(S)-HPOTrE and 13-(S)-HOTrE on generation of NO and ROS in RAW 264.7 cells and mouse peritoneal macrophages.*** **A)** Nitrite levels in the culture medium of RAW 264.7 cells pre-incubated with different concentrations (1, 50 and 100 µM) of ALA metabolites or dexamethasone (10 µM) for 3 h. Then stimulated with or without LPS (100 ng/ml) for the next 24 h. 13-(S)-HPOTrE showed more effective dose-dependent reduction in NO level as compared to 13-(S)-HOTrE. Dexamethasone, a steroidal anti-inflammatory drug that suppresses NO production, is used as positive control. *Indicates significance ($p<0.05$) compared to LPS treated cells. **B)** Intracellular ROS level in RAW 264.7 cells following pretreatment with 100 µM of ALA metabolites for 3 h then stimulated with LPS for 16 h. 13-(S)-HPOTrE reduced ROS level more efficiently compared to 13-(S)-HOTrE. N-Acetyl Cysteine (NAC, 5 mM), a ROS inhibitor is used as positive control. The values represent mean ± SD of three independent experiments. *Indicates significance ($p<0.05$) compared to LPS treated cells. **C)** Intracellular ROS level in peritoneal macrophages following pre-incubation with 100 nM ALA metabolites for 3 h then challenged with LPS for 16 h. Similar to above result, 13-(S)-HPOTrE reduced ROS level more efficiently compared to 13-(S)-HOTrE. This is representative FACS chromatogram of the three independent experiments.

4.4.3 ALA metabolites inhibit the expression of iNOS and TNF-α in LPS stimulated RAW 264.7 cells.

iNOS is an enzyme associated with regulation of NO and ROS generation in monocytes, macrophages, and other cells [147]. The expression of iNOS and TNF-α, in RAW 264.7 cells stimulated with LPS in the presence and/or absence of ALA metabolites was studied. 13-(S)-HPOTrE and 13-(S)-HOTrE showed no effect on the expressions of either iNOS or TNF-α as compared to untreated RAW 264.7 cells, while LPS induced their expression. However, their expression in RAW 264.7 cells, pre-treated with 13-(S)-HPOTrE and 13-(S)-HOTrE and then challenged with LPS, was reduced in a dose-dependent manner (Figure 4-3A). The transcript levels of iNOS and TNF-α were also analyzed by semi-quantitative PCR. In LPS treated RAW 264.7 cells, the transcript levels of iNOS and TNF-α were increased but were reduced by pre-treatment with 13-(S)-HPOTrE and 13-(S)-HOTrE in a dose-dependent manner (Figure 4-3B).

NF-κB is known to regulate the expression of various pro-inflammatory genes, including iNOS and TNF-α [148,149] and ALA metabolites may affect its translocation to the nucleus to regulate gene expression. Therefore, the activation of NF-κB was monitored for its translocation to the nucleus by confocal microscopy. While LPS stimulation of RAW 264.7 cells showed a marked translocation of NF-κB, 13-(S)-HPOTrE and 13-(S)-HOTrE pre-treatments resulted in a decrease in NF-κB translocation (Figure 4-4A). Very similar effects were observed on NF-κB translocation when the mouse peritoneal macrophages were treated with 13-(S)-HPOTrE and 13-(S)-HOTrE at a lower dose (100 nM) and then challenged with LPS (Figure 4-4B).

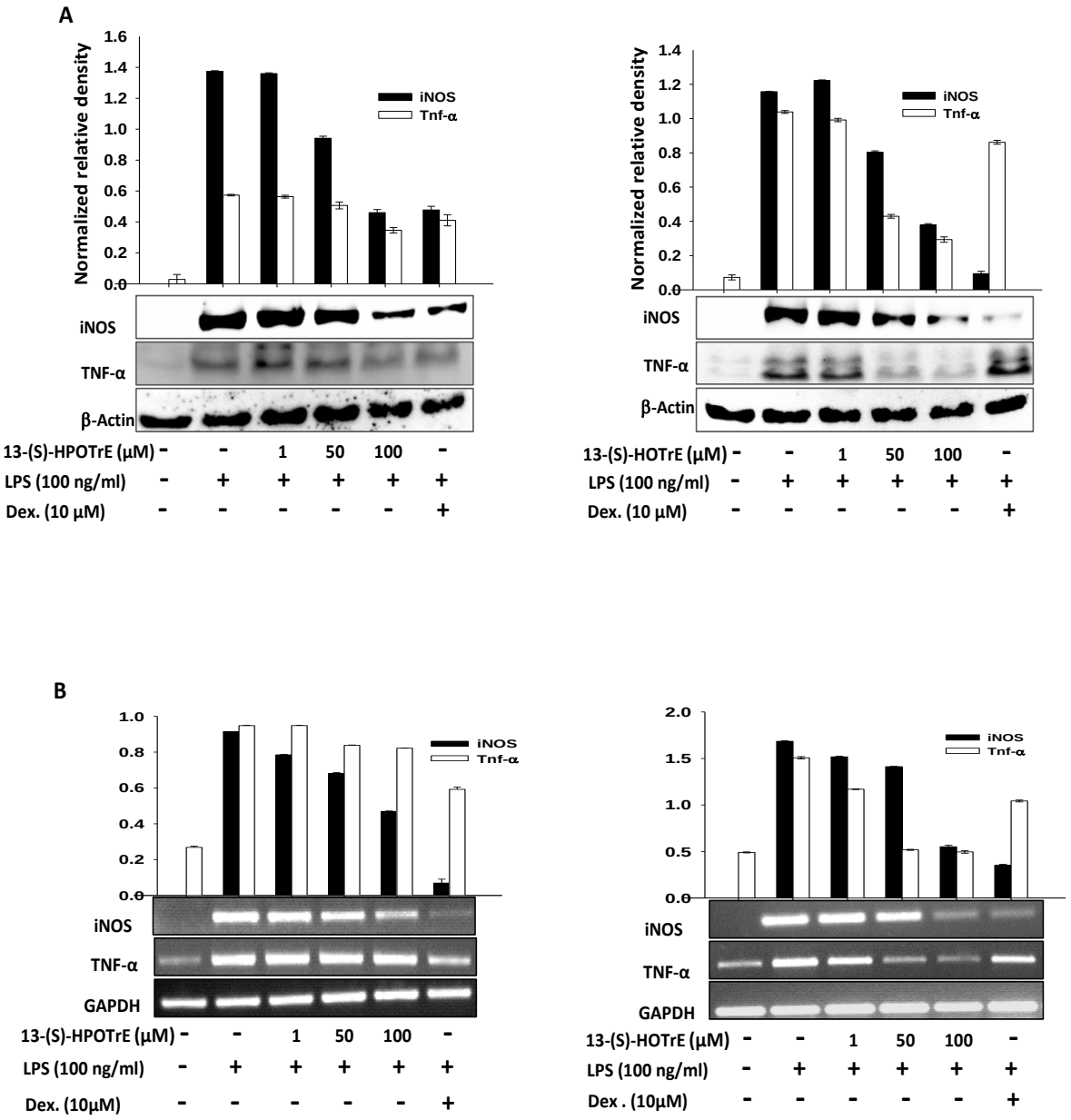

Figure 4-3: ***Anti-inflammatory effect of 13-(S)-HPOTrE and 13-(S)-HOTrE is mediated by inhibition of iNOS and TNF-α.*** **A)** Immunoblot analysis showing the expression of iNOS and TNF-α following treatment with 13-(S)-HPOTrE and 13-(S)-HOTrE (1, 50 and 100 μM) concentrations for 3 h and then stimulated with LPS for 24 h. β-Actin is used as an internal control. Dexamethasone (10 μM) is used as positive control. These are representative blots of the three independent experiments. **B)** RT-PCR analysis of transcripts of iNOS and TNF-α in RAW 264.7 cells pre-treated with ALA metabolites for 3 h then stimulated with LPS (100ng/ml) for 24 h. GAPDH is used as an internal control. Dexamethasone is used as positive control. These are representative gel images of the three independent experiments. The relative band intensities were measured by quantative scanning densitometry (Image J).

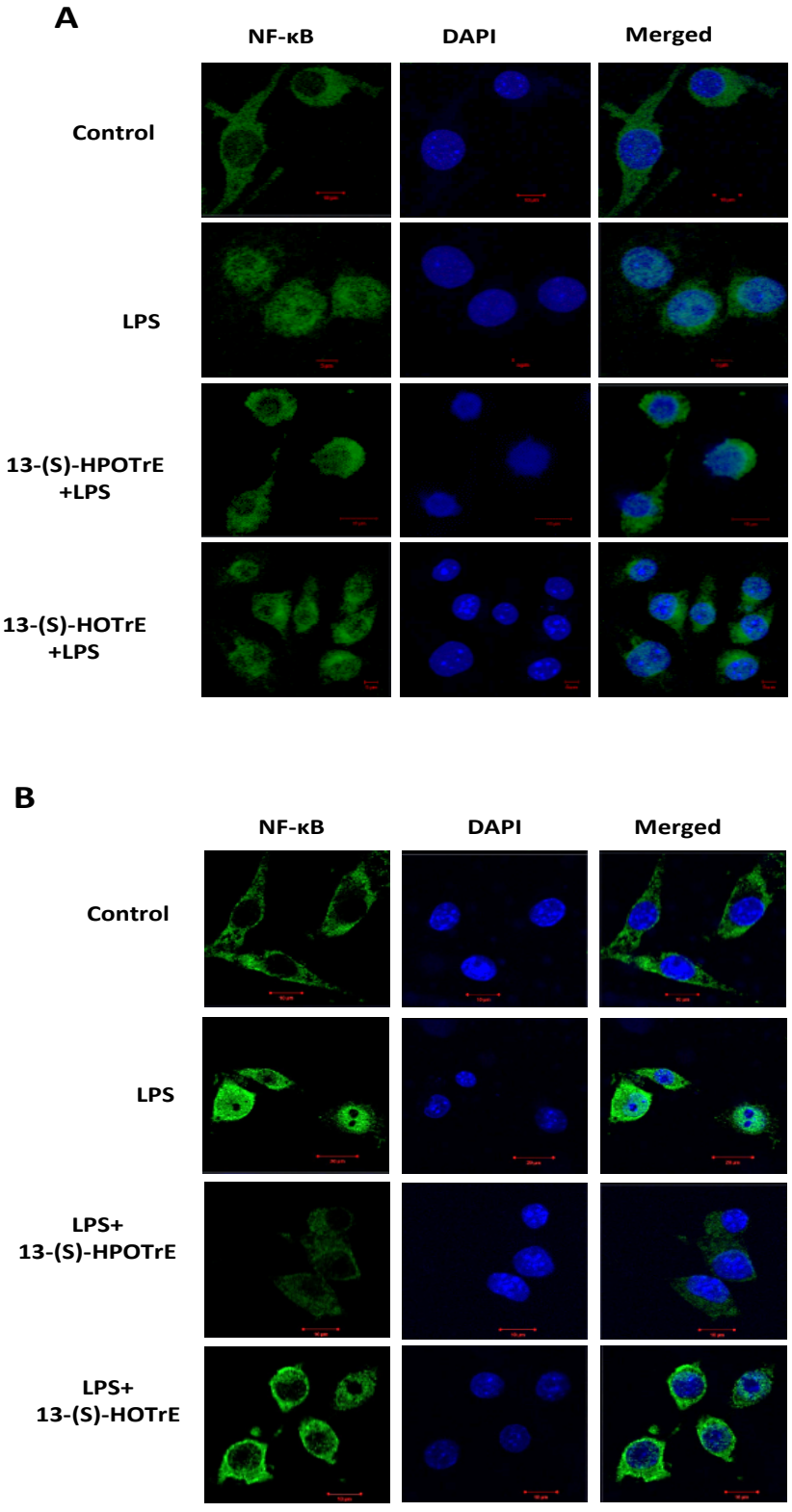

Figure 4-4: ***ALA metabolites inhibit the expression of iNOS and TNF-α in LPS stimulated RAW 264.7 cells through NF-κB pathway.*** **A)** Immunofluorescence microscopy of RAW 264.7 cells pre-treated with or without ALA metabolites (100 µM) for 3 h and then with LPS for 16 h. Immunostained for NF-κB (Green) and DAPI (Blue). Bar Scale: 10 µm. The image show representative of three independent experiments. **B)** Immunofluorescence microscopy of peritoneal macrophages pre-treated with or without ALA metabolites (100 nM) for 3 h and then challenged with LPS for 16 h. Immunostained for NF-κB (Green) and DAPI (Blue), Bar Scale: 10 µm. The image show representative of three independent experiments.

4.4.4 13-(S)-HPOTrE and 13-(S)-HOTrE inactivate inflammasome in PPAR-γ dependent manner in RAW 264.7 cells and peritoneal macrophages.

It is well known that NLRP3 inflammasome, an intracellular sensor that detects pathogens and sterile inflammation, gets activated in part through NF-κB in response to LPS treatment [150–152]. For analyzing, the effects of 15-LOX metabolites of ALA on NLRP3 inflammasome activation in LPS stimulated RAW 264.7 cells, the level of gene transcripts associated with inflammasome complex were quantified by semi-quantitative PCR. An increased transcript level of NLRP3, caspase-1, IL-1β and IL-18 in LPS activated RAW 264.7 cells showed an efficient dose-dependent reduction on treatment with both 13-(S)-HPOTrE and 13-(S)-HOTrE (Figure 4-5A). Since activated inflammasomes initiate the processing and secretion of IL-1β [153,154], we measured the level of IL-1β, in the culture medium of RAW 264.7 cells by ELISA. These studies showed a 4.4 fold increase in the level of IL-1β in response to LPS treatment in RAW 264.7 cells and this elevated level of IL-1β was significantly reduced by the treatment of 13-(S)-HPOTrE and 13-(S)-HOTrE, in a dose-dependent manner (Figure 4-5B). At 100 µM concentration, 13-(S)-HPOTrE and 13-(S)-HOTrE reduced IL-1β levels by 86.4% and 23% respectively.

LOX metabolites are natural ligands of PPAR-γ [155–158]. Interestingly, PPAR-γ and their coactivators were shown to promote macrophage's anti-inflammatory properties to increase insulin sensitivity [159]. In the present scenario, we studied the involvement of PPAR-γ on the NLRP3 inflammasome activation in LPS treated RAW 264.7 cells and peritoneal macrophages. Immunofluorescence microscopy studies showed activation of NLRP3 inflammasome complex along with upregulation of

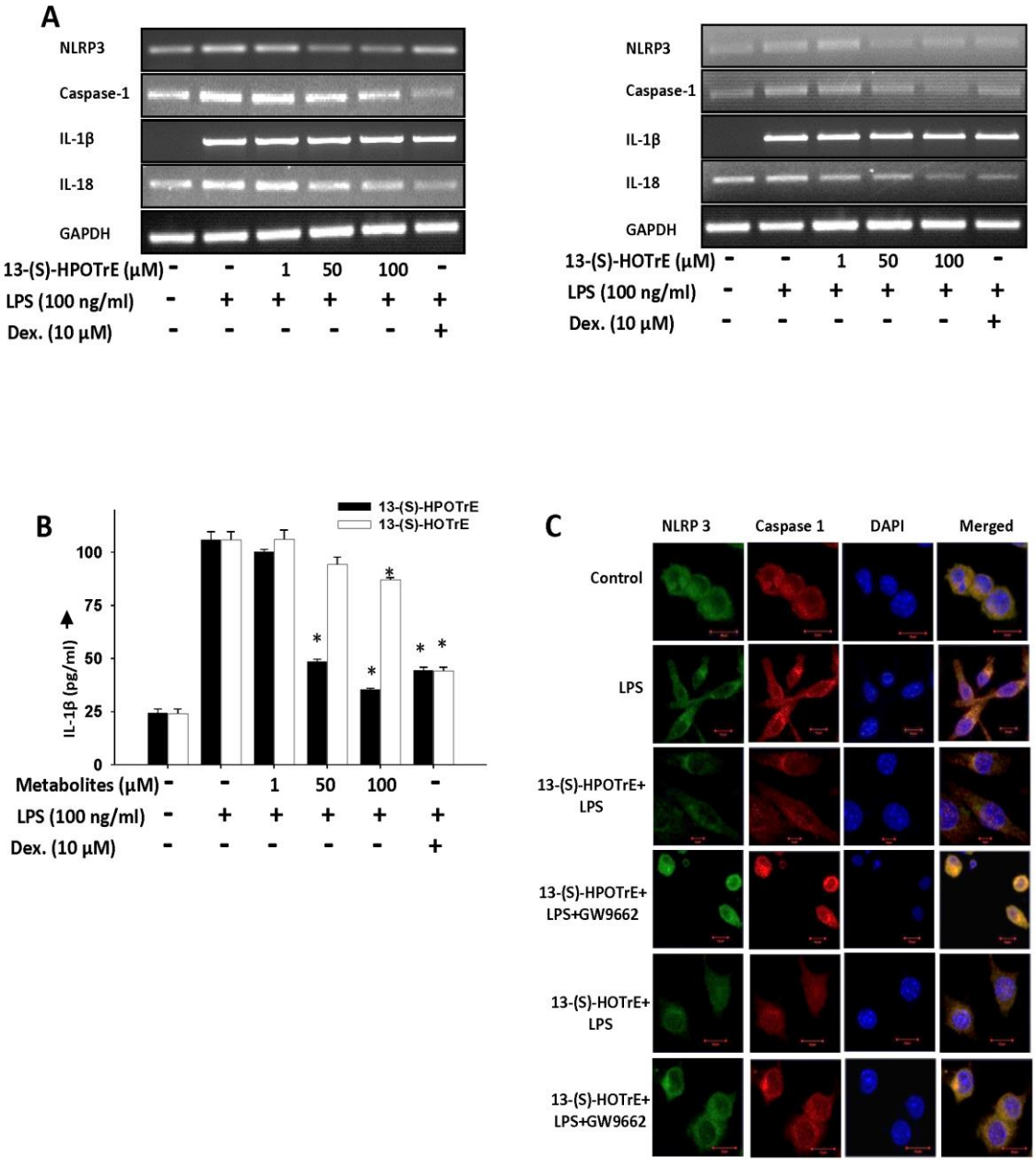

Figure 4-5: ***ALA metabolites, 13-(S)-HPOTrE and 13-(S)-HOTrE, inhibit inflammasome complex in RAW 264.7 cells.*** **A)** In semi-quantitative PCR analysis, 13-(S)-HPOTrE, and 13-(S)-HOTrE showed decrease in transcript level of NLRP3, caspase-1, IL-1β and IL-18 at various concentrations (1, 50 and 100 μM) pre-incubated for 3 h then stimulated with LPS for 24 h. GAPDH is used as an internal control**. B)** Estimation of IL-1β levels in the culture medium of cells as per the treatment described in (A). Dexamethasone (10 μM) is used as positive control. The values represent mean ± SD of three independent experiments. *Indicates significance ($p<0.05$) compared to LPS alone treated cells. **C)** Immunofluorescence microscopy of RAW 264.7 cells pre-treated with ALA metabolites (100 μM) for 3 h then stimulated with LPS for 24 h. Immunostained for NLRP3 (Green), caspase-1 (Red) and DAPI (Blue). Bars Scale: 10 μm. Data show representative of three independent experiments.

caspase-1 upon LPS treatment in RAW 264.7 cells (Figure 4-5C). However, pre-treatment of RAW 264.7 cells with 13-(S)-HPOTrE or 13-(S)-HOTrE and then challenged with LPS resulted in inactivation of NLRP3 inflammasome and thus downregulation of caspase-1. Interestingly, these effects of 13-(S)-HPOTrE and 13-(S)-HOTrE on inflammasome and caspase-1 were reversed when co-incubated with GW9662, a PPAR-γ antagonist.

To validate the findings observed in RAW 264.7 cells, further, studies were taken up on peritoneal macrophages at much lower doses (100 nM and 400 nM) of 13-(S)-HPOTrE and 13-(S)-HOTrE. Immunoblot analysis showed an increase in the expression of NLRP3 in LPS challenged peritoneal macrophages while cells pre-treated with ALA metabolites and challenged with LPS showed a reduction in the expression of NLPR3 (Figure 4-6A). Next, the IL-1β cytokine was probed in the culture medium by immunoblot analysis and quantified by ELISA. As shown in figure 4-6A & 4-6B, peritoneal macrophages pre-treated with 13-(S)-HPOTrE and 13-(S)-HOTrE and then challenged with LPS reduced the level of IL-1β by 59.5% and 54.5% respectively, when compared to LPS alone challenged macrophages. These metabolites also increased the levels of anti-inflammatory cytokine-IL-10 in culture medium (Figure 4-6C). Similarly, the involvement of PPAR-γ in the regulation of inflammasome by ALA metabolites was validated on peritoneal macrophages at lower concentrations. Immunofluorescent microscopy showed decreased expression of NLRP3 inflammasome and caspase-1 in macrophages pre-treated with ALA metabolites and challenged with LPS. However, the effects of ALA metabolites were reversed when co-incubated with GW9662, PPAR-γ antagonist (Figure 4-7). The foregoing results suggest that inactivation of the inflammasome by 13-(S)-HPOTrE and 13-(S)-HOTrE in LPS challenged RAW 264.7 cells

and peritoneal macrophages is mediated through PPAR-γ dependent pathway. Immunoblot analysis of the LPS stimulated RAW 264.7 cells revealed an increase in the COX-2 expression (Figure 4-8A). The LPS induced expression of COX-2 was further enhanced by both 13-(S)-HPOTrE and 13-(S)-HOTrE in a dose-dependent manner.

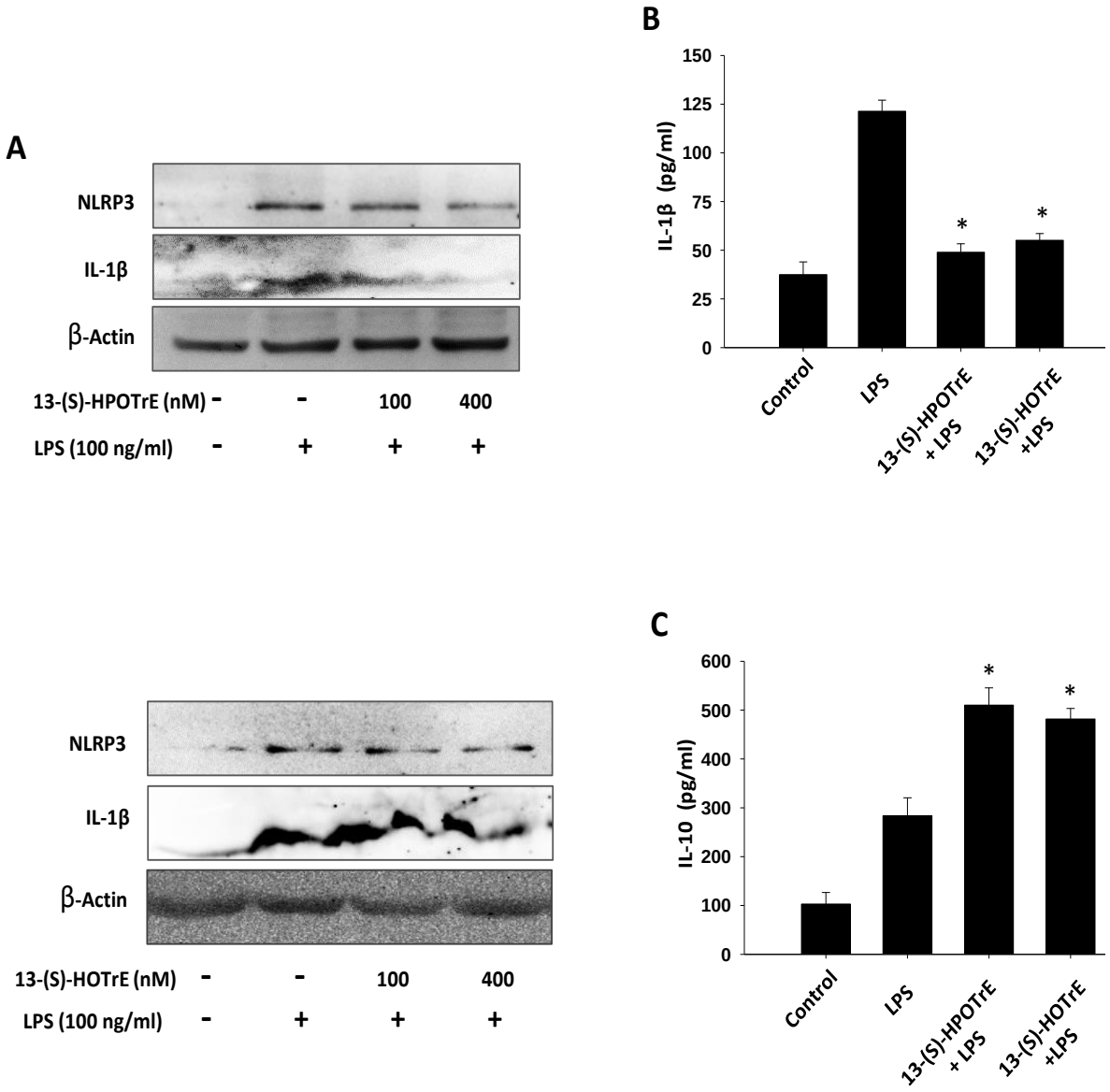

Figure 4-6: ***ALA metabolites inhibit inflammasome complex activation in mouse peritoneal macrophages***. **A)** Immunoblot analysis of NLRP3 and IL-1β (in culture medium) expression in peritoneal macrophages, pre-incubated with ALA metabolites (100 nM and 400 nM) for 3 h then challenged with LPS (100 ng/ml) for next 24 h. β-Actin is used as an internal control. **B)** Estimation of IL-1β levels in the culture medium by ELISA as per the treatment described above. The values represent mean ± SD of three independent experiments. *Indicates significance ($p<0.05$) compared to LPS treated peritoneal macrophages. **C)** Estimation of IL-10 levels in the culture medium by ELISA as per the treatment described above (at 100 nM). The values represent mean ± SD of three independent experiments. *Indicates significance ($p<0.05$) compared to LPS treated peritoneal macrophages.

Coinciding with the changes observed in COX-2, the downstream metabolites of COX-2, PGE_2, and PGD_2, also showed similar trend of enhanced production with LPS treatment (Figure 4-8B). These studies reveal that COX-2, a key enzyme involved in mediating inflammation, may also be playing a role in the resolution of inflammation through the generation of PGD_2 which is a PPAR-γ ligand [133].

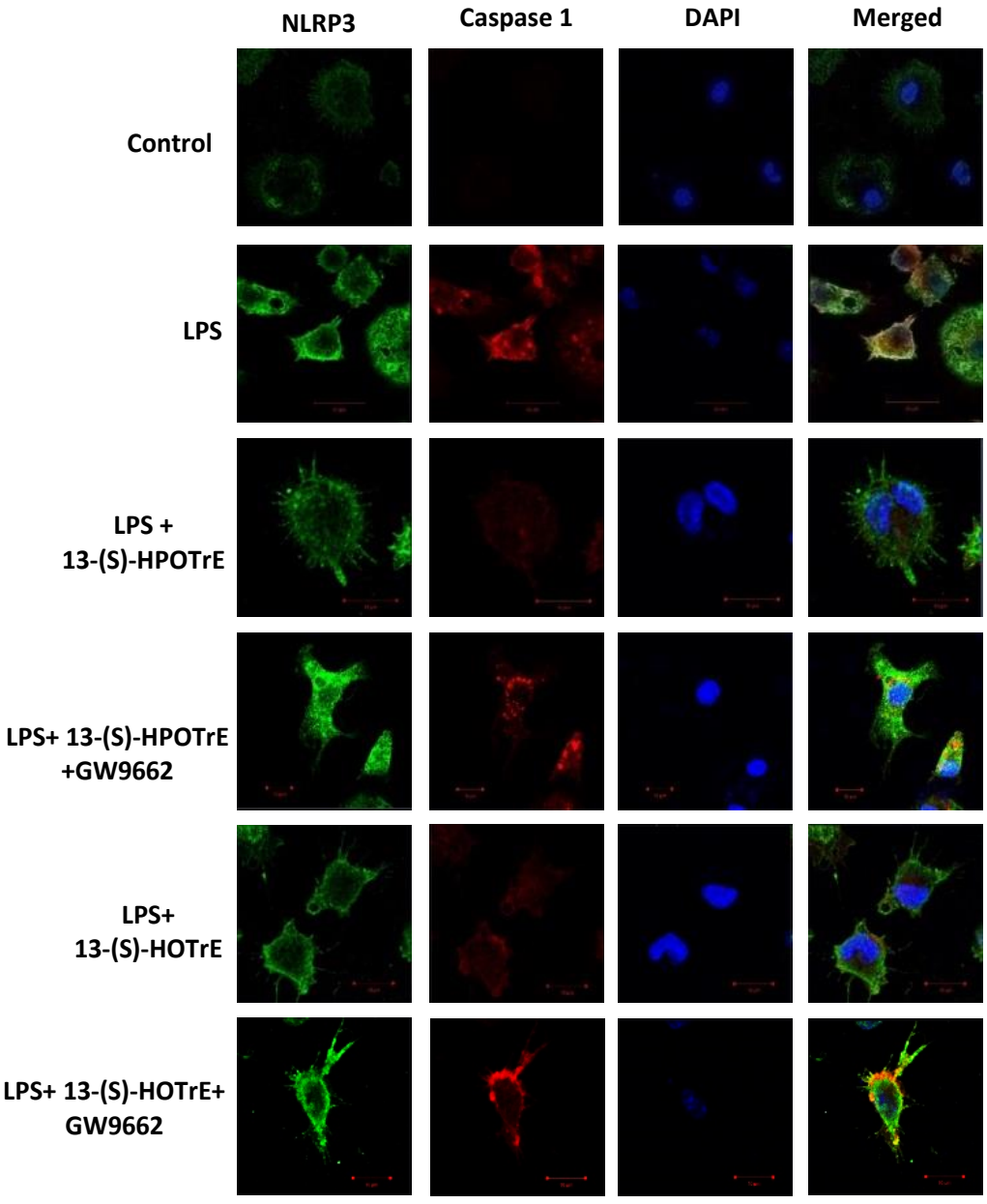

Figure 4-7: ***ALA metabolites inhibit inflammasome complex activation in mouse peritoneal macrophages.*** Immunofluorescence microscopy of peritoneal macrophages treated with ALA metabolites (100 nM) for 3 h then stimulated with LPS for 24 h. Immunostained for NLRP3 (Green), caspase-1 (Red) and DAPI (Blue). Bars Scale: 10 µm. Images show representative of three independent experiments.

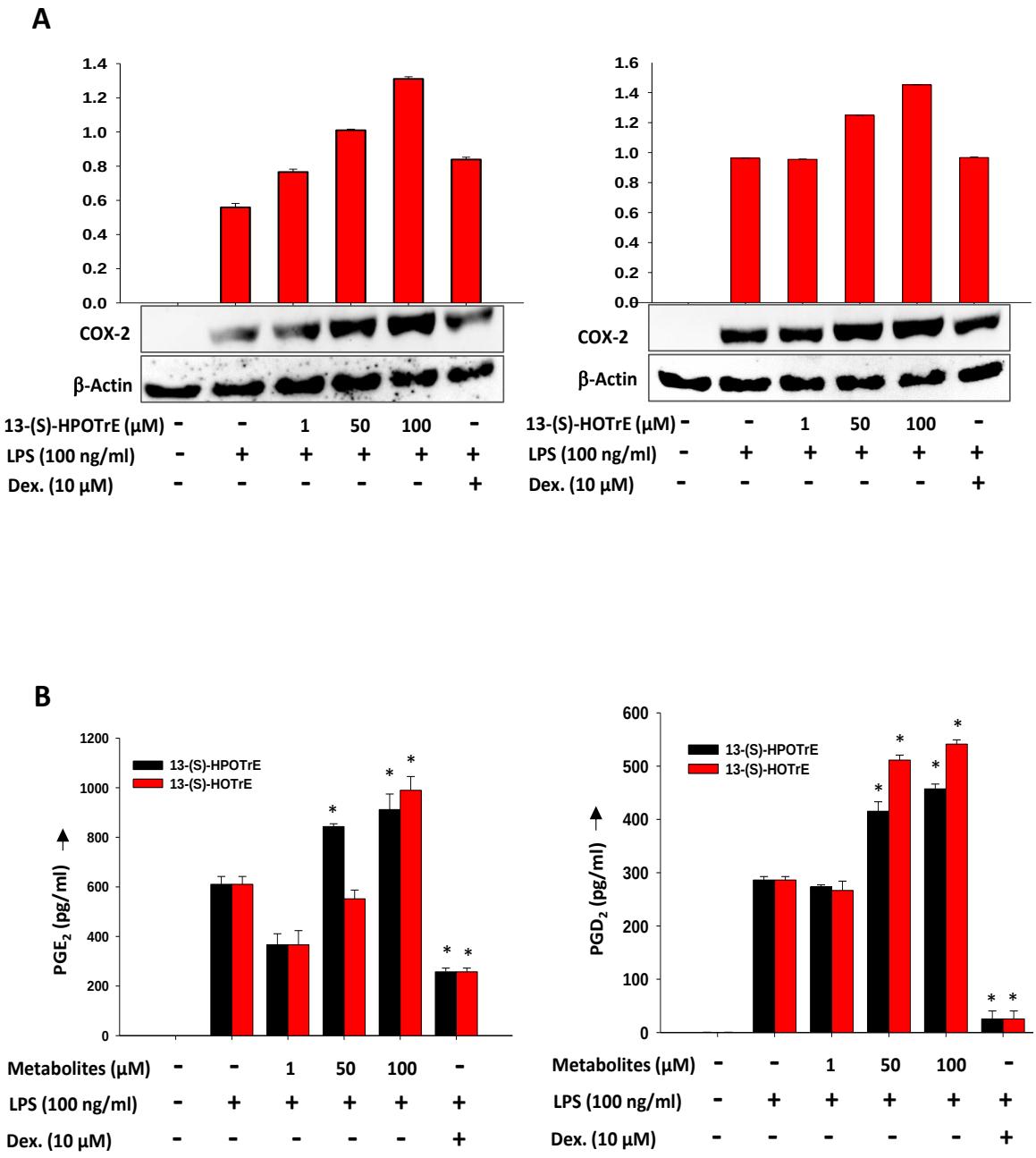

Figure 4-8: ***13-(S)-HPOTrE and 13-(S)-HOTrE show anti-inflammatory effects by upregulating expression of COX-2.*** **A)** Immunoblot analysis of COX-2 expression in RAW 264.7 cells pre-incubated with ALA metabolites at different concentrations (1, 50 and 100 µM) for 3 h then further stimulated by LPS (100 ng/ml) for next 24 h. β-Actin is used as an internal control and Dexamethasone is used as positive control. Western blot shows representative of three independent experiments. **B)** Estimation of PGE_2 and PGD_2 level in the culture medium of RAW 264.7 cells when pre-incubated with ALA metabolites for 3 h and then stimulated with LPS for 24 h. Dexamethasone is used as positive control. The values represent mean± SD of three independent experiments. *Indicates significance ($p<0.05$) compared to LPS treated cells.

4.4.5 ALA metabolites induce apoptosis in LPS treated RAW 264.7 cells.

It is known that apoptosis plays a vital role in the resolution of inflammation and Beclin-1 dependent inhibition of autophagy by apoptosis enhances its anti-inflammatory effects [106]. Apoptosis blocks Beclin-1 dependent autophagy by blocking autophagosome synthesis [160]. Moreover, LPS and activated inflammasomes also induce autophagy in mesothelial cells [107]. Since ALA metabolites showed anti-inflammatory effects, we examined whether they affect induction of apoptosis and autophagy in LPS stimulated RAW 264.7 cells. 13-(S)-HPOTrE treatment increased apoptosis in LPS challenged RAW 264.7 cells in a dose-dependent manner (Figure 4-9) although, 13-(S)-HPOTrE and 13-(S)-HOTrE showed no effect on apoptosis in unchallenged cells. A significant increase in autophagy with the enhanced conversion of soluble LC3-I into lipid bound LC3-II and increased puncta formation were observed in LPS challenged RAW 264.7 cells. However, these effects were greatly reduced or undetectable in RAW 264.7 cells pre-treated with ALA metabolites and challenged with LPS (Figure 4-10A, B). Moreover, immunoblot analysis also showed induced expression of beclin-1, an autophagic marker, which was greatly reduced when RAW 264.7 cells was treated with ALA metabolites in a dose-dependent manner (Figure 4-10C).

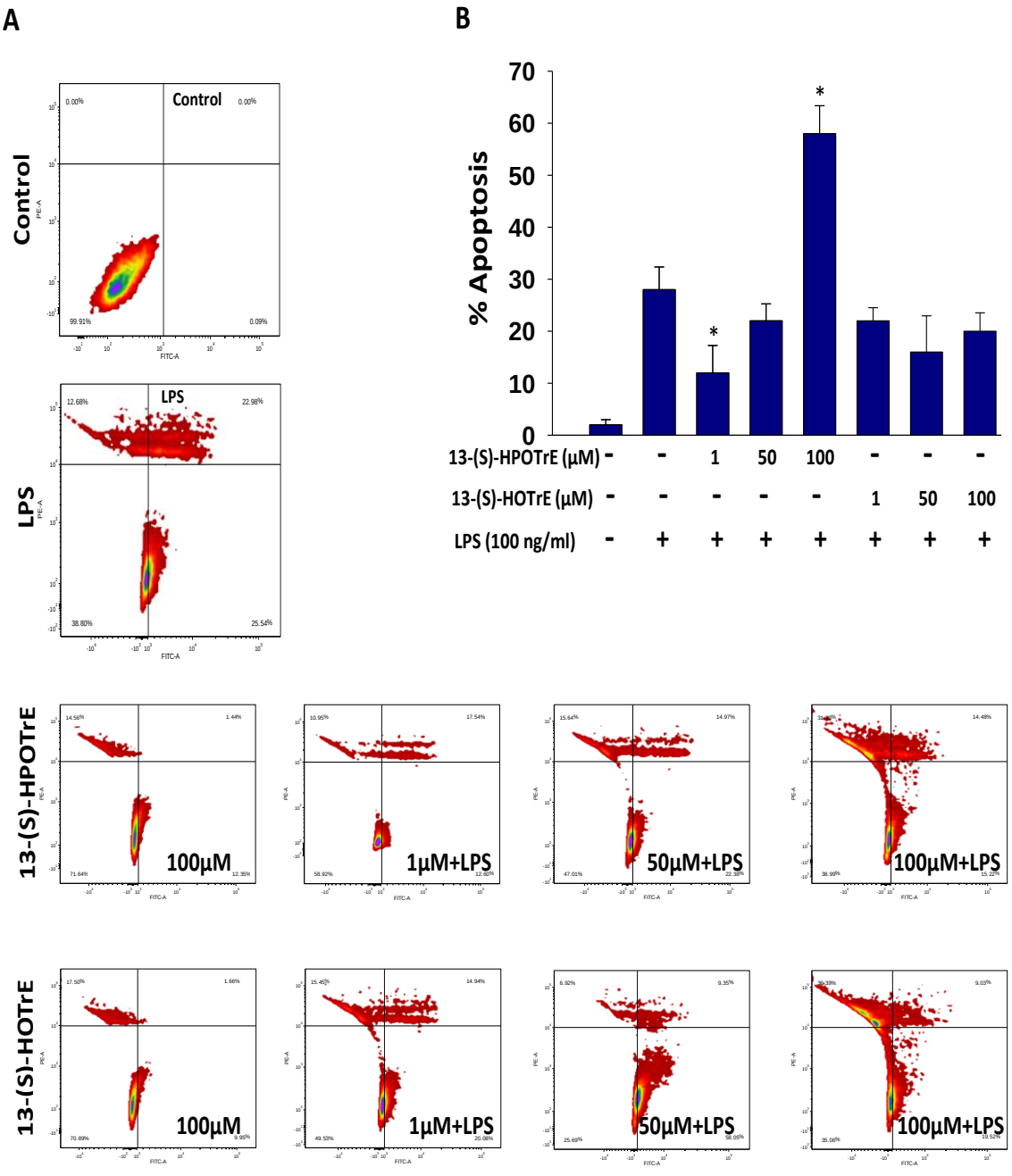

Figure 4-9: ***13-(S)-HPOTrE and 13-(S)-HOTrE induce apoptosis in LPS stimulated RAW 264.7 cells*. A)** Flow cytometric analysis showing the effects of ALA metabolites on apoptosis in RAW 264.7 cells challenged with LPS. Apoptosis is assayed by Propidium Iodide and FITC conjugated Annexin V at 24 h, by flow cytometric Analysis. The apoptosis level was calculated as % of AnnexinV^{+} PI^{-} cells in density plot distribution. The dead cells were gated and analysis was performed only on live cells. *Indicates significance ($p<0.05$) compared to LPS treated cells. **B)** Bar graph is representation of above data.

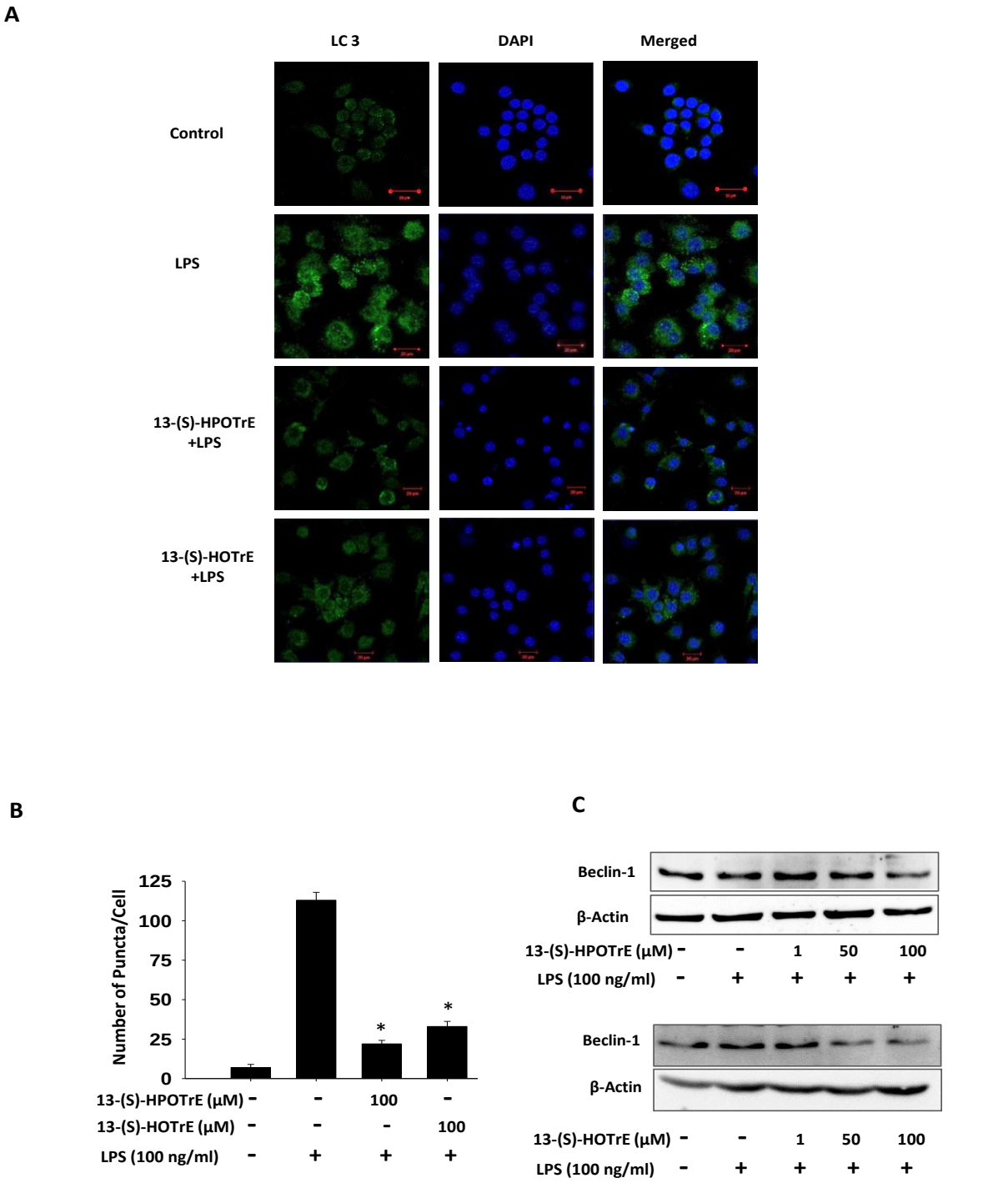

Figure 4-10: ***13-(S)-HPOTrE and 13-(S)-HOTrE inhibit Beclin-1 mediated autophagy in LPS stimulated RAW 264.7 cells.*** **A)** Confocal microscopy of RAW 264.7 cells treated with or without ALA metabolites (100 µM) for 3 h then challenged with LPS for 24 h. Immunostained for LC 3 (Green) and DAPI (Blue). Bars Scale: 10 µm. Images show representative of three experiments. **B)** Bar graph shows puncta/cell calculated by ImageJ LC3 macro.*Indicates significance ($p<0.05$) compared to LPS treated cells. **C)** Beclin-1 Immunoblotting of RAW 264.7 cells pre-incubated with ALA metabolites for 3 h and then challenged with LPS for 24 h. Western blots show representative of three independent experiments.

4.4.6 ALA metabolites extend BALB/c mice survival and show anti-inflammatory properties by regulating cytokines and inflammasome.

Septic shock is a complication of inflammation in which infections or toxins induce an inflammatory response in the entire body. Endotoxin-mediated septic shock is often integrated with high mortality [161]. On the other hand, saturated fatty acid had shown major impact on the survival of mice in bacterial infection [98] and these ALA metabolites showed anti-inflammatory effects in *in vitro* model system. We then wanted to validate the effects of ALA metabolites *in vivo* on the survival of mice in septic shock induced by LPS in toxemia model. These studies showed features of septic shock in all the mice received LPS such as increase in heartbeat rate, decrease in body weight, apathy, dullness and diarrhea, which began to die within 12 h. Contrary to this, the mice pre-treated with ALA metabolites and then challenged with LPS were quite active. However, loss of weight was observed in all except control mice. The results from this experiment showed that survival rate in ALA metabolites pre-treated mice were 40% and 10% extended than LPS alone challenged mice (Figure 4-11A).

Since ALA metabolites showed a decrease in mortality rate in mice with endotoxin-mediated septic shock, studies were further extended to mice with sepsis induced by polymicrobial infection in a CLP mouse model. Results showed up-regulation of iNOS and NLRP3 expression in CLP mice and their down-regulation in mice pre-treated with ALA metabolites (Figure 4-11B). The levels of IL-1β and IL-10 were increased in liver tissue and serum of CLP mice. However, the level of pro-inflammatory cytokine-IL-1β was decreased while the level of anti-inflammatory cytokine-IL-10 was further increased in mice treated with ALA metabolites (Figure 4-11C).

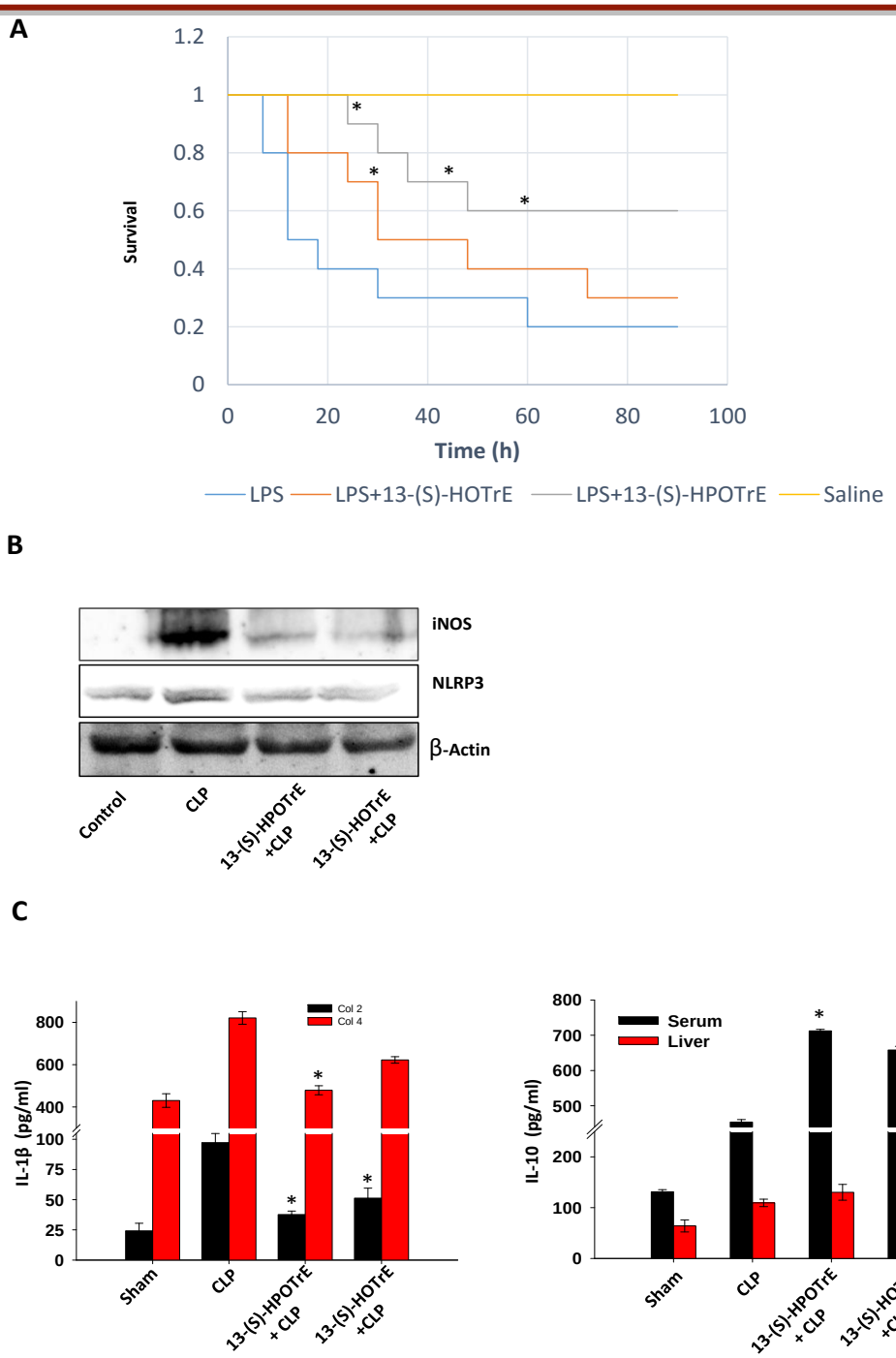

Figure 4-11: ***Effects of ALA metabolites during sepsis in BALB/c mice.*** **A)** ALA metabolites showed an increase in survival of BALB/c mice (n=10 mice/group) in endotoxin-induced Septic Shock in toxemia model. LPS (30 mg/kg) was injected i.p. and mice were monitored for 4 days then mortality was calculated. ALA metabolites showed decreased mortality rate in metabolites treated and LPS challenged mice as compared to LPS challenged mice. The survival curve is plotted on Kaplan-Meier method. *Indicates significance ($p<0.05$) compared to LPS treated mice. **B)** Sepsis was induced by polymicrobial infection in CLP mouse model (n=5 mice/group). Immunoblot analysis of iNOS and NLRP3 expression in CLP mice model, pre-treated with 13-(S)-HPOTrE and 13-(S)-HOTrE (0.1 mg/kg, 2.5 µg/mice) as described in methodology. Mice were sacrificed after 24 h of CLP and tissues were collected. β-Actin is used as an internal control. **C)** Estimation of IL-1β and IL-10 cytokines levels in serum and liver tissue. The values represent mean ± SD of three independent experiments. *Indicates significance ($p<0.05$) compared to CLP mice.

4.5 Discussion

The ratio of ω-6 PUFAs: ω-3 PUFAs in cell membranes reflect the physiological status of the tissues and regulate the inflammatory response to a variety of external or internal stimuli and thus maintenance of cellular homeostasis [100,101]. ω-3 PUFAs are known to exhibit anti-inflammatory effects and reduce the oxidative stress in the cells [51,100]. The findings of the present study also support this concept wherein ALA, ω-3 PUFA, and its metabolites, 13-(S)-HPOTrE and 13-(S)-HOTrE, significantly reduced the production of NO and ROS, as well as inflammatory cytokines, in LPS stimulated RAW 264.7 cells and in mouse peritoneal macrophages. Further studies on *in vivo* sepsis model and CLP mice model demonstrated the protective role of 13-(S)-HPOTrE and 13-(S)-HOTrE as evidenced by a decrease in the mortality rate and by the reduction of pro-inflammatory markers, in ALA metabolites treated BALB/c mice.

From previous studies, it has been established that ω-3 PUFAs exert their anti-inflammatory effects through several mechanisms, one of which being NF-κB signalling [51,100]. ω-3 PUFAs prevent the phosphorylation and degradation of Iκ-Bα protein by proteasome complex, thus inhibiting NF-κB signalling pathways [110]. The present study shows that 15-LOX metabolites of ALA [13-(S)-HPOTrE and 13-(S)-HOTrE] inhibit the translocation of NF-κB to the nucleus, along with the reduction of NO and ROS in LPS stimulated RAW 264.7 cells and peritoneal mouse macrophages. ALA metabolites also inhibited the activation of NLRP3 inflammasome as well as downstream signalling molecules such as caspase-1 and IL-1β at both transcriptional as well as translational levels. Interestingly, these effects of ALA metabolites on NLRP3 inflammasome were

blocked by the PPAR-γ antagonist-GW9662. These studies comprehensively suggest that inactivation of LPS induced NLRP3 inflammasome by 13-(S)-HPOTrE or 13-(S)-HOTrE in RAW 264.7 cells and peritoneal macrophages is dependent on PPAR-γ. Indeed a number of studies have shown that several PUFAs metabolites are ligands of PPAR-γ [137], further supporting such a possibility.

Recent studies have established that the inducible isoform of COX, COX-2, has dual roles, pro-and anti-inflammatory, depending on the downstream metabolites generated [129,162]. In the early stages, it is shown that COX-2 induction is mainly associated with the generation of pro-inflammatory prostaglandins, whereas at later stages the downstream metabolite is PGD_2, a ligand for PPAR-γ [133], which has been observed to possess anti-inflammatory roles [163]. In the present study, an increase in the expression of COX-2 and its downstream metabolites (PGE_2 and PGD_2) was observed in RAW 264.7 cells pre-treated with ALA metabolites and then stimulated with LPS. Here, COX-2 may be playing an anti-inflammatory role by shifting PGE_2 dominated prostaglandins in LPS stimulated macrophages to PGD_2 dominated prostaglandins upon treatment with ALA metabolites. It has been reported that PGD_2 derivative PGJ_2 and their metabolites $^{12}\Delta$ PGJ_2 and 15d-PGJ_2, often derived from induced COX-2, exhibit their anti-inflammatory effects in various *in vivo* systems [131,138,164]. In the present study the induced expression of COX-2 and increased the formation of PGD_2 upon treatment with ALA metabolites in LPS stimulated macrophages may be mediating the anti-inflammatory effects through its downstream metabolite, 15d-PGJ_2 a natural ligand for PPAR-γ [165]. This hypothesis is supported by the observation that PPAR-γ is maintaining the anti-inflammatory state, by inhibiting inflammasome and IL-1β, via induced COX-2 generated downstream metabolites, and when PPAR-γ is inhibited, it is

failing to inactivate the inflammasome. The reverse effects of ALA metabolites on inflammasome and caspase-1, when co-incubated with the PPAR-γ antagonist GW9662 supports such a possibility.

Macrophage differentiation, their subtypes and function depend on its surrounding environment. After differentiation, macrophages polarized into two subtypes, M1 and M2 with characteristic phenotypes and exhibit different behaviors [166]. While, the activation of M1 macrophage is associated with increased expression of iNOS [167] and increased level of pro-inflammatory cytokines such as TNF-α, IL-1β and IL-6 [19], the activation of M2 macrophages is associated with increased level of anti-inflammatory cytokines-IL-10 and scavenger receptor A [19]. LPS stimulated pro-inflammatory state is associated with M1 subtype macrophage, on the other hand, PPAR-γ activation and increased PGE_2 [135,136] is associated with shifting of M1 macrophages into M2 macrophages subtypes [168,169]. In the present study, ALA metabolites activated PPAR-γ, and increased PGE_2 level that might be responsible for shifting of M1 to M2 macrophages subtypes and thereby mediating anti-inflammatory effects. Furthermore, an increased cytokine IL-10 as well as decreased expression of iNOS and TNF-α which are associated with M2 subtype macrophages, further strengthen such a possibility.

Apoptosis is the major mechanism for safe clearance of PMNLs at inflammatory sites and thus limit pro-inflammatory signals and promote resolution of inflammation rather than persistence of tissue damage [170]. In the present study, 13-(S)-HPOTrE showed a dose-dependent increase in apoptosis in LPS activated RAW 264.7 cells and it is previously reported that activation of PPAR-γ induces apoptosis in differentiated

naive macrophages [171]. Therefore, it is possible that the apoptotic effects of 13-(S)-HPOTrE might be mediated through PPAR-γ dependent pathway. There is a correlation between apoptosis and regulation of autophagy. It is reported that apoptosis inhibits beclin-1 mediated autophagy [160]. It supports the present findings on immunofluorescence microscopy with LC3, in which pre-treatment of ALA metabolites remarkably diminished autophagy in LPS challenged RAW 264.7 cells. Furthermore, in immunoblot analysis, a decrease in beclin-1 expression was observed in ALA metabolites pre-treated and challenged with LPS. From these studies, it can be concluded that these ALA metabolites inhibit beclin-1 mediated autophagy through induction of apoptosis.

Sepsis is a critical state of the body because of systemic immune response induced by pathogens, microbes or endotoxins, also called systemic inflammatory response syndrome [172]. In endotoxin-induced septic shock model, mice pre-treated with ALA metabolites showed a significant decrease in mortality rate. Moreover, in another *in vivo* study, in CLP mouse model, mice treated with these ALA metabolites showed decrease in expression of NLRP3. It also showed reduction in IL-1β levels while elevation in IL-10 cytokine level as well. Thus, the *in vitro* anti-inflammatory effects of 13-(S)-HPOTrE and 13-(S)-HOTrE observed in RAW 264.7 cells and peritoneal macrophages also have been demonstrated *in vivo* as evidenced by the extension in the survival of mice in endotoxin-induced septic shock in toxemia model and inactivated inflammasome in polymicrobial-induced sepsis in CLP model.

In the present study, the hydroperoxy [13(S)-HPOTrE] and hydroxy [13(S)-HOTrE] metabolites of ALA showed anti-inflammatory effects, though the hydroperoxy

metabolite being more potent. As the hydroperoxy metabolite [13(S)-HPOTrE] is getting converted to the corresponding hydroxy [13(S)-HOTrE] metabolite with increasing period of time because of the reducing environment created by serum in culture medium, the effects of 13(S)-HPOTrE observed in the present study may be mediated by both the hydroperoxy and hydroxy metabolites of ALA.

The anti-inflammatory properties of ALA (ω-3 PUFA) observed in the present study thus are quite contrasting to those of AA (ω-6 PUFA) metabolites, wherein the hydroperoxy (15-(S)-HPETE) and hydroxy (15-(S)-HETE) metabolites of AA showed contrasting effects on angiogenesis, which is critically associated with inflammation [145,173,174]. While 15(S)-HPETE showed anti-angiogenic effects [145], the 15(S)-HETE induced angiogenesis [174] in adipose tissue. Also, such differential effects of the hydroperoxy and hydroxy metabolites of 15-LOX on angiogenesis were observed in human umbilical vein endothelial cells (HUVECs) [173]. Similar differential effects of hydroperoxy and hydroxy metabolites of 15-LOX with AA as the substrate were reported on chronic myeloid leukemia cell line [144]. Interestingly, in the present study, the hydroperoxy and hydroxy metabolites of ALA showed anti-inflammatory effects, however, the hydroperoxy metabolite being more potent than the hydroxy metabolite. These findings, thus strongly advocate the beneficial effects of ω-3 PUFAs in counteracting various inflammatory disorders, which are mainly mediated by the metabolites of ω-6 PUFAs.

In summary, ALA metabolites [13-(S)-HPOTrE and 13-(S)-HOTrE] exhibit anti-inflammatory effects in LPS challenged RAW 264.7 cells and mouse peritoneal macrophages by down-regulating LPS induced pro-inflammatory markers and by

inactivating the NLRP3 inflammasome complex. Additionally, the anti-inflammatory effects of ALA metabolites were mediated by the induction of apoptosis and inhibition of autophagy in the LPS challenged macrophages. These anti-inflammatory effects of ALA metabolites appear to be mediated by the inactivation of NLRP3 inflammasome complex and decrease in pro-inflammatory cytokines/enzymes along with simultaneous increase in anti-inflammatory cytokines. The present study also demonstrates the protective effects of ALA metabolites *in vivo* as evidenced by the extended survival of BALB/c mice in LPS induced septic shock.

Chapter 5

SUMMARY AND CONCLUSIONS

Inflammation is an essential part of host's response to infection or injury in order to maintain cellular homeostasis. Aberrant inflammation is associated with various disorders mediated by hyperactivation of inflammasome complexes and up-regulation of pro-inflammatory enzymes like iNOS [88,89] LOXs, and COXs [90–92]. The inflammatory response generated by eicosanoids is known to be mediated by pro-inflammatory cytokines such as IL-1β and TNF-α [93]. The types of PUFAs present and their ratio in cell membranes reflect the physiological status of the tissues and regulate the inflammatory response to a variety of external or internal stimuli and thus maintain cellular homeostasis [100,101].

The dietary intake of PUFAs such as AA, LA and ALA directly affects the ratio of ω-6 and ω-3 PUFAs in the cell membranes. The higher amount of ω-6 PUFAs is hypothesized to increase the pro-inflammatory eicosanoids production and thus the onset of various types of inflammatory disorders. A sufficiently high intake of ω-3 PUFAs, on the other hand, is shown to offer protection from inflammatory diseases by decreasing the production of pro-inflammatory eicosanoids, cytokines, ROS and RNS [51,100]. This concept is also supported by the findings of the present study wherein ω-3 PUFA, ALA and its metabolites [13-(S)-HPOTrE and 13-(S)-HOTrE], significantly reduce the production of pro-inflammatory mediators such as NO and ROS, as well as inflammatory cytokines, in LPS stimulated RAW 264.7 cells and in mouse peritoneal macrophages *in vitro*. Further, *in vivo* sepsis model and CLP mice model studies also demonstrates the protective effects of ALA metabolites as evidenced by a decrease in the mortality rate and by the maintenance of anti-inflammatory properties, in treated mice. For these studies, the 15-LOX metabolites of ALA [13-(S)-HPOTrE and 13-(S)-

HOTrE] were generated by employing novel 15-LOX source, linseed seedlings (*Linum usitatissimum*).

Linseed seedlings with abundant lipoxygenase activity

In the plants, LOXs play vital role during seed germination, growth, fruit ripening, and plant senescence [126]. Several studies reported that there are many folds increase in expression of LOXs during seed germination [114]. The present study also showed that the enzymatic activity of linseed seedlings increased during early days and further decreased as the seedlings mature. The specific activity of Day 2 linseed seedlings enzyme was significantly higher in comparison to the enzyme from other days seedlings. The linseed seedlings enzyme used both ω-6 and ω-3 PUFAs as substrates. Further, pH was optimized by measuring the enzyme activity of linseed seedlings at various pHs (pH 6.0 to 13.0), which showed many majors and minor peaks. The presence of such diverse pH optima reveals the possibility of different isoforms of LOXs. The possibility of 15-LOXs in linseed seedlings was further strengthened by comparing metabolites of linseed seedlings with metabolites of soybean 15-LOX on HPLC.

The linseed seedling enzyme is characterized as 15-LOX.

The Linseed seedling enzyme oxygenated PUFAs (AA, LA, and ALA) and generated corresponding hydroperoxy metabolites while hydroxy metabolites were generated by further reduction of hydroperoxy metabolites. When purified on SP-HPLC, the linseed seedlings hydroperoxy and hydroxy metabolites and soybean 15-LOX hydroperoxy [13-(S)-HPOTrE, 15-(S)-HPETE, and 13-(S)-HPODE] and hydroxy metabolites [13-(S)-HOTrE, 15-(S)-HETE, 13-(S)-HODE] showed very similar retention times

respectively and were co-eluted when linseed LOX metabolites were co-injected with those of soybean 15-LOX metabolites, suggesting that linseed enzyme is 15-LOX.

The new generation PDA detector associated with HPLC can efficiently detect any type of impurity if present in major peak such as impurity having either same elution time, or any minor peak eluting in the same area with major peak. The peak purity index obtained from this detector confirmed the purity of PUFAs metabolites synthesized by linseed seedling enzyme and separated on HPLC showed purity index of 1.00, a characteristic feature of a pure compound. These hydroperoxy and hydroxy metabolites of linseed seedlings enzyme synthesized using ALA, AA, and LA, were compared with corresponding standard hydroperoxy and hydroxy metabolites of soybean 15-LOX on SP-HPLC. When the hydroperoxy metabolites of linseed seedlings using ALA, AA, and LA as the substrate, compared with corresponding hydroperoxy metabolites [13-(S)-HPOTrE, 15-(S)-HPETE, and 13-(S)-HPODE] of soybean 15-LOX, showed same retention times. Similarly, the hydroxy metabolites of linseed seedlings using ALA, AA, and LA as the substrate, compared with corresponding hydroxy metabolites [13-(S)-HOTrE, 15-(S)-HETE, and 13-(S)-HODE] of soybean 15-LOX, also showed same retention times. The overlay HPLC chromatogram of hydroperoxy and hydroxy metabolites of linseed seedlings with standard soybean 15-LOX hydroperoxy and hydroxy metabolites indicated that linseed seedling enzyme might be 15-LOX.

The initial assays based on oxygraph indicated the possibility of LOXs in linseed seedling. Furthermore, the comparison of the retention time of hydroperoxy and hydroxy metabolites of linseed LOX with the hydroperoxy and hydroxy metabolites of soybean 15-LOX (standard) strengthens such a possibility. Finally, the presence of 15-

LOX in linseed seedlings was confirmed by analyzing the fragmentation patterns of a metabolite of linseed seedling with the corresponding metabolite of soybean 15-LOX on LC-MS/MS.

The omgea-3 PUFAs (ALA, and DHA) efficiently show anti-inflammatory effects in comparison to omgea-6 PUFAs (AA, and LA).

In the present study, mouse macrophage cell line, RAW 264.7 was used as *in vitro* model system to elucidate the ω-6 and ω-3 PUFAs role in inflammation. The findings of the present study support the previous reports regarding ω-6 and ω-3 PUFAs ratio in the body and their significances. While RAW 264.7 cells stimulated with LPS increased intracellular ROS levels, the macrophages pre-treated with ω-6 and ω-3 PUFAs and then stimulated with LPS showed a significant decrease in ROS generation. ω-3 PUFAs were more efficient in decreasing the intracellular ROS level as compared to ω-6 PUFAs.

NO is considered as a pro-inflammatory marker which regulates growth and inhibition of various cell types such as macrophages, immune cells and mast cells [46,109]. When their level in culture medium was measured, the result showed that macrophages pre-treated with ω-3 and ω-6 PUFAs decreased NO level in comparison to LPS alone treated macrophages. Again, ω-3 PUFAs were more effective in decreasing NO level compared to ω-6 PUFAs. The apoptosis provides strength to resolution phase of inflammation by removing the actively participating pro-inflammatory cells from the site of inflammation. RAW 264.7 cells challenged with LPS showed increased apoptosis, which was further increased in macrophages pre-treated with ω-6 and ω-3 PUFAs and challenged with LPS. However, apoptosis induced by ω-3 PUFAs was more prominent

than ω-6 PUFAs. These studies clearly demonstrate that ω-3 PUFAs (ALA, DHA) are more effective in either decreasing ROS generation or in inducing apoptosis when compared to ω-6 PUFAs and thus in the resolution of inflammation.

ALA metabolites show anti-inflammatory effects in RAW 264.7 CELLS and mouse primary peritoneal macrophages.

The studies presented in the earlier chapter suggest the possibility that the anti-inflammatory effects of ω-3 PUFAs might be mediated through their oxygenated metabolites generated through LOXs and COXs pathways. Based on this assumption, the *in vitro* studies on RAW 264.7 cells and mouse primary peritoneal macrophages were performed, which established the anti-inflammatory role of 15-LOX metabolites of ALA [13-(S)-HPOTrE, and 13-(S)-HOTrE]. The findings of the present study show the anti-inflammatory effects of these metabolites mediated by reducing the production of NO and ROS, as well as inflammatory cytokines, in LPS stimulated RAW 264.7 cells and in mouse peritoneal macrophages isolated from BALB/c mice. Further, the studies indicate that the anti-inflammatory effects of ALA metabolites are mediated by inactivation of NLRP3 inflammasome complex through the PPAR-γ dependent pathway.

Based on immunofluorescent confocal microscopy studies and FACS analysis, it is clear that the ALA metabolites inhibit the translocation of NF-κB to the nucleus, along with the reduction of NO (in culture medium) and ROS in LPS stimulated RAW 264.7 cells and peritoneal mouse macrophages. ALA metabolites also inhibit the activation of NLRP3 inflammasome as well as downstream signalling molecules such as caspase-1 and IL-1β at both transcriptional as well as translational levels. Interestingly, these effects of ALA metabolites on NLRP3 inflammasome were blocked by GW9662- a PPAR-γ antagonist. These studies systematically suggest that the inactivation of LPS induced

NLRP3 inflammasome by ALA metabolites in RAW 264.7 cells and peritoneal macrophages is mediated through PPAR-γ dependent pathway. Indeed, several studies have shown that PUFAs metabolites are ligands of PPAR-γ [137], further supporting such a possibility.

COX-2 functions as both pro-and anti-inflammatory marker, depending on the period and types of downstream metabolites generated [129,162]. In the early stages, it generates pro-inflammatory prostaglandins, whereas at later stages the downstream metabolite is PGD_2, a ligand for PPAR-γ [133], which has been observed to possess anti-inflammatory effects [163]. In this study, an increase in the expression of COX-2 and its downstream metabolites (PGE_2, and PGD_2) was observed in RAW 264.7 cells pre-treated with ALA metabolites and then stimulated with LPS. Here, COX-2 may be playing an anti-inflammatory role by its down-stream metabolite- PGD_2. It has been reported that PGD_2 derivative PGJ_2 and their metabolites $^{12}\Delta$ PGJ_2 and 15d-PGJ_2, often derived from induced COX-2, exhibit their anti-inflammatory effects in various *in vivo* systems [131,138,164]. In the present study the induced expression of COX-2 and increased the formation of PGD_2 upon treatment with ALA metabolites in LPS stimulated macrophages may be mediating the anti-inflammatory effects through its downstream metabolite, 15d-PGJ_2 a natural ligand for PPAR-γ [165]. This hypothesis is supported by the observation that PPAR-γ is maintaining the anti-inflammatory state, by inhibiting inflammasome and IL-1β, via induced COX-2 metabolites. This is further supported by the fact that PPAR-γ antagonist GW9662 could successfully block the ALA metabolites mediated inactivation of the inflammasome.

The surrounding environment affects the differentiation, subtypes and function of macrophages. Macrophages polarized into two subtypes, M1 and M2 after differentiation along with characteristic phenotypes that exhibit different behaviors [166]. While, the activation of M1 macrophages is associated with increased expression of iNOS [167] and increased level of pro-inflammatory cytokines such as TNF-α, IL-1β and IL-6 [19], the activation of M2 macrophages is associated with increased level of anti-inflammatory cytokines-IL-10 and scavenger receptor A [19]. LPS stimulated pro-inflammatory state is associated with M1 subtype macrophages, on the other hand, PPAR-γ activation and increased PGE_2 [135,136] shift the M1 macrophages into M2 macrophages [168,169]. In the present study, ALA metabolites activated PPAR-γ, and increased PGE_2 level that might be responsible for shifting of M1 to M2 macrophages subtypes and thereby mediating anti-inflammatory effects. Furthermore, an increased cytokine IL-10 as well as decreased expression of iNOS and TNF-α further strengthens such a possibility.

Apoptosis is the key machinery for clearance of pro-inflammatory cells from the inflammatory sites and support resolution phase of inflammation [170] and the activation of PPAR-γ induces apoptosis in differentiated naive macrophages [171]. In the present study 13-(S)-HPOTrE showed an increase in apoptosis in LPS stimulated RAW 264.7 cells. Therefore, it is possible that the apoptotic effects of 13-(S)-HPOTrE might be mediated through PPAR-γ dependent pathway. Further, there is a correlation between apoptosis and regulation of autophagy. It is reported that apoptosis inhibits beclin-1 mediated autophagy [160]. Again, it supports the present findings on immunofluorescence microscopy with LC3 in LPS challenged RAW 264.7 cells, in which pre-treatment of ALA metabolites remarkably diminished autophagy. Furthermore, in

immunoblot analysis, decrease in beclin-1 protein expression was observed in ALA metabolites pre-treated cells when challenged with LPS. From these studies, it can be concluded that ALA metabolites inhibit beclin-1 mediated autophagy through induction of apoptosis.

ALA metabolites extend survival of BALB/c mice and mediate anti-inflammatory effects by inactivating NLRP3 inflammasome: in vivo studies in sepsis model and CLP mice model.

The anti-inflammatory effects of ALA metabolites were further demonstrated *in vivo* in both the animal models, sepsis model induced by LPS and CLP mice model. These studies confirm the protective effects of 13-(S)-HPOTrE and 13-(S)-HOTrE as evidenced by a decrease in the mortality rate and by the maintenance of anti-inflammatory properties, in ALA metabolites treated BALB/c mice.

In LPS induced septic shock model, there was a significant decrease in the mortality rate in the mice pre-treated with ALA metabolites. Moreover, in another *in vivo* study, polymicrobial induced CLP mouse model, there was decrease in NLRP3 inflammasome expression in the mice treated with these ALA metabolites. It also showed reduction in pro-inflammatory cytokine- IL-1β levels along with elevation in anti-inflammatory cytokine- IL-10 levels. Thus, the *in vitro* anti-inflammatory effects of ALA metabolites observed in RAW 264.7 cells and peritoneal macrophages were further demonstrated *in vivo* as evidenced by the extension in the survival of mice in LPS-induced septic shock in toxemia model and inactivation of inflammasome in polymicrobial-induced sepsis in CLP model.

In conclusion the present study demonstrates that the ω-3 PUFAs (ALA, and DHA) exhibit significant anti-inflammatory effects *in vitro* in RAW 264.7 cells, much

higher than ω-6 PUFAs (AA, and LA), by reducing pro-inflammatory markers such as ROS, IL-1β, and NO. Further, the studies demonstrate that the LOX metabolites of ω-3 PUFAs

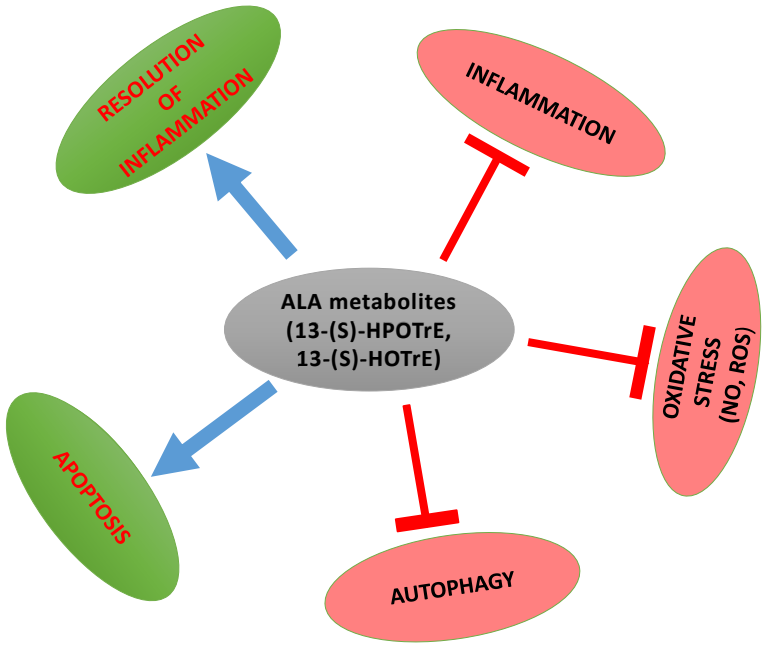

Figure 5-1: ***Effects of ALA metabolites [13-(S)-HPOTrE and 13-(S)-HOTrE] on different cellular processes/mechanism during inflammation.*** *Blue arrow- Positive effects, Red arrow- Negative effects*

Information based on: Kumar, N. *et al.* 15-Lipoxygenase metabolites of α-linolenic acid, [13-(S)-HPOTrE and 13-(S)-HOTrE], mediate anti-inflammatory effects by inactivating NLRP3 inflammasome. *Sci. Rep.* **6,** 31649 (2016).

are much more potent than the ω-6 PUFAs in exhibiting the anti-inflammatory effects, both *in vitro* and *in vivo*. The hydroperoxy and hydroxy metabolites of ALA, [13-(S)-HPOTrE and 13-(S)-HOTrE], exhibit their anti-inflammatory effects by down-regulating LPS induced pro-inflammatory markers and by inactivating the NLRP3 inflammasome complex in LPS challenged RAW 264.7 cells as well as in mouse peritoneal macrophages. Further, the ALA metabolites were shown to mediate the anti-inflammatory effects by the induction of apoptosis, inhibition of autophagy, inactivation of NLRP3 inflammasome complex and decrease in pro-inflammatory cytokines or enzymes along with simultaneous increase in anti-inflammatory cytokines. This study also

demonstrates for the first time the protective role of ALA metabolites *in vivo* in LPS-induced septic shock in toxemia model and inactivation of inflammasome in polymicrobial induced sepsis in CLP model, through induction of various anti-inflammatory pathways.

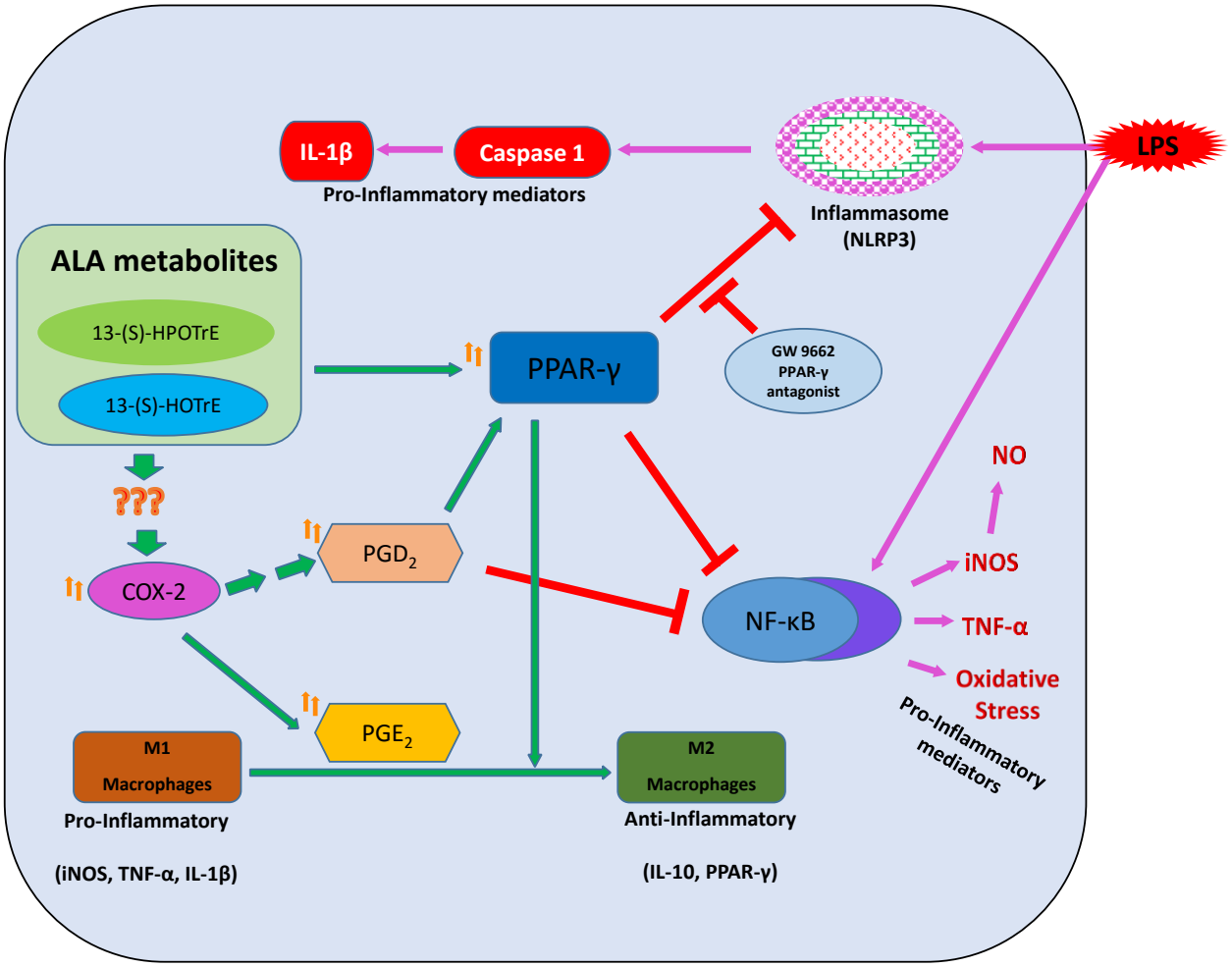

Figure : ALA metabolites mediate anti-inflammatory effects through PPAR-γ dependent pathways

Information based on: Kumar, N. *et al.* 15-Lipoxygenase metabolites of α-linolenic acid, [13-(S)-HPOTrE and 13-(S)-HOTrE], mediate anti-inflammatory effects by inactivating NLRP3 inflammasome. *Sci. Rep.* **6,** 31649 (2016).

REFERENCES

1. Ritchie RF, Palomaki GE, Neveux LM, Navolotskaia O, Ledue TB, Craig WY. Reference distributions for the negative acute-phase serum proteins, albumin, transferrin and transthyretin: a practical, simple and clinically relevant approach in a large cohort. J Clin Lab Anal. 1999;13: 273–9.
2. Ananian P, Hardwigsen J, Bernard D, Le Treut YP. Serum acute-phase protein level as indicator for liver failure after liver resection. Hepatogastroenterology. 52: 857–61.
3. Chua E, Clague JE, Sharma AK, Horan MA, Lombard M. Serum transferrin receptor assay in iron deficiency anaemia and anaemia of chronic disease in the elderly. QJM. 1999;92: 587–94.
4. Gotschlich EC, Liu TY, Oliveira E. Binding of C-reactive protein to C-carbohydrate and PC-substituted protein. Ann N Y Acad Sci. 1982;389: 163–71.
5. Kaplan MH, Volanakis JE. Interaction of C-reactive protein complexes with the complement system. I. Consumption of human complement associated with the reaction of C-reactive protein with pneumococcal C-polysaccharide and with the choline phosphatides, lecithin and sphingomyelin. J Immunol. 1974;112: 2135–47.
6. Kastrup CJ, Boedicker JQ, Pomerantsev AP, Moayeri M, Bian Y, Pompano RR, et al. Spatial localization of bacteria controls coagulation of human blood by “quorum acting”. Nat Chem Biol. NIH Public Access; 2008;4: 742–50.
7. Maintz L, Novak N. Histamine and histamine intolerance. Am J Clin Nutr. 2007;85: 1185–96.
8. Ryan GB, Majno G. Acute inflammation. A review. Am J Pathol. 1977;86: 183–276.
9. Owen J, Punt J, Stranford S, Jones P. Kuby IMMUNOLOGY. Kuby IMMUNOLOGY. W. H. Freeman; 2013.
10. Dunkelberger JR, Song W. Complement and its role in innate and adaptive immune responses. Cell Res. Nature Publishing Group; 2010;20: 34–50. doi:10.1038/cr.2009.139
11. Charles A Janeway J, Travers P, Walport M, Shlomchik MJ. The complement system and innate immunity. Garland Science; 2001;
12. Markiewski MM, Lambris JD. The role of complement in inflammatory diseases from behind the scenes into the spotlight. Am J Pathol. 2007;171: 715–27. doi:10.2353/ajpath.2007.070166
13. Smith WB, Noack L, Khew-Goodall Y, Isenmann S, Vadas MA, Gamble JR. Transforming growth factor-beta 1 inhibits the production of IL-8 and the transmigration of neutrophils through activated endothelium. J Immunol. American Association of Immunologists; 1996;157: 360–8.
14. Cho JH, Feldman M. Heterogeneity of autoimmune diseases: pathophysiologic insights from genetics and implications for new therapies. Nat Med. Nature Publishing Group; 2015;21: 730–8. doi:10.1038/nm.3897
15. Mantovani A, Mantovani A, Allavena P, Allavena P, Sica A, Sica A, et al. Cancer-related inflammation. Nature. 2008;454: 436–44. doi:10.1038/nature07205
16. Mantovani A. Cancer: Inflaming metastasis. Nature. 2009;457: 36–37. doi:10.1038/457036b

17. Kumar KA, Arunasree KM, Roy KR, Reddy NP, Aparna A, Reddy GV, et al. Effects of (15S)-hydroperoxyeicosatetraenoic acid and (15S)-hydroxyeicosatetraenoic acid on the acute-lymphoblastic-leukaemia cell line Jurkat: activation of the Fas-mediated death pathway. Biotechnol Appl Biochem. Blackwell Publishing Ltd; 2009;52: 121–133. doi:10.1042/BA20070264

18. Djavaheri-Mergny M, Maiuri MC, Kroemer G. Cross talk between apoptosis and autophagy by caspase-mediated cleavage of Beclin 1. Oncogene. Nature Publishing Group; 2010;29: 1717–1719. doi:10.1038/onc.2010.514

19. Grivennikov SI, Greten FR, Karin M. Immunity, Inflammation, and Cancer. Cell. 2011;140: 883–899. doi:10.1016/j.cell.2010.01.025.Immunity

20. Pikarsky E, Porat RM, Stein I, Abramovitch R, Amit S, Kasem S, et al. NF-kappaB functions as a tumour promoter in inflammation-associated cancer. Nature. 2004;431: 461–6. doi:10.1038/nature02924

21. Colotta F, Allavena P, Sica A, Garlanda C, Mantovani A. Cancer-related inflammation, the seventh hallmark of cancer: links to genetic instability. Carcinogenesis. 2009;30: 1073–1081. doi:10.1093/carcin/bgp127

22. Allavena P, Sica A, Garlanda C, Mantovani A. The Yin-Yang of tumor-associated macrophages in neoplastic progression and immune surveillance. Immunol Rev. Blackwell Publishing Ltd; 2008;222: 155–161. doi:10.1111/j.1600-065X.2008.00607.x

23. Apetoh L, Ghiringhelli F, Tesniere A, Obeid M, Ortiz C, Criollo A, et al. Toll-like receptor 4–dependent contribution of the immune system to anticancer chemotherapy and radiotherapy. Nat Med. Nature Publishing Group; 2007;13: 1050–1059. doi:10.1038/nm1622

24. Rathinam VA, Vanaja SK, Fitzgerald KA. Regulation of inflammasome signaling. Nat Immunol. 2012;13: 332–333. doi:ni.2237 [pii]\r10.1038/ni.2237 [doi]

25. McIntire CR, Yeretssian G, Saleh M. Inflammasomes in infection and inflammation. Apoptosis. 2009;14: 522–535. doi:10.1007/s10495-009-0312-3

26. Sokolovska A, Becker CE, Ip WKE, Rathinam VAK, Brudner M, Paquette N, et al. Activation of caspase-1 by the NLRP3 inflammasome regulates the NADPH oxidase NOX2 to control phagosome function. Nat Immunol. 2013;14: 543–553. doi:10.1038/ni.2595

27. Ren K, Torres R. Role of interleukin-1beta during pain and inflammation. Brain Res Rev. 2009;60: 57–64. doi:10.1016/j.brainresrev.2008.12.020

28. Church LD, Cook GP, McDermott MF. Primer: inflammasomes and interleukin 1β in inflammatory disorders. Nat Clin Pract Rheumatol. 2008;4: 34–42. doi:10.1038/ncprheum0681

29. Bergsbaken T, Fink SL, Cookson BT. Pyroptosis: host cell death and inflammation. Nat Rev Microbiol. 2009;7: 99–109. doi:10.1038/nrmicro2070

30. Allen IC, Scull MA, Moore CB, Holl EK, McElvania-TeKippe E, Taxman DJ, et al. The NLRP3 inflammasome mediates in vivo innate immunity to influenza A virus through recognition of viral RNA. Immunity. NIH Public Access; 2009;30: 556–65. doi:10.1016/j.immuni.2009.02.005

31. Duncan JA, Gao X, Huang MT-H, O'Connor BP, Thomas CE, Willingham SB, et al. Neisseria gonorrhoeae activates the proteinase cathepsin B to mediate the signaling activities of the NLRP3 and ASC-containing inflammasome. J Immunol. 2009;182: 6460–9.

doi:10.4049/jimmunol.0802696

32. Kim S, Bauernfeind F, Ablasser A, Hartmann G, Fitzgerald KA, Latz E, et al. Listeria monocytogenes is sensed by the NLRP3 and AIM2 inflammasome. Eur J Immunol. 2010;40: 1545–51. doi:10.1002/eji.201040425

33. Hise AG, Tomalka J, Ganesan S, Patel K, Hall BA, Brown GD, et al. An Essential Role for the NLRP3 Inflammasome in Host Defense against the Human Fungal Pathogen Candida albicans. Cell Host Microbe. Elsevier Ltd; 2009;5: 487–497. doi:10.1016/j.chom.2009.05.002

34. Muñoz-Planillo R, Franchi L, Miller LS, Núñez G. A critical role for hemolysins and bacterial lipoproteins in Staphylococcus aureus-induced activation of the Nlrp3 inflammasome. J Immunol. 2009;183: 3942–8. doi:10.4049/jimmunol.0900729

35. Meixenberger K, Pache F, Eitel J, Schmeck B, Hippenstiel S, Slevogt H, et al. Listeria monocytogenes-infected human peripheral blood mononuclear cells produce IL-1beta, depending on listeriolysin O and NLRP3. J Immunol. 2010;184: 922–30. doi:10.4049/jimmunol.0901346

36. Latz E, Xiao TS, Stutz A. Activation and regulation of the inflammasomes. Nat Rev Immunol. 2013;13: 397–411. doi:10.1038/nri3452

37. Hoffman HM, Brydges SD. Genetic and molecular basis of inflammasome-mediated disease. J Biol Chem. 2011;286: 10889–10896. doi:10.1074/jbc.R110.135491

38. Campbell L, Raheem I, Malemud C, Askari A. The Relationship between NALP3 and Autoinflammatory Syndromes. Int J Mol Sci. 2016;17: 725. doi:10.3390/ijms17050725

39. Hoffman HM, Mueller JL, Broide DH, Wanderer AA, Kolodner RD. Mutation of a new gene encoding a putative pyrin-like protein causes familial cold autoinflammatory syndrome and Muckle-Wells syndrome. Nat Genet. 2001;29: 301–5. doi:10.1038/ng756

40. Guo H, Callaway JB, Ting JP-Y. Inflammasomes: mechanism of action, role in disease, and therapeutics. Nat Med. 2015;21: 677–87. doi:10.1038/nm.3893

41. Wilson SP, Cassel SL. Inflammasome-Mediated Autoinflammatory Disorders. Postgrad Med. 2010;122: 125–133. doi:10.3810/pgm.2010.09.2209

42. Yuan C, Bloch K. ARTICLE : Conversion of Oleic Acid to Linoleic Acid Conversion of Oleic to Linoleic Acid *? 1961;236: 1277–1279.

43. Gurr M., Harwood J. Fatty Acid Structure and Metabolism. Lipid Biochemistry. Oxford, UK: Blackwell Science Ltd; 1991. pp. 13–92. doi:10.1002/9780470774366.ch2

44. Simopoulos AP. The importance of the ratio of omega-6/omega-3 essential fatty acids. Biomed Pharmacother = Biomédecine pharmacothérapie. 2002;56: 365–79.

45. Calder PC. Immunoregulatory and anti-inflammatory effects of n-3 polyunsaturated fatty acids. Brazilian J Med Biol Res = Rev Bras Pesqui médicas e biológicas / Soc Bras Biofísica . [et al]. 1998;31: 467–90.

46. Lee TH, Hoover RL, Williams JD, Sperling RI, Ravalese J, Spur BW, et al. Effect of dietary enrichment with eicosapentaenoic and docosahexaenoic acids on in vitro neutrophil and monocyte leukotriene generation and neutrophil function. N Engl J Med. 1985;312: 1217–24. doi:10.1056/NEJM198505093121903

47. Endres S, Ghorbani R, Kelley VE, Georgilis K, Lonnemann G, van der Meer JW, et al. The effect of dietary supplementation with n-3 polyunsaturated fatty acids on the synthesis

of interleukin-1 and tumor necrosis factor by mononuclear cells. N Engl J Med. 1989;320: 265–71. doi:10.1056/NEJM198902023200501

48. Gibney MJ, Hunter B. The effects of short- and long-term supplementation with fish oil on the incorporation of n-3 polyunsaturated fatty acids into cells of the immune system in healthy volunteers. Eur J Clin Nutr. 1993;47: 255–9.

49. Yaqoob P, Pala HS, Cortina-Borja M, Newsholme EA, Calder PC. Encapsulated fish oil enriched in alpha-tocopherol alters plasma phospholipid and mononuclear cell fatty acid compositions but not mononuclear cell functions. Eur J Clin Invest. 2000;30: 260–74.

50. Connor KM, SanGiovanni JP, Lofqvist C, Aderman CM, Chen J, Higuchi A, et al. Increased dietary intake of omega-3-polyunsaturated fatty acids reduces pathological retinal angiogenesis. Nat Med. Nature Publishing Group; 2007;13: 868–873. doi:10.1038/nm1591

51. Calder PC. Dietary modification of inflammation with lipids. Proc Nutr Soc. 2002;61: 345–358. doi:10.1079/PNS2002166

52. Dobrian AD, Lieb DC, Cole BK, Taylor-Fishwick DA, Chakrabarti SK, Nadler JL. Functional and pathological roles of the 12- and 15-lipoxygenases. Prog Lipid Res. 2011;50: 115–31. doi:10.1016/j.plipres.2010.10.005

53. Ivanov I, Heydeck D, Hofheinz K, Roffeis J, O'Donnell VB, Kuhn H, et al. Molecular enzymology of lipoxygenases. Arch Biochem Biophys. Elsevier Inc.; 2010;503: 161–174. doi:10.1016/j.abb.2010.08.016

54. Maccarrone M, Melino G, Finazzi-Agrò A. Lipoxygenases and their involvement in programmed cell death. Cell Death Differ. 2001;8: 776–784. doi:10.1038/sj.cdd.4400908

55. Koljak R. Identification of a Naturally Occurring Peroxidase-Lipoxygenase Fusion Protein. Science (80-). American Association for the Advancement of Science; 2011;277: 1–4. doi:10.1126/science.277.5334.1994

56. Brash AR. Lipoxygenases: Occurrence, Functions, Catalysis, and Acquisition of Substrate. J Biol Chem. 1999;274: 23679–23682. doi:10.1074/jbc.274.34.23679

57. Vogel R, Jansen C, Roffeis J, Reddanna P, Forsell P, Claesson HE, et al. Applicability of the triad concept for the positional specificity of mammalian lipoxygenases. J Biol Chem. 2010;285: 5369–5376. doi:10.1074/jbc.M109.057802

58. Hawkins DJ, Brash AR. Eggs of the sea urchin, Strongylocentrotus purpuratus, contain a prominent (11R) and (12R) lipoxygenase activity. J Biol Chem. 1987;262: 7629–7634.

59. Andreou A, Feussner I. Lipoxygenases - Structure and reaction mechanism. Phytochemistry. 2009;70: 1504–10. doi:10.1016/j.phytochem.2009.05.008

60. Oliw EH. Plant and fungal lipoxygenases. Prostaglandins Other Lipid Mediat. 2002;68–69: 313–323. doi:10.1016/S0090-6980(02)00037-0

61. Koeduka T, Kajiwara T, Matsui K. Cloning of lipoxygenase genes from a cyanobacterium, Nostoc punctiforme, and its expression in Eschelichia coli. Curr Microbiol. 2007;54: 315–319. doi:10.1007/s00284-006-0512-9

62. Porta H, Rocha-Sosa M. Lipoxygenase in bacteria: a horizontal transfer event? Microbiology. 2001;147: 3199–200. doi:10.1099/00221287-147-12-3199

63. Vance RE, Hong S, Gronert K, Serhan CN, Mekalanos JJ. The opportunistic pathogen Pseudomonas aeruginosa carries a secretable arachidonate 15-lipoxygenase. Proc Natl

Acad Sci U S A. 2004;101: 2135–9. doi:10.1073/pnas.0307308101

64. THEORELL H, HOLMAN RT, AKESON A. Crystalline lipoxidase. Acta Chem Scand. 1947;1: 571–6. doi:10.3891/acta.chem.scand.01-0571

65. Siedow JN. Plant Lipoxygenase: structure and function. Annu Rev Plant Physiol Plant Mol Biol. 1991;42: 145–188. doi:10.1146/annurev.pp.42.060191.001045

66. Hildebrand , D. F., Hamilton-Kemp T, R . , Legg, C . S . , Bookjans G. Plant lipoxygenases: occurrence, properties and possible functions. 1988.

67. Vick BA, Zimmerman DC. Characterization of 12-Oxo-Phytodienoic Acid Reductase in Corn: The Jasmonic Acid Pathway. Plant Physiol. 1986;80: 202–205.

68. Brady A V. Oxygenated fatty acids of the lipoxygenase pathways. Lipid Metab plant. 1993;In: Moore: 167–191.

69. Siedow JN. Plant Lipoxygenase: structure and function. Annual Review of Plant Physiology and Plant Molecular Biology. 1991. pp. 145–188. doi:10.1146/annurev.pp.42.060191.001045

70. Gardner HW. Soybean lipoxygenase-1 enzymically forms both (9S)- and (13S)-hydroperoxides from linoleic acid by a pH-dependent mechanism. Biochim Biophys Acta (BBA)/Lipids Lipid Metab. 1989;1001: 274–281. doi:10.1016/0005-2760(89)90111-2

71. Berry H. Oxygen Concentration Determines Regiospecificity in Soybean Lipoxygenase-1 Reaction Via a Branched Kinetic Scheme. J Biol Chem. 1998;273: 2769–2776. doi:10.1074/jbc.273.5.2769

72. Grechkin A. Recent developments in biochemistry of the plant lipoxygenase pathway. Prog Lipid Res. 1998;37: 317–352. doi:10.1016/S0163-7827(98)00014-9

73. Feussner I, Kühn H, Wasternack C. Lipoxygenase-dependent degradation of storage lipids. Trends Plant Sci. 2001;6: 268–273. doi:10.1016/S1360-1385(01)01950-1

74. Stelmach BA, M??ller A, Hennig P, Gebhardt S, Schubert-Zsilavecz M, Weiler EW. A Novel Class of Oxylipins, sn1-O-(12-Oxophytodienoyl)-sn2-O-(hexadecatrienoyl)-monogalactosyl Diglyceride, from Arabidopsis thaliana. J Biol Chem. 2001;276: 12832–12838. doi:10.1074/jbc.M010743200

75. Maccarrone M, Veldink GA, Agrò AF, Vliegenthart JF. Modulation of soybean lipoxygenase expression and membrane oxidation by water deficit. FEBS Lett. 1995;371: 223–6. doi:10.1016/0014-5793(95)00876-B

76. Fischer AM, Dubbs WE, Baker RA, Fuller MA, Stephenson LC, Grimes HD. Protein dynamics, activity and cellular localization of soybean lipoxygenases indicate distinct functional roles for individual isoforms. Plant J. Blackwell Science Ltd; 1999;19: 543–54. doi:10.1046/j.1365-313X.1999.00550.x

77. Melan MA, Dong X, Endara ME, Davis KR, Ausubel FM, Peterman TK. An Arabidopsis thaliana lipoxygenase gene can be induced by pathogens, abscisic acid, and methyl jasmonate. Plant Physiol. 1993;101: 441–450.

78. Creelman RA, Mullet JE. Biosynthesis and Action of Jasmonates in Plants. Annu Rev Plant Physiol Plant Mol Biol. Annual Reviews 4139 El Camino Way, P.O. Box 10139, Palo Alto, CA 94303-0139, USA; 1997;48: 355–381. doi:10.1146/annurev.arplant.48.1.355

79. Porta H, Rueda-Benítez P, Campos F, Colmenero-Flores JM, Colorado JM, Carmona MJ, et al. Analysis of lipoxygenase mRNA accumulation in the common bean (Phaseolus

vulgaris L.) during development and under stress conditions. Plant Cell Physiol. 1999;40: 850–8.

80. Kolomiets M V. Lipoxygenase Is Involved in the Control of Potato Tuber Development. Plant Cell Online. 2001;13: 613–626. doi:10.1105/tpc.13.3.613

81. Griffiths a., Barry C, Alpuche-Solis a. G, Grierson D. Ethylene and developmental signals regulate expression of lipoxygenase genes during tomato fruit ripening. J Exp Bot. 1999;50: 793–798. doi:10.1093/jxb/50.335.793

82. Liu Y, Ahn J-E, Datta S, Salzman R a, Moon J, Huyghues-Despointes B, et al. Arabidopsis vegetative storage protein is an anti-insect acid phosphatase. Plant Physiol. 2005;139: 1545–56. doi:10.1104/pp.105.066837

83. Tranbarger TJ, Franceschi VR, Hildebrand DF, Grimes HD. The Soybean 94-Kilodalton Vegetative Storage Protein Is a Lipoxygenase That Is Localized in Paravenous Mesophyll Cell Vacuoles. Plant Cell. 1991;3: 973–987. doi:10.1105/tpc.3.9.973

84. Porta H. Plant Lipoxygenases. Physiological and Molecular Features. Plant Physiol. 2002;130: 15–21. doi:10.1104/pp.010787

85. Bate NJ, Rothstein SJ. C6-volatiles derived from the lipoxygenase pathway induce a subset of defense-related genes. Plant J. 1998;16: 561–569. doi:10.1046/j.1365-313X.1998.00324.x

86. Parchmann S, Gundlach H, Mueller MJ. Induction of 12-oxo-phytodienoic acid in wounded plants and elicited plant cell cultures. Plant Physiol. 1997;115: 1057–1064. doi:10.1104/pp.115.3.1057

87. Agrawal AA. Mechanisms, ecological consequences and agricultural implications of tri-trophic interactions. Curr Opin Plant Biol. 2000;3: 329–335. doi:10.1016/S1369-5266(00)00089-3

88. Xie Q, Nathan C. The high-output nitric oxide pathway: role and regulation. J Leukoc Biol. 1994;56: 576–582.

89. Kanwar JR, Kanwar RK, Burrow H, Baratchi S. Recent advances on the roles of NO in cancer and chronic inflammatory disorders. Curr Med Chem. 2009;16: 2373–94. doi:10.2174/092986709788682155

90. Kim SY, Kim T-B, Moon K, Kim TJ, Shin D, Cho YS, et al. Regulation of pro-inflammatory responses by lipoxygenases via intracellular reactive oxygen species in vitro and in vivo. Exp Mol Med. Korean Society of Medical Biochemistry and Molecular Biology; 2008;40: 461–76. doi:10.3858/emm.2008.40.4.461

91. Ulivi V, Giannoni P, Gentili C, Cancedda R, Descalzi F. p38/NF-kB-dependent expression of COX-2 during differentiation and inflammatory response of chondrocytes. J Cell Biochem. 2008;104: 1393–1406. doi:10.1002/jcb.21717

92. Taketo MM. Wnt signaling and gastrointestinal tumorigenesis in mouse models. Oncogene. 2006;25: 7522–7530. doi:10.1038/sj.onc.1210058

93. Reuter S, Gupta SC, Chaturvedi MM, Aggarwal BB. Oxidative stress, inflammation, and cancer: how are they linked? Free Radic Biol Med. Elsevier Inc.; 2010;49: 1603–16. doi:10.1016/j.freeradbiomed.2010.09.006

94. Astrup A. The role of dietary fat in obesity. Semin Vasc Med. 2005;5: 40–7. doi:10.1055/s-2005-871740

95. Medzhitov R. Origin and physiological roles of inflammation. Nature. 2008;454: 428–435. doi:10.1038/nature07201

96. Calder PC. Polyunsaturated fatty acids and inflammation. Prostaglandins, Leukot Essent Fat Acids. 2006;75: 197–202. doi:10.1016/j.plefa.2006.05.012

97. Calder PC. n-3 polyunsaturated fatty acids, inflammation, and inflammatory diseases. Am J Clin Nutr. 2006;83: 1505S–1519S.

98. Svahn SL, Grahnemo L, Pálsdóttir V, Nookaew I, Wendt K, Gabrielsson B, et al. Dietary Polyunsaturated Fatty Acids Increase Survival and Decrease Bacterial Load during Septic Staphylococcus aureus Infection and Improve Neutrophil Function in Mice. McCormick BA, editor. Infect Immun. 2015;83: 514–521. doi:10.1128/IAI.02349-14

99. Kaithwas G, Majumdar DK. Effect of L. usitatissimum (Flaxseed/Linseed) Fixed Oil against Distinct Phases of Inflammation. ISRN Inflamm. 2013;2013: 1–4. doi:10.1155/2013/735158

100. Ren J, Chung SH. Anti-inflammatory Effect of α-Linolenic Acid and Its Mode of Action through the Inhibition of Nitric Oxide Production and Inducible Nitric Oxide Synthase Gene Expression via NF-κB and Mitogen-Activated Protein Kinase Pathways. J Agric Food Chem. American Chemical Society; 2007;55: 5073–5080. doi:10.1021/jf0702693

101. Barceló-Coblijn G, Murphy EJ. Alpha-linolenic acid and its conversion to longer chain n−3 fatty acids: Benefits for human health and a role in maintaining tissue n−3 fatty acid levels. Prog Lipid Res. Elsevier Ltd; 2009;48: 355–374. doi:10.1016/j.plipres.2009.07.002

102. Hartley JW, Evans LH, Green KY, Naghashfar Z, Macias AR, Zerfas PM, et al. Expression of infectious murine leukemia viruses by RAW264.7 cells, a potential complication for studies with a widely used mouse macrophage cell line. Retrovirology. 2008;5: 1. doi:10.1186/1742-4690-5-1

103. Mosmann T. Rapid colorimetric assay for cellular growth and survival: application to proliferation and cytotoxicity assays. J Immunol Methods. 1983;65: 55–63. doi:10.1016/0022-1759(83)90303-4

104. Dinarello C a. Historical Review of Cytokines. Eur J Immunol. 2007;37: S34–S45. doi:10.1002/eji.200737772.Historical

105. Sims JE, Smith DE. The IL-1 family: regulators of immunity. Nat Rev Immunol. Nature Publishing Group; 2010;10: 89–102. doi:10.1038/nri2691

106. Hortelano S, Castrillo a, Alvarez a M, Boscá L. Contribution of cyclopentenone prostaglandins to the resolution of inflammation through the potentiation of apoptosis in activated macrophages. J Immunol. 2000;165: 6525–6531.

107. Wang J, Feng X, Zeng Y, Fan J, Wu J, Li Z, et al. Lipopolysaccharide (LPS)-induced autophagy is involved in the restriction of Escherichia coli in peritoneal mesothelial cells. BMC Microbiol. BMC Microbiology; 2013;13: 255. doi:10.1186/1471-2180-13-255

108. Merriam-Webster. Food (n.d.) [Internet]. Merriam-Webster; [cited 21 Jun 2016]. Available: http://www.merriam-webster.com/dictionary/food

109. Coleman JW. Nitric oxide in immunity and inflammation. International Immunopharmacology. 2001. pp. 1397–1406. doi:10.1016/S1567-5769(01)00086-8

110. Ren J, Chung SH. Anti-inflammatory Effect of α-Linolenic Acid and Its Mode of Action through the Inhibition of Nitric Oxide Production and Inducible Nitric Oxide Synthase Gene Expression via NF-κB and Mitogen-Activated Protein Kinase Pathways. J Agric Food

Chem. 2007;55: 5073–5080. doi:10.1021/jf0702693

111. Komatsu W. Docosahexaenoic acid suppresses nitric oxide production and inducible nitric oxide synthase expression in interferon-γ plus lipopolysaccharide-stimulated murine macrophages by inhibiting the oxidative stress. Free Radic Biol Med. 2003;34: 1006–1016. doi:10.1016/S0891-5849(03)00027-3

112. Oelze-Karow H, Schopfer P, Mohr H. Phytochrome-mediated repression of enzyme synthesis (lipoxygenase): a threshold phenomenon. Proc Natl Acad Sci U S A. 1970;65: 51–7.

113. Matsui K, Kajiwara T, Hayashi K, Hatanaka A. Tissue Specific Heterogeneity of Lipoxygenase in Cucumber Seedlings. Agric Biol Chem. 1988;52: 3219–3221. doi:10.1080/00021369.1988.10869218

114. Ohta H (Kyoto U. U (Japan). RI for FS, Ida S, Mikami B, Morita Y. Changes in lipoxygenase components of rice seedlings during germination. Plant Cell Physiol. 1986;

115. Dupont J. Lipoxygenase- mediated cleavage of fatty acids in plant mitochondria. Physiol Plant. Blackwell Publishing Ltd; 1981;52: 225–232. doi:10.1111/j.1399-3054.1981.tb08497.x

116. Reddanna P, Whelan J, Maddipati KR, Reddy CC. Purification of arachidonate 5-lipoxygenase from potato tubers. Methods Enzymol. 1990;187: 268–277. doi:http://dx.doi.org/10.1016/0076-6879(90)87031-W

117. Pérez-Gilabert M, López-Nicolás JM, García Carmona F. Purification of a novel lipoxygenase from eggplant (Solanum melongena) fruit chloroplasts. Physiol Plant. Munksgaard International Publishers; 2001;111: 276–282. doi:10.1034/j.1399-3054.2001.1110303.x

118. Martinchik AN, Baturin AK, Zubtsov V V, Molofeev VI. [Nutritional value and functional properties of flaxseed]. Vopr Pitan. 2012;81: 4–10.

119. Oomah BD, Kenaschuk EO, Mazza G. Lipoxygenase Enzyme in Flaxseed †. JAgricFood chem. 1997;8561: 2426–2430.

120. Zimmerman DC, Vick BA. Specificity of flaxseed lipoxidase. Lipids. Springer-Verlag; 1970;5: 392–397. doi:10.1007/BF02532104

121. Grosch W, Laskawy G, Weber F. Formation of volatile carbonyl compounds and cooxidation of beta-carotene by lipoxygenase from wheat, potato, flax, and beans. J Agric Food Chem. 24: 456–9.

122. Vernooy Gerritsen M GAV and VJFG. Specification of Antisera Directed Against Soybean Lipoxygenases-1 and -2 and purification of Lipoxygenases-2 by Affinity Chromatography. Biochemica et Biophysica Acta; 1982. pp. 330–334.

123. Sailesh S, Kumar Y V, Prasad M, Reddanna P. Sheep uterus dual lipoxygenase in the synthesis of 14,15-leukotrienes. Arch Biochem Biophys. 1994;315: 362–8. doi:10.1006/abbi.1994.1512

124. Reddy GR, Reddanna P, Reddy CC, Curtis WR. 11-hydroperoxyeicosatetraenoic acid is the major dioxygenation product of lipoxygenase isolated from hairy root cultures of Solanum tuberosum. Biochem Biophys Res Commun. 1992;189: 1349–52. doi:10.1016/0006-291X(92)90222-7

125. Rabinovitch-Chable H, Cook-Moreau J, Breton JC, Rigaud M. Purification of lipoxygenase and hydroperoxide dehydrase in flaxseeds: Interaction between these enzymatic

activities. Biochem Biophys Res Commun. 1992;188: 858–864. doi:10.1016/0006-291X(92)91135-D

126. Thompson JE, Froese CD, Madey E, Smith MD, Hong Y. Lipid metabolism during plant senescence. Prog Lipid Res. 1998;37: 119–141. doi:10.1016/S0163-7827(98)00006-X

127. Serhan CN, Hong S, Gronert K, Colgan SP, Devchand PR, Mirick G, et al. Resolvins: A Family of Bioactive Products of Omega-3 Fatty Acid Transformation Circuits Initiated by Aspirin Treatment that Counter Proinflammation Signals. J Exp Med. 2002;196: 1025–1037. doi:10.1084/jem.20020760

128. Kalinski P. Regulation of Immune Responses by Prostaglandin E2. J Immunol. 2012;188: 21–28. doi:10.4049/jimmunol.1101029

129. Serhan CN, Chiang N, Van Dyke TE. Resolving inflammation: dual anti-inflammatory and pro-resolution lipid mediators. Nat Rev Immunol. 2008;8: 349–361. doi:10.1038/nri2294

130. Ricciotti E, FitzGerald GA. Prostaglandins and Inflammation. Arterioscler Thromb Vasc Biol. 2011;31: 986–1000. doi:10.1161/ATVBAHA.110.207449

131. Shibata T, Kondo M, Osawa T, Shibata N, Kobayashi M, Uchida K. 15-Deoxy- 12,14-prostaglandin J2: A PROSTAGLANDIN D2 METABOLITE GENERATED DURING INFLAMMATORY PROCESSES. J Biol Chem. 2002;277: 10459–10466. doi:10.1074/jbc.M110314200

132. Poligone B, Baldwin AS. Positive and negative regulation of NF-kappaB by COX-2: roles of different prostaglandins. J Biol Chem. 2001;276: 38658–64. doi:10.1074/jbc.M106599200

133. Gilroy DW, Colville-Nash PR, Willis D, Chivers J, Paul-Clark MJ, Willoughby D a. Inducible cyclooxygenase may have anti-inflammatory properties. Nat Med. 1999;5: 698–701. doi:10.1038/9550

134. Serhan CN, Chiang N. Endogenous pro-resolving and anti-inflammatory lipid mediators: a new pharmacologic genus. Br J Pharmacol. 2009;153: S200–S215. doi:10.1038/sj.bjp.0707489

135. Li Q, Liu L, Zhang Q, Liu S, Ge D, You Z. Interleukin-17 Indirectly Promotes M2 Macrophage Differentiation through Stimulation of COX-2/PGE2 Pathway in the Cancer Cells. Cancer Res Treat. 2014;46: 297–306. doi:10.4143/crt.2014.46.3.297

136. Heusinkveld M, de Vos van Steenwijk PJ, Goedemans R, Ramwadhdoebe TH, Gorter A, Welters MJ, et al. M2 macrophages induced by prostaglandin E2 and IL-6 from cervical carcinoma are switched to activated M1 macrophages by CD4+ Th1 cells. J Immunol. 2011;187: 1157–1165. doi:10.4049/jimmunol.1100889

137. Straus DS, Pascual G, Li M, Welch JS, Ricote M, Hsiang CH, et al. 15-deoxy-delta 12,14-prostaglandin J2 inhibits multiple steps in the NF-kappa B signaling pathway. Proc Natl Acad Sci U S A. 2000;97: 4844–9. doi:10.1073/pnas.97.9.4844

138. Genovese T, Esposito E, Mazzon E, Di Paola R, Muià C, Meli R, et al. EFFECT OF CYCLOPENTANONE PROSTAGLANDIN 15-deoxy-Δ12,14PGJ2 ON EARLY FUNCTIONAL RECOVERY FROM EXPERIMENTAL SPINAL CORD INJURY. Shock. 2007;30: 1. doi:10.1097/shk.0b013e31815dd381

139. Mueller E, Smith M, Sarraf P, Kroll T, Aiyer a, Kaufman DS, et al. Effects of ligand activation of peroxisome proliferator-activated receptor gamma in human prostate cancer. Proc Natl Acad Sci U S A. 2000;97: 10990–10995. doi:10.1073/pnas.180329197

140. Horn T, Adel S, Schumann R, Sur S, Kakularam KR, Polamarasetty A, et al. Evolutionary aspects of lipoxygenases and genetic diversity of human leukotriene signaling. Prog Lipid Res. Elsevier Ltd; 2015;57: 13–39. doi:10.1016/j.plipres.2014.11.001

141. Martel-Pelletier J, Lajeunesse D, Reboul P, Pelletier J-P. Therapeutic role of dual inhibitors of 5-LOX and COX, selective and non-selective non-steroidal anti-inflammatory drugs. Ann Rheum Dis. 2003;62: 501–509. doi:10.1136/ard.62.6.501

142. Uderhardt S, Krönke G. 12/15-Lipoxygenase during the regulation of inflammation, immunity, and self-tolerance. J Mol Med. 2012;90: 1247–1256. doi:10.1007/s00109-012-0954-4

143. Kühn H, O'Donnell VB. Inflammation and immune regulation by 12/15-lipoxygenases. Prog Lipid Res. 2006;45: 334–356. doi:10.1016/j.plipres.2006.02.003

144. Mahipal SVK, Subhashini J, Reddy MC, Reddy MM, Anilkumar K, Roy KR, et al. Effect of 15-lipoxygenase metabolites, 15-(S)-HPETE and 15-(S)-HETE on chronic myelogenous leukemia cell line K-562: Reactive oxygen species (ROS) mediate caspase-dependent apoptosis. Biochem Pharmacol. 2007;74: 202–214. doi:10.1016/j.bcp.2007.04.005

145. Soumya SJ, Binu S, Helen A, Reddanna P, Sudhakaran PR. 15-LOX metabolites and angiogenesis: angiostatic effect of 15(S)-HPETE involves induction of apoptosis in adipose endothelial cells. PeerJ. 2014;2: e635. doi:10.7717/peerj.635

146. Zhang X, Goncalves R, Mosser DM. The isolation and characterization of murine macrophages. Curr Protoc Immunol. 2008;Chapter 14: Unit 14.1. doi:10.1002/0471142735.im1401s83

147. Guzik TJ, Korbut R, Adamek-Guzik T. Nitric oxide and superoxide in inflammation and immune regulation. J Physiol Pharmacol. 2003;54: 469–487.

148. Sweet MJ, Hume DA. Endotoxin signal transduction in macrophages. J Leukoc Biol. 1996;60: 8–26.

149. Ben-Neriah Y, Karin M. Inflammation meets cancer, with NF-κB as the matchmaker. Nat Immunol. 2011;12: 715–723. doi:10.1038/ni.2060

150. Andreakos E, Sacre SM, Smith C, Lundberg A, Kiriakidis S, Stonehouse T, et al. Distinct pathways of LPS-induced NF-kappa B activation and cytokine production in human myeloid and nonmyeloid cells defined by selective utilization of MyD88 and Mal/TIRAP. Blood. 2004;103: 2229–37. doi:10.1182/blood-2003-04-1356

151. Bauernfeind FG, Horvath G, Stutz A, Alnemri ES, MacDonald K, Speert D, et al. Cutting edge: NF-kappaB activating pattern recognition and cytokine receptors license NLRP3 inflammasome activation by regulating NLRP3 expression. J Immunol. 2009;183: 787–91. doi:10.4049/jimmunol.0901363

152. Qiao Y, Wang P, Qi J, Zhang L, Gao C. TLR-induced NF-κB activation regulates NLRP3 expression in murine macrophages. FEBS Lett. Federation of European Biochemical Societies; 2012;586: 1022–6. doi:10.1016/j.febslet.2012.02.045

153. Ciraci C, Janczy JR, Sutterwala FS, Cassel SL. Control of innate and adaptive immunity by the inflammasome. Microbes Infect. Elsevier Masson SAS; 2012;14: 1263–1270. doi:10.1016/j.micinf.2012.07.007

154. Shenoy AR, Wellington D a., Kumar P, Kassa H, Booth CJ, Cresswell P, et al. GBP5 promotes NLRP3 inflammasome assembly and immunity in mammals. Science (80-). 2012;336: 481–5. doi:10.1126/science.1217141

155. Im D-S. Omega-3 fatty acids in anti-inflammation (pro-resolution) and GPCRs. Prog Lipid Res. Elsevier Ltd; 2012;51: 232–237. doi:10.1016/j.plipres.2012.02.003

156. Nixon JB, Kamitani H, Baek SJ, Eling TE. Evaluation of eicosanoids and NSAIDs as PPARγ ligands in colorectal carcinoma cells. Prostaglandins, Leukot Essent Fat Acids. Elsevier; 2003;68: 323–330. doi:10.1016/S0952-3278(03)00023-1

157. Itoh T, Fairall L, Amin K, Inaba Y, Szanto A, Balint BL, et al. Structural basis for the activation of PPARgamma by oxidized fatty acids. Nat Struct Mol Biol. Nature Publishing Group; 2008;15: 924–31. doi:10.1038/nsmb.1474

158. Edwards IJ, O'Flaherty JT. Omega-3 fatty acids and PPARγ in cancer. PPAR Res. 2008;2008: 1–14. doi:10.1155/2008/358052

159. Miao H, Ou J, Ma Y, Guo F, Yang Z, Wiggins M, et al. Macrophage CGI-58 Deficiency Activates ROS-Inflammasome Pathway to Promote Insulin Resistance in Mice. Cell Rep. 2014;7: 223–235. doi:10.1016/j.celrep.2014.02.047

160. Luo S, Rubinsztein DC. Apoptosis blocks Beclin 1-dependent autophagosome synthesis: an effect rescued by Bcl-xL. Cell Death Differ. 2010;17: 268–277. doi:10.1038/cdd.2009.121

161. Morrison DC, Ryan JL. Endotoxins and disease mechanisms. Annu Rev Med. Annual Reviews 4139 El Camino Way, P.O. Box 10139, Palo Alto, CA 94303-0139, USA; 1987;38: 417–32. doi:10.1146/annurev.me.38.020187.002221

162. Serhan CN, Krishnamoorthy S, Recchiuti A, Chiang N. Novel anti-inflammatory--pro-resolving mediators and their receptors. Curr Top Med Chem. 2011;11: 629–47. doi:10.1016/j.bbi.2008.05.010

163. Scher JU, Pillinger MH. The anti-inflammatory effects of prostaglandins. J Investig Med. 2009;57: 703–8. doi:10.231/JIM.0b013e31819aaa76

164. Scher JU, Pillinger MH. 15d-PGJ2: The anti-inflammatory prostaglandin? Clin Immunol. 2005;114: 100–109. doi:10.1016/j.clim.2004.09.008

165. Powell WS. 15-deoxy-D12,14-PGJ2: endogenous PPARg ligand or minor eicosanoid degradation product? J Clin Invest. 2003;112: 828–830. doi:10.1172/JCI200318337.2.

166. Araujo JA, Zhang M, Yin F. Heme Oxygenase-1, Oxidation, Inflammation, and Atherosclerosis. Front Pharmacol. 2012;3: 119. doi:10.3389/fphar.2012.00119

167. Gordon S, Taylor PR. Monocyte and macrophage heterogeneity. Nat Rev Immunol. Nature Publishing Group; 2005;5: 953–964. doi:10.1038/nri1733

168. Sharma AM, Staels B. Peroxisome Proliferator-Activated Receptor γ and Adipose Tissue—Understanding Obesity-Related Changes in Regulation of Lipid and Glucose Metabolism. J Clin Endocrinol Metab. 2007;92: 386–395. doi:10.1210/jc.2006-1268

169. Castrillo A, Tontonoz P. NUCLEAR RECEPTORS IN MACROPHAGE BIOLOGY: At the Crossroads of Lipid Metabolism and Inflammation. Annu Rev Cell Dev Biol. 2004;20: 455–480. doi:10.1146/annurev.cellbio.20.012103.134432

170. Kim CW, Lee CD. Apoptosis and diagnosis of nonalcoholic steatohepatitis. Korean J Hepatol. 2011;17: 247. doi:10.3350/kjhep.2011.17.3.247

171. Chinetti G, Griglio S, Antonucci M, Torra IP, Delerive P, Majd Z, et al. Activation of proliferator-activated receptors alpha and gamma induces apoptosis of human monocyte-derived macrophages. J Biol Chem. 1998;273: 25573–80.

doi:10.1074/jbc.273.40.25573

172. Nemzek JA, Hugunin KMS, Opp MR. Modeling sepsis in the laboratory: Merging sound science with animal well-being. Comp Med. 2008;58: 120–128.

173. Soumya SJ, Binu S, Helen A, Anil Kumar K, Reddanna P, Sudhakaran PR. Effect of 15-lipoxygenase metabolites on angiogenesis: 15(S)-HPETE is angiostatic and 15(S)-HETE is angiogenic. Inflamm Res. 2012;61: 707–18. doi:10.1007/s00011-012-0463-5

174. Soumya SJ, Binu S, Helen A, Reddanna P, Sudhakaran PR. 15(S)-HETE-induced angiogenesis in adipose tissue is mediated through activation of PI3K/Akt/mTOR signaling pathway. Biochem Cell Biol. NRC Research Press; 2013;91: 498–505. doi:10.1139/bcb-2013-0037

INDEX

LIST OF PUBLICATIONS AND MANUSCRIPTS

1. **Kumar, N.,** Gupta, G., Kotha, A., Fatima, N., Karnati, R., Gorla, G.V., Voorigiri, P., & Reddanna, P. 15-Lipoxygenase metabolites of α-linolenic acid, [13-(S)-HPOTrE and 13-(S)-HOTrE], mediate anti-inflammatory effects by inactivating NLRP3 inflammasome. ***Nature Sci. Rep.*** 6, 31649 (2016).

2. Kamatham, S., **Kumar, N.** & Gudipalli, P. Isolation and characterization of gallic acid and methyl gallate from the seed coats of Givotia rottleriformis Griff. and their anti-proliferative effect on human epidermoid carcinoma A431 cells. *Toxicol. Reports* 2, 520–529 (2015).

3. Rupa, S., **Kumar, N.,** Kumari, D. S., Tamvada & Lakshminarasu, M. Chemoprevention Efficacy of the Biovlavanoid and its potentiation effect on Conventional Chemotherapeutic Drug on Human Cancer Cell Lines. *Technology Spectrum*, 4, 36-41 (2010).

4. Fatima, N., Ramakrishna, B. P., **Kumar, N.,** & Reddanna, P. 12R-Lipoxygenase expression, purification and characterisation: Inhibition by the subfractions of Acalypha indica leaves. *Asian Pacific Journal of Tropical Biomedicine* (Submitted, Under Revision).

5. **Kumar, N.,** Gupta, G., Kotha, A., & Reddanna, P. Isolation, purification and characterization of Lipoxygenase from Linseed seedlings (Manuscript in preparation).

6. Kamatham, S., **Kumar, N.,** Reddanna, P., & Gudipalli, P. Does benzoylsalicylic acid is an alternative of Acetylsalicylic acid? (Manuscript in preparation).

7. Gupta, G., **Kumar, N**., Venkat, Karnati, R., Gupta A. D., & Reddanna. P. A pivotal role of 12R-Lipoxygenase in late terminal differentiation of human keratinocytes (Manuscript in preparation).

8. Gupta, G., Kumar, K., **Kumar, N.,** Karnati, R., Gupta A. D., & Reddanna. P. 12R-Lipoxygenase knockdown affects expression of TGM-1 and Filaggrin epidermoid carcinoma cell line, A431 (Manuscript in preparation).

9. Gupta, G., **Kumar, N.,** Karnati, R., & Reddanna. P. Synergistic effects of COX-2 and 5-LOX dual inhibitor, chebulagic acid and 12S- LOX inhibitor, baicalein on growth inhibition and induction of apoptosis in human breast cancer cell line (MCF-7) (Manuscript in preparation).

SCIENTIFIC REPORTS

OPEN

Received: 10 November 2015
Accepted: 22 July 2016
Published: 18 August 2016

15-Lipoxygenase metabolites of α-linolenic acid, [13-(S)-HPOTrE and 13-(S)-HOTrE], mediate anti-inflammatory effects by inactivating NLRP3 inflammasome

Naresh Kumar[1], Geetika Gupta[1], Kotha Anilkumar[2], Naireen Fatima[1], Roy Karnati[1], Gorla Venkateswara Reddy[1], Priyanka Voori Giri[1] & Pallu Reddanna[1]

The ratio of ω-6 to ω-3 polyunsaturated fatty acids (PUFAs) appears to be critical in the regulation of various pathophysiological processes and to maintain cellular homeostasis. While a high proportion of dietary intake of ω-6 PUFAs is associated with various inflammatory disorders, higher intake of ω-3 PUFAs is known to offer protection. It is now well established that beneficial effects of ω-3 PUFAs are mediated in part by their oxygenated metabolites mainly via the lipoxygenase (LOX) and cyclooxygenase (COX) pathways. However, the down-stream signaling pathways that are involved in these anti-inflammatory effects of ω-3 PUFAs have not been elucidated. The present study evaluates the effects of 15-LOX metabolites of α-linolenic acid (ALA, ω-3 PUFA) on lipopolysaccharide (LPS) induced inflammation in RAW 264.7 cells and peritoneal macrophages. Further, the effect of these metabolites on the survival of BALB/c mice in LPS mediated septic shock and also polymicrobial sepsis in Cecal Ligation and Puncture (CLP) mouse model was studied. These studies reveal the anti-inflammatory effects of 13-(S)-hydroperoxyoctadecatrienoic acid [13-(S)-HPOTrE] and 13-(S)-hydroxyoctadecatrienoic acid [13-(S)-HOTrE] by inactivating NLRP3 inflammasome complex through the PPAR-γ pathway. Additionally, both metabolites also deactivated autophagy and induced apoptosis. In mediating all these effects 13-(S)-HPOTrE was more potent than 13-(S)-HOTrE.

Inflammation is an essential part of host's response to infection or injury in order to maintain cellular homeostasis. Aberrant inflammation is associated with various disorders mediated by hyperactivation of inflammasome complexes and up-regulation of pro-inflammatory enzymes like inducible nitric oxide synthase (iNOS)[1,2], LOX[3] and COX[4,5]. The inflammatory response generated by eicosanoids, the oxygenated metabolites of PUFAs such as arachidonic acid (AA) is known to be mediated by pro-inflammatory cytokines such as IL-1β and tumor necrosis factor-α (TNF-α)[6].

Increased ratio of ω-6 to ω-3 PUFAs is hypothesized to elevate pro-inflammatory eicosanoid production and thus the onset of inflammatory diseases. A sufficiently high intake of ω-3 PUFAs, on the other hand, was shown to offer protection from inflammatory diseases by decreasing the production of pro-inflammatory eicosanoids, cytokines, ROS and RNS[7,8]. In addition, it is reported that increasing ω-3 PUFAs tissue levels by dietary or genetic means decrease the pathological retinal angiogenesis by suppressing TNF-α[9]. These beneficial effects of ω-3 PUFAs appear to be mediated by the oxygenated metabolites formed via the LOX and COX pathways[10–14].

COX-2, an inducible enzyme that converts ω-6 PUFAs such as AA to pro-inflammatory prostaglandins, has been widely recognized as the major pathway responsible for inflammation as it triggers the production of other pro-inflammatory chemokines and cytokines[14]. However, this concept is challenged by recent findings on COX-2 derived oxidative metabolites of ω-3 PUFAs possessing anti-inflammatory and anti-oxidant properties[15,16]. These studies suggest that the ultimate pro/anti-inflammatory effects of COX depend on the substrate

[1]School of Life Sciences, University of Hyderabad, Hyderabad 500046, India. [2]National Institute of Animal Biotechnology, Hyderabad 500049, India. Correspondence and requests for materials should be addressed to P.R. (email: prsl@uohyd.ernet.in)

on which these enzymes act, ω-6 or ω-3 PUFAs[17,18] and their down-stream metabolites-PGE_2 and/or PGD_2. While PGE_2 is generally pro-inflammatory in nature[13], PGD_2 exhibits anti-inflammatory effects by its conversion to PGJ_2 and subsequently 15-deoxy-$\Delta^{12,14}$ PGJ_2 (15d-PGJ_2) a well-known ligand with high affinity for peroxisome proliferator-activated receptor-γ (PPAR-γ)[19–21]. LOXs, on the other hand, are majorly classified into 5-, 12- and 15-LOXs, depending on the position at which AA is oxygenated. These LOX isoforms have been implicated in a variety of inflammatory and hyperproliferative and neurodegenerative diseases[22]. While 5-LOX is pro-inflammatory in nature[23], the 15-LOX exhibits anti-inflammatory properties[24,25]. Earlier we have shown the anti-inflammatory and anti-cancer properties of 15-LOX metabolites of AA and elucidated the mechanisms involved[26–28]. In the present study, we report the anti-inflammatory effects of 15-LOX metabolites of ALA, the precursor for eicosapentaenoic acid (EPA) and docosahexaenoic acid (DHA), on LPS stimulated mouse macrophage cell line, RAW 264.7 and primary peritoneal macrophages isolated from BALB/c mice and demonstrated that these effects are mediated by inactivating NLRP3 inflammasome complex through the PPAR-γ pathway. Further, we report on the extended survival of BALB/c mice in endotoxin-mediated septic shock and polymicrobial sepsis in CLP mouse model.

Results

Hydroperoxy metabolites exhibit more cytotoxic effects on RAW 264.7 cells as compared to hydroxy metabolites of ALA. The cytotoxic effects of 15-LOX metabolites of ALA [13-(S)-HPOTrE and 13-(S)-HOTrE] on RAW 264.7 cells were evaluated by MTT (3-(4, 5-dimethylthiazol-2-yl)-2, 5-diphenyl tetrazolium bromide) assay. Among this, hydroperoxy metabolite, 13-(S)-HPOTrE showed more cytotoxic effect compared to the hydroxy metabolite, 13-(S)-HOTrE, when incubated at different concentrations for 24 h (Fig. 1A). Treatment with both metabolites decreased the proliferation of the cells in a dose and time-dependent manner. However, 13-(S)-HPOTrE and 13-(S)-HOTrE showed more cytotoxic effects when compared to ω-3 (ALA & DHA) and ω-6 (AA & Linoleic acid-LA) PUFAs (Supplementary Figure S1). A 50% decrease in RAW 264.7 cell proliferation was observed at a concentration (IC_{50} value) of 114 μM 13-(S)-HPOTrE, which was much lower than 13-(S)-HOTrE (>200 μM) at 24 h. Based on these results, further experiments on RAW 264.7 cells were carried out up to 100 μM concentration of ALA metabolites for analysis of their anti-inflammatory effects.

ALA metabolites reduce nitric oxide levels and ROS generation in RAW 264.7 cells and peritoneal macrophages. Next, it was aimed to evaluate the effects of ALA metabolites on LPS induced inflammation by examining effects on pro-inflammatory parameters: NO- a second messenger and ROS- an oxidative stress marker. For this, RAW 264.7 cells were first treated with and/or without metabolites and challenged with LPS as described in the methods. There was significant elevation in NO production and ROS generation in cells when stimulated with LPS and this elevated NO level was reduced by 52.7% and 29% in the presence of 13-(S)-HPOTrE and 13-(S)-HOTrE at 100 μM, respectively (Fig. 1B). Similarly, LPS stimulated RAW 264.7 cells, pre-treated with 13-(S)-HPOTrE and 13-(S)-HOTrE, resulted in the reduction of ROS generation, in a dose-dependent manner and at 100 μM concentration, decreased ROS generation by 96.4% and 92.7% respectively (Fig. 1C). Not only ALA metabolites, the substrate fatty acid ALA also showed the similar pattern of decreased ROS and NO production in LPS stimulated RAW 264.7 cells, though lower (18.6% and 89.5%) compared to its metabolites (Supplementary Figure S2). Similar effects were observed on ROS level when the mouse peritoneal macrophages were pre-treated with ALA metabolites at lower doses (100 nM) and then challenged with LPS (Fig. 1D). The significant reduction in the production of the pro-inflammatory markers by the ALA metabolites suggest their strong anti-inflammatory effects on LPS stimulated macrophages.

ALA metabolites inhibit the expression of iNOS and TNF-α in LPS stimulated RAW 264.7 cells. iNOS is an enzyme associated with regulation of NO and ROS generation in monocytes, macrophages, and other cells[29]. The expression of iNOS and TNF-α, in RAW 264.7 cells stimulated with LPS in the presence and/or absence of ALA metabolites was studied. 13-(S)-HPOTrE or 13-(S)-HOTrE showed no effect on the expressions of either iNOS or TNF-α as compared to untreated RAW 264.7 cells (Supplementary Figure S3), while LPS induced their expression. However, their expression in RAW 264.7 cells, pre-treated with 13-(S)-HPOTrE and 13-(S)-HOTrE and then challenged with LPS, was reduced in a dose-dependent manner (Fig. 2A). The transcript levels of iNOS and TNF-α were also analyzed by semi-quantitative PCR. In LPS treated RAW 264.7 cells, the transcript levels of iNOS and TNF-α were increased but were reduced by pre-treatment with 13-(S)-HPOTrE and 13-(S)-HOTrE in a dose-dependent manner (Supplementary Figure S4). NF-κB is known to regulate the expression of various pro-inflammatory genes, including iNOS and TNF-α[30,31] and ALA metabolites may affect its translocation to the nucleus to regulate gene expression. Therefore the activation of NF-κB was monitored for its translocation to the nucleus by confocal microscopy. While LPS stimulation of RAW 264.7 cells showed a marked translocation of NF-κB, 13-(S)-HPOTrE and 13-(S)-HOTrE pre-treatments resulted in a decrease in NF-κB translocation (Fig. 2B). Very similar effects were observed on NF-κB translocation when the mouse peritoneal macrophages were treated with 13-(S)-HPOTrE and 13-(S)-HOTrE at a lower dose (100 nM) and then challenged with LPS (Fig. 2C).

13-(S)-HPOTrE and 13-(S)-HOTrE inactivate inflammasome in PPAR-γ dependent manner in RAW 264.7 cells and peritoneal macrophages. It is well known that NLRP3 inflammasome, an intracellular sensor that detects pathogens and sterile inflammation, gets activated in part through NF-κB in response to LPS treatment[32–34]. For analyzing the effects of 15-LOX metabolites of ALA on NLRP3 inflammasome activation in LPS stimulated RAW 264.7 cells, the level of gene transcripts associated with inflammasome complex were quantified by semi-quantitative PCR. An increased transcript level of NLRP3, caspase-1, IL-1β and IL-18 in LPS activated RAW 264.7 cells showed an efficient dose-dependent reduction on treatment with both 13-(S)-HPOTrE

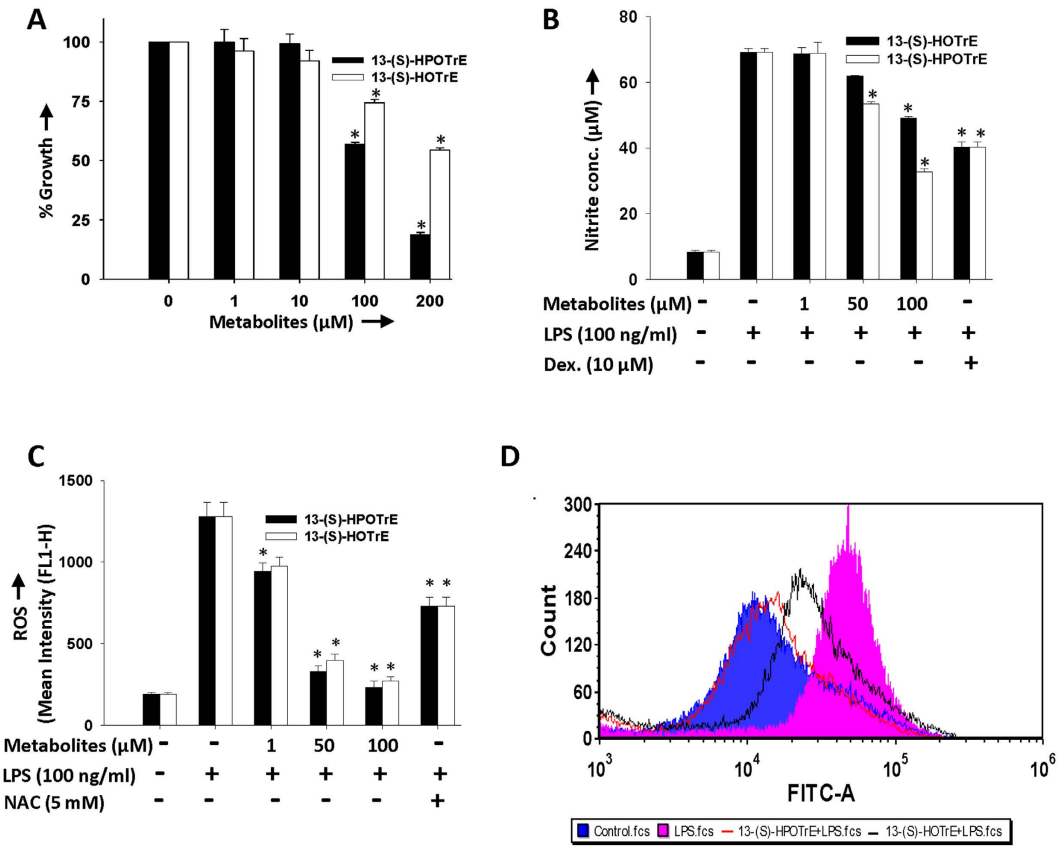

Figure 1. Effects of 13-(S)-HPOTrE and 13-(S)-HOTrE on cells viability, generation of NO and ROS in RAW 264.7 cells and mouse peritoneal macrophages. (**A**) Effects of 13-(S)-HPOTrE and 13-(S)-HOTrE on the viability of RAW 264.7 cells were measured by MTT assay. Cells were treated with different concentrations (1, 10, 100 and 200 μM) of ALA metabolites for 24 h. The percent cell growth following treatment was calculated, in comparison with untreated control cells. The values represent mean ± SD of three independent experiments. *Indicates significance ($p < 0.05$) when compared with untreated control cells. (**B**) Nitrite levels in the culture medium of RAW 264.7 cells pre-incubated with different concentrations (1, 50 and 100 μM) of ALA metabolites or dexamethasone (10 μM) for 3 h and further stimulated with or without LPS (100 ng/ml) for the next 24 h. 13-(S)-HPOTrE showed more effective dose-dependent reduction in NO level as compared to 13-(S)-HOTrE. Dexamethasone, a steroidal anti-inflammatory drug that suppresses NO production, is used as positive control. *Indicates significance ($p < 0.05$) compared to LPS treated cells. (**C**) Intracellular ROS level in RAW 264.7 cells following pretreatment with 100 μM of ALA metabolites for 3 h then stimulated with LPS for 16 h. 13-(S)-HPOTrE reduced ROS level more efficiently compared to 13-(S)-HOTrE. N-Acetyl Cysteine (NAC, 5 mM), a ROS inhibitor was used as positive control. The values represent mean ± SD of three independent experiments. *Indicates significance ($p < 0.05$) compared to LPS treated cells. (**D**) Intracellular ROS level in peritoneal macrophages following pre-incubation with 100 nM ALA metabolites for 3 h then challenged with LPS for 16 h. Similar to above result, 13-(S)-HPOTrE reduced ROS level more efficiently compared to 13-(S)-HOTrE. This is representative FACS chromatogram of the three independent experiments.

and 13-(S)-HOTrE (Fig. 3A). Since activated inflammasomes initiate the processing and secretion of IL-1β[35,36], we measured the level of IL-1β, in the culture medium of RAW 264.7 cells by ELISA. These studies showed a 4.4 fold increase in the level of IL-1β in response to LPS treatment in RAW 264.7 cells and this elevated level of IL-1β was significantly reduced by the treatment of 13-(S)-HPOTrE and 13-(S)-HOTrE, in a dose-dependent manner (Fig. 3B). At 100 μM concentration, 13-(S)-HPOTrE and 13-(S)-HOTrE reduced IL-1β levels by 86.4% and 23% respectively.

LOX metabolites are natural ligands of PPAR-γ[37–40]. Interestingly, PPAR-γ and their coactivators were shown to promote macrophage's anti-inflammatory properties to increase insulin sensitivity[41]. In the present scenario, we studied the involvement of PPAR-γ on the NLRP3 inflammasome activation in LPS treated RAW 264.7 cells and peritoneal macrophages. Immunofluorescence microscopy studies showed activation of NLRP3 inflammasome complex along with upregulation of caspase-l upon LPS treatment in RAW 264.7 cells (Fig. 3C). However, pre-treatment of RAW 264.7 cells with 13-(S)-HPOTrE or 13-(S)-HOTrE and then challenged with LPS resulted in inactivation of NLRP3 inflammasome and thus downregulation of caspase-1. Interestingly, these effects of 13-(S)-HPOTrE and 13-(S)-HOTrE on inflammasome and caspase-1 were reversed when co-incubated with GW9662, a PPAR-γ antagonist.

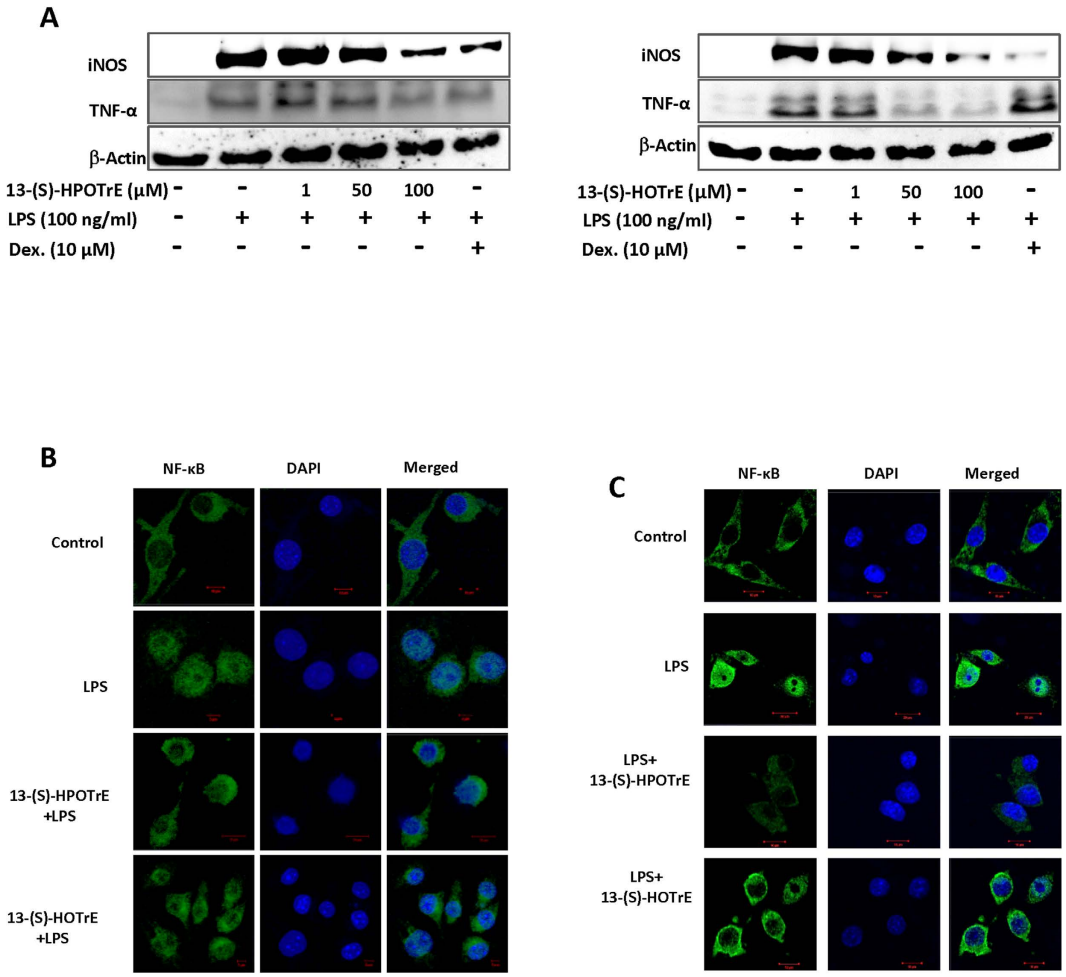

Figure 2. Anti-inflammatory effect of 13-(S)-HPOTrE and 13-(S)-HOTrE is mediated by inhibition of iNOS and TNF-α. (**A**) Immunoblot analysis showing the expression of iNOS and TNF-α following treatment with 13-(S)-HPOTrE and 13-(S)-HOTrE (1, 50 and 100 μM) concentrations for 3 h and then stimulated with LPS for 24 h. β-Actin was used as an internal control. Dexamethasone (10 μM) was used as positive control. These are representative blots of the three independent experiments. (**B**) Immunofluorescence microscopy of RAW 264.7 cells pre-treated with or without ALA metabolites (100 μM) for 3 h and then with LPS for 16 h. Immunostained for NF-κB (Green) and DAPI (Blue). Bar Scale: 10 μm. The image showed representative of three independent experiments. (**C**) Immunofluorescence microscopy of peritoneal macrophages pre-treated with or without ALA metabolites (100 nM) for 3 h and then challenged with LPS for 16 h. Immunostained for NF-κB (Green) and DAPI (Blue), Bar Scale: 10 μm. The image showed representative of three independent experiments.

To validate the findings observed in RAW 264.7 cells, further, studies were taken up on peritoneal macrophages at much lower doses (100 nM and 400 nM) of 13-(S)-HPOTrE and 13-(S)-HOTrE. Immunoblot analysis showed an increase in the expression of NLRP3 in LPS challenged peritoneal macrophages while cells pre-treated with ALA metabolites and challenged with LPS showed a reduction in the expression of NLPR3 (Fig. 4A). Next, the IL-1β cytokine was probed in the culture medium by immunoblot analysis and quantified by ELISA. As shown in Fig. 4A,B, peritoneal macrophages pre-treated with 13-(S)-HPOTrE and 13-(S)-HOTrE and then challenged with LPS reduced the level of IL-1β by 59.5% and 54.5% respectively, when compared to LPS alone challenged macrophages. Similarly, the involvement of PPAR-γ in the regulation of inflammasome by ALA metabolites was validated on peritoneal macrophages at lower concentrations. Immunofluorescent microscopy showed decreased the expression of NLRP3 inflammasome and caspase-1 in macrophages pre-treated with ALA metabolites and challenged with LPS. However, the effects of ALA metabolites were reversed when co-incubated with GW9662, PPAR-γ antagonist (Fig. 4C). These metabolites also increased the levels of anti-inflammatory cytokine-IL-10 in culture medium (Fig. 4D).

The foregoing results suggest that inactivation of the inflammasome by 13-(S)-HPOTrE and 13-(S)-HOTrE in LPS challenged RAW 264.7 cells and peritoneal macrophages is mediated through PPAR-γ dependent pathway. Immunoblot analysis of the LPS stimulated RAW 264.7 cells revealed an increase in the COX-2 expression (Fig. 5A). The LPS induced expression of COX-2 was further enhanced by both 13-(S)-HPOTrE and 13-(S)-HOTrE in a dose-dependent manner. Coinciding with the changes observed in COX-2, the downstream

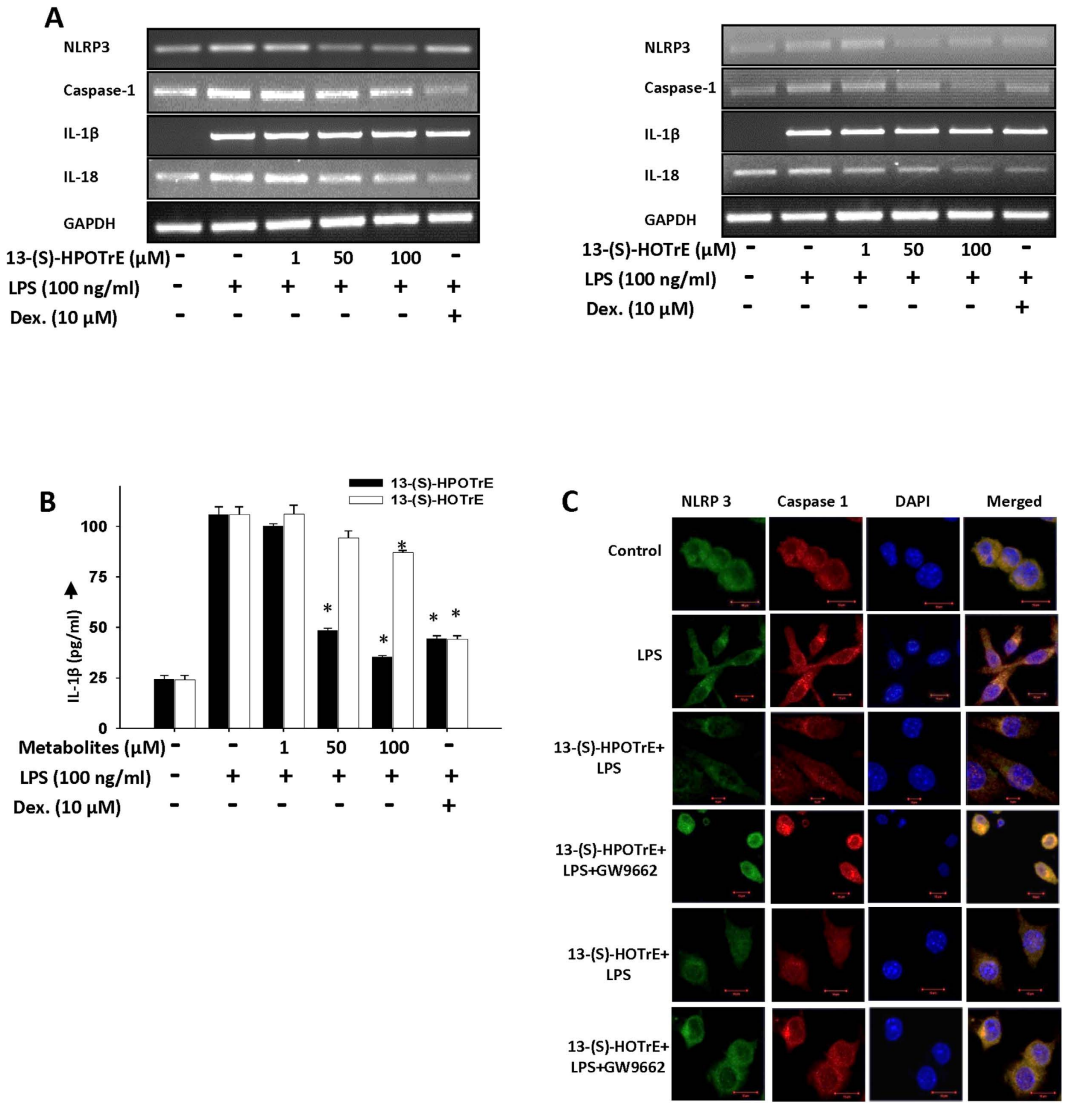

Figure 3. ALA metabolites, 13-(S)-HPOTrE and 13-(S)-HOTrE, inhibit inflammasome complex in RAW 264.7 cells. (**A**) In semi-quantitative PCR analysis, 13-(S)-HPOTrE, and 13-(S)-HOTrE showed decrease in transcript level of NLRP3, caspase-1, IL-1β and IL-18 at various concentrations (1, 50 and 100 μM) pre-incubated for 3 h then stimulated with LPS for 24 h. GAPDH was used as an internal control. (**B**) Estimation of IL-1β levels in the culture medium of cells as per the treatment described in (**A**). Dexamethasone (10 μM) was used as positive control. The values represent mean ± SD of three independent experiments. *Indicates significance ($p < 0.05$) compared to LPS alone treated cells. (**C**) Immunofluorescence microscopy of RAW 264.7 cells pre-treated with ALA metabolites (100 μM) for 3 h then stimulated with LPS for 24 h. Immunostained for NLRP3 (Green), caspase-1 (Red) and DAPI (Blue). Bars Scale: 10 μm. Data show representative of three independent experiments.

metabolites of COX-2, PGE_2 and PGD_2, also showed similar trend of enhanced production with LPS treatment (Fig. 5B). These studies reveal that COX-2, a key enzyme involved in mediating inflammation, may also be playing a role in the resolution of inflammation through the generation of PGD_2 which is a PPAR-γ ligand[17].

ALA metabolites induce apoptosis in LPS treated RAW 264.7 cells. It is known that apoptosis plays a vital role in the resolution of inflammation and Beclin-1 dependent inhibition of autophagy by apoptosis enhances its anti-inflammatory effects[42]. Apoptosis blocks Beclin-1 dependent autophagy by blocking autophagosome synthesis[43]. Moreover, LPS and activated inflammasomes also induce autophagy in mesothelial cells[44]. Since ALA metabolites showed anti-inflammatory effects, we examined whether they affect induction of apoptosis and autophagy in LPS stimulated RAW 264.7 cells. 13-(S)-HPOTrE treatment increased apoptosis in LPS challenged RAW 264.7 cells in a dose-dependent manner (Fig. 6A) although, 13-(S)-HPOTrE and 13-(S)-HOTrE showed no effect on apoptosis in unchallenged cells (Supplementary Figure S5). A significant increase in autophagy with the enhanced conversion of soluble LC3-I into lipid bound LC3-II and increased puncta formation was observed in LPS challenged RAW 264.7 cells. However, these effects were greatly reduced or undetectable in RAW 264.7

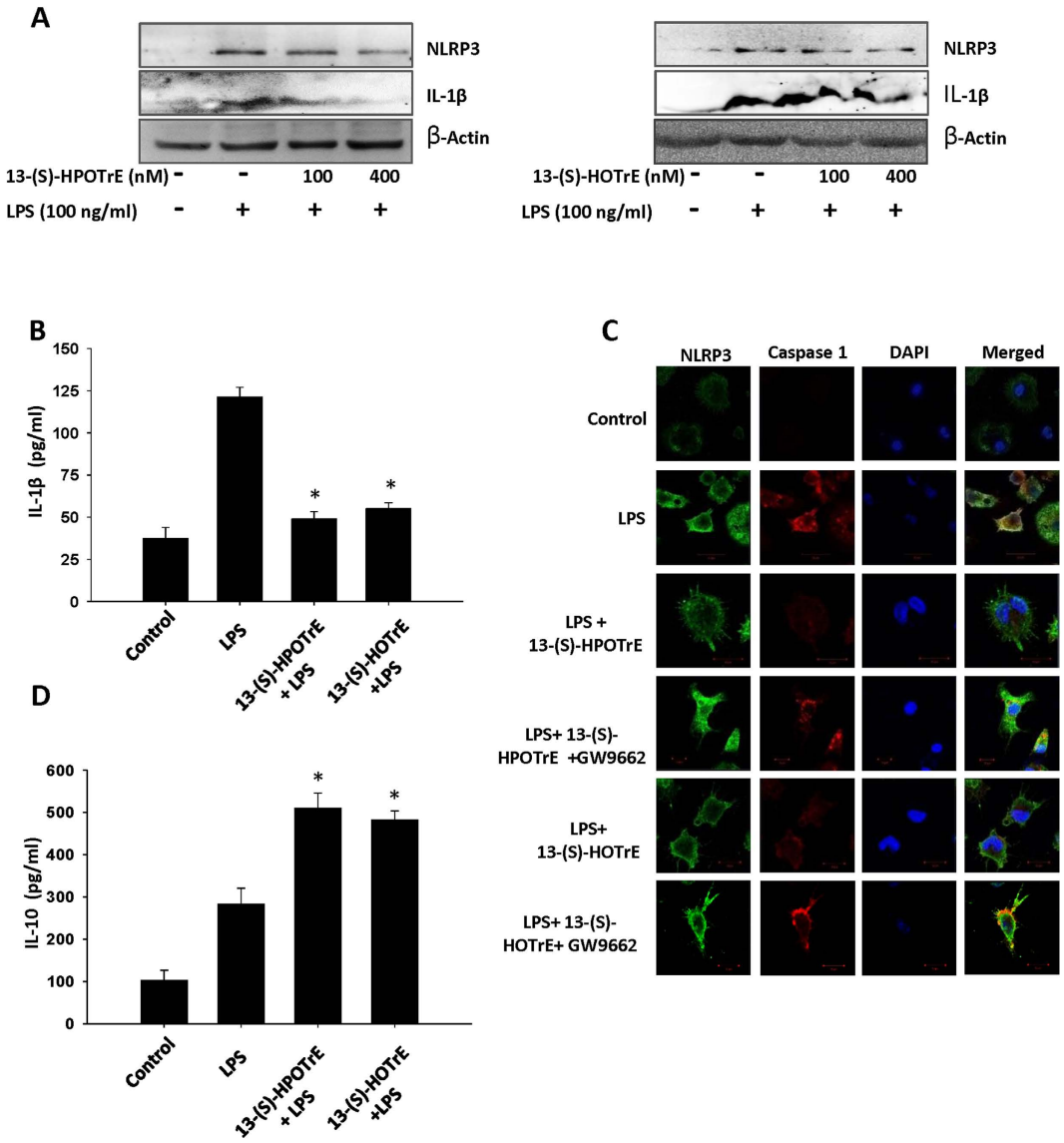

Figure 4. ALA metabolites inhibit inflammasome complex activation in mouse peritoneal macrophages. (**A**) Immunoblot analysis of NLRP3 and IL-1β (in culture medium) expression in peritoneal macrophages, pre-incubated with ALA metabolites (100 nM and 400 nM) for 3 h then challenged with LPS (100 ng/ml) for next 24 h. β-Actin was used as an internal control. (**B**) Estimation of IL-1β levels in the culture medium by ELISA as per the treatment described above. The values represent mean ± SD of three independent experiments. *Indicates significance ($p < 0.05$) compared to LPS treated peritoneal macrophages. (**C**) Immunofluorescence microscopy of peritoneal macrophages treated with ALA metabolites (100 nM) for 3 h then stimulated with LPS for 24 h. Immunostained for NLRP3 (Green), caspase-1 (Red) and DAPI (Blue). Bars Scale: 10 μm. Images show representative of three independent experiments. (**D**) Estimation of IL-10 levels in the culture medium by ELISA as per the treatment described above (at 100 nM). The values represent mean ± SD of three independent experiments. *Indicates significance ($p < 0.05$) compared to LPS treated peritoneal macrophages.

cells pre-treated with ALA metabolites and challenged with LPS (Fig. 6B). Moreover, immunoblot analysis also showed induced expression of beclin-1, an autophagic marker, which was greatly reduced when RAW 264.7 cells were treated with ALA metabolites in a dose-dependent manner (Fig. 6C).

ALA metabolites extend BALB/c mice survival and show anti-inflammatory properties by regulating cytokines and inflammasome. Septic shock is a complication of inflammation in which an infection or toxin induces inflammatory response in the entire body. Endotoxin-mediated septic shock is often integrated with high mortality[45]. On the other hand, saturated fatty acid had shown major impact on the survival of mice in bacterial infection[46] and these ALA metabolites showed anti-inflammatory effects in *in vitro* model system. We then wanted to validate the effects of ALA metabolites *in vivo* on the survival of mice in a septic shock induced by LPS in toxemia model. These studies showed features of septic shock in all the mice received LPS such as an increase in heartbeat rate, decrease in body weight, apathy, dullness and diarrhea, which began to die

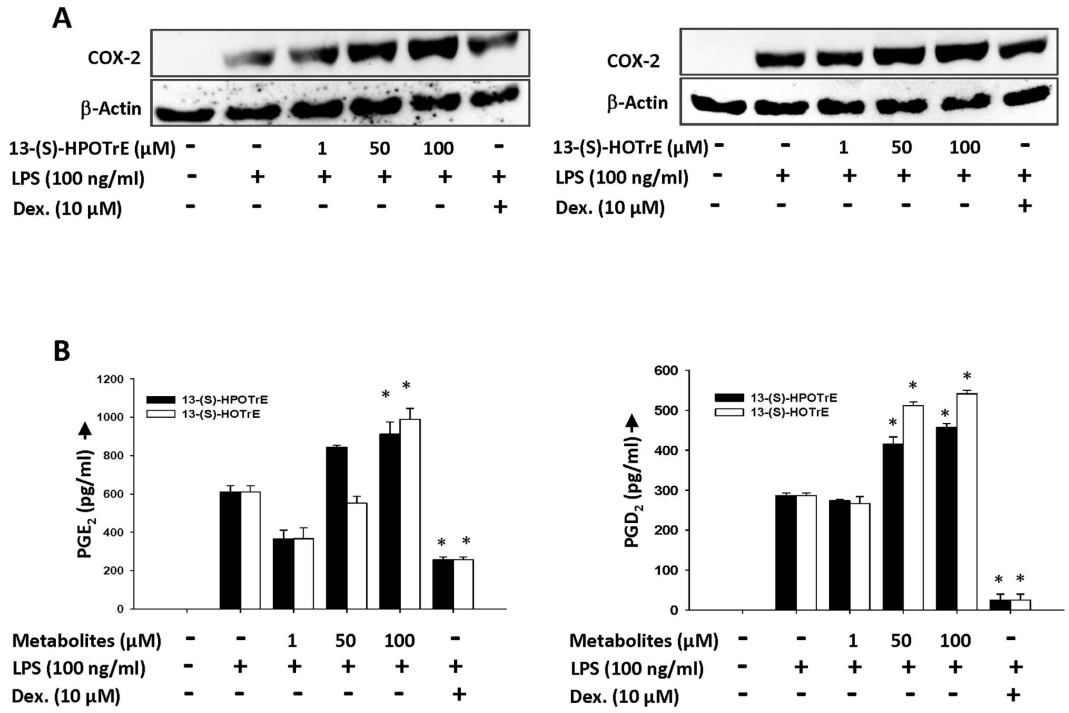

Figure 5. 13-(S)-HPOTrE and 13-(S)-HOTrE show anti-inflammatory effects by upregulating expression of COX-2. (**A**) Immunoblot analysis of COX-2 expression in RAW 264.7 cells pre-incubated with ALA metabolites at different concentrations (1, 50 and 100 μM) for 3 h then further stimulated by LPS (100 ng/ml) for next 24 h. β-Actin was used as an internal control and Dexamethasone was used as positive control. Western blot shows representative of three independent experiments. (**B**) Estimation of PGE_2 and PGD_2 level in the culture medium of RAW 264.7 cells when pre-incubated with ALA metabolites for 3 h and then stimulated with LPS for 24 h. Dexamethasone was used as positive control. The values represent mean ± SD of three independent experiments. *Indicates significance ($p < 0.05$) compared to LPS treated cells.

within 12 h. Contrary to this, the mice pre-treated with ALA metabolites and then challenged with LPS were quite active. However, loss of weight was observed in all except control mice. The result from this experiment showed that survival rate in ALA metabolites pre-treated mice were 40% and 10% extended than LPS alone challenged mice (Fig. 7A).

Since ALA metabolites showed a decrease in mortality rate in mice with endotoxin-mediated septic shock, the study was further extended to mice with sepsis induced by polymicrobial infection in a CLP mouse model. Results showed upregulation of iNOS and NLRP3 expression in CLP mice and their down-regulation in mice pre-treated with ALA metabolites (Fig. 7B). The levels of IL-1β and IL-10 were increased in liver tissue and serum of CLP mice. However, the level of pro-inflammatory cytokine-IL-1β was decreased while the level of anti-inflammatory cytokine-IL-10 was further increased in mice treated with ALA metabolites (Fig. 7C).

Discussion

The ratio of ω-6 PUFAs: ω-3 PUFAs in cell membranes reflects the physiological status of the tissues and regulates the inflammatory response to a variety of external or internal stimuli and thus maintains cellular homeostasis[7,8]. ω-3 PUFAs are known to exhibit anti-inflammatory effects and reduce the oxidative stress in the cells[7,47]. The findings of the present study also support this concept wherein ALA, ω-3 PUFA, and its metabolites, 13-(S)-HPOTrE and 13-(S)-HOTrE, significantly reduced the production of NO and ROS, as well as inflammatory cytokines, in LPS stimulated RAW 264.7 cells and in mouse peritoneal macrophages. Further studies on *in vivo* sepsis model and CLP mice model demonstrated the protective role of 13-(S)-HPOTrE and 13-(S)-HOTrE as evidenced by a decrease in the mortality rate and by the maintenance of anti-inflammatory properties, in ALA metabolites treated BALB/c mice.

From previous studies, it has been established that ω-3 PUFAs exert their anti-inflammatory effects through several mechanisms, one of which being NF-κB signaling[7,47]. ω-3 PUFAs prevent the phosphorylation and degradation of Iκ-Bα protein by proteasome complex, thus inhibiting NF-κB signaling pathways[48]. The present study shows that 15-LOX metabolites of ALA [13-(S)-HPOTrE and 13-(S)-HOTrE] inhibit the translocation of NF-κB to the nucleus, along with the reduction of NO and ROS in LPS stimulated RAW 264.7 cells and peritoneal mouse macrophages. ALA metabolites also inhibited the activation of NLRP3 inflammasome as well as downstream signaling molecules such as caspase-1 and IL-1β at both transcriptional as well as translational levels. Interestingly, these effects of ALA metabolites on NLRP3 inflammasome were blocked by the PPAR-γ antagonist-GW9662. These studies comprehensively suggest that inactivation of LPS induced NLRP3 inflammasome by 13-(S)-HPOTrE or 13-(S)-HOTrE in RAW 264.7 cells and peritoneal macrophages is dependent on

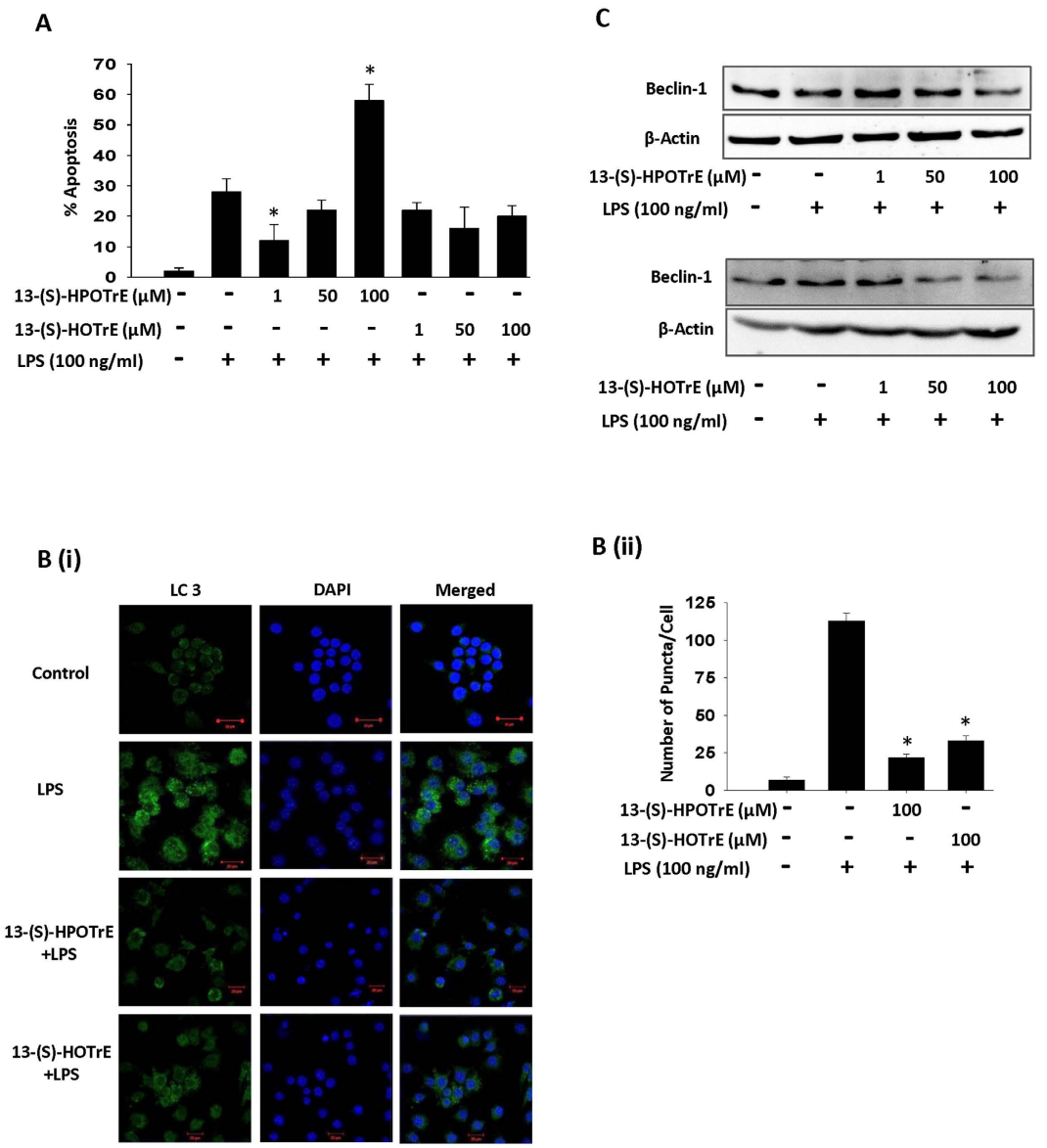

Figure 6. 13-(S)-HPOTrE and 13-(S)-HOTrE inhibit Beclin-1 mediated autophagy in LPS stimulated RAW 264.7 cells. (**A**) Flow cytometric analysis showing the effects of ALA metabolites on apoptosis in RAW 264.7 cells challenged with LPS. Apoptosis was assayed by Propidium Iodide and FITC conjugated Annexin V at 24 h, by flow cytometric Analysis. The apoptosis level was calculated as % of AnnexinV^{+} PI^{-} cells in density plot distribution. The dead cells were gated and analysis was performed only on live cells. *Indicates significance ($p < 0.05$) compared to LPS treated cells. (**B**) **(i)** Confocal microscopy of RAW 264.7 cells treated with or without ALA metabolites (100 μM) for 3 h then challenged with LPS for 24 h. Immunostained for LC 3 (Green) and DAPI (Blue). Bars Scale: 10 μm. Images show representative of three experiments. **(ii)** Bar graph shows puncta/cell calculated by ImageJ LC3 macro. *Indicates significance ($p < 0.05$) compared to LPS treated cells. (**C**) Beclin-1 Immunoblotting of RAW 264.7 cells pre-incubated with ALA metabolites for 3 h and then challenged with LPS for 24 h. Western blots show representative of three independent experiments.

PPAR-γ. Indeed a number of studies have shown that several PUFA metabolites are ligands of PPAR-γ[19], further supporting such a possibility.

Recent studies have established that the inducible isoform of COX, COX-2, has dual roles, pro-and anti-inflammatory, depending on the downstream metabolites generated[13,49]. In the early stages, it is shown that COX-2 induction is mainly associated with the generation of pro-inflammatory prostaglandins, whereas at later stages the downstream metabolite is PGD_2, a ligand for PPAR-γ[17], which has been observed to possess anti-inflammatory roles[50]. In the present study, an increase in the expression of COX-2 and its downstream metabolites (PGE_2 and PGD_2) was observed in RAW 264.7 cells pre-treated with ALA metabolites and then stimulated with LPS. Here, COX-2 may be playing an anti-inflammatory role by shifting PGE_2 dominated prostaglandins in LPS stimulated macrophages to PGD_2 dominated prostaglandins upon treatment with ALA metabolites. It has been reported that PGD_2 derivative PGJ_2 and their metabolites $^{12}\Delta$ PGJ_2 and 15d-PGJ_2, often derived from

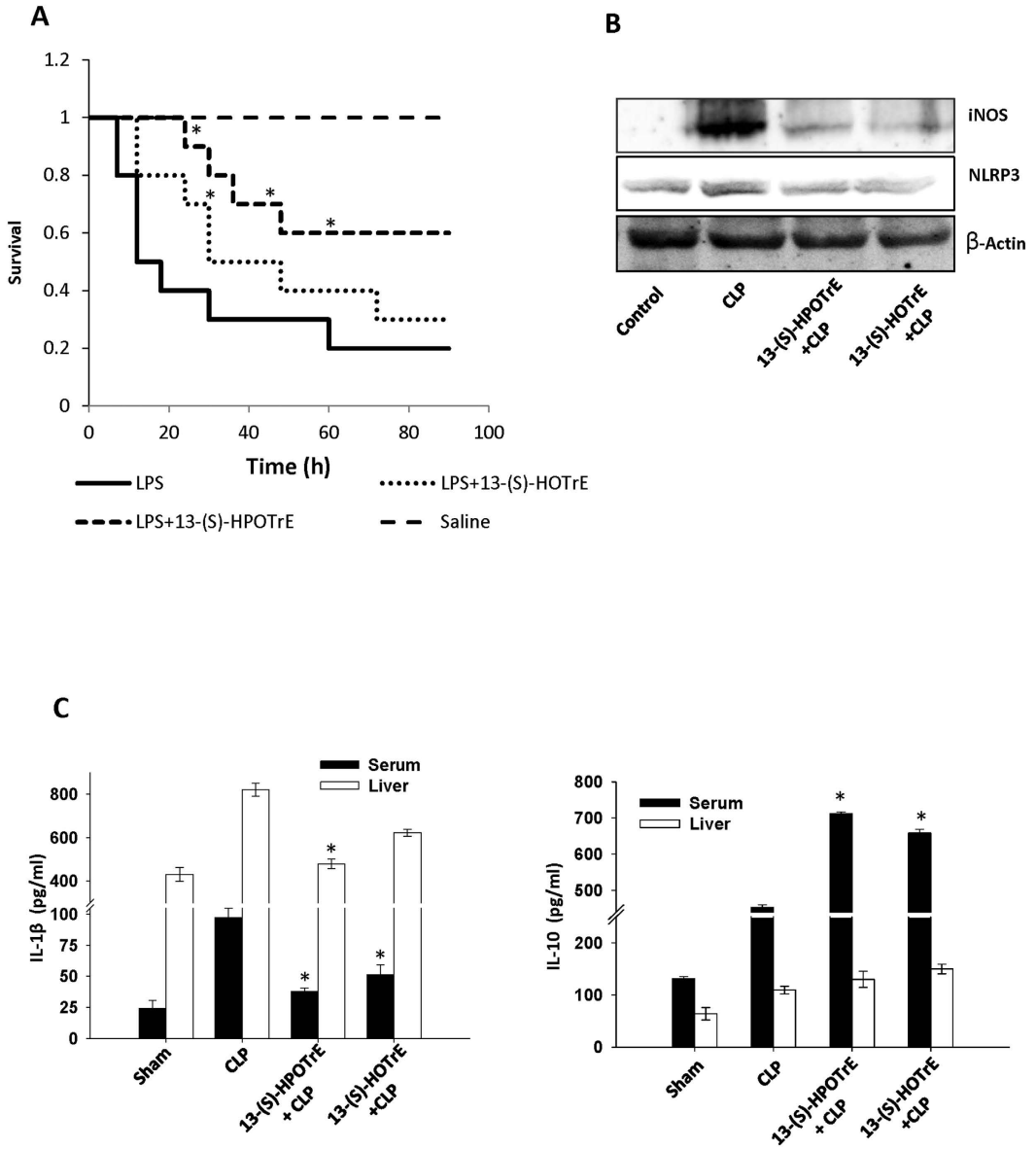

Figure 7. Effects of ALA metabolites during sepsis in BALB/c mice. (**A**) ALA metabolites showed an increase in survival of BALB/c mice (n = 10 mice/group) in endotoxin-induced Septic Shock in toxemia model. LPS (30 mg/kg) was injected i.p. and mice were monitored for 4 days then mortality was calculated. ALA metabolites showed decreased mortality rate in metabolites treated and LPS challenged mice as compared to LPS challenged mice. The survival curve is plotted on Kaplan-Meier method. *Indicates significance ($p < 0.05$) compared to LPS treated mice. (**B**) Sepsis was induced by polymicrobial infection in CLP mouse model (n = 5 mice/group). Immunoblot analysis of iNOS and NLRP3 expression in CLP mice model, pre-treated with 13-(S)-HPOTrE and 13-(S)-HOTrE (0.1 mg/kg, 2.5 μg/mice) as described in methodology. Mice were sacrificed after 24 h of CLP and tissues were collected. β-Actin was used as an internal control. (**C**) Estimation of IL-1β and IL-10 cytokines levels in serum and liver tissue. The values represent mean ± SD of three independent experiments. *Indicates significance ($p < 0.05$) compared to CLP mice.

induced COX-2, exhibit their anti-inflammatory effects in various *in vivo* systems[20,15,51]. In the present study, the induced expression of COX-2 and increased formation of PGD_2 upon treatment with ALA metabolites in LPS stimulated macrophages may be mediating the anti-inflammatory effects through its downstream metabolite, 15d-PGJ_2 a natural ligand for PPAR-γ[52]. This hypothesis is supported by the observation that PPAR-γ is maintaining the anti-inflammatory state, by inhibiting inflammasome and IL-1β, via induced COX-2 generated downstream metabolites, and when PPAR-γ is inhibited, it is failing to inactivate the inflammasome. The reversed effects of ALA metabolites on inflammasome and caspase-1, when co-incubated with the PPAR-γ antagonist GW9662 support such a possibility.

Macrophage differentiation, their subtypes and function depend on its surrounding environment. After differentiation, macrophages polarized into two subtypes, M1 and M2 with characteristic phenotypes and exhibit

different behaviours[53]. While, the activation of M1 macrophage is associated with increased expression of iNOS[54] and increased level of pro-inflammatory cytokines such as TNF-α, IL-1β and IL-6[55], the activation of M2 macrophages is associated with increased level of anti-inflammatory cytokines-IL-10 and scavenger receptor A[55]. LPS stimulated pro-inflammatory state is associated with M1 subtype macrophage, on the other hand, PPAR-γ activation and increased PGE_2[56,57] is associated with shifting of M1 macrophages into M2 macrophages subtypes[58,59]. In the present study, ALA metabolites activated PPAR-γ, and also increased PGE_2 level that might be responsible for shifting of M1 to M2 macrophages subtypes and thereby mediating anti-inflammatory effects. Furthermore, an increased cytokine IL-10 as well as decreased expression of iNOS and TNF-α which are associated to M2 subtype macrophages further strengthen such possibility.

Apoptosis is the major mechanism for safe clearance of PMNLs at inflammatory sites and thus limit pro-inflammatory signals and promote resolution of inflammation rather than persistence of tissue damage[60]. In the present study, 13-(S)-HPOTrE showed a dose-dependent increase in apoptosis in LPS activated RAW 264.7 cells and it is previously reported that activation of PPAR-γ induces apoptosis in differentiated naive macrophages[61]. Therefore, it is possible that the apoptotic effects of 13-(S)-HPOTrE might be mediated through PPAR-γ dependent pathway. There is a correlation between apoptosis and regulation of autophagy. It is reported that apoptosis inhibits beclin-1 mediated autophagy[43]. It supports the present findings on immunofluorescence microscopy with LC3, in which pre-treatment of ALA metabolites remarkably diminished autophagy in LPS challenged RAW 264.7 cells. Furthermore, in immunoblot analysis, a decrease in beclin-1 expression was observed in ALA metabolites pre-treated and challenged with LPS. From these studies, it can be concluded that these ALA metabolites inhibit beclin-1 mediated autophagy through induction of apoptosis.

Sepsis is a critical state of the body because of systemic immune response induced by pathogens, microbes or endotoxins, also called systemic inflammatory response syndrome[62]. In endotoxin-induced septic shock model, mice pre-treated with ALA metabolites showed a significant decrease in mortality rate. Moreover, in another *in vivo* study, in CLP mouse model, mice treated with these ALA metabolites showed a decrease in expression of NLRP3. It also showed a reduction in IL-1β levels while elevation in IL-10 cytokine level as well. Thus the *in vitro* anti-inflammatory effects of 13-(S)-HPOTrE and 13-(S)-HOTrE observed in RAW 264.7 cells and peritoneal macrophages also have been demonstrated *in vivo* as evidenced by the extension in the survival of mice in endotoxin-induced septic shock in toxemia model and inactivated inflammasome in polymicrobial induced sepsis in CLP model.

In the present study, the hydroperoxy [13(S)-HPOTrE] and hydroxy [13(S)-HOTrE] metabolites of ALA showed anti-inflammatory effects, though the hydroperoxy metabolite being more potent. As the hydroperoxy metabolite [13(S)-HPOTrE] is getting converted to the corresponding hydroxy [13(S)-HOTrE] metabolite with increasing period of time because of the reducing environment created by serum in culture medium, the effects of 13(S)-HPOTrE observed in the present study may be mediated by both the hydroperoxy and hydroxy metabolites of ALA.

The anti-inflammatory properties of ALA (ω-3 PUFA) observed in the present study thus are quite contrasting to those of AA (ω-6 PUFA) metabolites, wherein the hydroperoxy (15-(S)-HPETE) and hydroxy (15-(S)-HETE) metabolites of AA showed contrasting effects on angiogenesis, which is critically associated with inflammation[27,63,64]. While 15(S)-HPETE showed anti-angiogenic effects[27], the 15(S)-HETE induced angiogenesis[64] in adipose tissue. Also, such differential effects of the hydroperoxy and hydroxy metabolites of 15-LOX on angiogenesis were observed in human umbilical vein endothelial cells (HUVECs)[63]. Similar differential effects of hydroperoxy and hydroxy metabolites of 15-LOX with AA as the substrate were reported on chronic myeloid leukemia cell line[26]. Interestingly, in the present study, the hydroperoxy and hydroxy metabolites of ALA showed anti-inflammatory effects, however, the hydroperoxy metabolite being more potent than the hydroxy metabolite. These findings, thus strongly advocate the beneficial effects of ω-3 PUFAs in counteracting various inflammatory disorders, which are mainly mediated by the metabolites of ω-6 PUFAs.

In summary, ALA metabolites [13-(S)-HPOTrE and 13-(S)-HOTrE] exhibit anti-inflammatory effects in LPS challenged RAW 264.7 cells and mouse peritoneal macrophages by down-regulating LPS induced pro-inflammatory markers and by inactivating the NLRP3 inflammasome complex. Additionally, the anti-inflammatory effects of ALA metabolites were mediated by the induction of apoptosis and inhibition of autophagy in the LPS challenged macrophages. These anti-inflammatory effects of ALA metabolites appear to be mediated by the inactivation of NLRP3 inflammasome complex and decrease in pro-inflammatory cytokines/enzymes along with a simultaneous increase in anti-inflammatory cytokines. The present study also demonstrates the protective effects of ALA metabolites *in vivo* as evidenced by the extended survival of BALB/c mice in LPS induced septic shock.

Materials and Methods

Chemicals and Reagents. Culture medium DMEM, penicillin, streptomycin, PBS, Trypsin-EDTA and fetal bovine serum (FBS) were purchased from Gibco. MTT, 2′-7′-Dichlorodihydrofluorescein diacetate (DCFH-DA), LPS (lipopolysaccharide from *E. coli, 0127:B8)*, Griess reagent, Dexamethasone (Dex) and GW9662 were purchased from Sigma-Aldrich, USA. Anti-Beclin-1, anti-Caspase-1, anti-NF-κB and anti-TNF-α antibodies were purchased from Abcam (MA, USA). Anti-LC-3 antibody was purchased from Cell Signaling while Anti-COX-2 antibody was obtained from Santa Cruz Biotechnology Inc. (Texas, USA). Anti-iNOS antibody was purchased from Thermo Fisher Scientific (MA, USA). Enzyme immunoassay kit for IL-1β, IL-10 and PGE_2 were purchased from R&D system, Inc. (MN, USA) whereas PGD_2 assay kit was purchased from Cayman Chemical Company (Ann Arbor, MI, USA). AA, LA, ALA and DHA were procured from Nu-Chek-Prep (MN, USA). The 15-LOX metabolites of ALA, 13-(S)-HPOTrE and 13-(S)-HOTrE, were generated (Supplementary Figure S6) essentially employing the methods described earlier for generation of 5-LOX metabolites[65–67].

Cell culture and Treatments. The mouse macrophage cell line, RAW 264.7 was obtained from NCCS (Pune, India) grown and maintained in DMEM supplemented with 10% heat-inactivated fetal bovine serum (FBS), 100 IU/ml penicillin and 100 μg/ml streptomycin in a humidified atmosphere with 5% CO_2 at 37 °C. Subculturing of cells was done twice a week. Fresh culture medium was used before each treatment. Cells were pre-incubated with different concentrations (1, 50 and 100 μM) of ALA metabolites, 13-(S)-HPOTrE and 13-(S)-HOTrE or with Dexamethasone (10 μM) for 3 h then challenged with LPS (100 ng/ml) for different time points as mentioned in experiments. The anti-inflammatory drug, dexamethasone was used as positive control. For inhibitor study, cells were pre-incubated with 10 μM GW9662 (2-chloro-5-nitrobenzanilide), for specific time period as mentioned in experiments. For analysis of the inflammasomes and IL-1β measurements, RAW 264.7 cells and peritoneal macrophages were incubated with 1 mM ATP for 30 min prior to end time points.

Animal. BALB/c, male mice, 4-week old weighing 20–25 g were purchased from Centre for Cellular and Molecular Biology, Hyderabad, India. Mice were housed at constant room temperature (23 ± 1 °C) and allowed to water and food *ad libitum* in 12 h dark/light cycle. The mice were kept at least 1 week in animal house before performing any experiment. The mice used in this study were handled carefully and according to the *Guide for the care and use of Laboratory animals* published by NIH (National Institute of Health). The experimental protocol was approved by Institutional Animal Ethics Committee (IAEC), University of Hyderabad, India.

LPS Induced Septic Shock. BALB/c male mice (20 to 25 g) were divided into 4 different groups (10 mice in each group), control, LPS, LPS+13-(S)-HPOTrE and LPS+13-(S)-HOTrE. LPS was dissolved in saline (0.9% NaCl) and injected (30 mg/kg body weight) intraperitoneal (i.p.) in all mice except control. In control mice, 0.9% saline was injected. ALA metabolites were dissolved in saline having Tween 80 (0.9% NaCl + 0.5% Tween 80). Two i.p. doses of 13-(S)-HPOTrE and 13-(S)-HOTrE (0.1 mg/kg body weight, 2.5 μg/mice) metabolites were injected, first at 1 h prior to LPS and second, soon after LPS administration. 250 μl saline with Tween 80 (vehicle control) was injected in control and LPS treated groups. All mice were kept in normal conditions with an extra vigilance. Mice were monitored initially at 2 h intervals for 12 h then for 4 days.

Cecal Ligation and Puncture (CLP) model. Cecal Ligation and Puncture was performed in BALB/c male mice (20 to 25 g). Mice were divided into 4 groups (5 mice/group), Sham, CLP, CLP+13-(S)-HPOTrE and CLP+13-(S)-HOTrE. The mice were anesthetized with 60 μg/g ketamine and 10 μg/g xylazine. After cleaning and disinfecting the lower abdomen by iodine solution to prevent infection, a 1.5 to 2 cm incision was made through linea alba. Then, the cecum was spotted and ligated with disinfected 3–0 silk suture and perforated twice using a 22-gauge needle. Wound strength was ensured by squeezing out a small amount of stool. Then the cecum was replaced into the abdomen, and the incision was closed properly. In Sham, mice undergone surgery but ligation and puncture were not performed. Tramadol hydrochloride (20 μg/g body wt.) was injected i.p. with 1 ml warm saline in all mice. In ALA metabolites treated mice, two i.p. doses of 13-(S)-HPOTrE and 13-(S)-HOTrE (0.1 mg/kg body weight, 2.5 μg/mice) metabolites were given, first at 1 h prior to CLP and second, soon after CLP surgery. Finally, all mice were kept at normal conditions with an extra vigilance. The mice were sacrificed after 24 h of CLP surgery then blood, peritoneal fluid and liver were collected.

Isolation of Primary Peritoneal Macrophages. Primary peritoneal macrophages were isolated from thioglycolate-elicited BALB/c male mice as described by Xia Zhang *et al.*[68]. Briefly, in BALB/c male mice, 3% thioglycolate broth (1 ml) was injected through i.p. After 3 days, mice were euthanized by cervical dislocation. 5 ml ice-cold DMEM was injected into the peritoneal cavity. The abdomen was finger tapped 4–5 times and peritoneal lavage was aspirated and collected in a cold sterile centrifuge tube. Further, centrifugation was done at 1500 rpm for 5 min, pellets were resuspended in DMEM and cell counting was done by haemocytometer. Appropriate number of cells were grown and maintained in DMEM, macrophages enrichment was done by washing and removing unattached cells from culture plate, further grown as described above for RAW 264.7 cells, and treated with 13-(S)-HPOTrE and 13-(S)-HOTrE as mentioned in experiments for RAW 264.7 cells.

Cytotoxicity Assay. Cytotoxicity of PUFAs and their metabolites were assayed by MTT assay. To perform this assay, RAW 264.7 cells were seeded in 96 well plates at a density of 5×10^4 cells/well then treated with ω-6 PUFAs (AA and LA), ω-3 PUFAs (ALA and DHA) and 15-LOX metabolites of ALA [13-(S)-HPOTrE and 13-(S)-HOTrE] at various concentrations (1, 50, 100 and 200 μM) for different time points. Cell viability was measured colorimetrically by MTT (3-(4,5-dimethylthiazol-2-yl)-2,5-diphenyl tetrazolium bromide) assay as described by Mossman[69].

Nitrite Estimation. RAW 264.7 cells were seeded in 6 well plates for 12 h then pre-incubated with different concentrations (1, 50 and 100 μM) of ALA metabolites [13-(S)-HPOTrE and 13-(S)-HOTrE], or dexamethasone for 3 h then stimulated with or without LPS (100 ng/ml) for the next 24 h. At the end of the time point, stable nitrite level in the culture supernatant was measured by Griess Reagent. For this, 50 μl of cell culture medium was mixed with 50 μl of Griess reagent and incubated at room temperature for 10 min in the dark. Then absorbance was measured at 540 nm using multi-mode plate reader (BioTek, SynergyMx). Nitrite level in samples was determined by using the standard curve of sodium nitrite. Culture medium was taken as blank for all experiments.

Estimation of IL-1β, IL-10, PGD_2 and PGE_2. Levels of IL-1β, IL-10, PGE_2 and PGD_2 in culture medium were measured by ELISA kit according to manufacturer's protocol. Their levels in culture medium were determined by using standard curves of respective cytokine or prostaglandin standards provided along with the kit.

Measurement of Reactive Oxygen Species (ROS). RAW 264.7 cells were seeded in 6 well plates at a density of 2×10^5 cells/well then pre-incubated with different concentrations (1, 50 and 100 μM) of ALA metabolites [13-(S)-HPOTrE and 13-(S)-HOTrE] and/or N-Acetyl Cysteine (NAC, 5 mM), for 3 h. Then cells were further stimulated with or without LPS (1 μg/ml) for next 16 h. After that cells from each well were harvested and washed twice with PBS and further incubated with 10 mM DCFH-DA for 30 min in dark at 37 °C and then two times washed with PBS. About 10,000 cells per sample were taken for analysis. The measurement was performed on a Flow Cytometer and data analysis was done by Cell Quest software (FACS Calibur, Becton Dickinson, CA, USA) with excitation of DCF at λ488 nm and emission at λ525 nm. Primary macrophages isolated from peritoneal cavity were seeded in 12 well plate and grown as mentioned earlier. Then pre-treated with 13-(S)-HPOTrE and 13-(S)-HOTrE at 100 nM for 3 h. Then stimulated with LPS and ROS was measured as described above.

Immunoblot Analysis. RAW 264.7 cells seeded in 100 mm plates at a density of 5×10^5 cells/well and then after 12 h pre-incubated with different concentrations (1, 50 and 100 μM) of either ALA metabolites or dexamethasone (10 μM) for 3 h. For Immunoblot analysis of primary cells, mouse peritoneal macrophages were isolated and seeded in 60 mm plates. Then pre-treated with lower doses (100 nM and 400 nM) of ALA metabolites for 3 h. Cells were then stimulated with or without LPS (100 ng/ml) for next 24 h. Cells were harvested at the end of time point, pelleted down and stored at −80 °C for further use. Cell pellets were lysed in RIPA buffer containing 1x protease inhibitor at 4 °C. Protein estimation was done by Bradford method using BSA as standard. An equal amount of protein was loaded and separated on 8–15% SDS-PAGE and transferred to nitrocellulose membrane. Then membranes were blocked with 5% (w/v) fat-free dry milk in TBST for 1 h at room temperature followed by washing three times with TBST. Membranes were incubated with primary antibodies (0.5–1.0 μg/ml) for 12 h at 4 °C on a shaker incubator with gentle shaking followed by thrice washing with TBST. The membranes were then incubated with respective secondary antibodies conjugated with HRP. Signals were then detected with western lightning plus ECL kit (PerkinElmer) and captured on Kodak Imaging System (KODAK Image station 4000 mm Pro).

Reverse Transcription Polymerase Chain Reaction (RT-PCR). RAW 264.7 cells were seeded in 6 well culture plate. At 60% confluency, cells were pre-incubated with different concentrations of either ALA metabolites (1, 50 and 100 μM) or dexamethasone (10 μM) for 3 h and then stimulated with LPS (100 ng/ml) for 24 h. Total cellular RNA was extracted from each well using TRIzol® Reagent according to the manufacturer's instructions (Invitrogen Bio Services, India, Pvt. Ltd). RNA quantification was performed by nanodrop (NanoDrop 2000TM, Thermo Scientific, DE, USA). cDNA of each sample was prepared by using 2 μg of RNA, 1 μl MLV reverse transcriptase, 1 mM dNTP and 1 μl oligo dT according to manufacturer's standardized protocol (Promega Corporation, WI, USA). PCR analyses were performed on aliquots of the cDNA prepared to detect iNOS, TNF-α, NLRP3, Caspase-1, IL-1β, IL-18 and GAPDH. The reactions were carried out in a volume of 20 μl containing (final concentration) 1 U Taq DNA polymerase, 0.2 mM dNTP, 100 pM of forward primers and reverse primers (Supplementary Table S1), and 10 μl reaction buffer. After amplification, PCR products were electrophoresed on 1% agarose gels and visualized by ethidium bromide staining on UV irradiation (BIO-RAD, Universal hood II).

Analysis of the inflammasome, autophagy and NF-κB translocation by confocal microscopy. RAW 264.7 cells were seeded in 6 well culture plates on sterile culture grade coverslips. When cells were 60% confluent, cells were pre-incubated with ALA metabolites (100 μM) and/or with GW9662, PPAR-γ inhibitor, for 3 h, then stimulated with LPS (100 ng/ml) for 24 h. For the study of inflammasome and autophagy, stimulation of cells with LPS was done for 24 h and for NF-κB translocation, it was done for 16 h. However, for study NF-κB translocation on peritoneal macrophages, cells were treated with ALA metabolites at lower concentration (100 nM) for 16 h. Fixation of cells was done by ice-cold 4% paraformaldehyde for 10 min at 4 °C followed by washing in PBS with 0.2% Tween 20. Permeabilization in cells was done by ice-cold acetone: methanol (1:3) for 15 min at room temperature followed by washing in PBS with 0.2% Tween 20. To avoid nonspecific binding, blocking was done by incubating cells in 5% FBS in PBST for 1 h at room temperature followed by twice washing in PBS with 0.2% Tween 20. Cells were then incubated with targeted primary antibody (1:100 dilution) in 3% BSA in PBST for 12 h at 4 °C followed by washing thrice in PBS with 0.2% tween 20. Cells were then incubated with the fluorescent conjugated respective secondary antibody (1:300 dilutions) in 3% BSA in PBST for 1 h at room temperature in the dark. Finally, washings were done and coverslips mounted on slides by anti-fade reagent with DAPI (ProLong Gold Antifade reagent, Invitrogen, USA). Image analysis was done on a confocal microscope (Zeiss LSM700, USA).

Analysis of Apoptosis by FACS. RAW 264.7 cells were seeded in 6 well cultures plate. When cells were 60% confluent, cells were pre-incubated with different concentrations of either ALA metabolites (1, 50 and 100 μM) and/or doxorubicin (10 μM) for 3 h, then stimulated with LPS (100 ng/ml) for 24 h. Staining of cells was done by FITC Annexin V Apoptosis Detection Kit (BD Biosciences, CA, USA), according to manufacturer's standardized protocol. Samples were run on Flow Cytometer (BD, LSR Fortessa, CA, USA) and data analyses were done on BD FACS Diva™ software.

Statistical Analyses. All the experiments were performed in triplicates and the values represented as mean ± SD. Data were correlated, analyzed and p-values were obtained using student's t-test. The p-value < 0.05 was considered as statistically significant.

References

1. Xie, Q. & Nathan, C. The high-output nitric oxide pathway: role and regulation. *J. Leukoc. Biol.* **56,** 576–582 (1994).
2. Kanwar, J. R., Kanwar, R. K., Burrow, H. & Baratchi, S. Recent advances on the roles of NO in cancer and chronic inflammatory disorders. *Curr. Med. Chem.* **16,** 2373–2394 (2009).
3. Kim, S. Y. *et al.* Regulation of pro-inflammatory responses by lipoxygenases via intracellular reactive oxygen species *in vitro* and *in vivo*. *Exp. Mol. Med.* **40,** 461–476 (2008).
4. Ulivi, V., Giannoni, P., Gentili, C., Cancedda, R. & Descalzi, F. p38/NF-kB-dependent expression of COX-2 during differentiation and inflammatory response of chondrocytes. *J. Cell. Biochem.* **104,** 1393–1406 (2008).
5. Taketo, M. M. Wnt signaling and gastrointestinal tumorigenesis in mouse models. *Oncogene* **25,** 7522–7530 (2006).
6. Reuter, S., Gupta, S. C., Chaturvedi, M. M. & Aggarwal, B. B. Oxidative stress, inflammation, and cancer: how are they linked? *Free Radic. Biol. Med.* **49,** 1603–1616 (2010).
7. Ren, J. & Chung, S. H. Anti-inflammatory Effect of α-Linolenic Acid and Its Mode of Action through the Inhibition of Nitric Oxide Production and Inducible Nitric Oxide Synthase Gene Expression via NF-κB and Mitogen-Activated Protein Kinase Pathways. *J. Agric. Food Chem.* **55,** 5073–5080 (2007).
8. Barceló-Coblijn, G. & Murphy, E. J. Alpha-linolenic acid and its conversion to longer chain n–3 fatty acids: Benefits for human health and a role in maintaining tissue n−3 fatty acid levels. *Prog. Lipid Res.* **48,** 355–374 (2009).
9. Musiek, E. S. *et al.* Electrophilic cyclopentenone neuroprostanes are anti-inflammatory mediators formed from the peroxidation of the omega-3 polyunsaturated fatty acid docosahexaenoic acid. *J. Biol. Chem.* **283,** 19927–19935 (2008).
10. Serhan, C. N. *et al.* Resolvins: A Family of Bioactive Products of Omega-3 Fatty Acid Transformation Circuits Initiated by Aspirin Treatment that Counter Proinflammation Signals. *J. Exp. Med.* **196,** 1025–1037 (2002).
11. Calder, P. C. n–3 polyunsaturated fatty acids, inflammation, and inflammatory diseases. *Am. J. Clin. Nutr.* **83,** 1505S–1519S (2006).
12. Kalinski, P. Regulation of Immune Responses by Prostaglandin E2. *J. Immunol.* **188,** 21–28 (2012).
13. Serhan, C. N., Chiang, N. & Van Dyke, T. E. Resolving inflammation: dual anti-inflammatory and pro-resolution lipid mediators. *Nat. Rev. Immunol.* **8,** 349–361 (2008).
14. Ricciotti, E. & FitzGerald, G. A. Prostaglandins and Inflammation. *Arterioscler. Thromb. Vasc. Biol.* **31,** 986–1000 (2011).
15. Shibata, T. *et al.* 15-Deoxy- 12,14-prostaglandin J2: A prostaglandin D2 metabolite generated during inflammatory processes. *J. Biol. Chem.* **277,** 10459–10466 (2002).
16. Poligone, B. & Baldwin, A. S. Positive and negative regulation of NF-kappaB by COX-2: roles of different prostaglandins. *J. Biol. Chem.* **276,** 38658–38664 (2001).
17. Gilroy, D. W. *et al.* Inducible cyclooxygenase may have anti-inflammatory properties. *Nat. Med.* **5,** 698–701 (1999).
18. Serhan, C. N. & Chiang, N. Endogenous pro-resolving and anti-inflammatory lipid mediators: a new pharmacologic genus. *Br. J. Pharmacol.* **153,** S200–S215 (2009).
19. Straus, D. S. *et al.* 15-deoxy-delta 12,14-prostaglandin J2 inhibits multiple steps in the NF-kappa B signaling pathway. *Proc. Natl. Acad. Sci. USA* **97,** 4844–4849 (2000).
20. Genovese, T. *et al.* Effect of cyclopentanone prostaglandin 15-deoxy-δ12,14pgj2 on early functional recovery from experimental spinal cord injury. *Shock* **30,** 1 (2007).
21. Mueller, E. *et al.* Effects of ligand activation of peroxisome proliferator-activated receptor gamma in human prostate cancer. *Proc. Natl. Acad. Sci. USA* **97,** 10990–10995 (2000).
22. Horn, T. *et al.* Evolutionary aspects of lipoxygenases and genetic diversity of human leukotriene signaling. *Prog. Lipid Res.* **57,** 13–39 (2015).
23. Martel-Pelletier, J., Lajeunesse, D., Reboul, P. & Pelletier, J.-P. Therapeutic role of dual inhibitors of 5-LOX and COX, selective and non-selective non-steroidal anti-inflammatory drugs. *Ann. Rheum. Dis.* **62,** 501–509 (2003).
24. Uderhardt, S. & Krönke, G. 12/15-Lipoxygenase during the regulation of inflammation, immunity, and self-tolerance. *J. Mol. Med.* **90,** 1247–1256 (2012).
25. Kühn, H. & O'Donnell, V. B. Inflammation and immune regulation by 12/15-lipoxygenases. *Prog. Lipid Res.* **45,** 334–356 (2006).
26. Mahipal, S. V. K. *et al.* Effect of 15-lipoxygenase metabolites, 15-(S)-HPETE and 15-(S)-HETE on chronic myelogenous leukemia cell line K-562: Reactive oxygen species (ROS) mediate caspase-dependent apoptosis. *Biochem. Pharmacol.* **74,** 202–214 (2007).
27. Soumya, S. J., Binu, S., Helen, A., Reddanna, P. & Sudhakaran, P. R. 15-LOX metabolites and angiogenesis: angiostatic effect of 15(S)-HPETE involves induction of apoptosis in adipose endothelial cells. *PeerJ* **2,** e635 (2014).
28. Kumar, K. A. *et al.* Effects of (15S)-hydroperoxyeicosatetraenoic acid and (15S)-hydroxyeicosatetraenoic acid on the acute-lymphoblastic-leukaemia cell line Jurkat: activation of the Fas-mediated death pathway. *Biotechnol. Appl. Biochem.* **52,** 121–133 (2009).
29. Guzik, T. J., Korbut, R. & Adamek-Guzik, T. Nitric oxide and superoxide in inflammation and immune regulation. *J. Physiol. Pharmacol.* **54,** 469–487 (2003).
30. Sweet, M. J. & Hume, D. A. Endotoxin signal transduction in macrophages. *J. Leukoc. Biol.* **60,** 8–26 (1996).
31. Ben-Neriah, Y. & Karin, M. Inflammation meets cancer, with NF-κB as the matchmaker. *Nat. Immunol.* **12,** 715–723 (2011).
32. Andreakos, E. *et al.* Distinct pathways of LPS-induced NF-kappa B activation and cytokine production in human myeloid and nonmyeloid cells defined by selective utilization of MyD88 and Mal/TIRAP. *Blood* **103,** 2229–2237 (2004).
33. Bauernfeind, F. G. *et al.* Cutting edge: NF-kappaB activating pattern recognition and cytokine receptors license NLRP3 inflammasome activation by regulating NLRP3 expression. *J. Immunol.* **183,** 787–791 (2009).
34. Qiao, Y., Wang, P., Qi, J., Zhang, L. & Gao, C. TLR-induced NF-κB activation regulates NLRP3 expression in murine macrophages. *FEBS Lett.* **586,** 1022–1026 (2012).
35. Ciraci, C., Janczy, J. R., Sutterwala, F. S. & Cassel, S. L. Control of innate and adaptive immunity by the inflammasome. *Microbes Infect.* **14,** 1263–1270 (2012).
36. Shenoy, A. R. *et al.* GBP5 promotes NLRP3 inflammasome assembly and immunity in mammals. *Science* (*80-*) **336,** 481–485 (2012).
37. Im, D.-S. Omega-3 fatty acids in anti-inflammation (pro-resolution) and GPCRs. *Prog. Lipid Res.* **51,** 232–237 (2012).
38. Nixon, J. B., Kamitani, H., Baek, S. J. & Eling, T. E. Evaluation of eicosanoids and NSAIDs as PPARγ ligands in colorectal carcinoma cells. *Prostaglandins, Leukot. Essent. Fat. Acids* **68,** 323–330 (2003).
39. Itoh, T. *et al.* Structural basis for the activation of PPARgamma by oxidized fatty acids. *Nat. Struct. Mol. Biol.* **15,** 924–931 (2008).
40. Edwards, I. J. & O'Flaherty, J. T. Omega-3 fatty acids and PPARγ in cancer. *PPAR Res.* **2008,** 1–14 (2008).
41. Miao, H. *et al.* Macrophage CGI-58 Deficiency Activates ROS-Inflammasome Pathway to Promote Insulin Resistance in Mice. *Cell Rep.* **7,** 223–235 (2014).
42. Hortelano, S., Castrillo, A., Alvarez, A. M. & Boscá, L. Contribution of cyclopentenone prostaglandins to the resolution of inflammation through the potentiation of apoptosis in activated macrophages. *J. Immunol.* **165,** 6525–6531 (2000).
43. Luo, S. & Rubinsztein, D. C. Apoptosis blocks Beclin 1-dependent autophagosome synthesis: an effect rescued by Bcl-xL. *Cell Death Differ.* **17,** 268–277 (2010).
44. Wang, J. *et al.* Lipopolysaccharide (LPS)-induced autophagy is involved in the restriction of Escherichia coli in peritoneal mesothelial cells. *BMC Microbiol.* **13,** 255 (2013).
45. Morrison, D. C. & Ryan, J. L. Endotoxins and disease mechanisms. *Annu. Rev. Med.* **38,** 417–432 (1987).
46. Svahn, S. L. *et al.* Dietary Polyunsaturated Fatty Acids Increase Survival and Decrease Bacterial Load during Septic Staphylococcus aureus *Infection and Improve Neutrophil Function in Mice* **83,** 514–521 (2015).

47. Calder, P. C. Dietary modification of inflammation with lipids. *Proc. Nutr. Soc.* **61,** 345–358 (2002).
48. Ren, J. & Chung, S. H. Anti-inflammatory Effect of α-Linolenic Acid and Its Mode of Action through the Inhibition of Nitric Oxide Production and Inducible Nitric Oxide Synthase Gene Expression via NF-κB and Mitogen-Activated Protein Kinase Pathways. *J. Agric. Food Chem.* **55,** 5073–5080 (2007).
49. Serhan, C. N., Krishnamoorthy, S., Recchiuti, A. & Chiang, N. Novel anti-inflammatory--pro-resolving mediators and their receptors. *Curr. Top. Med. Chem.* **11,** 629–647 (2011).
50. Scher, J. U. & Pillinger, M. H. The anti-inflammatory effects of prostaglandins. *J. Investig. Med.* **57,** 703–708 (2009).
51. Scher, J. U. & Pillinger, M. H. 15d-PGJ2: The anti-inflammatory prostaglandin? *Clin. Immunol.* **114,** 100–109 (2005).
52. Powell, W. S. 15-deoxy-D12,14-PGJ2: endogenous PPARg ligand or minor eicosanoid degradation product? *J Clin Invest* **112,** 828–830 (2003).
53. Araujo, J. A., Zhang, M. & Yin, F. Heme Oxygenase-1, Oxidation, Inflammation, and Atherosclerosis. *Front. Pharmacol.* **3,** 119 (2012).
54. Gordon, S. & Taylor, P. R. Monocyte and macrophage heterogeneity. *Nat. Rev. Immunol.* **5,** 953–964 (2005).
55. Grivennikov, S. I., Greten, F. R. & Karin, M. Immunity, Inflammation, and Cancer. *Cell* **140,** 883–899 (2011).
56. Li, Q. *et al.* Interleukin-17 Indirectly Promotes M2 Macrophage Differentiation through Stimulation of COX-2/PGE2 Pathway in the Cancer Cells. *Cancer Res. Treat.* **46,** 297–306 (2014).
57. Heusinkveld, M. *et al.* M2 macrophages induced by prostaglandin E2 and IL-6 from cervical carcinoma are switched to activated M1 macrophages by CD4+ Th1 cells. *J Immunol* **187,** 1157–1165 (2011).
58. Sharma, A. M. & Staels, B. Peroxisome Proliferator-Activated Receptor γ and Adipose Tissue—Understanding Obesity-Related Changes in Regulation of Lipid and Glucose Metabolism. *J. Clin. Endocrinol. Metab.* **92,** 386–395 (2007).
59. Castrillo, A. & Tontonoz, P. NUCLEAR RECEPTORS IN MACROPHAGE BIOLOGY: At the Crossroads of Lipid Metabolism and Inflammation. *Annu. Rev. Cell Dev. Biol.* **20,** 455–480 (2004).
60. Kim, C. W. & Lee, C. D. Apoptosis and diagnosis of nonalcoholic steatohepatitis. *Korean J. Hepatol.* **17,** 247 (2011).
61. Chinetti, G. *et al.* Activation of proliferator-activated receptors alpha and gamma induces apoptosis of human monocyte-derived macrophages. *J. Biol. Chem.* **273,** 25573–25580 (1998).
62. Nemzek, J. A., Hugunin, K. M. S. & Opp, M. R. Modeling sepsis in the laboratory: Merging sound science with animal well-being. *Comp. Med.* **58,** 120–128 (2008).
63. Soumya, S. J. *et al.* Effect of 15-lipoxygenase metabolites on angiogenesis: 15(S)-HPETE is angiostatic and 15(S)-HETE / is angiogenic. *Inflamm. Res.* **61,** 707–718 (2012).
64. Soumya, S. J., Binu, S., Helen, A., Reddanna, P. & Sudhakaran, P. R. 15(S)-HETE-induced angiogenesis in adipose tissue is mediated through activation of PI3K/Akt/mTOR signaling pathway. *Biochem Cell Biol* **91,** 498–505 (2013).
65. Reddanna, P., Whelan, J., Maddipati, K. R. & Reddy, C. C. Purification of arachidonate 5-lipoxygenase from potato tubers. *Methods Enzymol.* **187,** 268–277 (1990).
66. Sailesh, S., Kumar, Y. V., Prasad, M. & Reddanna, P. Sheep uterus dual lipoxygenase in the synthesis of 14,15-leukotrienes. *Arch. Biochem. Biophys.* **315,** 362–368 (1994).
67. Reddy, G. R., Reddanna, P., Reddy, C. C. & Curtis, W. R. 11-hydroperoxyeicosatetraenoic acid is the major dioxygenation product of lipoxygenase isolated from hairy root cultures of Solanum tuberosum. *Biochem. Biophys. Res. Commun.* **189,** 1349–1352 (1992).
68. Zhang, X., Goncalves, R. & Mosser, D. M. The Isolation and Characterization of Murine Macrophages. *Curr. Protoc. Immunol./Ed. by* John E. *Coligan …*[*et al.*] chapter, Unit-14 (2008).
69. Mosmann, T. Rapid colorimetric assay for cellular growth and survival: application to proliferation and cytotoxicity assays. *J. Immunol. Methods* **65,** 55–63 (1983).

Acknowledgements

The authors gratefully acknowledge the financial support from Department of Science and Technology (DST) under FIST and University Grants Commission (UGC) under UPE-II programs.

Author Contributions

N.K. and P.R. designed research, N.K. performed the experiments, N.K. and R.K. analyzed the data, N.K. and N.F. drafted manuscript. N.K., P.R., G.G., K.A., G.V.R. and P.V.G. reviewed the manuscript. All the authors approved the manuscript.

Additional Information

Supplementary information accompanies this paper at http://www.nature.com/srep

Competing financial interests: The authors declare no competing financial interests.

How to cite this article: Kumar, N. *et al.* 15-Lipoxygenase metabolites of α-linolenic acid, [13-(S)-HPOTrE and 13-(S)-HOTrE], mediate anti-inflammatory effects by inactivating NLRP3 inflammasome. *Sci. Rep.* **6**, 31649; doi: 10.1038/srep31649 (2016).

Toxicology Reports 2 (2015) 520–529

Contents lists available at ScienceDirect

Toxicology Reports

journal homepage: www.elsevier.com/locate/toxrep

Isolation and characterization of gallic acid and methyl gallate from the seed coats of *Givotia rottleriformis* Griff. and their anti-proliferative effect on human epidermoid carcinoma A431 cells

Samuel Kamatham [a], Naresh Kumar [b], Padmaja Gudipalli [c,*]

[a] Department of Biochemistry, School of Life Sciences, University of Hyderabad, Hyderabad, Telangana, India
[b] Department of Animal Biology, School of Life Sciences, University of Hyderabad, Hyderabad, Telangana, India
[c] Department of Plant Sciences, School of Life Sciences, University of Hyderabad, Hyderabad, Telangana, India

ARTICLE INFO

Article history:
Received 3 December 2014
Received in revised form 6 March 2015
Accepted 6 March 2015
Available online 14 March 2015

Keywords:
Givotia rottleriformis
Gallic acid
Methyl gallate
A431 cells
Cyclooxygenases
HaCaT

ABSTRACT

Gallic acid (GA) and its derivative methyl gallate (MG) are well studied plant phenolics. They have exhibited anticancer effects in several cancer cell lines. However, the presence of GA/MG in the seed coats of *Givotia rottleriformis* and their inhibitory effect on human epidermoid carcinoma (A431) skin cancer cells were not reported. In this study we have isolated and chemically characterized the bioactive compounds GA and MG from the bioassay guided methanolic (MeOH) seed coat extracts of *G. rottleriformis*. The fractions obtained from open silica column chromatography were subjected to in vitro enzymatic assays. Among seven fractions we found that only fractions 5 and 6 showed significant inhibition activity toward COX-1 with an IC_{50} value of 28 μg/mL and 9.3 μg/mL and COX-2 with an IC_{50} value of 35 μg/mL and 7.0 μg/mL respectively. However, we could not find 5-LOX enzyme inhibition activity. MG (10 mg/g DW) and GA (6 mg/g DW) were the major compounds of seed coats. Cell viability was analyzed by 3-(4,5-dimethylthiazol-2-yl)-2,5-diphenyl tetrazolium bromide (MTT) assay, which showed that GA/MG significantly reduced the growth of A431 cells with an IC_{50} value of 25 μg/mL and 53 μg/mL and 11 μg/mL and 43 μg/mL at 24 h and 48 h, respectively. However the cytotoxic effect of GA/MG on HaCaT normal skin keratinocyte cell line was found to be less. Western blot analysis has shown that GA/MG treatment down regulated Bcl-2 and up regulated cleaved caspase-3 with respect to increasing doses. Our results conclude that GA and MG have potential anticancer effects and can be used as therapeutic agents for skin cancers.

1. Introduction

Skin diseases are becoming more common worldwide, because of increasing environmental pollutants, such as chemical hazards and radiations. Diverse factors influence skin cancers, e.g. solar radiation, UV irradiation. More than one million new skin cancer cases were reported annually in USA [1]. Increasing incidence of skin cancers was reported in AIDS (Acquired immune deficiency syndrome)

* Corresponding author at: Department of Plant Sciences, School of Life Sciences, University of Hyderabad, Gachibowli, Hyderabad, Telangana 500 046, India.
E-mail addresses: gudipallipadmaja@gmail.com, gprsl@uohyd.ernet.in (P. Gudipalli).

http://dx.doi.org/10.1016/j.toxrep.2015.03.001

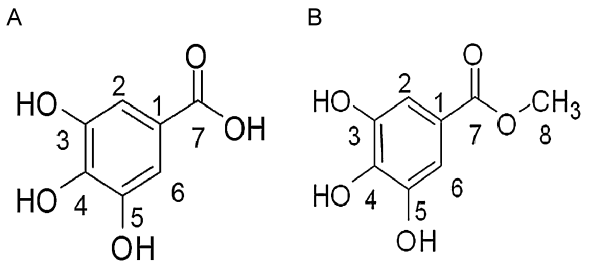

Fig. 1. Chemical structure of (A) gallic acid and (B) methyl gallate.

patients [2]. The cancer chemoprevention by natural agents such as phytochemicals, minerals and vitamins were shown to have effective results on various malignancies [3,4]. The curcumin isolated from plants inhibits UV-irradiation-induced oxidative stress and enhanced apoptosis in A431 cells [1,5]. The isolated resveratrol from plants was reported to have potential anti-cancer effect that enhanced apoptosis in A431 cells [6].

In this study we used the seed coats of *Givotia rottleriformis*, a tree species that belongs to Euphorbiaceae family. This plant grows in limited areas and particularly in the forests of Andhra Pradesh, Karnataka, Tamil Nadu and West Bengal in India. In our previous study we have observed that the seeds of this plant were rich in phenolics [7] and were reported to have anti-rheumatic, anti-psoriatic and anti-dandruff medicinal properties [8].

The gallic acid is isolated from plants [9,10] and the antioxidant and anticancer effect of GA were well reported in most of the cancer cells [9,11–17]. Many of GA derived chemical derivatives were also shown to have good anticancer properties [18]. Methyl gallate, a methyl ester of GA, was also isolated from several plants [19,20]. The biosynthesis of GA and MG takes place via dihydroshikimate, a derivative of phenylpropanoid biosynthesis [21]. The anticancer and anti oxidant effects of MG was reported in different cancer cells [22–27]. In addition MG was also shown to have anti-bacterial and anti-viral properties [28–30].

Cyclooxygenases (COX-1 and COX-2) and lipoxygenases (5-LOX, 12-LOX, 15-LOXa and 15-LOXb) are the key enzymes of arachidonic acid (AA) metabolism [31]. Previous reports suggested that inducible form of COX-1 and COX-2 leads to the biosynthesis of prostaglandins and thus causes inflammation and cancer [32–34]. Inhibition of 5-LOX blocks production of 5-LOX metabolites and triggers apoptosis in prostate cancer cells [35]. Therefore, identification of natural dual COX-2/5-LOX inhibitors is an interesting area of research to control cancer progression [36].

The over expression of Bcl-2 protein causes reduction of apoptosis in cancer cells [37–40]. In contrast, the up-regulation of cleaved caspase-3 activated by other caspases [41,42], enhances apoptosis and thus reduces cancer cell survival [43–45].

In the present study, we have isolated GA and MG from the seed coats of *G. rottleriformis* using chromatographic techniques and chemically characterized them using IR, NMR and LC–MS analysis (Fig. 1). The inhibitory effect of GA or MG on COX-1, COX-2 and 5-LOX was determined. We further studied the cytotoxic effect of purified GA and MG on human epidermoid carcinoma (A431) skin cancer cell line and normal human skin keratinocyte cell line HaCaT using MTT assay. The apoptotic effect of GA/MG was studied by western blotting analysis of Bcl-2 and cleaved caspase-3 in a dose dependent manner.

2. Materials and methods

2.1. General procedure

IR spectra was determined in the KBr pellet using a JASCO FT-IR model 5300 spectrophotometer with polystyrene as reference. NMR spectra were recorded at 400 MHz for ^{1}H NMR and 100 MHz for ^{13}C NMR on Bruker-Avance-400 spectrometer with chloroform-d as solvent and tetramethylsilane (TMS) as reference ($\delta = 0$ ppm) in DMSO-d6 at 25 °C. The chemical shift was expressed in δ, downfield from the signal of internal TMS. Mass spectra were recorded using LC–MS-2010 (Shimadzu).

2.2. Plant materials

Mature and dry seeds of *G. rottleriformis* were collected during summer from Regional Forest Research Centre (RFRC), Rajahmundry, Andhra Pradesh, India.

2.3. Cell lines and reagents

A431 skin cancer cell line and normal HaCaT skin cell line were obtained from National Centre for Cell Science (NCCS), Pune, India. Dulbeco's modified Eagle's medium (DMEM), fetal bovine serum (FBS), phosphate buffered saline (PBS), penicillin and streptomycin were purchased from GIBCO, Ltd. (BRL Life Technologies, Inc., Grand Island, NY). MTT [3-(4,5-dimethylthiazol-2-yl)-2,5-diphenyl tetrazolium bromide] and dimethyl sulfoxide (DMSO) were obtained from Sigma; poly-L-lysine, glutaraldehyde, proteinase inhibitor K, propidium iodide (PI), phenyl methyl sulfonyl fluoride (PMSF), luepeptin, aprotinin, pepstatin A, trypsin, Tween 20, Triton X-100, TMPD (*N,N,N,N′*-tetramethyl-*p*-phenylenediamine) were purchased from Sigma Chemical Company (St. Louis, USA). The primary antibodies for Bcl-2 and cleaved caspase-3 were obtained from Upstate Biotechnology (Charlottesville, VA, USA). The GA and MG were purified from the seed coats of *G. rottleriformis*. All other chemicals and reagents used in the study were obtained either from Merck or Sigma.

2.4. Extraction and reverse phase HPLC analysis of crude extract

The seed coats were macerated into fine powder and were extracted in methanol (MeOH). The crude extract was filtered using Whatman No.1 filter paper and was concentrated using Rotavapor (R3, Buchi). The extract was further analyzed with RP-HPLC (Shimadzu) using C18 reverse phase column (Shim-pack column with dimensions 250 mm × 4.6 mm, particle size 5 μM), with flow rate of

6 mL/min and detection at 280 nm. The mobile phase used was a complex gradient of solvent-A (water:acetic acid, 1000:1), and solvent-B (MeOH:acetic acid, 1000:1).

2.5. Open silica column and RPHPLC

The crude extract (10 g) was chromatographed using (Acme's) silica gel (100–200 mesh). Hexane and ethyl acetate was used as a mobile phase. Each fraction was passed through a thin layer chromatography (TLC) using silica gel plates (Merck $60F^{254}$) and visualized by irradiation with UV light and/or by iodine vapors. COX-1, COX-2 and 5-LOX assays were performed for all the fractions (see below). Only fractions that showed significant bioactivity were resolved using RP-HPLC (method mentioned above), isolated and concentrated by lyophilizer. The purified compounds were stored at room temperature and were used for bioassays and further analysis.

2.6. Isolation of COX-1 enzyme

We isolated COX-1 enzyme from Ram seminal vesicles using Hemler and Lands [46] method with slight modifications. In brief, Ram seminal vesicles were minced and homogenized in Tris–HCl (pH 8.0) buffer for 1 min; the homogenate was filtered through cheese cloth and centrifuged at 13,000 × *g* at 4 °C for 30 min. Finally 0.01% sodium azide was added to the supernatant. It was stored as small aliquots at −80 °C and was used as COX-1 enzyme source.

2.7. Isolation of COX-2 enzyme

The enzyme COX-2 was isolated according to the method of Reddy et al. [47] with slight modifications. In brief, human recombinant COX-2 enzyme was expressed in Sf-9 cells. Cells were pelleted down by centrifugation at 2000 rpm and the cells were further resuspended in 50 mM Tris–HCl buffer (pH 7.2) and sonicated for 3 min followed by centrifugation at 90,000 × *g* at 4 °C for 1 h 20 min using ultracentrifuge (Hitachi, Himac CP-100α). The obtained pellet was re-suspended in 2.5 mM Tris–HCl buffer (pH 7.2), 0.8% Tween 20, 1 mM phenol, and 0.5% glycerol. It was stored as small aliquots at −80 °C and used as COX-2 enzyme source.

2.8. COX-1 and COX-2 enzyme activity

We used the method of Copeland et al. [48] with slight modifications to measure the enzymatic activities of both COX-1 and COX-2, based on the chromogenic assay and oxidation of TMPD during the reduction of prostaglandin G2 (PGG2) to prostaglandin H2 (PGH2). In brief, the assay mixture contained Tris–HCl buffer (100 mM, pH 8.0), hematin (15 μM), EDTA (3 μM), enzyme (COX-1 or COX-2) and test compound. The assay mixture was pre-incubated at 25 °C for 15 min and the reaction was initiated by addition of AA and TMPD to a final volume of 1 mL. The activity was measured by estimating the rate of TMPD oxidation with an increase in absorbance at 603 nm during 1 min. A low rate of non-enzymatic TMPD oxidation observed in the absence of COX-1 or COX-2 enzymes was used as control reaction and was subtracted from the test experimental values while calculating the percent inhibition.

2.9. 5-LOX assay

The 5-LOX enzyme was extracted from potato tubers and assayed according to Reddanna et al. [49]. The enzyme activity was measured using polarographic method with a Clark's oxygen electrode on Strathkelvin instruments, model 782, RC-300. The typical reaction mixture contained 50–100 μL of enzyme and 10 μL of substrate (133 μM of AA), 100 mM phosphate buffer (pH 6.3) in a total volume of 3 mL. The rate of decrease in the oxygen concentration was taken as a measure of enzyme activity. The stock solutions of the test compounds were freshly prepared before use and were dissolved in DMSO. Various concentrations of the test compound were prepared and the 5-LOX was initiated by the addition of the substrate. The assay was performed at 25 °C and the maximum slope generated was taken for calculating the activity. The percent inhibition was calculated by the comparison of 5-LOX activity in the presence or absence of the inhibitor and IC_{50} value was calculated from the concentration–inhibition response curve.

2.10. Cell culture

A431 cells and HaCaT cells were grown as a monolayer in petriplates and supplemented with DMEM that contains 10% heat inactivated FBS, 100 IU/mL penicillin, 100 μg/mL streptomycin, 2 mM L-glutamine and maintained at 37 °C in a humidified atmosphere with 5% CO_2. The cells were subcultured twice in a week and the exponentially growing cells were used for the analysis.

2.11. MTT assay

A431 cells and HaCaT cells (5×10^3 cells per well) were seeded in 96 well plates and were treated with or without GA/MG at various concentrations (0.1, 10, 25, 50 and 100 μg/mL) in a final volume of 100 μL and incubated for 24 h and 48 h. Later 20 μL of MTT (5 mg/mL in PBS) was added to each well and incubated for an additional 3 h at 37 °C. The culture medium was removed and 50 μL of DMSO was added to each well to dissolve the purple-blue formazan crystals and optical density was measured at 570 nm using ELISA multi mode plate reader (SYNERGYMX, Bioteck).

2.12. Preparation of whole cell extract and Western blot analysis

The cells were treated with or without GA or MG at various concentrations (25, 50 and 100 μg/mL) for 24 h. Then the cells were washed with PBS and harvested by trypsinization and finally cell pellets were resuspended in RIPA buffer containing 1× protease inhibitor cocktail followed by incubation for 30 min at 4 °C with frequent vortex. The lysate was centrifuged at 10,000 rpm for 30 min and the supernatant was collected as whole-cell extract

[50]. The protein concentration was estimated by Bradford method Bradford [51]. The total protein was resolved on 12% SDS-PAGE and transferred onto nitrocellulose (NC) membrane. The NC membrane was then incubated in 5% (w/v) non-fat dry milk powder at room temperature for 1 h to block non-specific sites. The NC membrane was incubated with the primary antibody of interest for 12 h at 4 °C under shaking (cleaved caspase-3, and Bcl-2) and washed thrice with TBST. The NC membrane was again incubated with the respective secondary antibody conjugated with HRP for 1 h at room temperature, and again washed thrice with TBST. The blot was developed by adding HRP substrate (PerkinElmer; Western lightning Plus-ECL).

2.13. Statistical analyses

The data was presented graphically as the mean ± standard deviation (SD). Statistical analysis was done using Sigma Plot 12.0 software and the graphs were plotted using Graph pad prism 6.0 software.

3. Results

3.1. RP-HPLC analysis and column chromatography of seed coat extract

The crude seed coat extract subjected to RP-HPLC and the resolved chromatogram showed 10 major peaks at different retention times (RTs). Peak-1 eluted at 9.0 min, peak-2 at 25.9 min, peak-3 at 28.6 min, peak-4 at 33.1 min, peak-5 at 40.8 min, peak-6 at 42.1 min, peak-7 at 44.7 min, peak-8 at 47.7 min, peak-9 at 50.0 min and peak-10 at 57.0 min (Fig. 2). The crude seed coat extract (10 g) was fractionated into one to seven fractions, fraction 1 (0.6 g), fraction 2 (5.0 g), fraction 3 (1 g), fraction 4 (0.8 g), fraction 5 (1.0 g), fraction 6 (1.2 g), fraction 7 (0.4 g) according to the polarity using open silica chromatography and the purity of each fraction was monitored with TLC.

3.2. COX-1, COX-2 and 5-LOX enzymatic essays

COX-1, COX-2 and 5-LOX activity were estimated for fractions 1–7. However, only fractions 5 and 6 inhibited COX-1 with an IC_{50} value of 7 μg/mL and 5.1 μg/mL and COX-2 with an IC_{50} value of 9 μg/mL and 6.44 μg/mL respectively (Fig. 3A–D). None of the fractions showed 5-LOX inhibition activity.

3.3. Isolation and chemical characterization of active compound from fraction 5

The bioassay guided fraction 5 that showed only a single peak at RT of 41.5 min, when resolved by RP-HPLC was collected (Fig. 4A). The isolated compound was subjected to IR, ^{1}H, ^{13}C NMR and LC–MS analysis and identified as MG (Supplementary Fig. S1–S4). IR (KBr) cm^{-1}: 3506 (O—H), 1697 (●C=O), 1618 (C=C), 1541, 1471, 1439, 1313, 1251, 1195, 1037, 767, 746 (Supplementary Fig. S1). ^{1}H NMR (400 MHz, $CDCl_3$) δ ppm: 7.26 (S, 2H, A), 4.01 (S, 2H, B) (Supplementary Fig. S2). ^{13}C NMR (200 MHz, $CDCl_3$) δ ppm: 165.67 (C7, ●C=O) 144.10 (C3, C5), 136.99 (C4), 118.82 (C1) 107.86 (C2, C5) 50.36 (C8) (Supplementary Fig. S3). The molecular mass of isolated MG was determined as 184 using LC–MS analysis (Supplementary Fig. S4).

3.4. Isolation and chemical characterization of active compound from fraction 6

RP-HPLC chromatogram of fraction 6 that showed a mixture of 3 compounds eluted at different RTs, C1 (600 mg) at RT 27.49 min, C2 (250 mg) at RT 40.8 min and C3 (350 mg) at RT 51.4 min were isolated separately (Fig. 4B). MTT assay results showed that significant inhibition of A431 cell proliferation was seen when treated with C1, whereas treatment with C2 or C3 did not show any inhibitory effect on cell proliferation. The active C1 was subjected to IR, ^{1}H, ^{13}C NMR and LC–MS analysis and its chemical structure was identified as GA. IR (KBr) cm^{-1} 33.71 (—COOH), 3057 (C—H), 1705 (=C=O), 1620 (C=C), 1452, 1338, 1248, 1026, 702 (Supplementary Fig. S5). ^{1}H NMR δ ppm: 12.52 (S, H acid OH), 7.22 (S, 2H) (Supplementary Fig. S6). ^{13}C NMR δ ppm: 167.01 (C7=C=O), 143.98 (C3, C5), 136.61 (C4), 119.87 (C1) 108.14 (C2, C6); (Supplementary Fig. S7). The mass of the purified GA was determined as 169 by LC–MS (Supplementary Fig. S8).

3.5. MTT assay

Dose and time dependent effect of GA and MG on A431 and HaCaT cell proliferation was investigated. A431 cells that were treated with various concentrations of GA/MG (1, 10, 25, 50 and 100 μg/mL) showed significantly reduced cell proliferation due to enhanced cell death (Fig. 5A and B). GA treatment enhanced A431 cell death in a dose dependent manner with calculated IC_{50} value of 25 μg/mL at 24 h. The cell death was increased further when the GA treatment time increased to 48 h with an IC_{50} value of 11 μg/mL (Fig. 5Ai–iv). Similarly MG treatment also reduced A431 cell proliferation in a dose dependent manner. MG treatment showed reduced A431 cell proliferation with an IC_{50} value of 53 μg/mL at 24 h. However when the MG treatment time increased to 48 h the rate of cell death also increased further with an IC_{50} value of 43 μg/mL (Fig. 5Bi–iv). HaCaT cells that were treated with same GA concentrations (1, 10, 25, and 100 μg/mL) showed low level of reduction in cell proliferation with the calculated IC_{50} values of 84.2 μg/mL at 24 h and 64.4 μg/mL at 48 h, respectively (Fig. 6Ai–iv). MG treatment also showed reduced effect on HaCaT cell proliferation with an IC_{50} value of 79.4 μg/mL at 48 h (Fig. 6Bi–iv).

3.6. Western blot analysis

Treatment of A431 cells with GA and MG down regulated Bcl-2 and thus enhanced apoptosis in dose (25, 50 and 100 μg/mL) dependent manner (Fig. 7Ai and Bi). The cleaved caspase-3 was also induced in a dose dependent manner with increasing doses of GA and MG treatment (Figs. 7Aii and 6Bii). β-Actin was used as a loading control (Fig. 7Aiii and Biii).

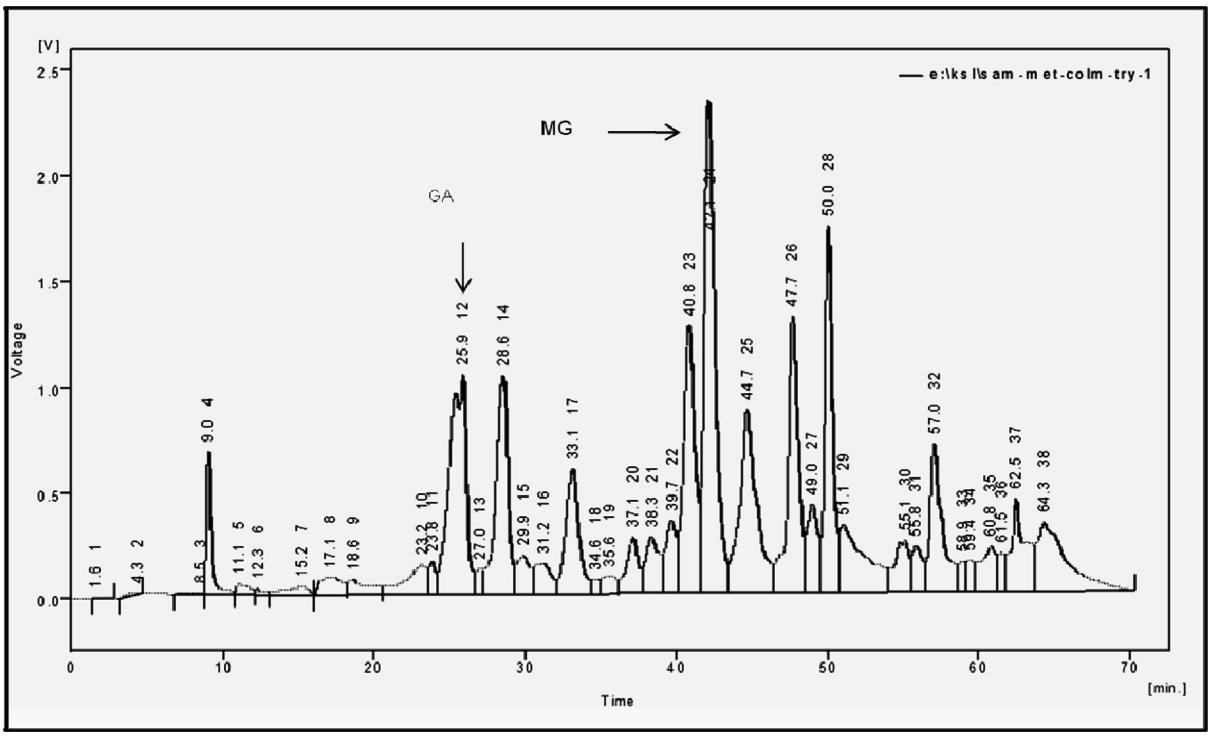

Fig. 2. High-performance liquid chromatography (HPLC) analysis of crude extract of *G. rottleriformis* seed coats using a reverse phase C_{18} column. High-performance liquid chromatography (HPLC) chromatogram showing crude compounds resolved at their respective retention times (RTs).

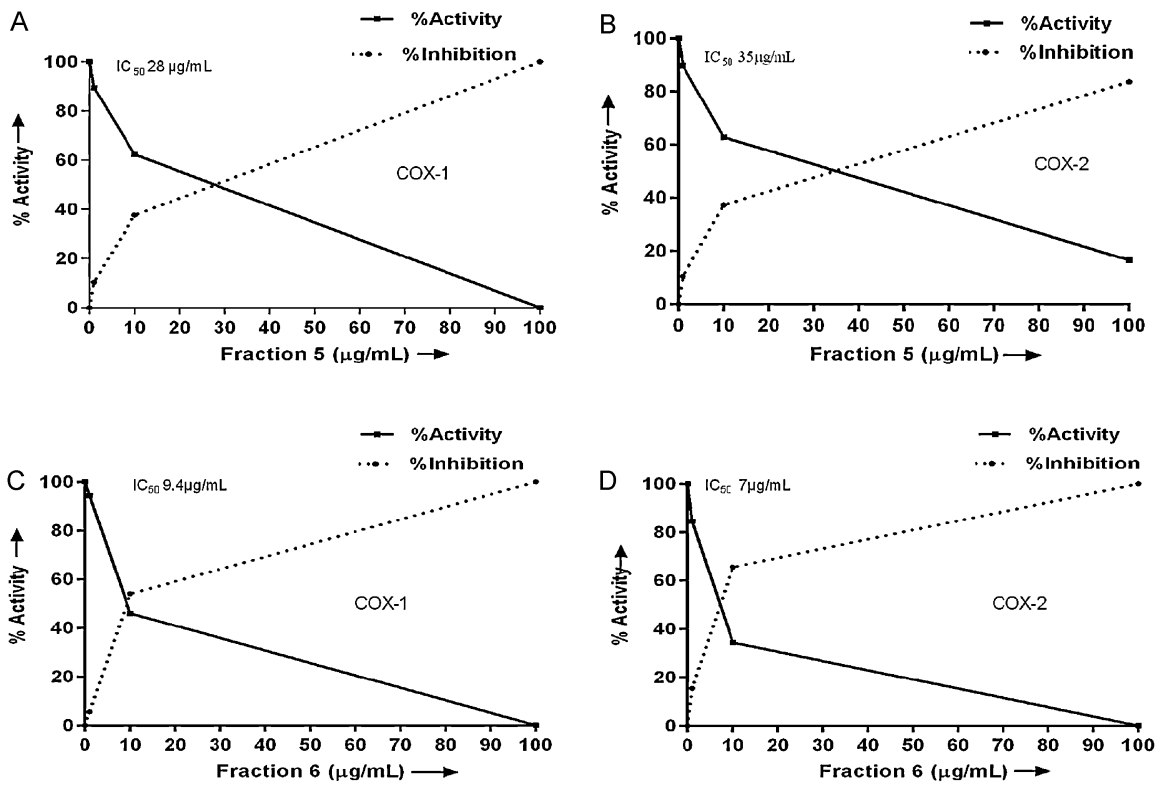

Fig. 3. COX-1 and COX-2 inhibition activity of fractions 5 and 6. (A) COX-1 inhibition of fraction 5, (B) COX-2 inhibition of fraction 5, (C) COX-1 inhibition of fraction 6 and (D) COX-2 inhibition of fraction 6.

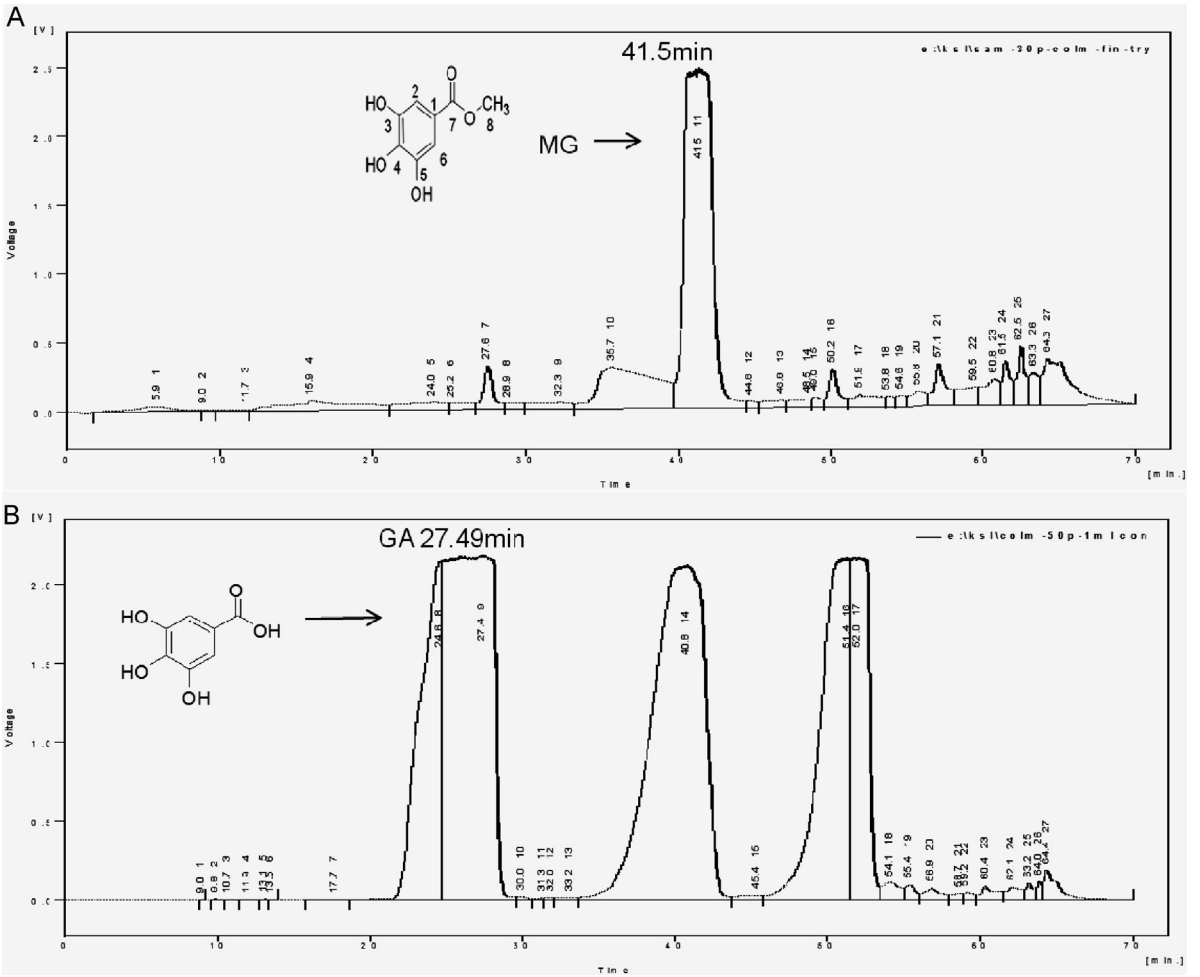

Fig. 4. Purification of methyl gallate (MG) from fraction 5 and gallic acid (GA) from fraction 6 by high-performance liquid chromatography (HPLC) using a reverse phase C_{18} column. (A) MG from fraction 5. (B). GA from fraction 6.

4. Discussion

Plants synthesize a wide range of metabolites for their survival, growth, development and protection from a broad spectrum of bacterial, fungal and viral pathogens. Some of the plant metabolites work as anti-oxidant and anti-cancer drugs because of their toxic effect toward cancer cells [6,26,52]. In this study we isolated GA and MG as major metabolites from the seed coats of *G. rottleriformis*. The total seed coat extract was fractionated and subjected to COX-1/COX-2/5-LOX assays and cytotoxic efficiency was conducted on A431 cells and HaCaT cells. The HPLC chromatogram data of MeOH seed coat extract revealed a group of peaks that were fractionated from one to seven by open silica column chromatography. Among all the fractions, only 5 and 6 fractions significantly inhibited COX-1 and COX-2 enzyme activity (Fig. 3a–d). However, these fractions did not show any significant inhibition on 5-LOX enzyme activity. Earlier studies have demonstrated that COXs and LOXs are the key enzymes that play an important role in inflammation and carcinogenesis [10,11,52]. Only 5 and 6 chromatographed fractions that inhibited the A431 cell proliferation was further subjected to active compound isolation by RP-HPLC. The active compounds of fractions 5 and 6 were purified by RP-HPLC (Fig. 4A and B) and were identified as GA and MG using IR, NMR and LC–MS analysis. GA and MG are natural constituents isolated from different plants [19,25,29]. Phenylpropanoid metabolism produce enormous array of secondary metabolites. The biosynthesis of GA and its derivative MG takes place via phenylpropanoid metabolism [21]. Our results suggest that MG (10 mg/g DW) and GA (6 mg/g DW) are the major compounds of the seed coats of this plant. We have also isolated several phenylpropanoid metabolites both known and unknown and studied their role in inducing plant immunity (Samuel et al., unpublished data). It was well demonstrated that some plant compounds such as curcumin, resveratrol and α-santalol suppressed cell proliferation and enhanced apoptosis in A431 cells [1,5,6].

Treatment of A431 cells with GA/MG suppressed cell survival by enhanced apoptosis in a dose and time dependent manner (Fig. 5Ai–iv and Bi–iv). The cytotoxic effect of GA and MG was investigated in various cancer cells [11,26,53–55]. The GA isolated from *Terminalia bellerica*

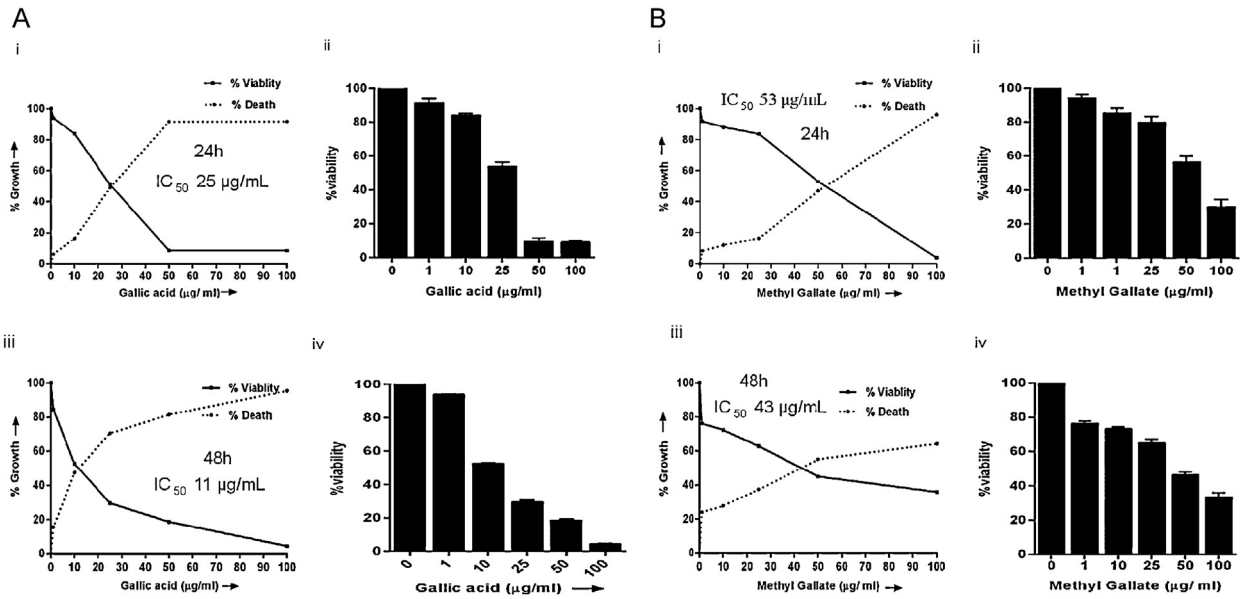

Fig. 5. Gallic acid (GA) and methyl gallate (MG) reduced the cell viability of A431 cells. Cells were seeded at a density of 1×10^6 cells/mL in 96 well polystyrene culture plates and maintained at 37 °C with 5% (v/v) CO_2 for 1 day. After 24 h the cells were incubated with GA/MG at the indicated concentrations for 24 h and 48 h and then processed for MTT assay. (Ai–iv) Percentage of cell death and viability of A431 cells treated with GA in a dose dependent manner at 24 h and 48 h. (Bi–iv) Percentage of cell death and viability of A431 cells after treatment with MG at 24 h and 48 h. The data presented as the mean ± SD of three independent experiments. The bars represent statistical significance over control ($P < 0.05$).

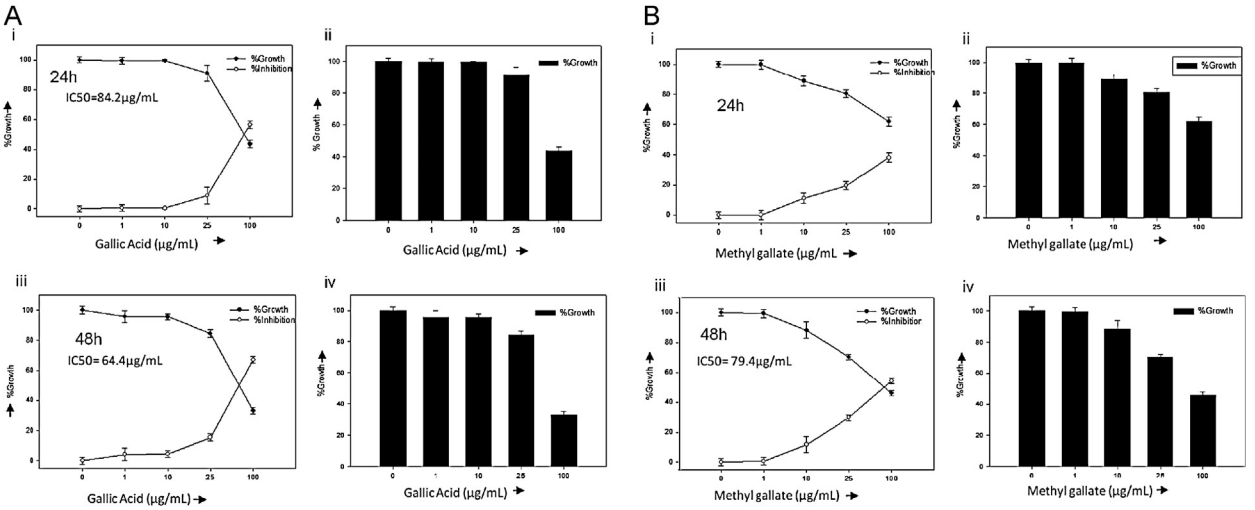

Fig. 6. Gallic acid (GA) and methyl gallate (MG) reduced the cell viability of HaCaT normal skin keratinocyte cell line. Cells were seeded at a density of 1×10^6 cells/mL in 96 well polystyrene culture plates at 37 °C with 5% (v/v) CO_2 for 1 day. After 24 h the cells were incubated with GA/MG at the indicated concentrations for 24 h and 48 h and then processed for MTT assay. (Ai–iv) Percentage of cell death and viability in HaCaT cells when treated with GA in a dose dependent manner at 24 h and 48 h. (Bi-iv) Percentage of cell death and viability in HaCaT cells when treated with MG in a dose dependent manner at 24 h and 48 h. The data presented as the mean ± SD of three independent experiments. Bars represent statistical significance over control ($P < 0.05$).

potentially inhibited COX-1 and COX-2 enzymes in a concentration dependent manner [10]. Similarly, MG also showed dual COX-2/5-LOX inhibitory activity; however, 5-LOX inhibition was based on the leukotriene C_4 [36]. Similar results were observed with our data with GA inhibiting both COX-1 and COX-2 enzymes in a dose dependent manner [10]. The inhibition of COX-2 enzyme by MG was similar as that mentioned by Kim et al. [36]. The COX-1 activity of fraction 5 and the purified MG were the same (IC_{50} value of 28 µg/mL). Here we report for the first time the COX-1 inhibition activity of MG. We have not observed any effect of GA on 5-LOX activity and our results were consistent with the findings from previous reports [10]. Whereas the 5-LOX activity of MG could not be observed even at increasing concentrations though it was earlier reported that MG exhibits 5-LOX inhibition activity [36].

The anti-oxidant and anti-proliferative effects of GA/MG were well studied [11,19,20,22,26,28,30,53]. In our results,

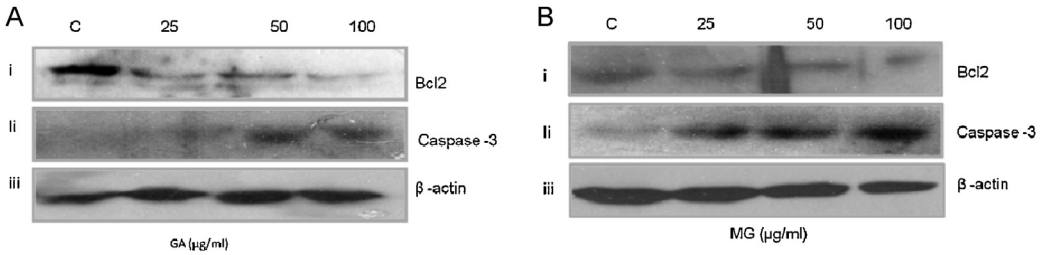

Fig. 7. Western blotting analysis showing Bcl-2 and cleaved caspase-3 protein up regulation in A431 cells that were treated with purified gallic acid (GA)/methyl gallate (MG). (Ai) A431 cells treated with GA down regulated Bcl-2 expression with respect to increasing doses. (Aii) Up regulation of the expression of cleaved caspase-3 in GA treated A431 cells. (Bi) Down regulation of the expression of Bcl-2 levels with increasing doses of MG treated A431 cells. (Bii) Up regulation of the expression of cleaved caspase-3 with increasing doses of MG treated A431 cells.

the treatment of A431 cells with purified GA suppressed the growth of A431 cells in a dose dependent manner with an IC_{50} value of 25 μg/mL and 11 μg/mL at 24 h and 48 h, respectively (Fig. 5Ai–iv). On the other hand, GA has shown much less cytotoxic effect on HaCaT normal skin keratinocyte cell line and showed IC_{50} value of 84.2 μg/mL and 62.4 μg/mL at 24 h and 48 h, respectively (Fig. 6Ai–iv). The anti-proliferative and apoptotic properties of phytochemicals were demonstrated in A431 cells [1,5,6]. However this is the first observation that reported the effect of GA on A431 cells. Similarly MG reduced the cell proliferation with an IC_{50} value of 53 μg/mL and 48 μg/mL at 24 h and 48 h respectively (Fig. 5Bi–iv). In the same way, normal skin HaCaT cells that were treated with MG showed less cytotoxicity with an IC_{50} value of 79.4 μg/mL than A431 cancer cells (Fig. 6Bi–iv). It was suggested by previous reports that MG inhibits cancer cells [25,53]. Our data showed that the treatment of A431 cells with GA and MG down regulated Bcl-2 (Fig. 7Ai and Bi). Bcl-2 promotes cell proliferation and reduced apoptosis in cancer cells [56–59]. Treatment of A431 cells with GA or MG also upregulated the protein levels of cleaved caspase-3 in a dose dependent manner (Fig. 7Aii and Bii). Caspase-3 was reported as an apoptotic marker protein, the expression of which enhances apoptosis, cleaves key cellular proteins and promotes cell death in cancer cells [56,60–62]. Apart from cancer, because of antioxidant property of GA, GA and its ester derivatives were widely used as additives in food industry [63]. In summary, this study demonstrates that the seeds coats of *G. rottleriformis* are a rich source of GA/MG and may play significant role in treatment of various cancers. These results demonstrate and encourage the need of further studies to establish the role of GA or MG as potential anti-inflammatory drugs to avoid the risk of various skin and other cancer problems.

Conflict of interest

The author has received grants from University Grants commission, Council of Scientific and Industrial Research, and Department of Science and Technology, during the conduct of the study.

Transparency document

The Transparency document associated with this article can be found in the online version.

Acknowledgements

The authors acknowledge the support of Prof. Pallu Reddanna, UOH for lab facilities. The study was supported by the fellowship received from University Grants Commission (UGC), New Delhi; Council of Scientific and Industrial Research (CSIR), New Delhi, India; Young Scientist grant from Department of Science and Technology under Science and Engineering Research Board (DST-SERB). The infrastructural facilities at School of Life Sciences, University of Hyderabad established with the support of UGC-SAP-CAS, DST-FIST and DBT-CREBB have been utilized in the present study.

Appendix A. Supplementary data

Supplementary data associated with this article can be found, in the online version, at doi:10.1016/j.toxrep.2015.03.001.

References

[1] M. Kaur, C. Agarwal, R.P. Singh, X. Guan, C. Dwivedi, R. Agarwal, Skin cancer chemopreventive agent, {alpha}-santalol, induces apoptotic death of human epidermoid carcinoma A431 cells via caspase activation together with dissipation of mitochondrial membrane potential and cytochrome c release, Carcinogenesis 26 (2005) 369–380.
[2] R.N. Saladi, A.N. Persaud, The causes of skin cancer: a comprehensive review, Drugs Today (Barc.) 41 (2005) 37–53.
[3] A. Gescher, U. Pastorino, S.M. Plummer, M.M. Manson, Suppression of tumour development by substances derived from the diet – mechanisms and clinical implications, Br. J. Clin. Pharmacol. 45 (1998) 1–12.
[4] M.M. Manson, Cancer prevention – the potential for diet to modulate molecular signalling, Trends Mol. Med. 9 (2003) 11–18.
[5] W.H. Chan, C.C. Wu, J.S. Yu, Curcumin inhibits UV irradiation-induced oxidative stress and apoptotic biochemical changes in human epidermoid carcinoma A431 cells, J. Cell. Biochem. 90 (2003) 327–338.
[6] N. Ahmad, V.M. Adhami, F. Afaq, D.K. Feyes, H. Mukhtar, Resveratrol causes WAF-1/p21-mediated G(1)-phase arrest of cell cycle and induction of apoptosis in human epidermoid carcinoma A431 cells, Clin. Cancer Res. 7 (2001) 1466–1473.
[7] K. Samuel, D. Debashish, B. Madhumita, G. Padmaja, Siva Ram Prasad, R.M.V. Bhaskara, P.S. Rao, In vitro germination and micropropagation of *Givotia rottleriformis* Griff., In Vitro Cell. Dev. Biol. Plant. 45 (2009) 466–473.
[8] Thammanna, K. Narayana Rao, Medicinal Plants of Tirumala, Tirumala Tirupati Devasthanam (TTD), Tirupati, Andhra Pradesh, 1990.
[9] H.M. Chen, Y.C. Wu, Y.C. Chia, F.R. Chang, H.K. Hsu, Y.C. Hsieh, C.C. Chen, S.S. Yuan, Gallic acid, a major component of *Toona sinensis* leaf extracts, contains a ROS-mediated anti-cancer activity in human prostate cancer cells, Cancer Lett. 286 (2009) 161–171.
[10] T.C. Reddy, P. Aparoy, N.K. Babu, K.A. Kumar, S.K. Kalangi, P. Reddanna, Kinetics and docking studies of a COX-2 inhibitor

isolated from *Terminalia bellerica* fruits, Protein Pept. Lett. 17 (2010) 1251–1257.
[11] T. Chandramohan Reddy, D. Bharat Reddy, A. Aparna, K.M. Arunasree, G. Gupta, C. Achari, G.V. Reddy, V. Lakshmipathi, A. Subramanyam, P. Reddanna, Anti-leukemic effects of gallic acid on human leukemia K562 cells: downregulation of COX-2, inhibition of BCR/ABL kinase and NF-kappaB inactivation, Toxicol. In Vitro 26 (2012) 396–405.
[12] A.J. Hou, L.Y. Peng, Y.Z. Liu, Z.W. Lin, H.D. Sun, Gallotannins and related polyphenols from *Pistacia weinmannifolia*, Planta Med. 66 (2000) 624–626.
[13] M. Inoue, R. Suzuki, N. Sakaguchi, Z. Li, T. Takeda, Y. Ogihara, B.Y. Jiang, Y. Chen, Selective induction of cell death in cancer cells by gallic acid, Biol. Pharm. Bull. 18 (1995) 1526–1530.
[14] M. Kaur, B. Velmurugan, S. Rajamanickam, R. Agarwal, C. Agarwal, Gallic acid, an active constituent of grape seed extract, exhibits anti-proliferative, pro-apoptotic and anti-tumorigenic effects against prostate carcinoma xenograft growth in nude mice, Pharm. Res. 26 (2009) 2133–2140.
[15] R. Veluri, R.P. Singh, Z. Liu, J.A. Thompson, R. Agarwal, C. Agarwal, Fractionation of grape seed extract and identification of gallic acid as one of the major active constituents causing growth inhibition and apoptotic death of DU145 human prostate carcinoma cells, Carcinogenesis 27 (2006) 1445–1453.
[16] R.D. Yeh, J.C. Chen, T.Y. Lai, J.S. Yang, C.S. Yu, J.H. Chiang, C.C. Lu, S.T. Yang, C.C. Yu, S.J. Chang, H.Y. Lin, J.G. Chung, Gallic acid induces G(0)/G(1) phase arrest and apoptosis in human leukemia HL-60 cells through inhibiting cyclin D and E, and activating mitochondria-dependent pathway, Anticancer Res. 31 (2011) 2821–2832.
[17] Y. Zuo, H. Chen, Y. Deng, Simultaneous determination of catechins, caffeine and gallic acids in green, Oolong, black and pu-erh teas using HPLC with a photodiode array detector, Talanta 57 (2002) 307–316.
[18] H.O. Saxena, U. Faridi, S. Srivastava, J.K. Kumar, M.P. Darokar, S. Luqman, C.S. Chanotiya, V. Krishna, A.S. Negi, S.P. Khanuja, Gallic acid-based indanone derivatives as anticancer agents, Bioorg. Med. Chem. Lett. 18 (2008) 3914–3918.
[19] M.M. Abou-Zaid, D.A. Lombardo, C. Nozzolillo, Methyl gallate is a natural constituent of maple (Genus Acer) leaves, Nat. Prod. Res. 23 (2009) 1373–1377.
[20] C.J. Kane, J.H. Menna, Y.C. Yeh, Methyl gallate, methyl-3,4,5-trihydroxybenzoate, is a potent and highly specific inhibitor of herpes simplex virus in vitro. I. Purification and characterization of methyl gallate from *Sapium sebiferum*, Biosci. Rep. 8 (1988) 85–94.
[21] T. Vogt, Phenylpropanoid biosynthesis, Mol. Plant 3 (2010) 2–20.
[22] R. Chaubal, V.H. Deshapande, N.R. Deshpande, Methyl gallate, the medicinally important compound: a review, J. Environ. Agric. Food Chem. 4 (2005) 956–962.
[23] S.L. Da Silva, J.daS. Chaar, T. Yano, Chemotherapeutic potential of two gallic acid derivative compounds from leaves of *Casearia sylvestris* Sw (Flacourtiaceae), Eur. J. Pharmacol. 608 (2009) 76–83.
[24] S.M. Fiuza, C. Gomes, L.J. Teixeira, M.T. Girao da Cruz, M.N. Cordeiro, N. Milhazes, F. Borges, M.P. Marques, Phenolic acid derivatives with potential anticancer properties – a structure-activity relationship study. Part 1: Methyl, propyl and octyl esters of caffeic and gallic acids, Bioorg. Med. Chem. 12 (2004) 3581–3589.
[25] T.J. Hsieh, T.Z. Liu, Y.C. Chia, C.L. Chern, F.J. Lu, M.C. Chuang, S.Y. Mau, S.H. Chen, Y.H. Syu, C.H. Chen, Protective effect of methyl gallate from *Toona sinensis* (Meliaceae) against hydrogen peroxide-induced oxidative stress and DNA damage in MDCK cells, Food Chem. Toxicol. 42 (2004) 843–850.
[26] H. Lee, Y. Kwon, J.H. Lee, J. Kim, M.K. Shin, S.H. Kim, H. Bae, Methyl gallate exhibits potent antitumor activities by inhibiting tumor infiltration of CD4+CD25+ regulatory T cells, J. Immunol. 185 (2010) 6698–6705.
[27] D. Lizarraga, S. Tourino, F.J. Reyes-Zurita, T.M. de Kok, J.H. van Delft, L.M. Maas, J.J. Briede, J.J. Centelles, J.L. Torres, M. Cascante, Witch hazel (*Hamamelis virginiana*) fractions and the importance of gallate moieties – electron transfer capacities in their antitumoral properties, J. Agric. Food Chem. 56 (2008) 11675–11682.
[28] J.G. Choi, O.H. Kang, Y.S. Lee, Y.C. Oh, H.S. Chae, H.J. Jang, J.H. Kim, D.H. Sohn, D.W. Shin, H. Park, D.Y. Kwon, In vitro activity of methyl gallate isolated from galla rhois alone and in combination with ciprofloxacin against clinical isolates of salmonella, J. Microbiol. Biotechnol. 18 (2008) 1848–1852.
[29] C.J. Kane, J.H. Menna, C.C. Sung, Y.C. Yeh, Methyl gallate, methyl-3,4,5-trihydoxybenzoate, is a potent and highly specific inhibitor of herpes simplex virus in vitro. II. Antiviral activity of methyl gallate and its derivatives, Biosci. Rep. 8 (1988) 95–102.
[30] M.S. Kang, J.S. Oh, I.C. Kang, S.J. Hong, C.H. Choi, Inhibitory effect of methyl gallate and gallic acid on oral bacteria, J. Microbiol. 46 (2008) 744–750.
[31] E.R. Greene, S. Huang, C.N. Serhan, D. Panigrahy, Regulation of inflammation in cancer by eicosanoids, Prostaglandins Other Lipid Mediat. 96 (2011) 27–36.
[32] G. Dannhardt, W. Kiefer, Cyclooxygenase inhibitors – current status and future prospects, Eur. J. Med. Chem. 36 (2001) 109–126.
[33] M.T. Rizzo, Cyclooxygenase-2 in oncogenesis, Clin. Chim. Acta 412 (2011) 671–687.
[34] X. Tang, Y.J. Sun, E. Half, M.T. Kuo, F. Sinicrope, Cyclooxygenase-2 overexpression inhibits death receptor 5 expression and confers resistance to tumor necrosis factor-related apoptosis-inducing ligand-induced apoptosis in human colon cancer cells, Cancer Res. 62 (2002) 4903–4908.
[35] S. Sarveswaran, V. Thamilselvan, C. Brodie, J. Ghosh, Inhibition of 5-lipoxygenase triggers apoptosis in prostate cancer cells via down-regulation of protein kinase C-epsilon, Biochim. Biophys. Acta 1813 (2011) 2108–2117.
[36] S.J. Kim, M. Jin, E. Lee, T.C. Moon, Z. Quan, J.H. Yang, K.H. Son, K.U. Kim, J.K. Son, H.W. Chang, Effects of methyl gallate on arachidonic acid metabolizing enzymes: cyclooxygenase-2 and 5-lipoxygenase in mouse bone marrow-derived mast cells, Arch. Pharm. Res. 29 (2006) 874–878.
[37] S. Cory, J.M. Adams, The Bcl2 family: regulators of the cellular life-or-death switch, Nat. Rev. Cancer 2 (2002) 647–656.
[38] Y. Fernandez, B. Gu, A. Martinez, A. Torregrosa, A. Sierra, Inhibition of apoptosis in human breast cancer cells: role in tumor progression to the metastatic state, Int. J. Cancer 101 (2002) 317–326.
[39] D.S. Huang, K.Z. Shen, J.F. Wei, T.B. Liang, S.S. Zheng, H.Y. Xie, Specific COX-2 inhibitor NS398 induces apoptosis in human liver cancer cell line HepG2 through BCL-2, World J. Gastroenterol. 11 (2005) 204–207.
[40] H. Joensuu, L. Pylkkanen, S. Toikkanen, Bcl-2 protein expression and long-term survival in breast cancer, Am. J. Pathol. 145 (1994) 1191–1198.
[41] M. Enari, R.V. Talanian, W.W. Wong, S. Nagata, Sequential activation of ICE-like and CPP32-like proteases during Fas-mediated apoptosis, Nature 380 (1996) 723–726.
[42] T. Fernandes-Alnemri, G. Litwack, E.S. Alnemri, CPP32, a novel human apoptotic protein with homology to *Caenorhabditis elegans* cell death protein Ced-3 and mammalian interleukin-1 beta-converting enzyme, J. Biol. Chem. 269 (1994) 30761–30764.
[43] D. Dai, Y. Liang, Z. Xie, J. Fu, Y. Zhang, Z. Zhang, Survivin deficiency induces apoptosis and cell cycle arrest in HepG2 hepatocellular carcinoma cells, Oncol. Rep. 27 (2012) 621–627.
[44] Y. Fan, A. Bergmann, The cleaved-caspase-3 antibody is a marker of caspase-9-like DRONC activity in *Drosophila*, Cell Death Differ. 17 (2010) 534–539.
[45] L.F. Wu, Y.Q. Ye, G.Y. Huang, H.B. Li, G.P. Li, Z.J. Pu, B.L. Wei, J.L. Feng, Involvement of endoplasmic reticulum stress in adenosine-induced human hepatoma HepG2 cell apoptosis, Oncol. Rep. 26 (2011) 73–79.
[46] M. Hemler, W.E. Lands, Purification of the cyclooxygenase that forms prostaglandins. Demonstration of two forms of iron in the holoenzyme, J. Biol. Chem. 251 (1976) 5575–5579.
[47] C.M. Reddy, V.B. Bhat, G. Kiranmai, M.N. Reddy, P. Reddanna, K.M. Madyastha, Selective inhibition of cyclooxygenase-2 by C-phycocyanin, a biliprotein from *Spirulina platensis*, Biochem. Biophys. Res. Commun. 277 (2000) 599–603.
[48] R.A. Copeland, J.M. Williams, J. Giannaras, S. Nurnberg, M. Covington, D. Pinto, S. Pick, J.M. Trzaskos, Mechanism of selective inhibition of the inducible isoform of prostaglandin G/H synthase, Proc. Natl. Acad. Sci. U. S. A. 91 (1994) 11202–11206.
[49] P. Reddanna, J. Whelan, K.R. Maddipati, C.C. Reddy, Purification of arachidonate 5-lipoxygenase from potato tubers, Methods Enzymol. 187 (1990) 268–277.
[50] J. Sambrook, E.F. Fritsch, T. Maniatis, Molecular Cloning: A Laboratory Manual, 1st ed., Cold Spring Harbor Laboratory Press, 1989.
[51] M.M. Bradford, A rapid and sensitive method for the quantitation of microgram quantities of protein utilizing the principle of protein-dye binding, Anal. Biochem. 72 (1976) 248–254.
[52] D.B. Reddy, T.C. Reddy, G. Jyotsna, S. Sharan, N. Priya, V. Lakshmipathi, P. Reddanna, Chebulagic acid, a COX-LOX dual inhibitor isolated from the fruits of Terminalia chebula Retz., induces apoptosis in COLO-205 cell line, J. Ethnopharmacol. 124 (2009) 506–512.
[53] J.A. Crispo, M. Piche, D.R. Ansell, J.K. Eibl, I.T. Tai, A. Kumar, G.M. Ross, T.C. Tai, Protective effects of methyl gallate on H_2O_2-induced apoptosis in PC12 cells, Biochem. Biophys. Res. Commun. 393 (2010) 773–778.

[54] J.D. Hsu, S.H. Kao, T.T. Ou, Y.J. Chen, Y.J. Li, C.J. Wang, Gallic acid induces G2/M phase arrest of breast cancer cell MCF-7 through stabilization of p27(Kip1) attributed to disruption of p27(Kip1)/Skp2 complex, J. Agric. Food Chem. 59 (2011) 1996–2003.
[55] S.H. Lee, J.K. Kim, D.W. Kim, H.S. Hwang, W.S. Eum, J. Park, K.H. Han, J.S. Oh, S.Y. Choi, Antitumor activity of methyl gallate by inhibition of focal adhesion formation and Akt phosphorylation in glioma cells, Biochim. Biophys. Acta 1830 (2013) 4017–4029.
[56] C. Chang, Y. Zhu, X. Tang, W. Tao, The anti-proliferative effects of norcantharidin on human HepG2 cells in cell culture, Mol. Biol. Rep. 38 (2011) 163–169.
[57] S.J. Korsmeyer, BCL-2 gene family and the regulation of programmed cell death, Cancer Res. 59 (1999) 1693–1700.
[58] T.J. McDonnell, P. Troncoso, S.M. Brisbay, C. Logothetis, L.W. Chung, J.T. Hsieh, S.M. Tu, M.L. Campbell, Expression of the protooncogene bcl-2 in the prostate and its association with emergence of androgen-independent prostate cancer, Cancer Res. 52 (1992) 6940–6944.
[59] A.J. Raffo, H. Perlman, M.W. Chen, M.L. Day, J.S. Streitman, R. Buttyan, Overexpression of bcl-2 protects prostate cancer cells from apoptosis in vitro and confers resistance to androgen depletion in vivo, Cancer Res. 55 (1995) 4438–4445.
[60] E. Devarajan, A.A. Sahin, J.S. Chen, R.R. Krishnamurthy, N. Aggarwal, A.M. Brun, A. Sapino, F. Zhang, D. Sharma, X.H. Yang, A.D. Tora, K. Mehta, Down-regulation of caspase 3 in breast cancer: a possible mechanism for chemoresistance, Oncogene 21 (2002) 8843–8851.
[61] A.G. Porter, R.U. Janicke, Emerging roles of caspase-3 in apoptosis, Cell Death Differ. 6 (1999) 99–104.
[62] R.N. Winter, A. Kramer, A. Borkowski, N. Kyprianou, Loss of caspase-1 and caspase-3 protein expression in human prostate cancer, Cancer Res. 61 (2001) 1227–1232.
[63] A. Serrano, C. Palacios, G. Roy, C. Cespon, M.L. Villar, M. Nocito, P. Gonzalez-Porque, Derivatives of gallic acid induce apoptosis in tumoral cell lines and inhibit lymphocyte proliferation, Arch. Biochem. Biophys. 350 (1998) 49–54.

Evaluation of Cissus quadrangularis extracts as an inhibitor of COX, 5-LOX, and proinflammatory mediators

Article *in* Journal of ethnopharmacology · March 2012

DOI: 10.1016/j.jep.2012.03.044 · Source: PubMed

Journal of Ethnopharmacology xxx (2012) xxx–xxx

Contents lists available at SciVerse ScienceDirect

Journal of Ethnopharmacology

journal homepage: www.elsevier.com/locate/jethpharm

Evaluation of *Cissus quadrangularis* extracts as an inhibitor of COX, 5-LOX, and proinflammatory mediators

Arti M. Bhujade[a], Suhas Talmale[a], Naresh Kumar[b], Geetika Gupta[b], P. Reddanna[b], Samar K. Das[c], M.B. Patil[a,*]

[a] University Department of Biochemistry, L.I.T. Premises, R.T.M. Nagpur University, Nagpur 440 033, Maharashtra, India
[b] School of Life Science, Department of Animal Science, University of Hyderabad, Hyderabad 500046, India
[c] School of Chemistry, University of Hyderabad, Hyderabad 500046, India

ARTICLE INFO

Article history:
Received 1 November 2011
Received in revised form 6 March 2012
Accepted 21 March 2012
Available online xxx

Keywords:
Cissus quadrangularis
Cycloxygenase
Inflammation
COX-1
COX-2
5-LOX
COX–LOX inhibition
AA
Proinflammatory mediator
Nrf-2
HO-1

ABSTRACT

Ethnopharmacological relevance: Cissus quadrangularis is an ancient medicinal plant. It is an active ingredient of one Ayurvedic formula called "Laksha Gogglu". Its stem is used in food preparation in India. Traditionally it is used to treat various diseases like asthma, indigestion, ear diseases, irregular menstruation, skin diseases, piles, fractured bones, etc.
Aim of the study: This study aimed to evaluate the ability of the plant extracts to inhibit cycloxygenase (COX-1), cycloxygenase (COX-2), and 5-lipoxygenase (5-LOX) enzyme activity. Western blot analysis was also carried out in the quest to determine the effect of active acetone fraction of *Cissus quadrangularis* (AFCQ) on proinflammatory mediators as acetone extract is found to be the most effective in this study.
Materials and methods: The differential extract of the stem were tested for enzyme inhibition of COX and 5-LOX using spectroscopic and polarigraphic method. Effective acetone extract was partially purified by silica column, one of the active fraction showed dual inhibition against COX and 5-LOX. Western blotting shows downregulation of proinflammatory mediators as well as upregulation of phase-II enzymes.
Results: AFCQ extract showed COX and 5-LOX inhibition with IC_{50} values of 7 μg/ml, 0.4 μg/ml, and 20 μg/ml for COX-1, COX-2 and 5-LOX respectively. It also showed anti-inflammatory activity on RAW 264.7 cell line with IC_{50} value 65 μg/ml. In addition to this it is showing inhibition of proinflammatory mediators like iNOS and TNFα, along with translocation of Nrf-2 and upregulation of HO-1.
Conclusion: AFCQ is a COX and 5-LOX inhibitor isolated from the stems of *Cissus quadrangularis*. It is also effectively downregulate the iNOS, TNFα, and upregulation of HO-1.

1. Introduction

Cissus quadrangularis is an ancient medicinal plant that has been used in many traditional medicines. Traditionally it is used to treat diverse diseases like rheumatic diseases, allergies, skin diseases, piles, fracture, and bone diseases (Udupa et al., 1965; Deka et al., 1994). It is an active ingredient of Ayurvedic formula called "Laksha Gogglu" which is used for alleviating pain, reducing inflammation and promoting the healing of wounds or simple fracture (Kulkarni, 2001). Stem of *Cissus quadrangularis* is very important part of the plant and used as raw drug in Indian folk medicine (Panda, 1990). Leaves of *Cissus quadrangularis* is used to treat anorexia whereas dried powder of stem with honey is taken orally to reduce pain and inflammation. The stem and leaf of the *Cissus quadrangularis* are used in food preparation in India. Numerous studies demonstrated that methanolic and petroleum ether extract of the whole plant are used in treating osteoporosis and fracture (Deka et al., 1994; Shirwaikar et al., 2003; Sharpa et al., 2007). It possesses antioxidant (Jainu and Shyamaladevi, 2005), anti-inflammatory, antibacterial (Kashikar and George, 2006; Thakur et al., 2009), antiviral (Balasubramaniana et al., 2010), and antiulcerogenic (Jainu and Shyamaladevi, 2004, 2006; Jainu et al., 2010) properties. It has also solved the problems of weight loss and various metabolic syndromes (Oben et al., 2006, 2007). Phytochemical studies of *Cissus quadrangularis* have shown the presence of several phytochemical constituents, such as ascorbic acid, flavonoids, and triterpenoids (Potu et al., 2010).

Inflammatory and pathogenic condition activates the enzymes cycloxygenase (COX) and 5-lipoxygenase (5-LOX). COX and 5-LOX are the key enzymes in the synthesis of prostanoid and eicosonoids from poly unsaturated fatty acids (PUFAs), which are involved in various inflammatory and allergic disorders (Martel-Pelletier et al., 2003; Daniel et al., 2004). Nuclear factor E2 p45-related factor 2 (Nrf-2) is a member of leucine zipper transcription family

* Corresponding author. Tel.: +91 9542323509/+9860018333.
E-mail addresses: rtbiochem@hotmail.com, artibhujade@gmail.com (M.B. Patil).

0378-8741/$ – see front matter © 2012 Elsevier Ireland Ltd. All rights reserved.
http://dx.doi.org/10.1016/j.jep.2012.03.044

responsible for upregulation of genes of phase-II enzymes in response to oxidative stress and LPS treatment (Annukka et al., 2008). Heme oxygenase-1 (HO-1) is the phase-II enzyme catalyzes the degradation reaction of heme to convert biliverdin further to bilirubin. Deficiency of HO-1 isozyme reveals severe damage of iron metabolism, which leads to liver, and kidney oxidative damage and inflammation. Consequently HO-1 expression increases cell resistance to oxidative injury (Daniel et al., 2004). Inducible nitric oxide synthase (iNOS) and tumour necrosis factor alpha (TNFα) are the proinflammatory mediators. The concentration of iNOS is elevated in injury and inflammation, while TNFα is mainly formed through monocytes and activated macrophages. It is pleotropic proinflammatory cytokine with many actions like fever, macrophage activation, etc., that are central to the pathogenesis.

In the present study, we have examined the in vitro anti-inflammatory activity of different extracts of *Cissus quadrangularis* on COX, 5-LOX and proinflammatory mediators. Inhibition of COX-1 and COX-2 were evaluated by using chromogenic assay and inhibition of 5-LOX was evaluated by using polarigraphic method. Whole plant of *Cissus quadrangularis* was extracted with different organic solvents and the acetone extract gave the potential inhibition of COX and 5-LOX. Consequently number of partially purified fraction of acetone extract we have screened to examine the inhibition of COX and 5-LOX. Single active acetone fraction of *Cissus quadrangularis* have shown potent inhibition hence called AFCQ. AFCQ was further used to evaluate the eventual mechanism essentially its anti-inflammatory effect in LPS induced inflammation. We found that AFCQ have potentially inhibited COX-2, iNOS, and TNFα expression in LPS treated murine macrophages RAW 264.7 cells. Upregulation of HO-1 expression connected with activation and expression of Nrf-2 might be related in the anti-inflammatory activity of AFCQ.

2. Materials and methods

2.1. Plant material

Plant material was collected from Vidarbh region of Maharashtra in March 2008. The plants were authenticated at the Department of Botany, Rashtrasant Tukdoji Maharaj Nagpur University, Nagpur and voucher specimens were deposited in the herbarium. Botanical name is *Cissus quadrangularis* and voucher specimen number is 9433.

2.2. Preparation of extracts of Cissus quadrangularis

The stem of *Cissus quadrangularis* was shade dried for five to six months, powdered, and extracted successively using soxhlet apparatus with hexane, chloroform, acetone, ethyl acetate, methanol, ethanol, and water in the increasing polarity index. 250 g of dried plant powder was taken for the extraction. All extracts were concentrated to dryness using rotary evaporator. We obtained hexane extract 7.27 g, chloroform extract 5.10 g, acetone extract 2.17 g, ethyl acetate 1.7 g, methanol extract 3.53 g, ethanol extract 1.2 g, and water extract 1 g. The concentrated dry extracts were again dissolved in dimethyl sulphoxide (DMSO), mixed and vortexed for few min and then centrifuged 2000 × *g* for 10 min. Supernatant was subsequently used to check the inhibition of COX-1, COX-2, and 5-LOX.

2.3. Partial purification of acetone extract by column chromatography

Acetone extract partially purified by column chromatography. Active acetone extract passed through open silica column. We obtained around thirteen different fractions, this fractions were dried using rotary vaccum evaporator. Dried fractions again used to verify the inhibition of COX-1, COX-2, and 5-LOX. Out of thirteen fraction ninth fraction shows potent inhibition of COX and 5-LOX, hence called active fraction of *Cissus quadrangularis* (AFCQ) and used in further studies.

2.4. Reagents and chemicals

Phosphate buffered saline (PBS), RPMI 1640; fetal bovine serum (FBS), penicillin and streptomycin were purchased from Gibco BRL. TMPD (N,N,N,N-tetramethyl-*p*-phenylenediamine), Hematin, Trypsin, MTT (3-(4,5-dimethylthiazol-2-yl)-diphenyl tetrazolium bromide), β-actin antibody and lipopolysaccharide or LPS (*Escherichia coli* serotype), nitro blue tetrazolium (NBT) and 5-bromo-4-chloro-3-indolyl phosphate (BCIP) were purchased from Sigma–Aldrich chemical company (St. Louis, USA). Antibodies for COX-2, HO-1, TNFα, Nrf-2, iNOS and alkaline phosphatase conjugated anti-mouse, anti-goat and anti-rabbit antibodies were purchased from Santa Cruz Biotechnology (Santa Cruz, CA, USA). All other chemicals and solvents for chromatography were of HPLC grade. All other chemicals and solvents were of analytical grade purchased from authorized standard companies.

2.5. Extraction and isolation of cyclooxygenase-1 enzyme. (from Ram seminal vesicles)

Ram seminal vesicles were collected from local slaughter house and stored at −80 °C. Before starting the experiment, the ram seminal vesicles were taken out from −80 °C and kept at 4 °C overnight in refrigerator. All the process of Extraction and isolation were carried out below 7 °C.

2.5.1. Preparation of microsomes as a source of cycloxygenase-1

Preparation of microsome was carried out, according to the method of Hemler et al. (1976), with some modifications. Ram seminal vesicles were ground in a grinder. The ground material was homogenized with a waring blender in buffer containing 0.05 M Tris–HCl (pH 8), 5 mM EDTA disodium salt, 5 mM diethyl dithiocarbamate and 0.01% sodium azide. The homogenate was centrifuged at 13,000 × *g* for 15 min, 4 °C. The supernatant was filtered through cheesecloth. The filtered supernatant was again centrifuged at 42,000 rpm for 1 h 10 min, 4 °C by using ultracentrifuge (Himac, CP-100α HITACHI) to obtained microsomal pellet. This microsomal pellet was rehomogenized with a motor-driven Potter-Elvehjem homogenizer, connected to a teflon pestle in a buffer containing 0.05 M Tris–HCl (pH 8), 0.1 mM EDTA disodium salt, 0.1 mM diethyl dithiocarbamate and 0.01% sodium azide. This microsome fraction was stored as small aliquots at −80 °C, and used for further studies as enzyme source.

2.6. Extraction and isolation of cycloxygenase-2 enzyme (from Sf9 insect cell line)

2.6.1. Preparation of microsomes as a source of cyclooxygenase-2

Preparation of microsome was carried out according to the method of Reddy et al. (2000), with some modifications. Human recombinant COX-2 expressed in *Spodoptera frugiperda*. *Spodoptera frugiperda* (Sf9) cells were maintained at 28 °C in Grace's insect culture medium. Inscet Cells at 60% confluency were infected with recombinant baculovirus containing human COX-2. After 72 h of infection, the cells were collected by centrifugation at 2000 × *g* for 5 min at 4 °C. The pellet was suspended in minimum volume of Tris–HCl buffer (50 mM, pH 7.2) containing 5 mM EDTA, 300 mM sucrose, 5 mM diethyl thiocarbamate, 1 μg/ml pepstatin, 1 mM phenol and sonicated for 3 min. The cell lysate was centrifuged at 100,000 × *g* for 1 h 10 min at 4 °C by using ultracentrifuge (Himac,

Please cite this article in press as: Bhujade, A.M., et al., Evaluation of *Cissus quadrangularis* extracts as an inhibitor of COX, 5-LOX, and proinflammatory mediators. J. Ethnopharmacol. (2012), http://dx.doi.org/10.1016/j.jep.2012.03.044

CP-100α HITACHI), and the microsomal pellet obtained was suspended in Tris–HCl buffer (2.5 mM, pH 7.2) containing 0.5% glycerol, 0.8% Tween 20 and 1 mM phenol. This solubilized microsomal fraction was stored as small aliquots at −80 °C and used as enzyme source for further studies.

2.6.2. Cycloxygenase (COX-1 and COX-2) assay

Enzymatic activities of COX-1 and COX-2 were measured according to the method of Copeland et al. (1994), with slight modifications using a chromogenic assay based on the oxidation of N,N,N,N-tetramethyl-*p*-phenylene diamine (TMPD), during the reduction of PGG2 to PGH2 (Egan et al., 1976; Pagels et al., 1983). The assay mixture contained Tris–HCl buffer (0.5 M), hematin (5 mM), EDTA (0.5 M), enzyme (COX-1 or COX-2) and the test compound. The mixture was pre-incubated at 25 °C for 5 min and then the reaction was initiated by the addition of substrate AA and TMPD, in total volume of 1 ml reaction mixture. The enzyme activity was determined by estimating the rate of TMPD oxidation for the first 60 s of the reaction by following the increase in absorbance at 603 nm. A low rate of non-enzymatic oxidation, observed in the absence of COX-1 and COX-2, was subtracted from the experimental value while calculating the percent inhibition.

2.7. Purification and assay of 5-lipoxygenase (5-LOX)

Purification of 5-LOX from potato tubers was carried out and assayed according to the method of Reddanna et al. (1990). Enzyme activity was measured using polarigraphic method with a Clark's oxygen electrode on Strathkelvin Instruments (model 782, RC-300). Typical reaction mixture contained 50–100 μl of enzyme and 10 μl of substrate (Arachidonic acid, 40 mM) and final volume made to 3 ml with 100 mM potassium phosphate buffer of pH 6.3. Since LOX is an oxygen-consuming enzyme, the rate of decrease in oxygen was taken as a measure of enzyme activity. Reaction was allowed to proceed at 25 °C and the maximum slope generated was taken for calculating enzyme activity. The enzyme activity was expressed as moles of oxygen consumed min/mg protein.

2.8. Cell culture and treatment

RAW 264.7 cell line was maintained in monolayer in tissue culture petri dishes in RPMI-1640 medium supplemented with 10% heat inactivated fetal bovine serum (FBS), 100 IU/ml penicillin, 100 μg/ml streptomycin and 2 mM L-glutamine. The cultured cells were passaged twice a week. Cell cultures were maintained in a humidified atmosphere with 5% CO_2 at 37 °C. Before the treatment with test compound, cells were washed with PBS and fresh complete medium was added. The cells were incubated in the presence and absence of different concentration (50 μg/ml, 1 μg/ml, 10 ng/ml) of AFCQ, and stimulated with lipopolysaccharide (1 μg/ml) for 24 h. At the end of the treatment cells were washed with PBS and harvested to prepared cytoplasmic and nuclear extract for protein expression.

2.8.1. Cell proliferation assay of RAW 264.7 cell line

Cell proliferation was assessed by MTT (3-(4,5-dimethylthiazol-2-yl)-diphenyl tetrazolium bromide) assay as described by Mosmann (1983). The RAW 264.7 cell line used in this study were maintained in tissue culture petri dishes in complete RPMI-1640 medium. The cell line was maintained in a humidified atmosphere with 5% CO_2 at 37 °C. The cultured cells were passaged twice a week, seeding at a density of 5×10^4 cells per well in 96-well plates before the day of experiment. Before the treatment with test compound cells were washed with PBS and fresh complete RPMI-1640 medium was added, in the presence or absence of different concentration (100 μg/ml, 10 μg/ml, 1 μg/ml, 0.1 ng/ml) of AFCQ and were incubated for different time points (3, 6, 12, 24, and 48 h) in a final volume of 100 μl. At the end of the treatment, 20 μl of MTT (5 mg/ml) was added to each well and incubated for 4 h at 37 °C. The purple blue formazan precipitate was dissolved in 100 μl of DMSO and the optical density was measured at 570 nm on Synergy Mx, Bio-tek Instruments, Inc. micro titer plate reader. Each concentration was tested in three different experiments run in four replicates.

2.9. Preparation of cell extract and Western blot analysis

Cell pellets were lysed in lysis buffer (150 mM NaCl, 10 mM Tris–HCl, 1% Tween 20, 1 mM EDTA, 1 mM PMSF). Lysates were sonicated for 5 sec and centrifuged at 10,000 × *g* for 5 min. Protein concentrations were estimated by Bradford method, using BSA as a standard. Cell extracts were boiled in Laemmli sample buffer, resolved by SDS-PAGE on 12% polyacrylamide gels, and electroblotted onto nitrocellulose membrane. Membrane was stained with 0.5% ponceau in 1% acetic acid to confirm transfer of protein on membrane. Non-specific binding sites were blocked by incubating the membrane in 5% dried milk (fat free) in TBST solution, overnight at 4 °C. Blots were incubated with primary antibodies of COX-2 (1:1000 dilution), iNOS (1:500 dilution), TNFα (1:500 dilution), Nrf-2 (1:1000 dilution), HO-1 (1:1000 dilution) and β-actin (1:1000 dilution) dissolved in 5% bovine serum albumin solution prepared in TBST for overnight at 4 °C. Subsequently, blots were probed with a secondary antibodies of anti-goat, anti-mouse and anti-rabbit conjugated with alkaline phosphatase and incubated for 1 h at room temperature. After washing, protein expression was detected using Western blot detection reagent, nitro blue tetrazolium (NBT) and 5-bromo-4-chloro-3-indolyl phosphate (BCIP). NBT serve as oxidant and BCIP is the alkaline phosphatase substrate which gives dark blue dye.

2.9.1. Nuclear protein extraction

RAW 264.7 macrophages (3×10^6 cells/plate) were plated in 100-mm plates. Then, cells were treated with 1 μg/ml of LPS in the presence or absence of different concentration (50 μg/ml, 1 μg/ml, 10 ng/ml) of AFCQ for 24 h. Treated cells were scraped in cold PBS on ice, and centrifuged at 1000 rpm for 2 min at 4 °C. Each cell pellet was resuspended in 100 μl of cold lysis buffer (20 mM Tris–HCl, pH 7.5, 10 mM Magnessium acetate, 1% nonidet P-40, 1 mM PMSF). Cell suspensions were incubated on ice for 10 min and mixed by vortex stirring every 5 min. After incubation, Cell suspensions were centrifuged at 13,000 rpm for 15 min at 4 °C. Supernatant (Cytoplasmic extract) removed and nuclear pellet was resuspended in 100 μl of nuclear protein extraction buffer (420 mM NaCl, 10 mM HEPES, 10 mM $MgCl_2$, 1 mM EDTA, 0.1 mM DTT and 25% glycerol) incubated for 30 min on ice with intermittent vortexing of 10 sec each every 5 min. Followed, cell suspensions were centrifuged at 13,000 rpm for 30 min at 4 °C and supernatant were collected in new microcentrifuge tube as nuclear protein extracts. Protein concentrations were estimated by Bradford method, using BSA as a standard. Level and tranlocation of Nrf-2, HO-1 and β-actin in nuclear protein extract were determined by Western blotting analysis as described above.

2.10. Statistical analysis of data

All the data analysis was completed using the Sigma Plot 10 software. Numerical data, obtained from all the experiments, were presented as mean ± S.D. of three independent experiments, *P*-values were determined using the unpaired Student's *t*-test. *P*-value of less than 0.05 was considered as significant.

Please cite this article in press as: Bhujade, A.M., et al., Evaluation of *Cissus quadrangularis* extracts as an inhibitor of COX, 5-LOX, and proinflammatory mediators. J. Ethnopharmacol. (2012), http://dx.doi.org/10.1016/j.jep.2012.03.044

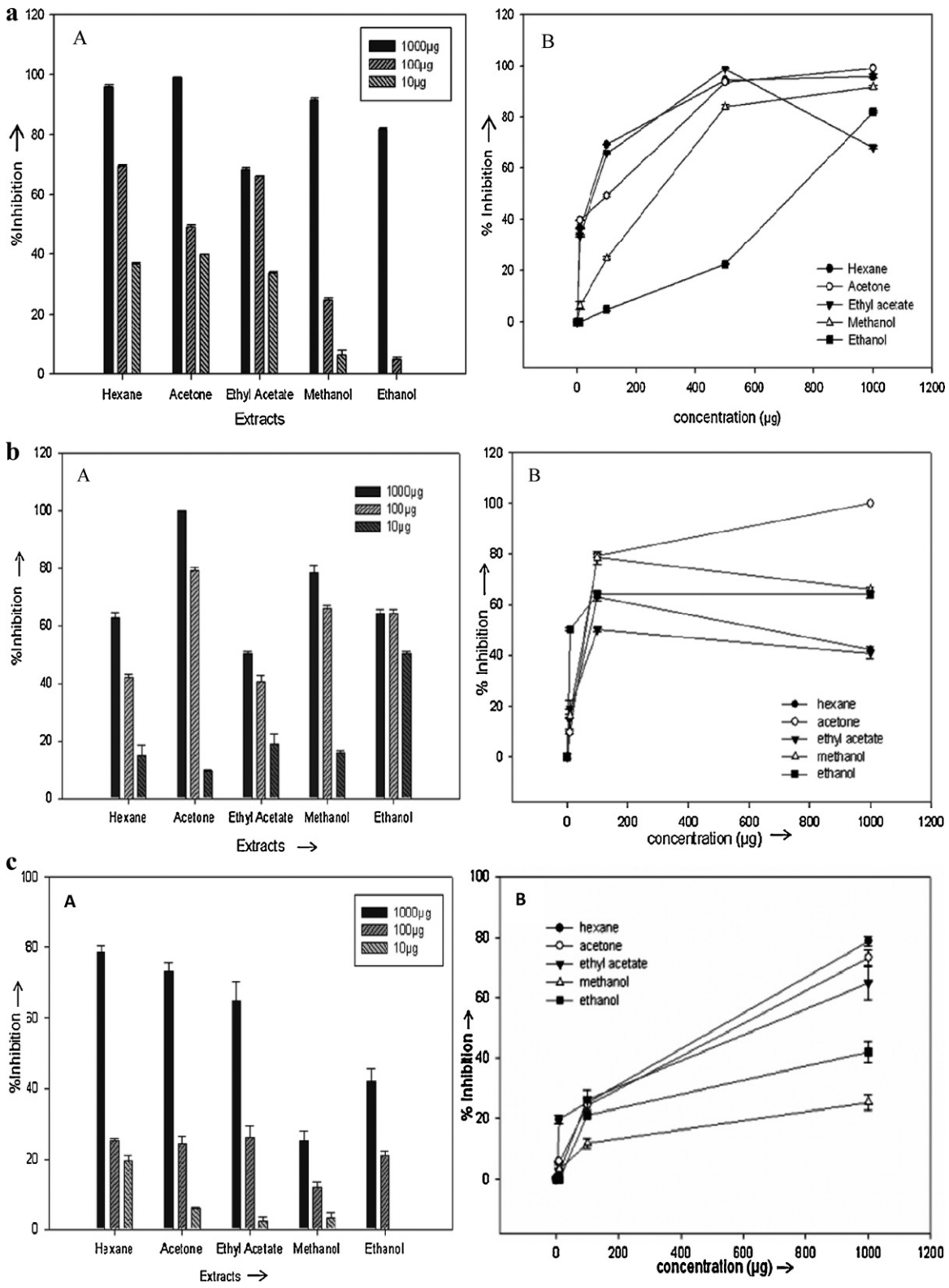

Fig. 1. (a) Effect of *Cissus quadrangularis* extracts on the enzyme activity of cycloxygenase-1. The inhibition properties of extracts were checked through spectroscopic method. The enzyme was incubated with different concentration (as shown in graph) of extracts for 5 min at 25 °C and the enzyme activity was observed by the oxidation of TMPD in presence of AA. Dose dependent inhibition of enzyme activity of COX-1 by hexane, acetone, ethyl acetate, methanol, and ethanol extracts were observed. Data are mean ± S.D. of three independent experiments. (b) Effect of *Cissus quadrangularis* extracts on the enzyme activity of cycloxygenase-2. The inhibition properties of extracts were checked through spectroscopic method. The enzyme was incubated with different concentration (as shown in graph) of extracts for 5 min at 25 °C and the enzyme activity was examined by the oxidation of TMPD in presence of AA. Dose dependent inhibition of enzyme activity of COX-2 by hexane, acetone, ethyl acetate, methanol, and ethanol extracts were observed. Data are mean ± S.D. of three independent experiments. (c) Effect of *Cissus quadrangularis* extracts on the enzyme activity of 5-lipoxygenase. The inhibition properties of extracts were checked through polarigraphic method with a Clark's oxygen electrode. The enzyme was incubated with different concentration (as shown in graph) of extracts for 5 min at 25 °C and the enzyme activity was examined by the rate of decrease in oxygen in presence of AA. Dose dependent inhibition of enzyme activity of 5-LOX by hexane, acetone, ethyl acetate, methanol, and ethanol extracts were observed. Data are mean ± S.D. of three independent experiments.

Please cite this article in press as: Bhujade, A.M., et al., Evaluation of *Cissus quadrangularis* extracts as an inhibitor of COX, 5-LOX, and proinflammatory mediators. J. Ethnopharmacol. (2012), http://dx.doi.org/10.1016/j.jep.2012.03.044

Table 1
IC_{50} values (μg/ml) of all extracts of *Cissus quadrangularis*, hexane, acetone ethyl acetate, methanol, and ethanol showed inhibition on activity of cycloxygenase-1, cycloxygenase-2, and 5-lipoxygenase enzymes were isolated from ram seminal vesicles, Sf9 cell line and potato tubers. The enzyme activity inhibition was estimated by decrease in the oxygen concentration in presence of extracts.

Plant extract (crude)	IC_{50} values (μg/ml)				
	Hexane	Acetone	Ethyl acetate	Methanol	Ethanol
COX-1	47.976	106.46	55.98	271.54	71.35
COX-2	441	25.9	100	59.29	65.81
5-LOX	367.86	550	654.9	–	–

3. Results

3.1. Effect of different extracts on cycloxygenase enzyme activity.

Preliminary studies with the plant extracts of *Cissus quadrangularis* exhibited inhibitory activity against both cycloxygenase (COX-1 and COX-2) enzymes. The IC_{50} values of all extracts are obtained on the inhibitory effect on COX-1 and COX-2 enzymes were given in Table 1. Hexane, acetone, ethyl acetate, methanol, and ethanol extracts of *Cissus quadrangularis* showed satisfactorily inhibition of enzyme COX-1 and COX-2 in dose dependent manner (1000 μg/ml, 100 μg/ml, 10 μg/ml) in (Fig. 1a and b), while chloroform and water extracts showed negligible inhibition against COX-1 and COX-2. Whereas the acetone extract showed potent inhibition of COX-1 and COX-2 with IC_{50} values of 106.46 μg/ml and 25.9 μg/ml, respectively, with 4-fold preference towards COX-2.

3.2. Inhibition of lipoxygenase enzyme activity

Inhibition of 5-LOX enzyme activity by the plant extracts was recorded as percentage inhibition, in terms of reducing enzyme activity. The enzyme activity inhibition was estimated by decrease in the oxygen concentration in presence of extracts. IC_{50} values of all extracts are given in Table 1. Bar graph (Fig. 1c) showing the comparison between hexane, acetone, ethyl acetate, methanol and ethanol extracts. From Fig. 1c we portrayed that the Acetone extract showed potent inhibition of 5-LOX enzyme with an IC_{50} value 550 μg/ml.

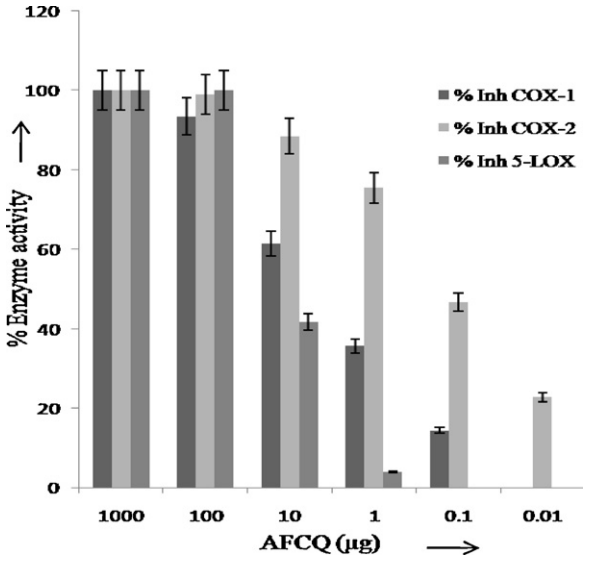

Fig. 2. Enzymatic inhibition activity of AFCQ on COX-1, COX-2 and 5-LOX. AFCQ more specifically inhibited COX-2 than COX-1 with 18-fold preference. The IC_{50} values for COX-1, COX-2 and 5-LOX were 7 μg/ml, 0.4 μg/ml, and 20 μg/ml, respectively. Data are mean ± SD of three independent experiments.

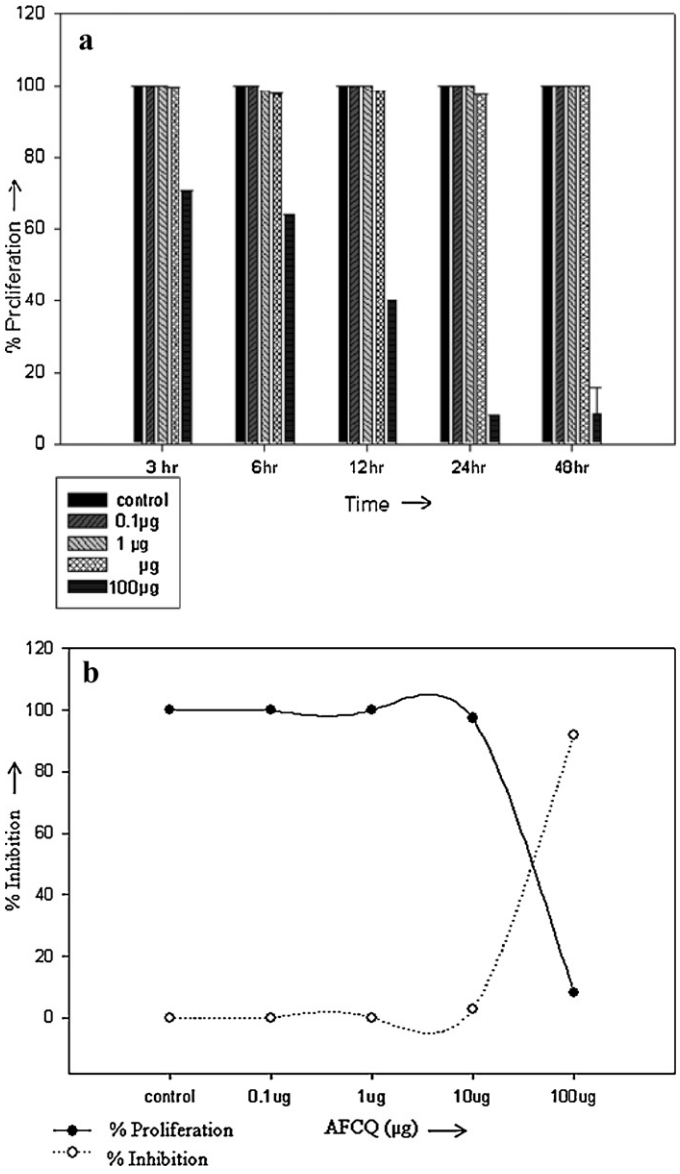

Fig. 3. (a) Effect of AFCQ on the proliferation of RAW 264.7 cell line. The cells were incubated with different concentrations (as shown in graph) of AFCQ for different time points (3, 6, 12, 24, and 48 h) and the cell viability was examined by MTT assay. Dose dependent inhibition was observed. Data are mean ± SD of three independent experiments. (b) IC_{50} value of AFCQ on RAW 264.7 cell line at 24 h was obtained 65 μg/ml. The cells were incubated with different concentrations (100 μg/ml, 10 μg/ml, 1 μg/ml, and 0.1 ng/ml) of AFCQ for 24 h and the cell viability was checked by MTT assay. Data are mean ± SD of three independent experiments.

3.2.1. Column chromatography, phytochemical study and inhibitory effect of AFCQ on COX and 5-LOX activity

The acetone extract of *Cissus quadrangularis* was fractionated through open silica column chromatography. We obtained around 13 fractions, all fractions were dried and concentrated by using rotary vacuum evaporator and checked for inhibitory action on COX and 5-LOX. Twelth fraction showed inhibition on COX-1 and COX-2 activity only. Ninth fraction showed dose dependent inhibition of COX-1, COX-2, and 5-LOX (Fig. 2) with IC_{50} values of 7 μg/ml, 0.4 μg/ml, and 20 μg/ml. The phytochemical studies of the AFCQ have showed the presence of tannin compounds. Partially purified AFCQ was used in all the experiments.

3.3. In vitro anti-inflammatory studies

RAW 264.7 cell lines was used in the present study for the evaluation of anti-inflammatory effect of AFCQ. RAW 264.7 cell line was incubated with different concentration of AFCQ (100 μg/ml, 10 μg/ml, 1 μg/ml, and 0.1 μg/ml) for different time points 3, 6, 12, 24, and 48 h. Cell viability was evaluated by MTT assay (Fig. 3a). AFCQ showed wide anti-inflammatory properties in dose dependent manner. The IC_{50} values of AFCQ for RAW 264.7 cell line was 65 μg/ml (Fig. 3b).

3.4. Effects of AFCQ on expression of iNOS, COX-2, TNFα

The potential anti-inflammatory effect of AFCQ were investigated by using murine macrophage cells, RAW 264.7, which can produce iNOS, COX-2, and TNFα upon stimulation with LPS. Cells were preincubated with AFCQ (50 μg/ml, 1 μg/ml, and 10 ng/ml,) for 3 h, and stimulated with or without LPS (1 μg/ml) for 24 h. iNOS, COX-2, and TNFα provide as key mediators of inflammation and thus the agents that suppress their expression have remedial importance for inflammatory diseases. iNOS, COX-2, and TNFα protein levels were markedly up-regulated in response to LPS treatment (Fig. 4), and AFCQ inhibited the expression of these proteins in a dose dependent manner. This study demonstrated the anti-inflammatory activity of AFCQ through down regulation of iNOS, COX-2, and TNFα.

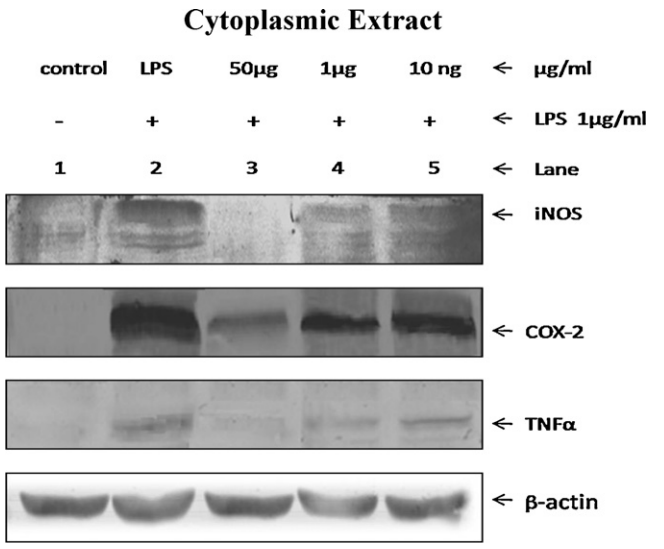

Fig. 4. AFCQ shows anti-inflammatory activity against LPS stimulated RAW 264.7 cells. Cells were preincubated with AFCQ (50 μg/ml, 1 μg/ml and 10 ng/ml,) for 3 h, and stimulated with or without LPS (1 μg/ml) for additional 24 h. iNOS, COX-2 and TNFα protein expression levels were monitored by Western blot analysis, β-actin was used as loading control.

3.5. Effects of AFCQ on expression of HO-1 and Nrf-2

Murine macrophage RAW 264.7 cells were preincubated with AFCQ (50 μg/ml, 1 μg/ml and 10 ng/ml) for 3 h, and stimulated with or without LPS (1 μg/ml) for 24 h. This study showing the translocation of Nrf-2 from cytoplasm to nucleus it leads to upregulation of anti-inflammatory protein HO-1 in dose dependent manner. Nrf-2 is in the cytosol under normal situation. But when it is activated, it get separated from keap-1 protein and phosphorylated, after that translocated to the nucleus, and binds to a promoter region called ARE, which is concerned in the regulation of downstream gene expression. Therefore we studied the effect of AFCQ on intracellular localization of Nrf-2 in RAW 264.7 cells. Western blot analysis of cytoplasmic extract exposed that Nrf-2 was translocated into the nucleus by AFCQ treatment at lower dose too in (Fig. 5). Whereas Western blot analysis of nuclear extract showed that AFCQ increased nuclear levels of Nrf-2 protein, indicating translocation from the cytoplasm into the nucleus (Fig. 5). Nrf-2 is a transcription factor regulating expression of phase-II antioxidant enzymes including HO-1 which are involved in the regulation of acute inflammatory responses. Western blot analysis of cytoplasmic and nuclear extract of AFCQ treated LPS stimulated RAW 264.7 cells showed increased level of HO-1 in cytoplasmic extract (Fig. 5) along with its level was decreased in nuclear extract (Fig. 5). HO-1 is a antioxidant enzymes induced in inflammatory or oxidative condition. AFCQ exerts anti-inflammatory activity through activating the translocation of Nrf-2 molecule from cytoplasm to nucleus and hence increasing the transcription of phase-II antioxidant enzyme HO-1 (Fig. 5). Here we found that lower concentration of AFCQ also activated the Nrf-2 for translocation (Fig. 5) and hence expression of antioxidant protein HO-1 was upregulated in cytoplasmic extract at lower dose.

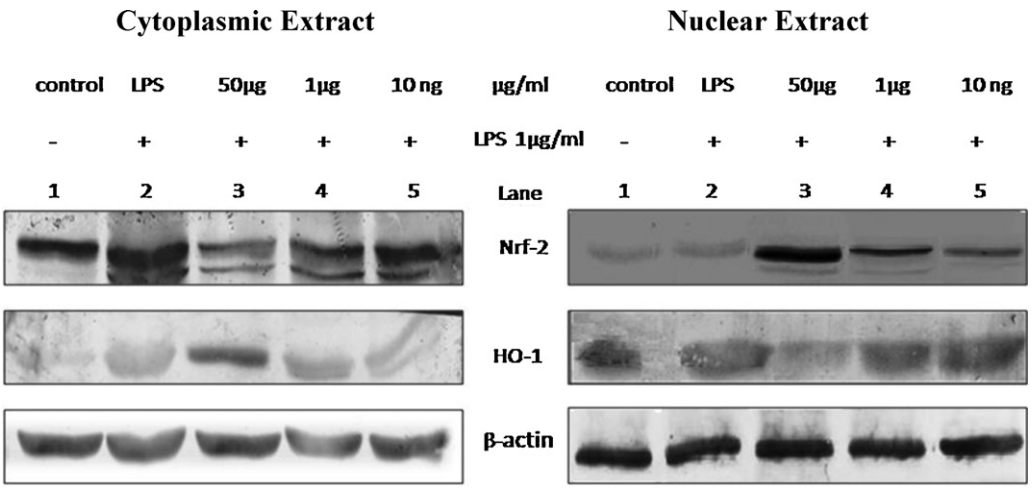

Fig. 5. RAW 264.7 cells were preincubated with AFCQ (50 μg/ml, 1 μg/ml, and 10 ng/ml) for 3 h, and stimulated with or without LPS (1 μg/ml) for 24 h and the levels of Nrf2 and HO-1 protein in cytoplasmic and nuclear fractions were analyzed by Western blot analysis. β-actin was used as loading markers for cytoplasmic and nuclear fractions, respectively.

Please cite this article in press as: Bhujade, A.M., et al., Evaluation of *Cissus quadrangularis* extracts as an inhibitor of COX, 5-LOX, and proinflammatory mediators. J. Ethnopharmacol. (2012), http://dx.doi.org/10.1016/j.jep.2012.03.044

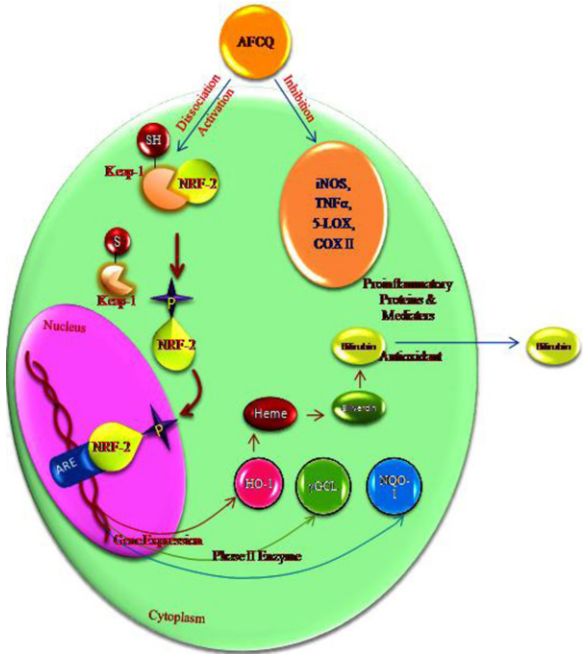

Fig. 6. Figure shows the effect of AFCQ on the Nrf-2 molecule which in turn increases the gene expression of antioxidant enzymes HO-1. It leads to the formation of bilirubin. AFCQ is also shows inhibition on the proinflammatory cytokines and mediators like TNFα, iNOS, 5-LOX, and COX-2.

4. Discussion

Almost all diseases are characterized by the inflammation and pain in response to different conditions like injuries, infection, etc. Inflammation and pain indicate the presence of COX and 5-LOX. The enzyme COX has two isoforms, COX-1 and COX-2. COX-1 is the constitutive enzyme, COX-2 is an inducible enzyme and its level is always found elevated in abnormal conditions like inflammation, arthritis and in carcinogenesis. Non steroidal anti-inflammatory drugs (NSAIDs) inhibit COX-2, but have many side effects, like cardiac failure, gastric ulcer, stroke, etc. (Pairet et al., 1996). A number of drugs, used in the treatment of chronic diseases, have been developed over the past few decades but these drugs have a lot of side effects. A very good example is of Aspirin which results in gastric ulceration, Vioxx (Rofecoxib) which results in heart attack, stroke, and serious cardiovascular events. That might be the reason behind its ban. Plant extracts are striking sources of new drugs. Traditional medicinal plant *Cissus quadrangularis*, commonly known as bone setter, is frequently used as a common food item in India. It is an edible plant found throughout the tropical parts of the world like India, Africa, Thailand, and Philippines (Parisuthiman et al., 2009). It is a multipurpose plant, used traditionally for different healing treatments. Our present study deals with COX and 5-LOX inhibition by using differential extracts of *Cissus quadrangularis*. Based on polarity, extraction was performed and six different extracts were prepared, *viz*. hexane, chloroform, acetone, ethyl acetate, methanol, and ethanol. Out of all these six extracts, acetone extract showed potent inhibition of COX-1, COX-2, and 5-LOX. Results show that acetone extract exhibit an effective inhibitor of both COX and 5-LOX. AFCQ is the active fraction of acetone extract isolated by column chromatography has shown inhibition on COX-1, COX-2, and 5-LOX enzyme activity with IC_{50} values of 7 μg/ml, 0.4 μg/ml, and 20 μg/ml. The phytochemical study of the AFCQ have shown the presence of tannin compounds. Partially purified AFCQ on cell proliferation of RAW 264.7 cell line shows IC_{50} value 65 μg/ml at 24 h. iNOS, COX-2, 5-LOX, and TNFα are key mediators of inflammation. The transcription factor Nrf-2 regulates the basal and inducible expression of numerous detoxifying and antioxidant genes. Western blotting studies have shown the downregulation of iNOS, COX-2, and TNFα by AFCQ treatment. In addition AFCQ have activated the translocation of Nrf-2 molecule which leads to increase in the synthesis of the antioxidant proteins HO-1, NQO-1, and γGCL, here we have verified the upregulation of HO-1. Isolation and characterization of active principle from AFCQ is in progress in our laboratory. Further studies with these extracts on arthritis, cancer and in other chronic diseases are also going on.

5. Conclusion

According to experimental results, AFCQ obtained from *Cissus quadrangularis*, was found to have better anti-inflammatory activity. AFCQ might be helping in the dissociation the Nrf-2-Keap-1 complex which in turn leads to activation of Nrf-2 protein by phosphorylation and translocation from cytoplasm into nucleus. Phosphorylated Nrf-2 binds with ARE which in turn activates the gene expression of phase-II enzymes. The antioxidant proteins like HO-1 get expressed through the Nrf-2 Pathway. It leads to synthesis of antioxidant like bilirubin. AFCQ also inhibit proinflammatory cytokines and mediators like TNFα, iNOS, 5-LOX, and COX-2 (Fig. 6). This might be due to the effect of the tannin compounds present in the AFCQ. Further studies are necessary to isolate active compounds and to elucidate their exact mechanism of action.

Acknowledgements

We are express our gratitude to Mr. G. Durgaprasad, Mr. Rambabu, Mr. Kishore, Mr. Tanmay, Ms. Monima, Mr. Bharat, urmi, Dr. Anil Kotha, Dr. Chandramohan, Dr. Pulla Reddy and Dr. G.V. Reddy for their support and guidance. We are also grateful to UGC Networking Resource Center, School of Chemistry, University of Hyderabad for providing the laboratory, instruments and other facilities.

References

Annukka, M.K., Emilia, K., Henna-Kaisa, J., Tarja, N., Seppo, Y.H., et al., 2008. Levonen enterolactone induces heme oxygenase-1 expression through nuclear factor-E2-related factor 2 activation in endothelial cells. The Journal of Nutrition 138, 1263–1268.

Balasubramaniana, P., Jayalakshmib, K., Vidhyab, N., Prasada, R., Khaleefathullah, A., Kathiravana, G., Rajagopala, K., et al., 2010. Antiviral activity of ancient system of ayurvedic medicinal plant *Cissus quadrangularis* linn. (Vitaceae). Journal of Basic Clinical Pharmacy 1, 37–40.

Copeland, R.A., Williams, J.M., Giannaras, J., Nurnberg, S., Covington, M., Pinto, D., et al., 1994. Mechanism of selective inhibition of the inducible isoform of prostaglandin G/H synthase. Proceedings of the National Academy Science of the United States of America 91, 11202–11206.

Deka, D.K., Lahon, L.C., Saikia, J., Mukit, A., 1994. Effect of *Cissus quadrangularis* in accelerating healing process of experimentally fractured radius-ulna of dog: a preliminary study. Indian Journal of Pharmacology 26, 44–45.

Daniel, M., Ana, I.R., Marta, S., Raquel, D., German, G., Jawed, A., et al., 2004. Regulation of heme oxygenase-1 expression through the phosphatidylinositol 3-kinase/akt pathway and the nrf-2 transcription factor in response to the antioxidant phytochemical carnosol. Journal of Biological Chemistry 279, 8919–8929.

Egan, R.W., Paxton, J., Kuehl Jr., F.A., 1976. Mechanism for irreversible self deactivation of prostaglandin synthetase. Journal of Biological Chemistry 251, 7329–7335.

Hemler, M., Lands, W.E., Smith, W.L., 1976. Purification of the cyclooxygenase that forms prostaglandins: demonstration of two forms of iron in the holoenzyme. Journal of Biological Chemistry 251, 5575–5579.

Jainu, M., Shyamaladevi, C., 2004. Effect of *Cissus quadrangularis* on gastric mucosal defensive factors in experimentally induced gastric ulcer—a comparative study with sucralfate. Journal of Medicinal Food 7, 372–376.

Jainu, M., Shyamaladevi, C.S., 2005. In vitro and in vivo evaluation of free radical scavenging potential of *Cissus quadrangularis*. African Journal of Biomedical Research 8, 95–99.

Jainu, M., Shyamaladevi, C., 2006. Gastroprotective action of *Cissus quadrangularis* extract against NSAID induced gastric ulcer: role of proinflammatory cytokines and oxidative damage. Chemico-Biological Interactions 161, 262–270.

Jainu, M., Vijaimohan, K., Kannan, K., 2010. *Cissus quadrangularis* l. extract attenuates chronic ulcer by possible involvement of polyamines and proliferating cell nuclear antigen. Pharmacognsy Magazine 23, 225–233.
Kashikar, N.D., George, I., 2006. Antibacterial activity of *Cissus quadrangularis*. International Journal of Pharmaceutical Science 68, 245–247.
Kulkarni, A.P., 2001. Lipoxygenase—a versatile biocatalyst for biotransformation of endobiotics and xenobiotics. Cell and Molecular Life Science 58, 1805–1825.
Martel-Pelletier, J.M., Lajeunesse, D., Reboul, P., Pelletier, J.P., 2003. Therapeutic role of dual inhibitors of 5-LOX and COX, selective and non-selective non-steroidal anti-inflammatory drugs. Annual Rheumatological Disease 62, 501–509.
Mosmann, T., 1983. Rapid colorimetric assay for cellular growth and survival: application to proliferation and cytotoxicity assays. Journal of Immunological Methods 65, 55–63.
Oben, J., Kuate, D., Agbor, G., Momo, C., Talla, X., 2006. The use of a *Cissus quadrangularis* formulation in the management of weight loss and metabolic syndrome. Lipid Health Disease 5, 1–7.
Oben, J.E., Enyegue, D.M., Fomekong, G.I., Soukontoua, Y.B., Agbor, G.A., 2007. The effect of *Cissus quadrangularis* (CQR-300) and a Cissus formulation (CORE) on obesity and obesity-induced oxidative stress. Lipids in Health Disease 6, 1–8.
Pagels, W.R., Sachs, R.J., Marnett, L.J., Dewitt, D.L., Day, J.S., Smith, W.L., 1983. Immunochemical evidence for the involvement of prostaglandin H synthase in hydroperoxide-dependent oxidations by ram seminal vesicle microsomes. Journal of Biological Chemistry 258, 6517–6523.
Pairet, M., Churchill, L., Trummlitz, G., Engelhardt, G., 1996. Differential inhibition of cyclooxygenase-1 (COX-1) and (COX-2) by NASAIDs: consequences on anti-inflammatory activity versus gastric and renal safety. Inflammopharmacology 4, 61–70.
Panda, 1990. Journal of Research Ayurvedic Siddha 11, 7.
Parisuthiman, D., Singhatanadgit, W., Dechatiwongse, T., Koontongkaew, S., 2009. *Cissus quadrangularis* extract enhances biomineralization through up-regulation of mapk-dependent alkaline phosphatase activity in osteoblasts. In Vitro Cellular and Developmental Biology - Animal 45, 194–200.
Potu, B.K., Rao, M.S., Nampurath, G.K., Rao, M.C., Nayak, S.R., Thomas, H., 2010. Anti-osteoporotic activity of the petroleum ether extract of *Cissus quadrangularis linn.* in ovariectomized wistar rats. Chang Gung Medical Journal 33, 252–257.
Reddanna, P., Whelan, J., Maddipati, K.R., Reddy, C.C., 1990. Purification of arachidonate 5-lipoxygenase from potato tubers. Methods in Enzymology 187, 268–277.
Reddy, C.M., Bhat, V.B., Kiranmai, G., Reddy, M.N., Reddanna, P., Madyastha, K.M., 2000. Selective inhibition of cyclooxygenase-2 by c-phycocyanin, a biliprotein from spirulina platensis. Biochemical and Biophysical Research Communication 277, 599–603.
Shirwaikar, A., Khan, S., Malini, S., 2003. Anti-osteoporotic effect of ethanol extract of *Cissus quadrangularis* linn on ovariectomized rat. Journal of Ethnopharmacology 89, 245–250.
Sharpa, H., Hollinsheada, J., Bartholomewa, B.B., Obenb, J., Watsona, A., Robert, J.N., 2007. Inhibitory effects of *Cissus quadrangularis l.* derived components on lipase, amylase and glucosidase activity in vitro. Natural Product Communication 2, 817–822.
Thakur, A., Jain, V., Hingorani, L., Laddha, K.S., 2009. Phytochemical studies on *Cissus quadrangularis* linn. Pharmacognocy Research 1, 213–215.
Udupa, K.N., Prasad, G., Sen, S.P., 1965. The effect of phytogenic anabolic steroid in the acceleration of fracture repairs. Life Sciences 4, 317–327.

Please cite this article in press as: Bhujade, A.M., et al., Evaluation of *Cissus quadrangularis* extracts as an inhibitor of COX, 5-LOX, and proinflammatory mediators. J. Ethnopharmacol. (2012), http://dx.doi.org/10.1016/j.jep.2012.03.044

Anti-inflammatory effects of 15-lipoxygenase metabolitcs of a -linolenic acid

ORIGINALITY REPORT

%12	%8	%8	%3
SIMILARITY INDEX	INTERNET SOURCES	PUBLICATIONS	STUDENT PAPERS

PRIMARY SOURCES

1	www.pubmedcentral.nih.gov Internet Source	%1
2	Kyu Lim. "ω-3 PUFAs and Other Cancers", Dietary Omega-3 Polyunsaturated Fatty Acids and Cancer, 2010 Publication	%1
3	Submitted to University of Birmingham Student Paper	%1
4	Mahipal, S.V.K.. "Effect of 15-lipoxygenase metabolites, 15-(S)-HPETE and 15-(S)-HETE on chronic myelogenous leukemia cell line K-562: Reactive oxygen species (ROS) mediate caspase-dependent apoptosis", Biochemical Pharmacology, 20070715 Publication	<%1
5	Iris J. Edwards. "ω-3 PUFAs, Breast and Prostate Cancer: Experimental Studies", Dietary Omega-3 Polyunsaturated Fatty Acids and Cancer, 2010 Publication	<%1

Rabelo, Thallita Kelly, Adriana Gibara

6	Guimarães, Marlange Almeida Oliveira, Juciano Gasparotto, Mairim Russo Serafini, Adriano Antunes de Souza Araújo, Lucindo José Quintans-Júnior, José Cláudio Fonseca Moreira, and Daniel Pens Gelain. "Shikimic acid inhibits LPS-induced cellular pro-inflammatory cytokines and attenuates mechanical hyperalgesia in mice", International Immunopharmacology, 2016. Publication	<%1
7	spandidos-publications.com Internet Source	<%1
8	journals.tubitak.gov.tr Internet Source	<%1
9	Araki, Shunsuke, Kazushige Dobashi, Kohtaro Asayama, and Akira Shirahata. "Simvastatin enhances induction of inducible nitric oxide synthase in 3T3-L1 adipocytes", Free Radical Research, 2007. Publication	<%1
10	www.strongparachutes.com Internet Source	<%1
11	www.ehponline.org Internet Source	<%1
12	Submitted to University of Bath Student Paper	<%1
13	Lee, Hwa Jin Jung, Hyeyoun Kwon, Junhye . "A germacranolide sesquiterpene lactone	<%1

	suppressed inducible nitric oxide synthase by downregulating ", Canadian Journal of Physiology and Pharm, March 2011 Issue Publication	
14	www.lipidworld.com Internet Source	<%1
15	www.e-emm.org Internet Source	<%1
16	Kimira, Yoshifumi Taniuchi, Yuri Nakatan. "Citrus limonoid nomilin inhibits osteoclastogenesis in vitro by suppression of NFATc1 and MAPK signa", Phytomedicine: International Journal of , Nov 15 2015 Issue Publication	<%1
17	effiloop.com Internet Source	<%1
18	lipidlibrary.aocs.org Internet Source	<%1
19	www.coursehero.com Internet Source	<%1
20	carcin.oxfordjournals.org Internet Source	<%1
21	ejcts.ctsnetjournals.org Internet Source	<%1
22	P. Sapieha. "5-Lipoxygenase Metabolite 4-HDHA Is a Mediator of the Antiangiogenic Effect of -3 Polyunsaturated Fatty Acids",	<%1

	Science Translational Medicine, 02/09/2011 Publication	
23	Antunes-Ricardo, Marilena Gutierrez-Urib. "Topical anti-inflammatory effects of isorhamnetin glycosides isolated from Opuntia ficus-indica.(Res", BioMed Research International, Annual 2015 Issue Publication	<%1
24	www.ors.org Internet Source	<%1
25	www.nature.com Internet Source	<%1
26	www.jcb.org Internet Source	<%1
27	www.plosone.org Internet Source	<%1
28	www.caymanchem.com Internet Source	<%1
29	www.plantphysiol.org Internet Source	<%1
30	iovs.arvojournals.org Internet Source	<%1
31	ar.iiarjournals.org Internet Source	<%1
32	fr.slideshare.net Internet Source	<%1

33	amsdottorato.unibo.it Internet Source	<%1
34	ip.com Internet Source	<%1
35	Submitted to University of Exeter Student Paper	<%1
36	Shamhart, Patricia E. Luther, Daniel J. . "Hyperglycemia enhances function and differentiation of adult rat cardiac fibroblasts. (Report)", Canadian Journal of Physiology and Pharm, July 2014 Issue Publication	<%1
37	Iliou, J.P.. "Monohydroperoxidized fatty acids but not 4-hydroxynonenal induced acute cardiac cell damage", Free Radical Biology and Medicine, 199512 Publication	<%1
38	Submitted to Loma Linda University Student Paper	<%1
39	www.ncbi.nlm.nih.gov Internet Source	<%1
40	Xu, Jun Chi, Feng Guo, Tongsheng Punj, Vasu Lee, W.N. Paul French, Samuel W. Tsukamoto, Hidekazu. "NOTCH reprograms mitochondrial metabolism for proinflammatory macrophage activation. (RESEARCH ARTICL", Journal of Clinical	<%1

Investigation, April 2015 Issue
Publication

41	Ganesan, Balasubramanian, Carl Brothersen, and Donald J. McMahon. "Fortification of Foods with Omega-3 Polyunsaturated Fatty Acids", Critical Reviews in Food Science and Nutrition, 2014. Publication	<%1
42	www.freepatentsonline.com Internet Source	<%1
43	Zhang*, H. J., Y. M. Guo, Y. Yang, and J. M. Yuan. "Dietary conjugated linoleic acid enhances spleen PPAR-γ mRNA expression in broiler chicks", British Poultry Science, 2006. Publication	<%1
44	Taechowisan, Thongchai, Chunhua Lu, Yuemao Shen, and Saisamorn Lumyong. "Anti-inflammatory Effects of 4-Arylcoumarins in LPS-induced Murine Macrophage RAW 264.7 Cells", Pharmaceutical Biology, 2006. Publication	<%1
45	www2007.igc.gulbenkian.pt Internet Source	<%1
46	Vijaya Juturu. "Fatty Acids, Insulin Resistance and Diabetes", Wild-Type Food in Health Promotion and Disease Prevention,	<%1

2008
Publication

47	archive.org Internet Source	<%1
48	Perica, M. M., and I. Delas. "Essential Fatty Acids and Psychiatric Disorders", Nutrition in Clinical Practice, 2011. Publication	<%1
49	molpharm.aspetjournals.org Internet Source	<%1
50	Gerber, Lukas C. Mohn, Dirk Fortunato, G. "Incorporation of reactive silver-tricalcium phosphate nanoparticles into polyamide 6 allows preparat", Polymer Engineering and Science, Jan 2011 Issue Publication	<%1
51	"Investigators from Konkuk University Have Published New Data on Myeloid Cells.", Biotech Week, July 4 2012 Issue Publication	<%1
52	Zhao, Xinwei Xu, Lina Zheng, Lingli Yin,. "Potent effects of dioscin against gastric cancer in vitro and in vivo.(Report)", Phytomedicine: International Journal of , March 15 2016 Issue Publication	<%1
53	www.tonicology.com Internet Source	<%1

54	www.cmj.org Internet Source	<%1
55	www.marshallplan.at Internet Source	<%1
56	Submitted to University of East London Student Paper	<%1
57	Submitted to University of Cambridge Student Paper	<%1
58	Youm, Yun-Hee Nguyen, Kim Y. Grant, Ryan. "The ketone metabolite [beta]-hydroxybutyrate blocks NLRP3 inflammasome-mediated inflammatory disease", Nature Medicine, March 2015 Issue Publication	<%1
59	"Findings on Cytokines Reported by Investigators at Dong Eui University (Fructus sophorae attenuates ", Health & Medicine Week, July 22 2016 Issue Publication	<%1
60	scialert.net Internet Source	<%1
61	Saini, Manpreet Kaur Sanyal, Sankar Nath. "Targeting angiogenic pathway for chemoprevention of experimental colon cancer using C-phycocyanin as", Biochemistry and Cell Biology, June 2014 Issue Publication	<%1

62	Wang, Jian-Yun Liu, Shuai Qin, Na Yang, . "Jak2/Stat1 pathway mediated tetrahydrobiopterin up-regulation contributes to nitric oxide overproduc", Canadian Journal of Physiology and Pharm, Jan 2015 Issue Publication	<%1
63	www.bodyofscience.com Internet Source	<%1
64	dare.ubn.kun.nl Internet Source	<%1
65	Granica, Sebastian Piwowarski, Jakub P. . "Ellagitannins modulate the inflammatory response of human neutrophils ex vivo. (Report)", Phytomedicine: International Journal of , Dec 15 2015 Issue Publication	<%1
66	www.faqs.org Internet Source	<%1
67	Pengjam, Yutthana Madhyastha, Harishkuma. "NF-[kappa]B pathway inhibition by anthrocyclic glycoside aloin is key event in preventing osteoclast", Phytomedicine: International Journal of , April 15 2016 Issue Publication	<%1
68	"Scientists at Korea Institute of Oriental Medicine Detail Research in Antioxidants.", Biotech Week, July 4 2012 Issue Publication	<%1

69	www.zftr.binoz.uj.edu.pl Internet Source	<%1
70	my.pbworks.com Internet Source	<%1
71	ebm.rsmjournals.com Internet Source	<%1
72	Ryter, Stefan W. Alam, Jawed Choi, Augus. "Heme oxygenase-1/carbon monoxide: from basic science to therapeutic applications.", Physiological Reviews, April 2006 Issue Publication	<%1
73	Dongxing Li; Woojin Kim; Dasom Shin; Yongjae Jung; Hyunsu Bae and Sun Kwang Kim. "Preventive Effects of Bee Venom Derived Phospholipase A_2 on Oxaliplatin-Induced Neuropathic Pain in Mice", Toxins, 2016. Publication	<%1
74	www.biomedcentral.com Internet Source	<%1
75	eprints.lib.hokudai.ac.jp Internet Source	<%1
76	etd.lsu.edu Internet Source	<%1
77	sadent.com Internet Source	<%1

78	www.bh4.org Internet Source	<%1
79	"Investigators from Nanjing Medical University Publish New Data on Myeloid Cells.(Report)", Blood Weekly, July 5 2012 Issue Publication	<%1
80	Submitted to Nottingham Trent University Student Paper	<%1
81	e-fas.org Internet Source	<%1
82	www.kidneychula.com Internet Source	<%1
83	highered.mcgraw-hill.com Internet Source	<%1
84	bentham.org Internet Source	<%1
85	lra.le.ac.uk Internet Source	<%1
86	nhmrc.gov.au Internet Source	<%1
87	www.imbhg.tcu.edu.tw Internet Source	<%1
88	"Study findings on life sciences are outlined in reports from Chungbuk National University, Departmen", Biotech Week,	<%1

	March 31 2010 Issue Publication	
89	carb.siobc.ras.ru Internet Source	<%1
90	wellcomelibrary.org Internet Source	<%1
91	scholarcommons.usf.edu Internet Source	<%1
92	Submitted to University of Glasgow Student Paper	<%1
93	Syahida, A., D.A. Israf, N.H. Lajis, S. Khozirah, M. Habsah, D. Permana, and I. Norhadiani. "Effect of Compounds Isolated from Natural Products on IFN-γ/LPS–Induced Nitric Oxide Production in RAW 264.7 Macrophages", Pharmaceutical Biology, 2006. Publication	<%1
94	www.aspergillus.org.uk Internet Source	<%1
95	www.scribd.com Internet Source	<%1
96	shop.micronplus.ro Internet Source	<%1
97	medicovegetariano.com.br Internet Source	<%1

98	nizetlab.ucsd.edu Internet Source	<%1
99	Andriy Podolyan. "Identification of the lipoxygenase gene family from *Vitis vinifera* and biochemical characterisation of two 13-lipoxygenases expressed in grape berries of Sauvignon Blanc", Functional Plant Biology, 2010 Publication	<%1
100	Woo, Hyun Ae Chae, Ho Zoon Hwang, Sung C. "Reversing the inactivation of peroxiredoxins caused by cysteine sulfinic acid formation. (Reports).", Science, April 25 2003 Issue Publication	<%1
101	"Patent Application Titled "Biocompatible Implant" Published Online.", Biotech Week, Jan 21 2015 Issue Publication	<%1
102	Wang, Wenwen Guan, Cuiwen Sun, Xiaozhe Z. "Tanshinone IIA protects against acetaminophen-induced hepatotoxicity via activating the Nrf2 pathway", Phytomedicine: International Journal of , June 1 2016 Issue Publication	<%1
103	Lin, Shan-Erh Wu, Fe-Lin Lin Wei, Ming-F. "Depletion of arginine by recombinant arginine deiminase induces nNOS-activated	<%1

neurotoxicity in neur", BioMed Research International, Annual 2014 Issue

Publication

EXCLUDE QUOTES	ON	EXCLUDE MATCHES	< 5 WORDS
EXCLUDE BIBLIOGRAPHY	ON		